DEVELOPMENT OF THE CORE TECHNOLOGY FOR THE CREATION OF ELECTRONICALLY-ACTIVE, SMART YARN

ANURA SARATHCHANDRA RATHNAYAKE

A thesis submitted in partial fulfilment of the requirements of Nottingham Trent University for the degree of Doctor of Philosophy

October 2015

COPYRIGHT STATEMENT

This work is the intellectual property of the author. You may copy up to 5% of this work for private study, or personal, non-commercial research. Any re-use of the information contained within this document should be fully referenced, quoting the author, title, university, degree level and pagination. Queries or requests for any other use, or if a more substantial copy is required, should be directed in the owner of the Intellectual Property Rights.

ACKNOWLEDGEMENTS

First of all, I would like to thank my Director of Studies Professor Tilak Dias for providing me with this great opportunity and incredible support throughout the PhD research work. It would have been impossible to complete this successful, unique piece of research work without his great supervision.

My thanks also go to my second supervisor Professor Philip Breedon for his support and guidance. My sincere thanks also go to Professor Tom Fisher for his incredible support and encouragement. And I was also very lucky to have the support of Dr. Colin Cork and Dr. Dorothy Hardy. I do appreciate their valuable support and guidance. My thanks also go to Carlos Oliveira, Ekael Mbise, Vajira Peiris, Dilusha Rajapaksha, Pasindu Lugoda, Dr. Katherine Townsend, Anna Piper, Sharon Haywood, Simon Johnson, Philip Stovell, Erica Just, Sue Turton, Susan Allcock, Jez Keeling and Richard Arm who provided me with professional support to carry out the research.

I would like to extend my appreciation to Professor Neil Gorman, the previous Vice Chancellor of Nottingham Trent University for the award of the Vice Chancellor’s Bursary.

I would like to take this opportunity to thank Dr. Nirmali De Silva, who was my BSc Engineering Degree supervisor, and Dr. Dilruk Yahathugoda for his encouragement and support that enabled me to carry out this research work successfully.

My thanks also go to all the members of staff of the Advanced Textiles Research Group and academic, non-academic staff and research colleagues at Nottingham Trent University who provided me wonderful, professional support to carry out the research.

Finally, I wish to give special thanks for my family, relatives and friends including Brigadier Jayalath Galgamuwa, Brigadier Hiran Halangoda, Chamara Perea, Piyumi Abeysinghe, Dr. Roshan de Silva, Nayomi Perera and W Wickremesinghe for their incredible moral support to achieve my desired tough target.

ABSTRACT

The general use of textiles began twenty-seven thousand years ago. However, today, textiles are used, not only in the production of clothing but are also found in numerous applications in medicine, the military, transport, construction sectors and in many industrial applications. Normally textiles are passive, however active textiles have been developed that exhibit the capability of adapting their functionality according to changes in their surroundings, i.e. environment. Such textiles are known as Smart and Interactive Textiles (SMIT) and are capable of sensing and being active. The integration of semiconductor devices into textiles has enormous potential in the creation of SMIT. Such SMIT structures will pave the way for the creation of truly-wearable electronic systems in the near future.

The aim of this research is the development of a core technology for embedding functional semiconductor devices within the fibres of a yarn, in order to create electronically-active yarns (e-yarn). Such electronically-active yarns will be the building blocks of the next generation of wearable electronics. Moreover, this will facilitate the creation of innovative solutions able to overcome current problems and difficulties which the manufacturers of wearable textiles are experiencing and open the doors for designers to develop the next generation of truly-wearable computers which are comfortable to wear, flexible and washable. The e-yarns could be used in medical applications such as monitoring of ECG, respiratory patterns, blood pressure and skin temperature. They could be adopted by industries such as automotive, retail, manufacturing, military, the internet of soft things, consumer products, sports, fashion and entertainment.

The development of the core technology required raw materials analysis in terms of physical, mechanical and electrical properties; creation of interconnections of electronic semi-conductor chips with copper filaments; encapsulation of the interconnections to improve washability and provide extra mechanical strength to the core filaments prior to making the final yarn. The final step was the process of manufacturing yarns using the knit braiding technique. A number of prototypes of e-textiles were produced including illuminated yarns, thermistor yarns, RFID yarns, magnetic yarns, vibration sensor yarns, illuminated garment, illuminated car seat, RFID-intergraded garments, a temperature-monitoring fabric mat and temperature-monitoring socks in order to investigate the manufacturing viability, identify practical issues, and to promote the technology to attract further funds and potential commercial partners.

CONTENTS

COPYRIGHT STATEMENT i
ACKNOWLEDGEMENTS ii
ABSTRACT iii
CONTENTS iv
LIST OF FIGURES ix
RESEARCH ACTIVITIES xix
i. Patent xix
ii. Publications and conference proceedings xix
iii. Exhibitions xx
CHAPTER ONE 1
1.0 Introduction 1
1.1 Background Information 1
1.1.1 Application of Electronic Textiles 1
1.1.2 Issues for Current Applications of Electronic Textiles 1
1.1.3 State of the Art of Electronic Textiles 2
1.2 The Aims and Objectives of the Study 3
1.3 Research Methodology 3
1.3.1 Conductive Yarn and Electronic Devices 5
1.3.2 Soldering 5
1.3.3 Encapsulation and Yarn Formation 5
1.4 Structure of Theses 6
CHAPTER TWO 8
2.0 Literature Review 8
2.1 Textiles 8
2.1.1 Textile Fibre Classification 8
2.1.2 Textile Yarn Classification 9
2.1.3 The Methodologies Available to Convert Fibres into Fabrics 10
2.2 Electronic Components 13
2.2.1 Semiconductor 14
2.3 Electronic Textiles 14
2.3.1 Early Examples 16
2.3.2 Attachment of Electronic Components into Pockets 16
2.3.3 Attachment of Electronic Components into Garments/Textiles 17
2.3.4 Integration of Electrically Conducting Fibres 20
2.3.5 Semi-Conductors Embedded Within Yarn 21
2.3.6 Highlighted Funded Projects on E-Textiles 22
2.3.7 Current Situation of Global Wearable Electronics and Electronic Textiles .. 24

2.4 Conclusion 26
CHAPTER THREE 28
3.0 Raw Materials Analysis 28
3.1 Conductive Yarns/Threads/Strands 28
3.1.1 Physical Properties Analysis of Copper Wires 29
3.1.1.1 Microscopic Analysis and Diameter Measuring Test 29
3.1.1.2 Measurement of Linear Density of Copper Wires 31
3.1.2 Mechanical Properties of Copper Wires 32
3.1.3 Mechanical Properties of Polyester Yarn 34
3.1.4 Mechanical Properties of Polyester Yarn and Copper Wires Combination 35
3.1.5 Electrical Properties of Copper Wires 36
3.2 Materials Used for Electrical Connection 37
3.2.1 Solder Paste 38
3.3 SMD Type Electronics Packaged Dies 39
3.3.1 Microscopic Analysis of Semiconductor Packaged dies 40
3.3.1.1 LED Silicon Wafer Bare Die 40
3.3.1.2 SMD Packaged Dies (0402 Type) 41
3.3.1.3 Radio Frequency Identification (RFID) Packaged Dies 41
3.3.2 Dimensions of Semiconductor Packaged Dies 42
3.4 Encapsulation Resin 43
3.4.1 Testing for Distance between UV Light Source and Resin to be Cured 43
3.4.2 Testing for Curing Time of UV Curable Resin 45
3.5 Conclusion 47
CHAPTER FOUR 48
4.0 Creation of Interconnections of Micro-Devices 48
4.1 Available Techniques of Solder Bonding 48
4.1.1 Hot Bar/Thermode Reflow Soldering 48
4.1.2 Hot plate 49
4.1.3 Resistance Soldering 49
4.1.4 Flame Soldering 49
4.1.5 Convection Oven 49
4.1.6 Focused Hot Air Soldering 50
4.1.7 Induction Soldering 50
4.1.8 Laser Soldering 50
4.1.9 Hand Soldering 50
4.1.10 Infra-Red (IR) Reflow Soldering 51
4.2 Creation of Interconnections using Hand Soldering Technique 53
4.3 Creation of Interconnections using Reflow Soldering 55

4.3.1: Determining the Solderability of Coated and Uncoated Copper Wires using the PDR IR Rework System 55
4.3.2: Polyester-Coated Copper Wire Soldering after Removal of the Coating 57
4.3.3: Method for Burning-off the Polyester Coating of the Copper Wire using Flux (Contactless Method) 58
4.3.4: Analysis of the Heating Profile Recommended by the Solder Paste Manufacturer for use with the PDR IR Rework System 59
4.3.5: Analysis of the Heating Profile Recommended by LED Manufacturer with PDR IR Rework System 62
4.3.6: Optimisation of the Heating Profile for Soldering Multi-Strand Copper Wires to Solder Pads 63
4.3.7: Development of Soldering Techniques for the 0201 Type Chips with Seven-Strand Copper 66
4.3.8: Development of Soldering Techniques for the 0201 Type Chips with Single-Strand Copper Wire 67
4.3.9: Development of Soldering Techniques for 0402 type Resistor Chips with Seven-Strand Copper 67
4.4 Analysis of Electrical Properties of Solder Joints 68
4.4.1 Development of a Method to Analyse the Electrical Properties of Solder Joints 68
4.4.2. Analysis of Solder Joints Created by Hand Soldering 69
4.4.3 Analysis of the Electrical Properties of Solder Joints Formed with the PDR IR Rework System 71
4.5 Analysis of Mechanical Performance of Solder Joints 72
4.5.1 Tensile Testing of Soldered 0201 Resistors with 4 Strands Copper Wires 72
4.5.2 Tensile Testing of Copper Wire Soldered with LEDs 75
4.5.3 Tensile Test for Soldered 0402 Red LEDs with 7 Strands Copper Wires 79
4.4 Analysis of the IR Beam of PDR IR Rework System 81
4.5 Conclusion 83
CHAPTER FIVE 84
5.0 Encapsulation 84
5.1 Introduction 84
5.1.1 Ultraviolet (UV) Radiation 85
5.1.2 UV Curing Technique 85
5.2 Preliminary Encapsulation Test 86
5.3 Encapsulation Process Using EFD Dispenser Unit 89
5.4 Encapsulation Process Using EFD Dispenser Unit and Teflon Tube Mould 90
5.5 Tensile Test of Soldered and Encapsulated 0402 Blue LEDs with 7-Strand Copper Filaments 92
5.5 Conclusion 93

CHAPTER SIX 95
6.0 Electronic Yarn Formation 95
6.1 Electronic Yarn (e-Yarn) 95
6.2 Study of Twisting Technique for e-Yarn Formation 95
6.2.1 The Issues of the Twisting Technique 96
6.3 Mini Circular Warp Knitting Technique for e-Yarn Formation 97
6.3.1 Preliminary Testing 98
6.3.2 Optimisation of the Uniformity of E-yarn 100
6.4 Tensile Test e-Yarns 105
6.4.1 Tensile Testing of Warp-Knitted Sleeves (Without Electronics) 105
6.4.2 Tensile Testing of E yarn with Blue LEDs 107
6.5 Conclusion 109
CHAPTER SEVEN 110
7.0 Development of Prototype Demonstrators with e-Yarn 110
7.1 Introduction 110
7.2 Illuminated Yarns 110
7.2.1 Producing Single-Colour LED Yarns 110
7.2.2 Production of Multi-Colour LED Yarns 113
7.3 Development of Illuminated Car Seat Cover 115
7.3.1 Design of the Positions of LED’s in the Fabric 116
7.3.2 Formation of LED Yarns for Car Seat Cover 116
7.3.3 Production of Car Seat Fabrics 117
7.3.3.1 Technical Specifications of Weaving the Car Seat Fabric. 117
7.3.4 Electronic-Circuit Design 117
7.3.5 Circuit Programming 119
7.3.5.1 Arduino Programming for the Blinking Effect 119
7.3.5.2. Arduino Programming for the Sequence Effect 120
7.3.6 Pilot Run with standard LED’s 120
7.3.7 Pilot Run with Illuminated Fabric Piece 121
7.3.8 Finishing the Car Seat Edge 121
7.3.9 Pilot Run with Illuminated Car Seat and Packing the Circuit Boards 122
7.4 Illuminated Garment 123
7.4.1 Design of LED’s Position in the Fabric 124
7.4.2 Fabrication of E-Yarn with LED’s 124
7.4.3 Weaving the Illuminated Garment 125
7.4.4 Electronics and Power Circuit Board and Design 126
7.4.5 Arduino Software Programming 127
7.4.6 Pilot Run with LilyPad Development Board and Illuminated Garment 129

7..4.7 Finishing of the Illuminated Garment and Connectivity of e-Yarns........... 129
7.5 Development of Temperature-Sensor Yarns and Fabrics 130
7.5.1 E-Yarns for Temperature Sensing.. 130
7.5.2 Development of a Fabric to Measure Temperature................................... 131
7.5.2.1 Hardware Development 132
7.5.2.2 Development of hardware to measure temperature with temperature sensor fabric 134
7.5.2.3 A Pilot Run.. 135
7.5.3 Development of Temperature Sensor Socks 136
7.6 Development of e-Yarns with Electronic Signatures... 138
7.6.1 RFID Technology 138
7.6.2 Creation of antenna for the RFID device 138
7.6.3 Optimisation of Read Distance 141
7.6.4 Integration of RFID e-Yarn with Garments 141
7.6.5 Washing of RFID e-Yarn Integrated Garment... 142
7.6.6 Results Discussion 143
7.7 Other Prototype Demonstrators with e-Textiles 143
7.8 Conclusion 147
CHAPTER EIGHT 148
8.0 Conclusion and Future Work 148
8.1 Thesis Summary.. 148
8.2 Conclusion 149
8.3 Contribution to Knowledge.. 150
8.4 Future Work 151
REFERANCES 154

LIST OF FIGURES

FIGURE 1. 1: SCHEMATIC OF THE TECHNOLOGY DEVELOPMENT 4

FIGURE 1. 2: SCHEMATIC OF THE STRUCTURE OF THESIS 7

FIGURE 2. 1: FIBRE CLASSIFICATION [5] 9

FIGURE 2. 2: CLASSIFICATION OF YARNS [6] 9

FIGURE 2. 3: MANUFACTURING STEPS FROM FIBRE TO FABRIC [5] 11

FIGURE 2. 4: ILLUSTRATION OF WOVEN FABRIC SHEARING PROPERTY 12

FIGURE 2. 5: CLASSIFICATION OF ELECTRONIC COMPONENTS [8] 13

FIGURE 2. 6: SOME EXAMPLE OF ELECTRONIC DEVICES [155] 13

FIGURE 2. 7: A TYPICAL VACUUM TUBE CIRCUIT [9] 13

FIGURE 2. 8: BORON ATOM ACTING AS AN ACCEPTOR IN THE SIMPLIFIED 2D SILICON LATTICE [156] 14

FIGURE 2. 9: PHOSPHORUS ATOM ACTING AS A DONOR IN THE SIMPLIFIED 2D SILICON LATTICE [156] 14

FIGURE 2. 10: NUMBER OF ARTICLES AND BOOKS PUBLISHED ON SMART TEXTILES LAST 15

FIGURE 2. 11: ICD+ JACKET [21] 16

FIGURE 2. 12: PROTOTYPE OF PROETEX GARMENT [23] 16

FIGURE 2. 13: ZEGNA SPORT JACKET [24] 17

FIGURE 2. 14: QTC™ MATERIAL USED FOR EMBEDDED FABRIC CONTROLS WITHIN A CAR DOOR PANEL TO OPERATE MIRRORS AND WINDOWS [25]. 17

FIGURE 2. 15: GEORGIA TECH WEARABLE MOTHERBOARD [29] 18

FIGURE 2. 16: LEFT: DEMO SET-UP WITH BELT PROTOTYPE, WORN BY A 12 WEEK OLD BABY. RIGHT: BABY SUIT PROTOTYPE, WORN BY A 21 WEEK OLD BABY [34]. 18

FIGURE 2. 17: FLEXIBLE SUBSTRATE WITH METALIZED CONTACT PADS INTERCONNECTED WITH EMBROIDERY [35]. 19

FIGURE 2. 18: NUMETREX HEART SENSING SPORT BRA (LEFT) ADIDAS MICOACH MEN'S TRAINING SHIRT (RIGHT) [36] 19

FIGURE 2. 19: CUTECIUTE GALAXY DRESS [44] 20

FIGURE 2. 20: CUTECIUTE M-DRESS [43] 20

FIGURE 2.21: VISIJAX HIGH VISIBILITY JACKETS [45] 20

FIGURE 2.22: EFS CONTROL GLOVE [46] 20

FIGURE 2.23: EXAMPLES OF WEARABLE ELECTRONIC DEVICES FROM FIBROTRONICS [12]. 21

FIGURE 2.24: THE STRAIN SENSOR DEVICES FOR MONITORING THE FLEXION ANGLE DURING (A) ELBOW AND (B) KNEE MOVEMENTS [48] ... 21

FIGURE 2.25: THE ELASTIC CONDUCTIVE WEBBING WITH A PLAIN STRUCTURE [48] ... 21

FIGURE 2.26: A SCHEMATIC ILLUSTRATING DIAS' CONCEPT OF AN ELECTRONICALLY-ACTIVE YARN [51] ... 22

FIGURE 2.27: A SNAPSHOT OF THE GLOBAL WEARABLE ELECTRONICS COMPONENT MARKET VALUE [71] ... 25

FIGURE 2.28: A SNAPSHOT OF THE GLOBAL WEARABLE ELECTRONICS FORECAST [71] ... 25

FIGURE 2.29: THE WEARABLE SENSORS MARKET FORECAST [72] ... 25

FIGURE 2.30: THE TRENDS OF SENSORS WHICH ARE IN WEARABLE ELECTRONICS [72] ... 25

FIGURE 2.31: SMART TEXTILES MARKET REVENUE SHARE BY APPLICATION IN 2012 [73] 25

FIGURE 3.1: ELECTRICAL CONDUCTIVITY OF MATERIALS [84] ... 29

FIGURE 3.2: COPPER WIRES FROM LUXION INDUSTRIES INC. LTD. ... 29

FIGURE 3. 3: SINGLE STRAND COPPER WIRE (LEFT: UNCOATED, RIGHT: COATED B) ... 30

FIGURE 3. 4: UNCOATED 4 STRAND (LEFT), 7 STRAND (RIGHT) COPPER WIRES ... 30

FIGURE 3. 5: UNCOATED 8 STRANDS COPPER WIRE ... 30

TABLE 3. 1: THE RESULTS OF DIAMETERS OF THE COPPER WIRES ... 30

FIGURE 3. 6: RELATIONSHIP BETWEEN YARN BREAKING FORCE, BREAKING ELONGATION AND TWIST OF A SPUN YARN [88] ... 31

TABLE 3. 2: THE LINEAR DENSITY OF COPPER WIRES ... 32

TABLE 3. 3: TENSILE TEST RESULTS FOR COPPER WIRES ... 33

FIGURE 3. 7: GRAPH OF COATED SINGLE STRAND WIRE ... 33

FIGURE 3. 8: GRAPH OF SINGLE STRAND WIRE ... 33

FIGURE 3. 9: GRAPH OF SINGLE STRAND WIRE B ... 33

FIGURE 3. 10: GRAPH OF 4 STRAND WIRE ... 33

FIGURE 3. 11: GRAPH OF 8 STRAND WIRE ... 34

FIGURE 3. 12: GRAPH OF 7 STRAND WIRE ... 34

TABLE 3. 4: TENSILE TEST RESULTS FOR POLYESTER YARN ... 34

FIGURE 3. 13: GRAPH OF ONE POLYESTER YARN ... 35

FIGURE 3. 14: GRAPH OF TWO POLYESTER YARN ... 35

TABLE 3. 5: TENSILE TEST RESULTS FOR COMBINATIONS OF POLYESTER YARN AND COPPER WIRE ... 35

FIGURE 3. 15: GRAPH OF TWO POLYESTER YARNS AND SINGLE COPPER WIRE ... 36

FIGURE 3. 16: GRAPH OF ONE POLYESTER YARN AND SINGLE STRAND COPPER WIRE 36

FIGURE 3. 17: GRAPH OF TWO POLYESTER YARNS AND 7 STRAND COPPER WIRE 36

FIGURE 3. 18: GRAPH OF ONE POLYESTER YARNS AND 7 STRAND COPPER WIRE 36

FIGURE 3. 19: AGILENT 6 ½ DIGIT MULTI-METER 37

TABLE 3. 6: THE RESISTANCE OF COPPER WIRES 37

FIGURE 3. 20: A MICROSCOPE IMAGE OF SOLDER PASTE (91) 38

FIGURE 3. 21: SOLDER PASTE DISPENSER, SLINGER AND TIPS [93] 39

FIGURE 3. 22: MICROSCOPE IMAGES OF SN96.5AG3.0CU0.5 TYPE VI SOLDER PASTE 39

FIGURE 3. 23: EXAMPLE OF SMD 0402 LEDS (YELLOW) AND 0201 RESISTORS (BLACK) 40

FIGURE 3. 24: MICROSCOPIC IMAGES OF LED SILICON WAFER BARE DIE (RIGHT: CLOSE IMAGE) 40

FIGURE 3. 25: MICROSCOPIC IMAGES OF 0402 TYPE LED PACKAGED DIE (LEFT: FRONT, RIGHT: BACK) 41

FIGURE 3. 26: MICROSCOPIC IMAGES OF RESISTOR PACKAGED DIE (0402 TYPE) 41

FIGURE 3. 27: MICROSCOPIC IMAGES OF RFID SILICON WAFER DIE (LEFT: BACK SIDE OF PACKAGED DIE, AND RIGHT: FRONT SIDE OF PACKAGED DIE) 42

FIGURE 3. 28: MICROSCOPIC IMAGES OF RFID PACKAGE DIE (LEFT: BACK SIDE OF CHIP, AND RIGHT: FRONT SIDE OF CHIP) 42

FIGURE 3. 29: MICROSCOPIC IMAGE OF 8-TERMINAL RFID PACKAGED DIE 42

TABLE 3. 7: DIMENSIONS OF SEMICONDUCTOR PACKAGED DIES 43

TABLE 3. 8: THE EQUIPMENT AND RAW MATERIALS USED FOR THE CURING TEST 44

FIGURE 3. 30: EQUIPMENT SET UP FOR RESIN CURING TEST 44

FIGURE 3. 31: EQUIPMENT SET UP FOR CURING 45

FIGURE 3. 32: : SCHEMATIC DIAGRAM OF EQUIPMENT SET UP 45

TABLE 3.9: CURING TEST RESULT 9001-E-V 3.5 RESIN AT FIX UV EXPOSURE TIME (5 SECONDS) 45

TABLE 3.10: CURING TEST RESULT 9001-E-V 3.5 RESIN AT FIX DISTANCE OF 1 CM BETWEEN THE UV LIGHT GUIDE TIP AND THE GLASS 46

TABLE 3.11: CURING TEST RESULT 9001-E-V 3.7 RESIN AT FIX DISTANCE OF 1 CM BETWEEN THE UV LIGHT GUIDE TIP AND THE GLASS 46

FIGURE 4. 1: AN EXAMPLE OF HAND SOLDERING [112] 51

FIGURE 4. 2: AN EXAMPLE OF PDR IR REWORK SYSTEM USED IN THIS RESEARCH 51

FIGURE 4. 3: THE USER INTERFACE OF THE CONTROL SOFTWARE OF THE PDR IR 52

REWORK SYSTEM 52

FIGURE 4. 4: A TYPICAL REFLOW HEATING PROFILE FROM EFD SOLDER PASTE SUPPLIER 53

FIGURE 4. 5: SMD CHIP AND COPPER WIRE SET UP FOR HAND SOLDERING 54

FIGURE 4. 6: A SOLDERED LED WHEN ENERGISED 54

FIGURE 4. 7: MICROSCOPIC IMAGE OF SOLDERED MICRO LED CHIP (5 X MAGNIFICATION) 54

FIGURE 4. 8: HEATING PROFILE 56

FIGURE 4. 9: SOLDERING ORIENTATION OF POLYESTER COATED COPPER 56

WIRE 57

FIGURE 4. 10: THE SOLDERING PROCESS 57

FIGURE 4. 11: THE COATED COPPER WIRE WHICH WAS SOLDERED SUCCESSFULLY 58

FIGURE 4. 12: THE ARRANGEMENT OF COATED, COPPER WIRE ON THE MICRO-MOULD ARRAY 59

FIGURE 4. 13: SMD CHIP AND COPPER WIRE SET UP FOR REFLOW SOLDERING (NOT ACCORDING TO DIMENSIONS) 60

FIGURE 4. 14: THE PDR IR REWORK SYSTEM HEATING PROFILE AS 61

RECOMMENDED IN THE TECHNICAL DATA SHEETS OF THE SOLDER PASTE 61

MANUFACTURER 61

FIGURE 4. 15: LED CHIP AND COPPER WIRE AFTER APPLYING HEAT 61

FIGURE 4. 16: PDR IR REWORK SYSTEM HEATING PROFILE WHICH IS 63

RECOMMENDED IN THE MANUFACTURER ‘S TECHNICAL DATA SHEET FOR THE 63

0402 SMD LED CHIP 63

FIGURE 4.17 A: HEATING PROFILE FIGURE 4.17 B: HEATING PROFILE 64

FIGURE 4.17 C: HEATING PROFILE FIGURE 4.17 D: HEATING PROFILE 64

FIGURE 4.17 E: HEATING PROFILE FIGURE 4.17 F: HEATING PROFILE 65

FIGURE 4. 17: HEATING PROFILES WHICH WERE USED IN THIS EXPERIMENT 65

FIGURE 4. 18: AN EXAMPLE OF AN ILLUMINATED LED JUST AFTER SOLDERING 65

FIGURE 4. 19: SOLDER JOINT FAILURE AFTER SOLDERING OF 0201 RESISTOR WITH 7 STRAND COPPER WIRE 66

FIGURE 4. 20: A MICROSCOPIC IMAGE OF THE SOLDER PADS OF A 0402 RESISTOR CHIP . 68

FIGURE 4. 21: SCHEMATIC OF RESISTANCES MEASURED IN SMD RESISTOR CHIP AND SOLDERED INTERCONNECTS 69

TABLE 4.1: DC RESISTANCES OF HAND SOLDERED SOLDER JOINTS 70

TABLE 4.2: THE RESULTS OF RESISTANCE MEASUREMENTS OF SOLDER JOINTS MADE WITH THE PDR IR REWORK SYSTEM 71

FIGURE 4. 22: TENSILE TEST AND RESISTANCE MEASUREMENT EQUIPMENT 73

TABLE 4.3: RESULTS OF THE TENSILE TESTS OF FOUR-STRAND COPPER WIRES SOLDERED TO SMD RESISTOR CHIPS 74

FIGURE 4. 23: THE LOAD – ELONGATION CURVE OF FOUR-STRAND COPPER WIRE SOLDERED TO AN SMD RESISTOR CHIP (SPECIMEN 1) 74

FIGURE 4. 24: MICROSCOPIC PICTURE OF SOLDERED 0201 CHIP AFTER TENSILE TEST 75

FIGURE 4. 25: AN EXAMPLE OF ILLUMINATED BLUE 0402 LED JUST AFTER 76

SOLDERED 76

FIGURE 4. 26: TENSILE TEST AND POWER SUPPLY ARRANGEMENT 77

TABLE 4.4: TENSILE TEST RESULTS FOR SOLDERED BLUE LEDS WITH 7-STRAND COPPER WIRE 77

FIGURE 4. 27: GRAPH OF TENSILE TEST OF TABLE 4.4 78

FIGURE 4. 28: MICROSCOPIC PICTURES OF SOLDERED 0402 CHIP AFTER 78

TENSILE TEST 78

TABLE 4.5: TENSILE TEST RESULTS FOR SOLDERED RED LEDS WITH 7-STRAND COPPER WIRES 79

FIGURE 4. 29: LOAD – ELONGATION CURVES OF SEVEN-STRAND COPPER WIRE SOLDERED TO RED LED'S TYPE 0402 80

FIGURE 4. 30: AN LED THAT WAS STILL FUNCTIONAL AFTER BREAKING OF THE ATTACHED COPPER WIRE DURING TENSILE TESTING 80

FIGURE 4. 31: A CROSS-SECTION OF LAMP AND IR REWORK LENS HOUSING OF THE PDR IR REWORK 81

FIGURE 4. 32: LENSES OF PDR SYSTEM [21] 81

FIGURE 4. 33: THE MAXIMUM SIZE OF THE IR BEAM OF THE PRD SYSTEM 82

FIGURE 4. 34: COMPARATIVE DIMENSIONS OF THE IR SPOT AND THE 0402 LED CHIP, WHEN THE APERTURE IS FULLY OPEN 82

FIGURE 5. 1: UV SPECTRUM [123] 85

FIGURE 5. 2: THE SCHEMATIC OF AN SMD CHIP ENCAPSULATED WITH UV-CURABLE RESIN BEFORE APPLICATION OF UV ENERGY [124] 86

FIGURE 5. 3: THE SCHEMATIC OF AN SMD CHIP ENCAPSULATED WITH UV-CURABLE RESIN DURING APPLICATION OF UV ENERGY [124] 86

FIGURE 5. 4: THE SCHEMATIC OF AN SMD CHIP ENCAPSULATED WITH UV-CURABLE RESIN AFTER CROSS-LINKING AND BECOMING A SOLID POLYMER MICRO-POD [124] 86

FIGURE 5. 5: THE EXPERIMENTAL RIG BUILT TO ENCAPSULATE SMD CHIPS 87

FIGURE 5. 6: SCHEMATIC OF AN ENCAPSULATED, PACKAGED DIE 87

TABLE 5.1: THE EQUIPMENT AND RAW MATERIALS FOR THE ENCAPSULATION PROCESS 88

FIGURE 5. 7: A CLOSE-UP PICTURE OF THE ENCAPSULATION PROCESS. 88

TABLE 5.2: THE EQUIPMENT AND RAW MATERIALS FOR THE ENCAPSULATION PROCESS 89

FIGURE 5. 8: SCHEMATIC OF THE ENCAPSULATION PROCESS 89

FIGURE 5. 9: SCHEMATIC DIAGRAM OF THE ENCAPSULATION PROCESS USING 90

TEFLON TUBE 90

FIGURE 5. 10: THE EXPERIMENTAL RIG BUILT TO ENCAPSULATE CHIP 91

AND SOLDER JOINTS 91

FIGURE 5. 11: MICROSCOPIC IMAGES OF ENCAPSULATED 0402 TYPE LEDS USING TEFLON TUBE 91

FIGURE 5. 12: BEFORE (LEFT) AND AFTER (RIGHT) TENSILE TEST 92

TABLE 5.3: TENSILE TEST RESULTS FOR SOLDERED & ENCAPSULATED BLUE LED'S WITH 7-STRAND COPPER FILAMENTS 93

FIGURE 5. 13: GRAPH OF TENSILE TEST OF CORE YARN SAMPLES IN TABLE 5.1 93

FIGURE 6. 1: THE EXPERIMENTAL RIG WHICH WAS BUILT TO TWIST CORE YARN WITH TEXTILE YARNS TO PRODUCE E-YARNS 96

FIGURE 6. 2: A SCHEMATIC DIAGRAM OF THE EXPERIMENTAL RIG WHICH WAS BUILT TO TWIST CORE YARN WITH TEXTILE YARNS TO PRODUCE E-YARNS 96

FIGURE 6. 3: A SCHEMATIC DIAGRAM SHOWING TWISTED YARNS [128] 97

FIGURE 6. 4: AN EXAMPLE OF THE FINAL, TWISTED E-YARN 97

FIGURE 6. 5: SCHEMATIC OF THE FORMATION OF THE FINAL E-YARN. 98

FIGURE 6. 6: A SCHEMATIC OF THE ARRANGEMENT OF YARN IN THE CIRCULAR WARP KNITTING MACHINE 99

FIGURE 6. 7: THE NEEDLE CYLINDER OF THE WARP KNITTING MACHINE AND YARN ARRANGEMENT 99

FIGURE 6. 8: A SCHEMATIC DIAGRAM OF THE FINAL E-YARN 100

FIGURE 6. 9: AN EXAMPLE OF FINAL E-YARN 100

FIGURE 6. 10: SMALL-DIAMETER CIRCULAR WARP KNITTING MACHINE RIUS MC WITH YARN CREEL 101

FIGURE 6. 11: SCHEMATIC TO ILLUSTRATE THE PREFERRED POSITION OF MICRO POD WITHIN E-YARN. 101

FIGURE 6. 12: SCHEMATIC TO ILLUSTRATE THE MICRO POD BEING SQUEEZED UP TO THE E-YARN SURFACE BY FILLER YARNS 102

FIGURE 6. 13: A PICTURE OF E-YARN WITH MICRO POD BEING PUSHED UP TO THE YARN SURFACE 102

FIGURE 6. 14: SCHEMATIC ILLUSTRATING THE CROSS SECTION OF THE MICRO POD WITH CORE YARN AND SEVEN-STRAND COPPER WIRE ON THE SAME SIDE OF THE PACKAGED DIE 103

FIGURE 6. 15: SCHEMATIC OF THE SIDE VIEW OF THE MICRO POD WHEN THE CARRIER YARNS ARE EITHER SIDE 103

FIGURE 6. 16: SCHEMATIC OF THE SIDE VIEW OF THE MICRO POD WHEN CARRIER YARNS ARE TOGETHER 103

FIGURE 6. 17: SCHEMATIC OF YARN ARRANGEMENT ON RIUS KNITTING MACHINE WITH THE NEW FILLER-YARN GUIDE DISC 104

FIGURE 6. 18: PICTURES OF THE FILLER YARN GUIDE DISC 104

FIGURE 6. 19: A SCHEMATIC DIAGRAM OF FIBRE-ORIENTATION IN THE FINAL E-YARN 105

FIGURE 6. 20: A SCHEMATIC DIAGRAM OF SHOWING A CROSS-SECTIONAL VIEW OF THE FINAL E-YARN 105

FIGURE 6. 21: AN EXAMPLE OF THE FINAL E-YARN 105

TABLE 6.1: TENSILE TEST RESULTS FOR WARP KNITTED SLEEVES PRODUCED WITH SIX NEEDLES 106

FIGURE 6. 22: GRAPH SHOWING TENSILE TEST RESULTS FOR THE SAMPLES LISTED IN TABLE 6.1 106

FIGURE 6. 23: BEFORE (LEFT) AND AFTER (RIGHT) TENSILE TEST 107

TABLE 6.2: TENSILE TEST RESULTS FOR SOLDERED WITH BLUE LED’S AND 7-STRAND COPPER WIRE, ENCAPSULATED AND BRAIDED 108

FIGURE 6. 24: GRAPH OF TENSILE TEST OF TABLE 6.2 108

FIGURE 7. 1: CIRCUIT DIAGRAM OF YARNS CONTAINING BLUE LED’S 111

FIGURE 7. 2: E-YARNS CONTAINING BLUE LED’S BEFORE AND AFTER ACTIVATION 111

FIGURE 7. 3: CIRCUIT DIAGRAM OF E-YARNS CONTAINING YELLOW LED’S 112

FIGURE 7. 4: ILLUMINATED E-YARNS CONTAINING YELLOW LED’S 112

FIGURE 7. 5: CIRCUIT DIAGRAM OF WHITE YARNS 113

FIGURE 7. 6: E-YARNS WITH WHITE LED’S BEFORE AND DURING ACTIVATION 113

FIGURE 7. 7: THE CIRCUIT USED TO POWER E-YARN WITH THREE COLOUR LED’S 114

FIGURE 7. 8: AFTER SOLDERING 2 COLOURS OF LED 114

FIGURE 7. 9: THREE- COLOUR ILLUMINATED 114

YARN 114

FIGURE 7. 10: THE PROTOTYPE DEMONSTRATOR OF AN ILLUMINATED CAR-SEAT COVER 115

FIGURE 7. 11. POSITIONS OF RED AND BLUE LED’S IN THE CAR-SEAT COVER 116

FIGURE 7. 12: WARP PLAN (LEFT) AND LIFTING PLAN (RIGHT) 117

FIGURE 7. 13: ARDUINO-LED INTERFACE – SCHEMATIC 118

FIGURE 7. 14: SCHEMATIC DIAGRAM OF POWER CIRCUIT BOARDS 118

FIGURE 7. 15: A PICTURE OF PILOT RUN ON BREADBOARD 121

FIGURE 7. 16: A PICTURE OF PILOT RUN ON ILLUMINATED FABRIC..................................... 121

FIGURE 7. 17: THE ILLUMINATED FABRIC WHILST FINISHING THE EDGES 122

FIGURE 7. 18: THE FINAL PILOT RUN WITH ILLUMINATED CAR SEAT COVER 122

FIGURE 7. 19. THE AUTHOR AT THE AUTOMOTIVE ENGINEERING SHOW IN BIRMINGHAM 123

FIGURE 7. 20: THE ILLUMINATED GARMENT.. 124

FIGURE 7. 21. LED’S POSITIONS IN THE ILLUMINATED GARMENT FABRIC.......................... 124

FIGURE 7. 22 : ILLUMINATED E – YARNS 125

FIGURE 7. 23: THE GARMENT JUST AFTER REMOVAL FROM WEAVING LOOM.................. 126

FIGURE 7. 24: THE WEAVING OF THE GARMENT BY ANNA PIPER 126

FIGURE 7. 25: IMAGE OF LILYPAD ARDUINO MICROCONTROLLER....................................... 126

FIGURE 7. 26: ELECTRIC POWER MANAGEMENT CIRCUIT BOARD 127

FIGURE 7. 27: LILYPAD DEVELOPMEN BOARD 129

FIGURE 7. 28: A PICTURE TAKEN DURING THE PILOT RUN ON THE ILLUMINATED GARMENT 129

FIGURE 7. 29: THE FABRIC CONNECTOR, WHICH WAS DEVELOPED TO CONNECT CONTROL HARDWARE TO THE GARMENT.. 130

FIGURE 7. 30: THE FINISHED, ILLUMINATED GARMENT 130

FIGURE 7. 31: A PROTOTYPE THERMISTOR E - YARN 131

FIGURE 7. 32: PICTURE OF THE TEMPERATURE-SENSOR FABRIC MAT 131

FIGURE 7. 33: ELECTRONIC CIRCUIT DIAGRAM (SCHEMATIC) 132

FIGURE 7. 34: PICTURE OF THE ELECTRONIC CIRCUIT BOARD 133

FIGURE 7. 35: PICTURE OF THE CIRCUIT BOARD WHICH IS COVERED WITH SILICONE RUBBER 133

FIGURE 7. 36: LABVIEW BLOCK DIAGRAM 134

FIGURE 7. 37: LABVIEW GRAPHICAL USER INTERFACE DEVELOPED TO SHOW THE MEASURED TEMPERATURES 134

FIGURE 7. 38: DEMONSTRATION OF THE RESPONSE OF TEMPERATURE WHEN FOUR FINGERS OF THE AUTHOR'S HAND ARE IN CONTACT WITH THE TEMPERATURE-SENSOR FABRIC MAT 135

FIGURE 7. 39: DEMONSTRATION OF THE RESPONSE WHEN ALL FIVE FINGERS OF THE AUTHOR'S HAND ARE IN CONTACT WITH THE TEMPERATURE-SENSOR FABRIC MAT 136

FIGURE 7. 40: A PAIR OF THERMISTOR SOCKS 136

FIGURE 7. 41: TECHNICAL SPEC OF KNITTING MACHINE 137

FIGURE 7. 42: SIMULARSION OF KNITTED FABRIC STRUCTURE OF SOCK 137

FIGURE 7. 43: AN EXAMPLE OF AN RFID TAG [141] 138

FIGURE 7. 44: AN EXAMPLE OF A BAR CODE [142] 138

FIGURE 7. 45: SCHEMATIC DEMONSTRATING RFID TECHNOLOGY (144) 138

FIGURE 7. 46: SMD CHIP AND COPPER WIRE SET UP FOR REFLOW SOLDERING 139

FIGURE 7. 47: A MICROSCOPIC IMAGE OF AN RFID CHIP WITH SOLDERED, SEVEN-STRAND COPPER WIRES 140

FIGURE 7. 48: THE CORE YARN CONTAINING RFID PACKAGED DIE, SOLDERED SEVEN-STRAND COPPER WIRE, TWO 167DTEX/47 PE YARNS AND MICRO PODS. 140

FIGURE 7. 49: TESTING OF RFID E-YARN USING AN RFID READER AND IPHONE APP 141

TABLE 7. 1: EFFECT OF DIPOLE LENGTH ON READ LENGTH 141

FIGURE 7. 50: RFID E-YARN AND RFID E-YARN-INTEGRATED GARMENTS 142

FIGURE 7. 51: TEST PROCEDURE FOR MEASURING READ DISTANCE 142

TABLE 7.2: TEST RESULTS OF READ DISTANCE AFTER WASHING AND TUMBLE DRYING 143

FIGURE 7. 52: A PROTOTYPE ILLUMINATED SUN VISOR FOR FUTURE CARS 144

FIGURE 7. 53: PROFESSOR TILAK DIAS HOLDING MAGNETIC YARN 144

FIGURE 7. 54: A PICTURE OF A VIBRATION-SENSING GLOVE 145

FIGURE 7. 55: AN ILLUMINATED YARN-INTEGRATED BLANKET 146

FIGURE 7. 56: ILLUMINATED YARN INTEGRATED INTO A COMPOSITE LAMINATE 146

FIGURE 8. 1: SCHEMATIC OF PICK AND PLACE MACHINE MODIFICATION 151

FIGURE 8. 2: A SCHEMATIC IMAGE OF MULTI-TERMINAL CONNECTIONS OF FUTURE E-YARN [151] 152

FIGURE 8. 3: SCHEMATIC OF YARN ARRANGEMENT RIUS KNITTING MACHINE 153

WITH NEW GUIDES 153

LIST OF TABLES

TABLE 3. 1: THE RESULTS OF DIAMETERS OF THE COPPER WIRES 30

TABLE 3. 2: THE LINEAR DENSITY OF COPPER WIRES 32

TABLE 3. 3: TENSILE TEST RESULTS FOR COPPER WIRES 33

TABLE 3. 4: TENSILE TEST RESULTS FOR POLYESTER YARN 34

TABLE 3. 5: TENSILE TEST RESULTS FOR COMBINATIONS OF POLYESTER YARN AND COPPER WIRE 35

TABLE 3. 6: THE RESISTANCE OF COPPER WIRES 37

TABLE 3. 8: DIMENSIONS OF SEMICONDUCTOR PACKAGED DIES 43

TABLE 3. 9: THE EQUIPMENT AND RAW MATERIALS USED FOR THE CURING TEST 44

TABLE 3.10: CURING TEST RESULT 9001-E-V 3.5 RESIN AT FIX UV EXPOSURE TIME (5 SECONDS) 45

TABLE 3.11: CURING TEST RESULT 9001-E-V 3.5 RESIN AT FIX DISTANCE OF 1 CM BETWEEN THE UV LIGHT GUIDE TIP AND THE GLASS 46

TABLE 3.12: CURING TEST RESULT 9001-E-V 3.7 RESIN AT FIX DISTANCE OF 1 CM BETWEEN THE UV LIGHT GUIDE TIP AND THE GLASS 46

TABLE 4.1: DC RESISTANCES OF HAND SOLDERED SOLDER JOINTS 70

TABLE 4.2: THE RESULTS OF RESISTANCE MEASUREMENTS OF SOLDER JOINTS MADE WITH THE PDR IR REWORK SYSTEM 71

TABLE 4.3: RESULTS OF THE TENSILE TESTS OF FOUR-STRAND COPPER WIRES SOLDERED TO SMD RESISTOR CHIPS 74

TABLE 4.4: TENSILE TEST RESULTS FOR SOLDERED BLUE LEDS WITH 7-STRAND COPPER WIRE 77

TABLE 4.5: TENSILE TEST RESULTS FOR SOLDERED RED LEDS WITH 7-STRAND COPPER WIRES 79

TABLE 5.1: THE EQUIPMENT AND RAW MATERIALS FOR THE ENCAPSULATION PROCESS 88

TABLE 5.2: THE EQUIPMENT AND RAW MATERIALS FOR THE ENCAPSULATION PROCESS 89

TABLE 5.3: TENSILE TEST RESULTS FOR SOLDERED & ENCAPSULATED BLUE LED'S WITH 7-STRAND COPPER FILAMENTS 93

TABLE 6.1: TENSILE TEST RESULTS FOR WARP KNITTED SLEEVES PRODUCED WITH SIX NEEDLES 106

TABLE 6.2: TENSILE TEST RESULTS FOR SOLDERED WITH BLUE LED'S AND 7-STRAND COPPER WIRE, ENCAPSULATED AND BRAIDED 108

TABLE 7. 1: EFFECT OF DIPOLE LENGTH ON READ LENGTH 141

TABLE 7.2: TEST RESULTS OF READ DISTANCE AFTER WASHING AND TUMBLE DRYING 143

RESEARCH ACTIVITIES

As a part of this research work, the following research and academic activities were carried out in order to gain an in-depth knowledge of manufacturing issues, project management skills, research practice methods, team working skills, and building-up of professional networks, scientific research skills such as producing research papers, book chapters, presentations and exhibiting effectively for general audiences. Examples of these, produced during the research, are listed below:

i. Patent

1. Dias, T., and Rathnayake, A,. Electronically Functional Yarn, patent number: PCT/GB2015/052553 4th September 2015

ii. Publications and conference proceedings

1. Book chapter: Dias. T., and Rathnayake, A., Electronic Textiles: Smart fabrics and wearable technology. Title:; Integration of micro-electronics with yarns for smart textiles, released May 2015. ISBN 9780081002018
2. Rathnayake, A., and Dias, T., 2015. Electronically functional yarns for wearables. In: Hoxley, M., and Crabbe, A., eds., CADBE Doctoral Student Conference [Nottingham Trent University, 9-10 June 2014] pp 113-122. www.ntu.ac.uk/adbe/document_uploads/CADBE-Summer-Conference-Proceedings-2014.pdf
3. Dias, T., Cork, C.R., Rathnayake, A., and Anastasopoulos, I., 2013. Electronically functional yarns for smart textiles. Nano, Issue/No: 27, pp. 11-12.
4. Rathnayake, A., and Dias. T., 2013. Electronically active smart textiles. Research and Researcher. Fifth Annual Conference, Nottingham Trent University. May 2013, AAS, pp. 80-85. https://nturesearchpracticeconference.files.wordpress.com/2013/05/research-and-the-researcher-ebook.pdf
5. Rathnayake, A., and Dias. T., 2013. Yarns with embedded electronics, ACM International Joint Conference on Pervasive and Ubiquitous Computing and Proceedings of the 2015 ACM International Symposium on Wearable Computers. pp. 385-388, ACM, New York, NY, USA. http://dx.doi.org/10.1145/2800835.2800919
6. Cork, C., Dias, T., Acti, T., Rathnayake, A,. Mbise, Ekael, Anastsopoulos, I., Piper, A. The next generation of electronic textiles, 2013. Proceedings of the 1st International Conference on Digital Technology for the Textile Industries, Manchester, UK, 5-6 Sep 2013.

7. Cork, C., Dias, T., Rathnayake, A,. Lugoda, P., Fibre Electronic Technology for Wearables. Advanced Textiles Research Group, School of Art and Design, Nottingham Trent University. Feb 2015 . www.academia.edu/10921783/Fibre_Electronic_Technology_for_Wearables
8. A. Ratnayaka and T. Dias (2013), E-Yarns for Interactive Illuminated Fashion Garments/ Textiles, Association of Fashion and Textile Conferance, Nottingham Trent University on 02nd of May 2013.
9. Ratnayaka, A. and Dias, T (2013), Electronically Active Smart Textiles, the third Art & Design and Built Environment research conference and festival, 28 Jun 2012.
10. Panel editor: Breaking Boundaries 2014: First Annual Professional Research Practice Conference, Nottingham Trent University, Nottingham, May 2014. http://breakingboundaries2014.blogspot.co.uk/

iii. Exhibitions

1. An illuminated garment was exhibited at the Future Textiles Exhibition, the Palace of Westminster (UK Parliament) from 10th to 14th December 2012. https://ntuadvancedtextiles.wordpress.com/2012/12/14/future-textiles-exhibition/
2. An illuminated car seat was exhibited at the Advanced Automotive Engineering Show 2013 in Birmingham. https://ntuadvancedtextiles.wordpress.com/2013/11/25/automotive-engineering-show/
3. E-yarns and E-textiles (illuminated garment, RFID interpreted garments, temperature sensing mat and sock) were exhibited at the International Symposium on Wearable Computers (ISWC) 2015, Osaka, Japan from 7th to 11th Sep 2015. https://ntuadvancedtextiles.wordpress.com/2015/10/12/anura-rathnayake-presents-electronic-textiles-at-iswc-2015-in-osaka-japan
4. Volunteer Student for conference and exhibition organising committee: International Symposium on Wearable Computers (ISWC) 2014, Seattle, USA from 13th to 17th Sep 2014. https://ntuadvancedtextiles.wordpress.com/2014/09/28/iswc-2014/

CHAPTER ONE

1.0 Introduction

1.1 Background Information

Currently, textiles can be designed to carry out a set of predetermined functions within certain boundary conditions, and would fail outside the defined conditions. However, the next generation of textiles will have the capability to adapt its functionality according to changes in the surroundings, i.e. the environment. Such textiles are known as Smart and Interactive Textiles (SMIT), and will be capable of sensing and be active. The electronics industry has made quantum leaps within the last eighty years in the design and construction of semi-conductor sensors, actuators and powerful micro-controllers with a very high degree of precision and performance. The electronic industry has also focused its efforts on miniaturising these semi-conductor devices. These micro-devices would provide an excellent platform for integration into yarns, in order to create a new generation of SMIT. Such SMIT structures will pave that way for the creation of truly-wearable, electronic systems in the near future.

The market for SMIT structures is expected to grow strongly. For example, in 2014 the US-based Market Research Company Markets & Markets, predicted that the global market volume of wearable electronics and technology market is expected to reach $ 11.61 Billion by the end of 2020, growing at a compound annual growth rate (CAGR) of 24.56% from 2014 to 2020 [1]. According to statista.com, the related global smart, intelligent, digital & interactive fabrics market revenue was $708 million in 2012 and is expected to reach to $2.03 billion by 2018, growing at an estimated CAGR of 17.7 % [2].

1.1.1 Application of Electronic Textiles

Some examples of applications of electronically-active yarns could be garments which are capable of continuous monitoring one's vital signs such as ECG, respiratory patterns, blood pressure and skin temperature. Other uses are flexible active display boards/screens, fashion garments (light-emitting garments), colour-changeable wall papers/curtains etc.

1.1.2 Issues for Current Applications of Electronic Textiles

Electronic textiles are currently used in areas that include medicine, automotive, aerospace, sports, military and fashion. However, despite these advances there are many disadvantages in such products available today, such as poor washabilty, excessive

weight and bulk, and poor flexibility, breathability and comfort. For example, various commercially available SMIT products are used in the medical sector to monitor the vital signs of the human body. Most of them include numerous wires which may lead to discomfort and inconvenience to patients. Usually, clothing is considered a second skin as it makes intimate contact with the body all the time and facilitates a comfortable and safe environment. Therefore, it is advantageous to integrate electronic component with the clothing rather than connecting components directly to the human body. Current applications of SMIT devices are, in general, quite limited and act solely as demonstrations of the potential of integration that can be possible in the future. Integrating functionality into flexible fibre form is thus the next progression in wearable electronics. The approach for realising this fibre technology, however, requires a paradigm shift in conventional thinking for it to occur. Thus the aim of the work described here is to address this gap in the knowledge base.

1.1.3 State of the Art of Electronic Textiles

In order to overcome the above disadvantages, a novel concept of electronically-active yarn has been developed in this research work. A smart yarn was produced by soldering semiconductor package dies with fine copper wires and creating a polymer micro-pod by encapsulation, and then forming the final yarn. The encasing of the package die has to be achieved in such a manner as to protect it from all forms of mechanical and thermal stresses. Such a smart yarn could then be used to manufacture electronically-active fabrics and garments. The concept was to create smart yarns that contained different microchips. Such smart yarns will be the building blocks of the next generation of wearable electronics. Moreover, this will facilitate solutions to overcome current problems and difficulties which the manufacturers of wearable textiles are experiencing and open the doors for designers to develop the next generation of truly-wearable computers which are comfortable, flexible and washable.

1.2 The Aims and Objectives of the Study

There are three main goals in this PhD research work:

1. To create the scientific knowhow for embedding semiconductor micro devices within the fibres of yarns, so as to create novel electronically-active yarn (EAY and also called e-yarn);
2. To investigate the mechanical and electrical properties of EAY's based on engineering and scientific knowledge;
3. To study methods of incorporating of EAYs into textile designs.

1.3 Research Methodology

The approach to the research can be largely described as quantitative. Once the experiments had been carried out on the samples, the data were collected and analysed. The knowledge gained was used to optimise the technology for creating EFY's. The research path utilised for the development of the technology is shown in Figure 1.1.

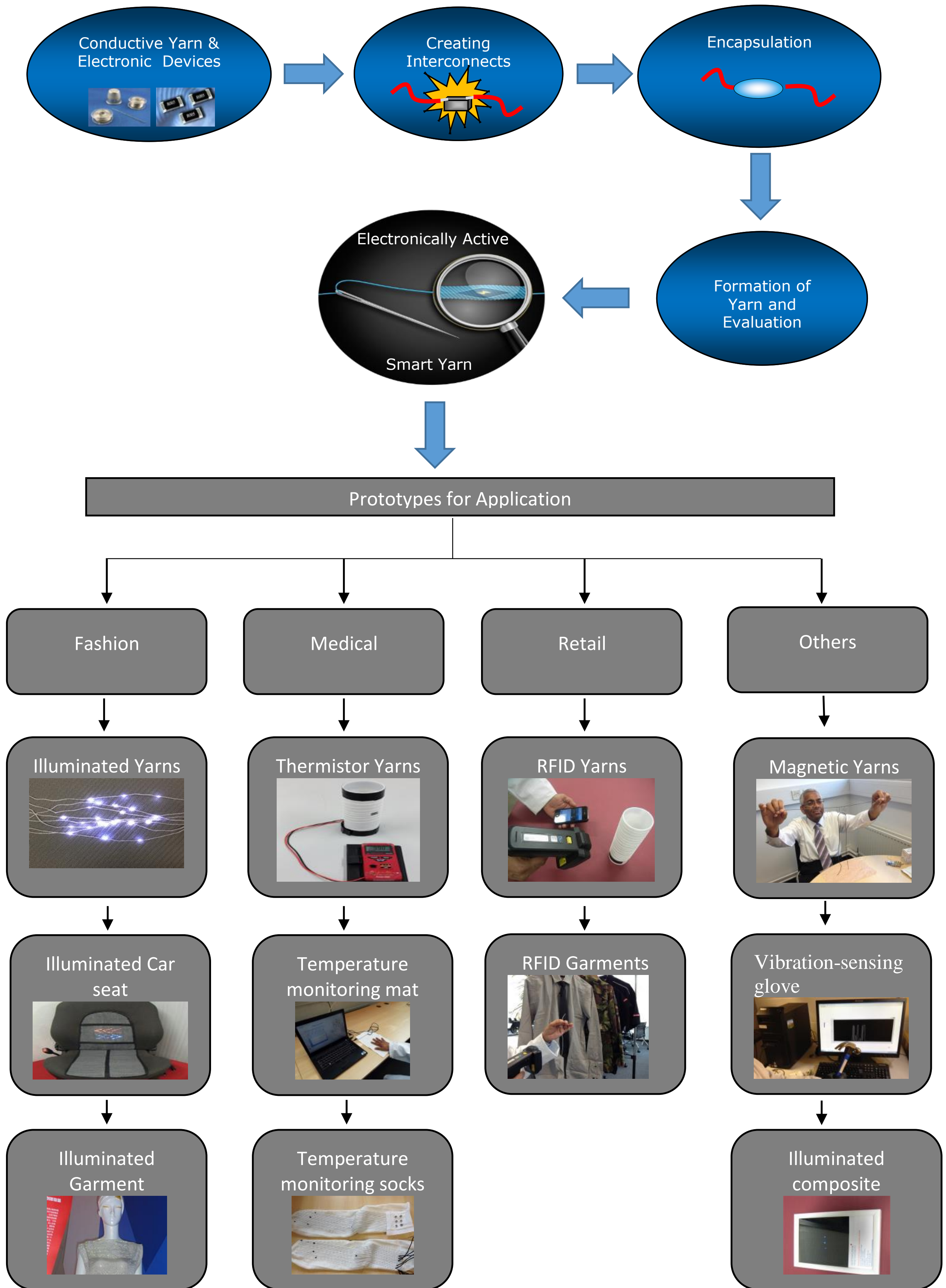

Figure 1. 1: Schematic of the technology development

1.3.1 Conductive Yarn and Electronic Devices

The interconnections of the micro devices have to be formed through use of very fine conductive micro-threads, usually in the order of 50 – 100 μm in diameter, with very low electrical DC resistance, and therefore multi-strand copper wire was identified to use in the research. The fine copper wire was also demonstrated good mechanical properties, excellent solderability and be covered by a thin non-conductive polymer film to prevent short-circuiting of the terminals of the microchips.

In the 19th century, the development of the vacuum tube was a great turning point in the electronics industry. The advances in semiconductor manufacture in the last few decades, resulted in the development of integrated circuits which are powerful, cost effective, reliable and small. Currently these semiconductor devices are available in a wide range of formats. The packaging format used in surface mount devices (SMD) is the most suitable for creating EAY's due to the absence of pins and leads. The miniature size of SMD that were used enabled the creation of fine EAYs. For the present research, surface mount devices of the formats SMD 0201 (0.60x0.30x0.23 mm) and SMD 0402 (1.0x0.5x0.5) were used in EAYs; the details are given in Annex 1.

1.3.2 Soldering

It is necessary to transfer thermal energy from a heat source to the soldering point to melt and reflow solder between terminals of the microchip (known as solder pads) and conductive thread(s) in order to create good bonds. There are three heat transfer mechanisms namely conduction, convection, and radiation. A focus IR reflow workstation from PDR was employed to carry out the soldering process. It uses a with a radiation heat transfer mechanism, and employs infrared (IR) electromagnetic rays to transfer heat energy required for the re-flow soldering process. The PDR system was a useful tool for creating good-quality soldered bonds between microchips (width: 500μm) and fine copper wires (diameter: 55μm) without damaging the microchip circuitry, thanks to contactless heat transfer mechanism. The experiments carried out with the PDR system are described in Chapter 4.

1.3.3 Encapsulation and Yarn Formation

After joining the solder pads of microchips to copper wires, it was necessary to protect the solder joints and strengthen the copper wires. Therefore, a composite yarn was crafted by mounting the copper wires and the soldered microchips onto two polyester yarns and the microchips and solder joints were encapsulated with a polymeric micro-pod made

from a UV-curable acrylated urethane-based conformable resin. This was used as the core yarn, which was encapsulated within a sheath of fibres to produce the final electronically active yarn (EAY, also called e-yarn). An ultra-small diameter warp knitting machine, (RIUS Model: MC), was employed to produce the fibre sheath.

1.4 Structure of Theses

This chapter gives the introduction. Chapter 2 covers the literature review of textiles and electronic textiles (e-textiles) in different applications with a timeline and the raw materials that were used in this project such as copper wires (strands), electronic devices, solders, and bonding techniques. The third chapter covers the mechanical and electrical properties of the raw materials that were used in this research. The fourth chapter covers the main part of this research work, which was the creation of interconnections using soldering techniques and reflow soldering, plus the optimisation of the mechanical and electrical properties of solder joints. The fifth chapter covers the encapsulation process including ultraviolet theory and the optimisation of the properties of the micro-pod. The sixth chapter describes the electronic yarn formation, including fibre and yarn classification, twisting and braiding techniques and optimisation of yarn appearance. Chapter seven covers the prototypes produced, including illuminated yarns, an illuminated garment, an illuminated car seat cover, a thermistor yarn, a thermistor mat, an RFID yarn, an RFID garment and a composite laminate. Chapter eight covers future work and conclusions. The structure of thesis is illustrated in the Figure 1.2.

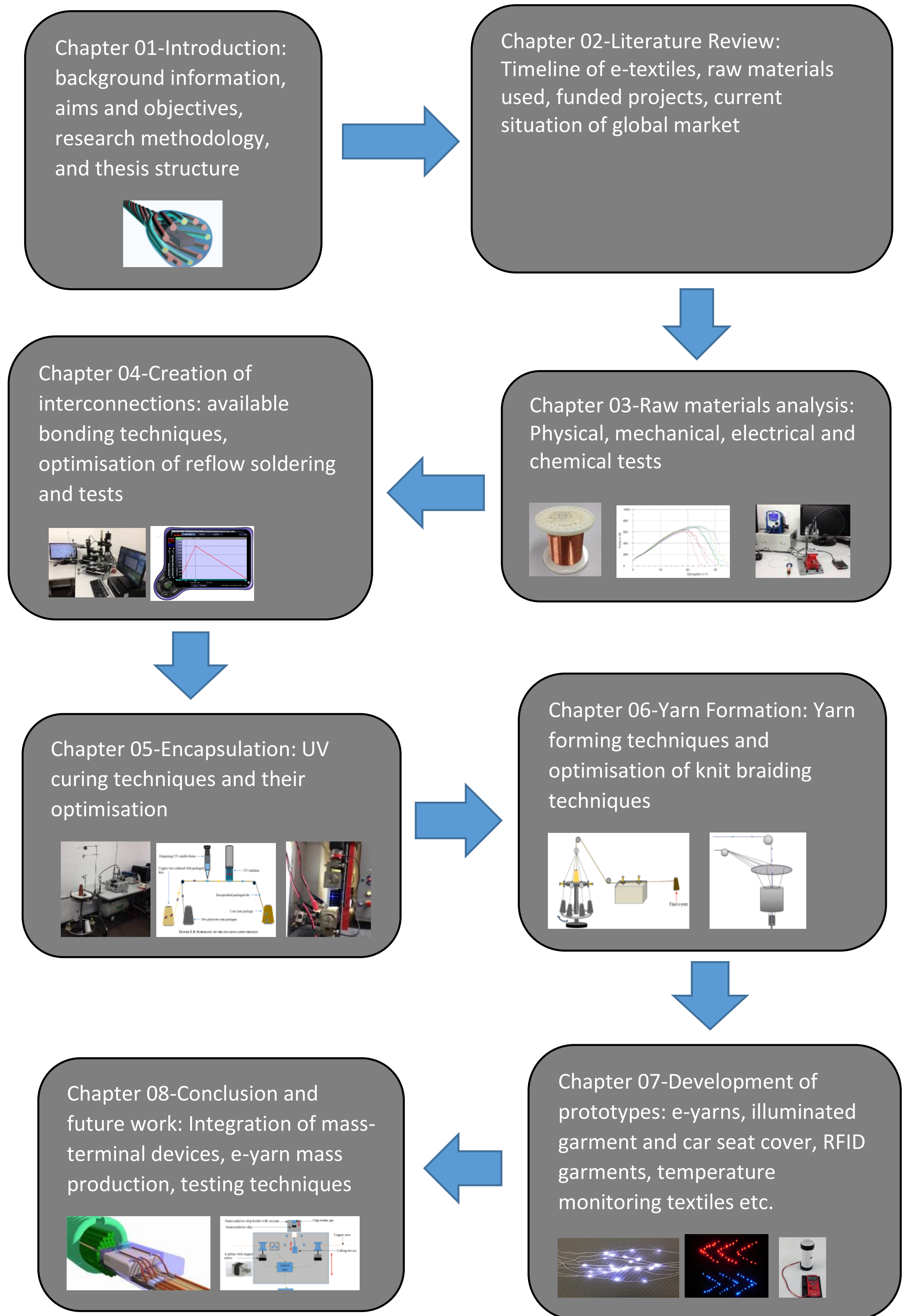

FIGURE 1. 2: SCHEMATIC OF THE STRUCTURE OF THESIS

CHAPTER TWO

2.0 Literature Review

As a part of the research work, it was important to study the results of other researchers and organisations who have been working in the electronic-textiles field, to understand the existing knowledge base, knowledge gap, advantages and disadvantages of commercially available wearable electronics products etc. Even though the main focus of this research work was on electronic textiles, it was necessary to discuss general textiles and electronics components before discussing electronic textiles. Therefore, the basic knowledge of textile technology and electronic components are described below. Then the history of electronic textiles and its timeline with some examples of developments in electronic textiles are summarised.

2.1 Textiles

The human body is in contact with textiles at least 70% of the time [3]. As such it is necessary to consider basic textile characteristics when electronic textiles are developed. Currently, most electronic textiles are manufactured by integrating electronic components into fabrics [4]. Therefore, the basic properties of textiles are often compromised.
Most of researchers who are in the e-textiles field, have not taken into account all of the basic textile characteristics. Therefore, most e-textiles are not comfortable in wear or washable in comparison to normal textiles [4]. Thus, if one wants to produce user-friendly, wearable electronics, it is wise to study the original core properties of textiles. A simple definition of a textile is a fabric that is made from fibres, which are converted into yarn as a first step and then made into fabrics by binding yarns using different techniques such as interlacing (weaving) and interlooping (knitting) (see Figure 2.3). There is also a category of textiles called non-woven that are made directly from fibre webs.

2.1.1 Textile Fibre Classification

According to the definition of textile fibres, ‘The length of a fibre has to be about one thousand times greater than its thicknesses’. The fibre is the basic unit of yarn. Textile fibres have properties such as fineness, pliability, a suitable length and strength. Natural fibres have a limited length while synthetic and man-made fibres are extruded in longer lengths and called filaments. Fibre classification is shown by Figure 2.1. Textile fibres can be divided into natural fibres and man-made fibres. Different types of fibres can be

used for production of e-yarns, depend on the application. Manufacturing techniques for producing e-yarns are described in Chapter 6.

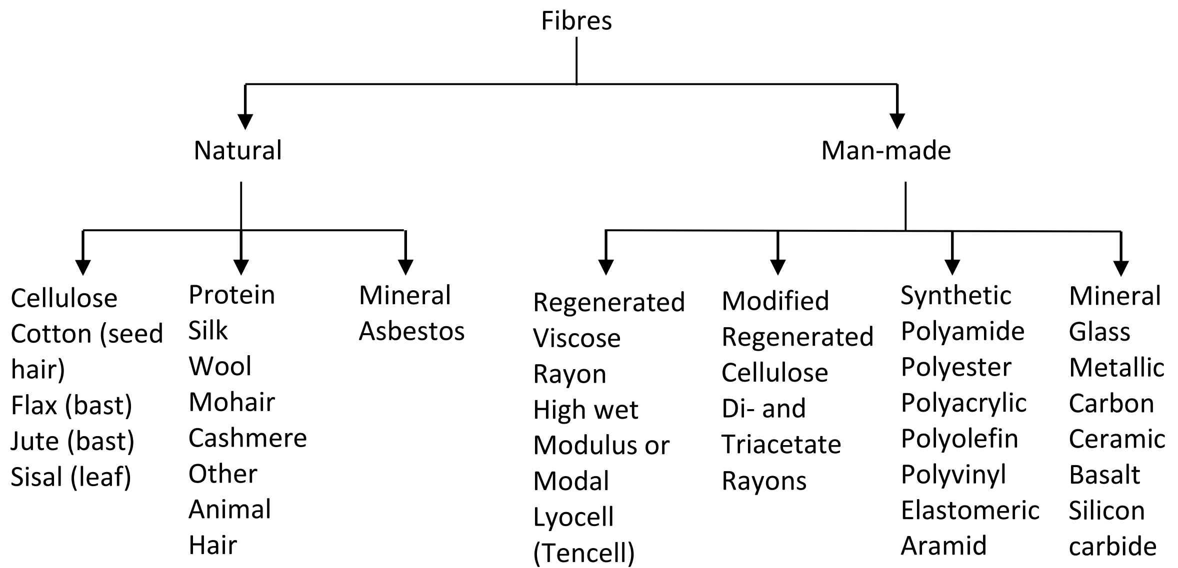

FIGURE 2. 1: FIBRE CLASSIFICATION [5]

2.1.2 Textile Yarn Classification

Yarns can be produced using different techniques (see Figure 2.3). The general classification of yarns is shown in Figure 2.2.

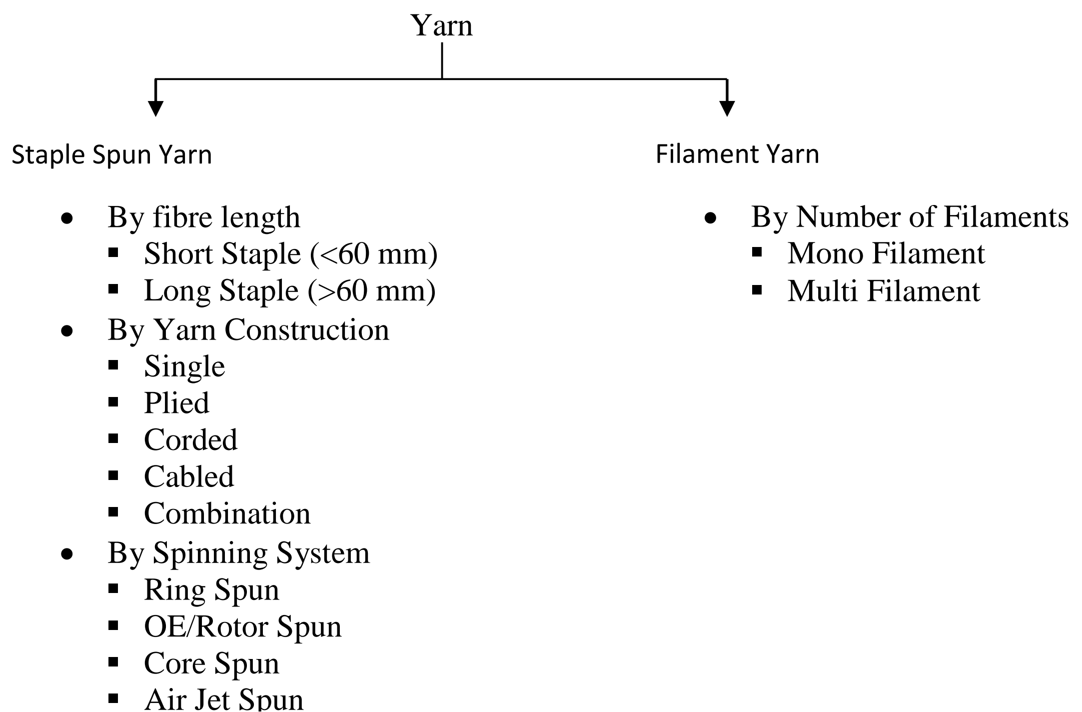

FIGURE 2. 2: CLASSIFICATION OF YARNS [6]

2.1.3 The Methodologies Available to Convert Fibres into Fabrics

The basic manufacturing process from fibre to fabric can be described briefly as below Figure 2.3.

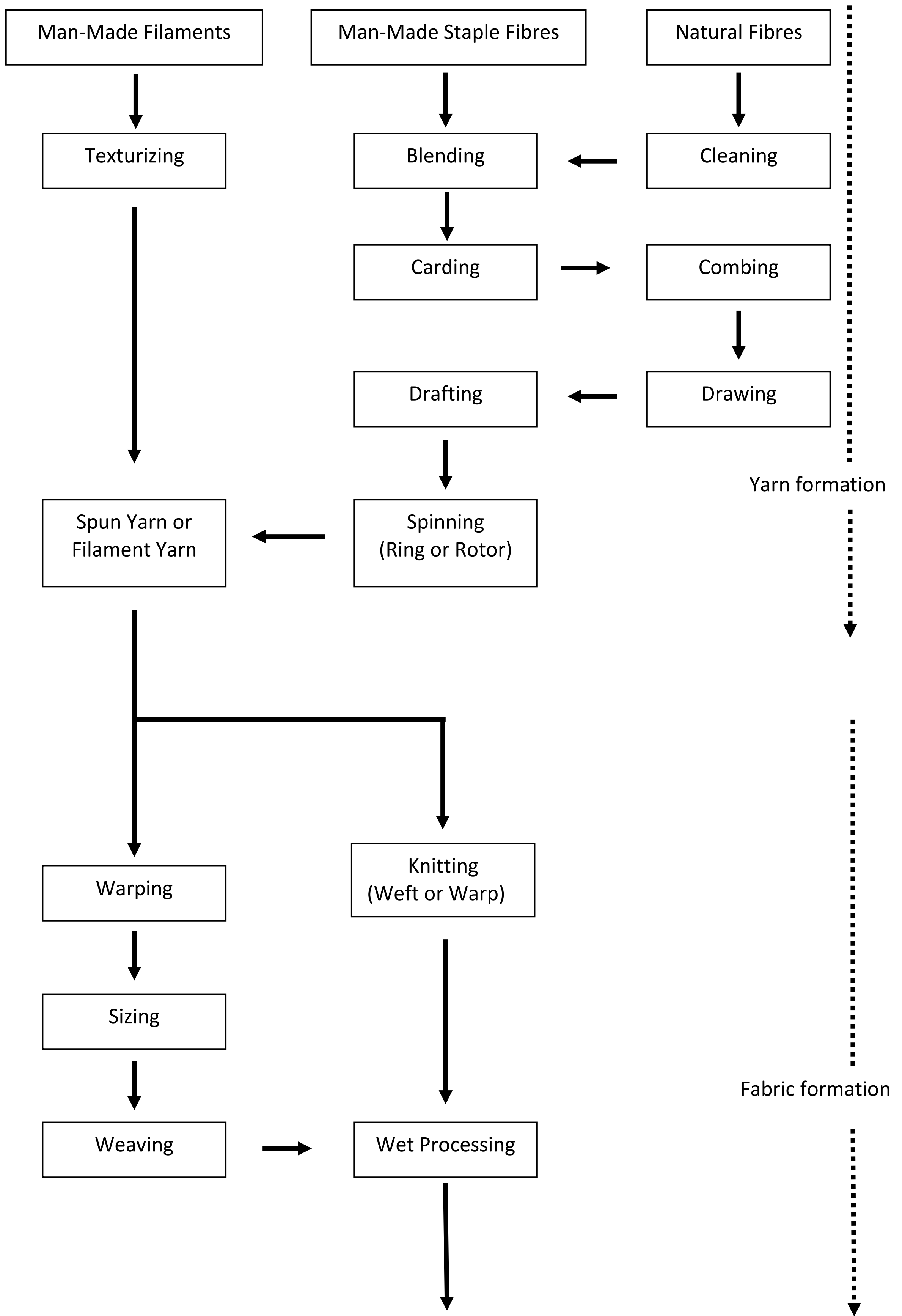

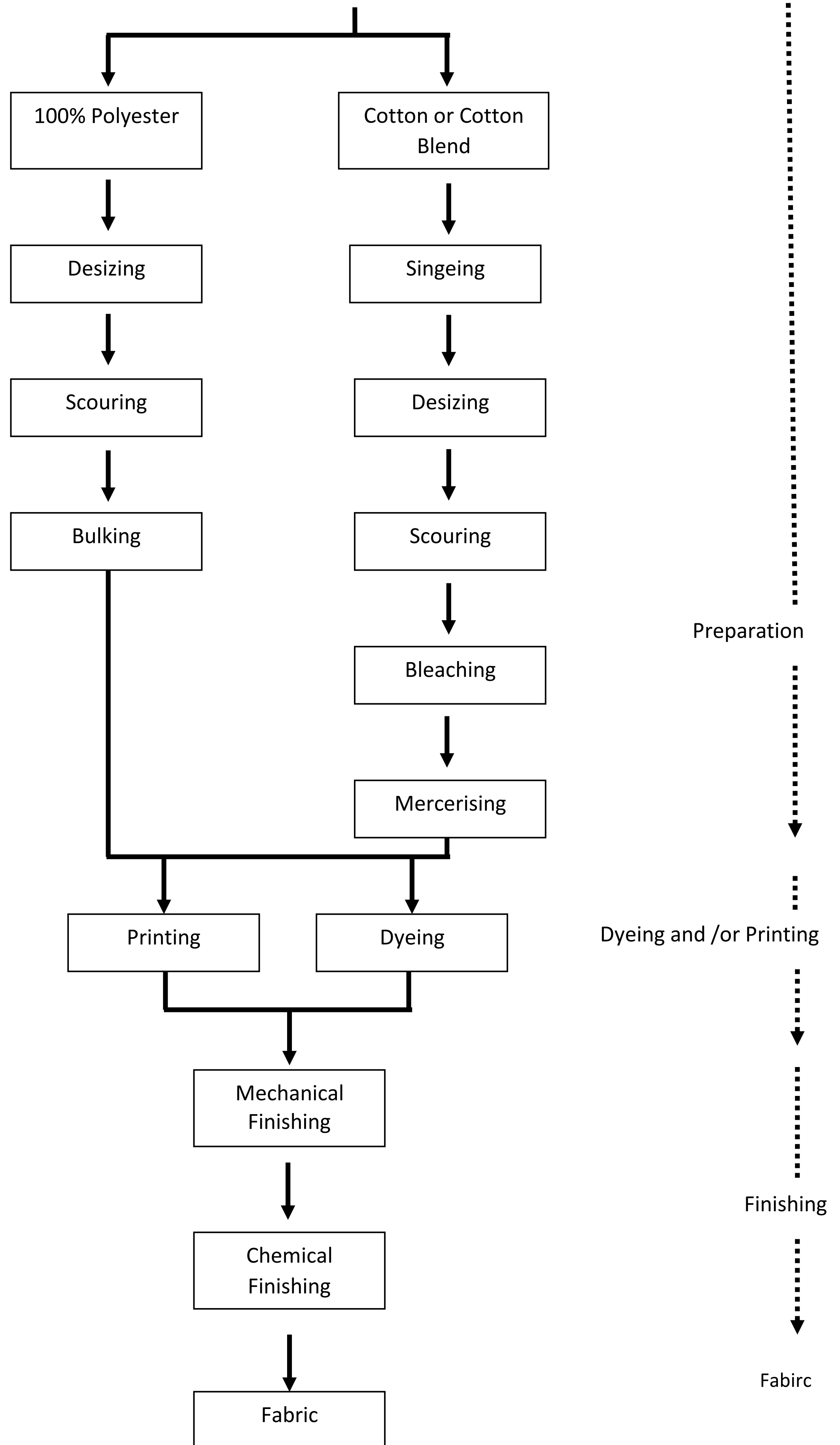

FIGURE 2. 3: MANUFACTURING STEPS FROM FIBRE TO FABRIC [5]

As described in Figure 2.3, fabrics are mostly made as woven and knitted fabrics, which can be used for producing garments. In the case of under-garments, they are considered to be a second skin on the human body and they are required to have special properties such as flexibility, softness, breathability, wicking properties and wetting ability. Therefore, textiles are more comfortable to wear as long as they retain these basic characteristics. Moreover, textiles are durable and washable due to their good mechanical properties; which can give protection from environmental changes to a certain degree, such as temperature, chemicals, wind, dust, viruses, bacteria and hazards. Another important property of textiles is that they can conform to almost any complex shape due to their shearing property [7]. For example, paper cannot undergo shear. Therefore, paper cannot be deformed without undergoing pleating or wrinkling. However, a fabric can shear as yarns/fibres can freely move whilst retaining their strong structure, which is as shown by Figure 2.4.

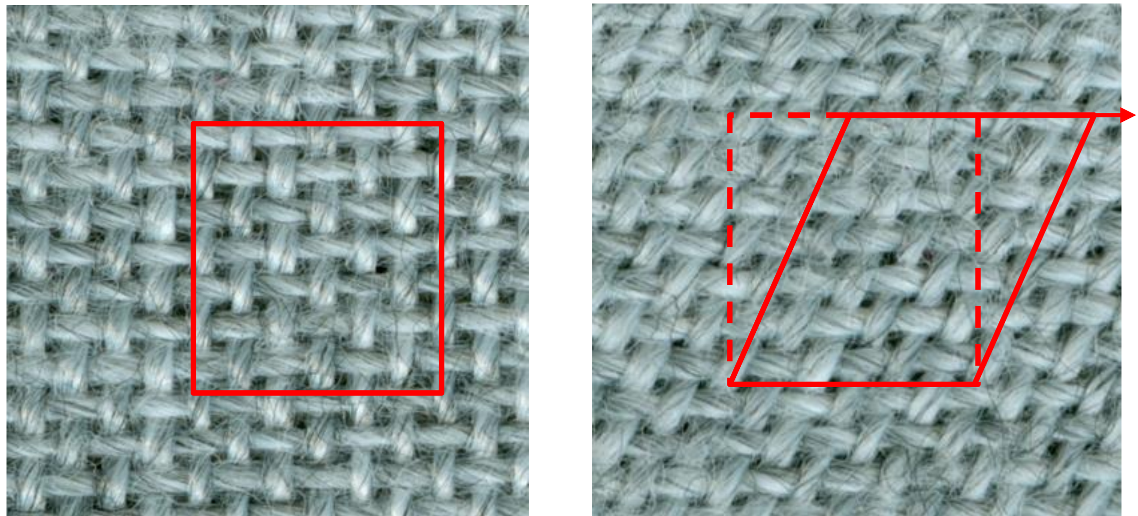

a. Before shearing of woven fabric b. After shearing of woven fabric

FIGURE 2. 4: ILLUSTRATION OF WOVEN FABRIC SHEARING PROPERTY

2.2 Electronic Components

Generally, electronic components can be classified broadly, as shown in Figure 2.5. It was necessary to become familiar with commercially-available electronic components in order to identify potential electronic devices which can be integrated into yarns whist retaining the required textile characteristics.

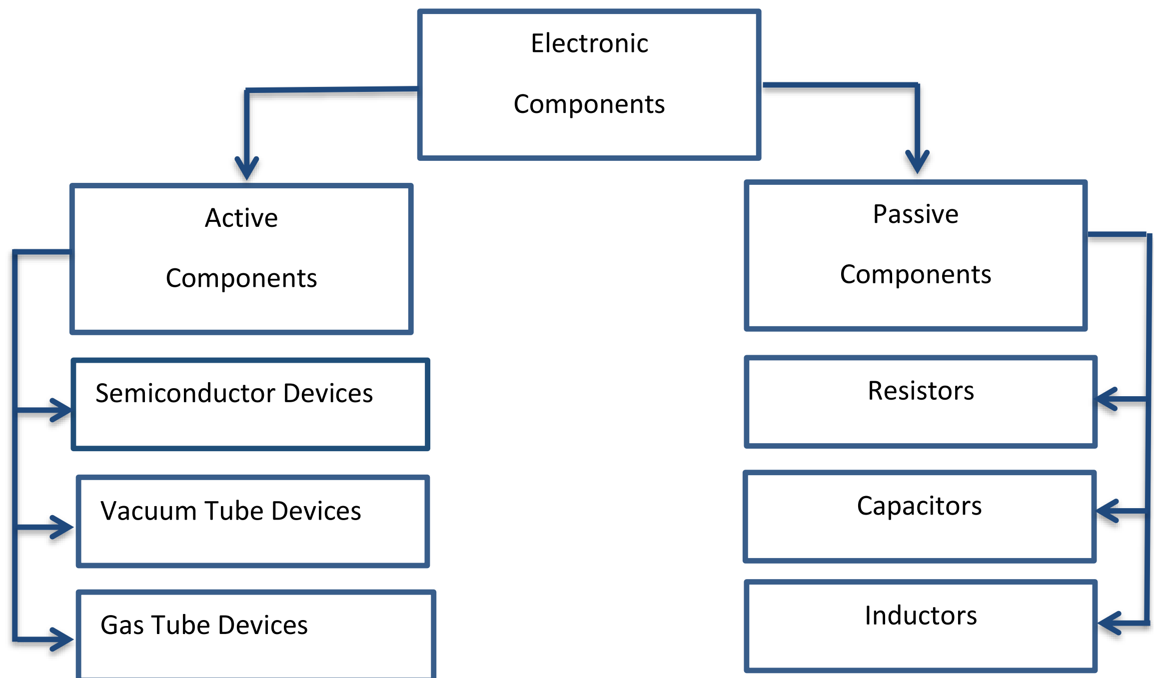

FIGURE 2. 5: CLASSIFICATION OF ELECTRONIC COMPONENTS [8]

In the 19th century, the development of the vacuum tube was a great turning point in the electronics industry. A typical vacuum tube circuit is shown as Figure 2.6. These were quite heavy, generated a lot of heat, had a short life-time, required warm-up and DC voltages of 300V or higher [9]. The advances in semiconductor manufacture in the last century resulted in the development of integrated circuits that are more efficient, cost effective, reliable and small. Currently these semiconductor devices are available in different formats as shown in Figure 2.7.

FIGURE 2.6: A TYPICAL VACUUM TUBE CIRCUIT [9]

FIGURE 2.7: SOME EXAMPLE OF ELECTRONIC DEVICES [155]

2.2.1 Semiconductor

A semiconductor is a solid, crystalline material which has electrical conductivity greater than that of insulators but less than of conductors. Usually they are used as a base material for the manufacture of semiconductor electronic circuits. The most common semiconductors are silicon and germanium. The conductivity of the semiconductors can be controlled by adding different types and amounts of impurities (which process is called doping). Moreover, the conductivity of a doped semiconductor can be controlled by the introduction of an electric field, by exposure to light, and even by pressure and heat; thus excellent sensors can be designed with doped semiconductors. Semiconductors doped with donor impurities (ex: phosphorus) are known as an n-type semiconductor, while those are doped with acceptor impurities (ex: boron) are known as p-type. By joining together these n and p types (called junctions), other components such as diodes (p-n junction) and transistors (n-p-n or p-n-p junctions) can be made [10]. Figures 2.8 and 2.9, show a boron atom acting as an acceptor and a phosphorus atom acting as a donor.

FIGURE 2. 6: BORON ATOM ACTING AS AN ACCEPTOR IN THE SIMPLIFIED 2D SILICON LATTICE [156]

FIGURE 2. 7: PHOSPHORUS ATOM ACTING AS A DONOR IN THE SIMPLIFIED 2D SILICON LATTICE [156]

2.3 Electronic Textiles

An intensive review of the literature on electronic textiles (e-textiles) was carried out in order to identify the gaps in the existing knowledge base of e-textiles. Although Smart Textiles are still in their infancy, it is evident from publications that this area is growing rapidly, as shown in Figure 2.10. The forecast for e-textiles is included at the end of this chapter.

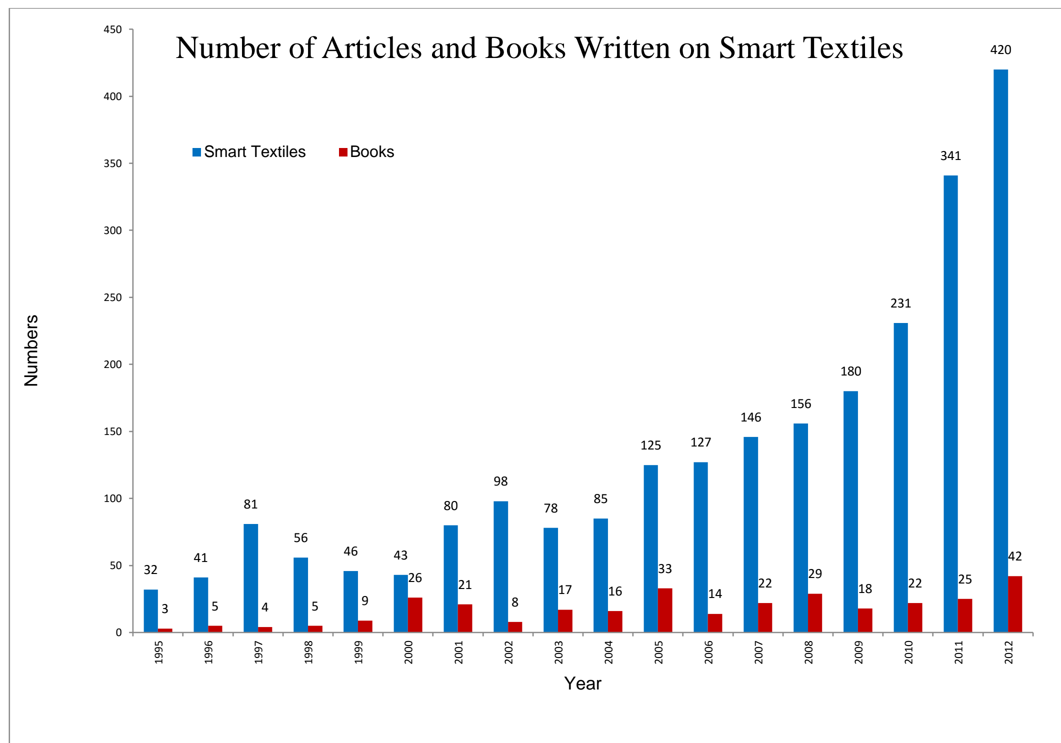

FIGURE 2. 8: NUMBER OF ARTICLES AND BOOKS PUBLISHED ON SMART TEXTILES LAST
18 years [Source science direct data base]

Most smart textiles are produced by using e-textiles. According to the level of intelligence, smart textiles can be divided into three groups, namely passive smart textiles (only able to sense the environment); active smart textiles (reactive sensing to stimuli from the environment); very smart textiles (able to sense, react and adapt according to environmental changes) [11].

E-textiles have gained an ever-increasing profile and have found applications in areas as diverse as medicine, sport, leisure, defence, automobile, fashion and entertainment, manufacturing and retail industry. However, most e-textiles available today are made by attaching either permanent or removable electronic functionality. In the first generation of these systems, electronic devices were simply attached to garments or included in pockets [12, 13] for examples; LifeShirt of Vivometrics and Fibertronics. In the second generation, electrical connectivity and functionality were introduced by the inclusion of conducting yarns within the fabric structure [14, 15] for example: Textronics, EFS control glove and SmartShirt. Van Langenhove [16] concludes that there are three categories of electronic textiles: embedded electronics, textronics and fibretronics. Embedded electronics include electronic devices such as MP3 players, mobile phones and head phones. These are inserted into garments by creating pockets for them. This is known as

the first generation of electronic textiles. The development of electronic textile is discussed in the following sections, starting with early examples.

2.3.1 Early Examples

In 1911, a heated glove was developed for drivers of motor boats, aeroplanes and automobiles which used manual steering-mechanisms. These ensured that drivers and pilots could grip the steering controls comfortably in freezing weather conditions [17]. In 1936, a patent application was filed for embedding electrical conductors into textiles such as blankets, pads, quilts, fabrics, clothing etc., [18]. In 1945, a heated glove was developed and patented by Summers, A. V., [19].

2.3.2 Attachment of Electronic Components into Pockets

First-generation electronic textiles involved attachment of electronic components into pockets of the garments. Some examples include the ICD+ suit, developed by Philips and Levi's and the Lifeshirt from Vivometrics. This ICD+ (Industrial Clothing Division) jacket (Figure 2.11) was developed in 2000. It was the first wearable electronic but it is no longer available on the market. Mobile phones and MP3 player were inserted into the pocket of the ICD+ jacket and wires were sewn into seams of the jacket [20].

FIGURE 2. 9: ICD+ JACKET [21]

The smart textiles that were produced between 2000 and 2010 were not commercially successful [22]. In 2010, a group of researchers worked on an EU-funded project called ProeTex to develop a garment (Figure 2.12) for fire fighters. Electronic components were integrated to detect CO_2 levels, environment and body temperatures and location [23].

FIGURE 2. 10: PROTOTYPE OF PROETEX GARMENT [23]

Bluetooth-enabled jackets with joystick controls were developed by Zegna Company. An example of jacket is shown in Figure 2.13. It incorporates integrated Bluetooth so it is possible to answer a mobile phone and to play music without removing the devices from the jacket [24].

FIGURE 2. 11: ZEGNA SPORT JACKET [24]

2.3.3 Attachment of Electronic Components into Garments/Textiles

In 1996, quantum tunnelling composite (QTC) materials were developed by Peratech Ltd., based on original ideas by David and Chris Lussey. QTC material is electrically conductive when pressed, whilst behave as an insulator when not under pressure. This material could be used in the automobile industry, for example in the switches shown below in Figure 2.14 [25]

FIGURE 2. 12: QTC™ MATERIAL USED FOR EMBEDDED FABRIC CONTROLS WITHIN A CAR DOOR PANEL TO OPERATE MIRRORS AND WINDOWS [25].

Textronics have been integrating electronics into textiles fabrics since 2004 [15]. This is one example of a second-generation electronic textile. Electronic textiles have gained great attention for use in military applications for more than fifteen years. As explained below in this page and the next, the US and UK governments have funded significant amounts of research in smart textiles. Smart textiles can sense, react and adapt according to environmental changes, providing extra support to soldiers in the battlefield. Some of the research work in this area is included below.

A report was published by a team of the US Army Soldier and Biological Chemical Command Soldier Systems Centre in 1998. The purpose of that report was to review interactive textile technologies that provide extra support for soldiers of the US Army, to increase their abilities and assess risks. The report described investigation of technologies and new materials such as new textile-manufacturing technologies, advanced fibre optics, conductive shape-memory materials, dendritic polymers, sensors and processors, gels and other coatings, composite materials, nano structures, biomimetics, micro-robotics and piezoelectric materials [26]. Van L., has mentioned that vital signs of soldiers can be monitored, such as socks which are integrated with pressure sensors to monitor blood pressure [16]. In 2001, the US Defence Advanced Research Projects Agency proposed a project to create a new class of wearable system made of fabric [27]. Georgia Tech wearable motherboard (GTWM) was developed by Jayaraman at Geogia Tech, Atalanta, USA. This smart shirt was developed for US Army soldiers to detect bullet wounds and monitor vital signs during combat conditions. The smart shirt consists of plastic optical fibres and other sensors [28, 29, 30]. “However, the smart shirt at this stage of

development only detects and alerts medical professionals of irregularities in patients' vital statistics or emergency situations, it does not respond to dangerous health conditions" [29]. The prototype GTWM is shown in Figure 2.15.

FIGURE 2. 13: GEORGIA TECH WEARABLE MOTHERBOARD [29]

In 2002, Engineers from the University of Southern California and Virginia Tech developed a large electronic fabric under the STRETCH programme. That prototype fabric was produced with interwoven micro-electronic components to use as a sensitive battlefield sensor to detect sounds such as gunfire and moving vehicles. This cloth was an example of a second generation e-textile [31]. Dr. Eugene Wilusz, who was working as a senior nuclear, biological, chemical scientist in the Warfighter Directorate, U.S. Army Natick Soldier Research, Development and Engineering Centre (NSRDEC) reported that the key factor for future advancements was the development of electronic circuits that are made entirely from fabric [32]. In 2002, Intelligent Textiles Ltd, which was founded by Asha Peta Thompson and Stan Swallow, developed conductive woven fabric to replace conventional wires that supply power to soldiers' systems and other devices [33].

Coosemans et al [34] investigated wireless ECG monitoring in textiles. The electronic circuits were emebeded onto the surface of fabrics, as shown in Figure 2.16. This garment does not appear to be comfortable or washable.

FIGURE 2. 14: LEFT: DEMO SET-UP WITH BELT PROTOTYPE, WORN BY A 12 WEEK OLD BABY. RIGHT: BABY SUIT PROTOTYPE, WORN BY A 21 WEEK OLD BABY [34].

The Institute for Reliability and Microintegration in Germany, and Samsung Electronics Co. Ltd, reported their attempts at combining electronic circuit boards with textiles, in order to develop clothes with wearable electronics (Figure 2.17). An electronic circuit was formed on a thin electronic substrate and was placed on the fabric using embroidery techniques. The disadvantages of this concept are the poor appearance, the washing difficulties and limited flexibility [35].

FIGURE 2. 15: FLEXIBLE SUBSTRATE WITH METALIZED CONTACT PADS INTERCONNECTED WITH EMBROIDERY [35].

In 2006, the NuMetrex heart sensing sport bra was released onto the market by Textronics Inc. [15]. Conductive yarns were used to knit localised electrodes into knitted fabrics as shown in Figure 2.18 [36]. This sensing fabric was able to pick up heart rates and transfer the signals to a watch, a smart phone or a cardio machine wirelessly using a small transmitter, which was inserted in a pocket in the bra. Later, seamless garments such as the Cardio shirt and miCoach (as shown Figure 2.18) for men were introduced, as well as a heart-sensing garment called "Racer Tank" for women, to monitor heart rate. In 2008 Adidas AG acquired Textronics to strengthen the technology [36]. These garments are fashionable and comfortable when compared with first generation e-textiles. However, there are still practical issues such as the feel of electronic components and washing problems with electronic components inserted into pockets of the garments.

FIGURE 2. 16: NUMETREX HEART SENSING SPORT BRA (LEFT) ADIDAS MICOACH MEN'S TRAINING SHIRT (RIGHT) [36]

E-textiles are also used in the fashion industry. Fashion can be described as a popular style or practice in clothing [37]. It can change from time to time and to suit people of different age groups, country, religion, professional status etc. Fashion can be influenced by famous personalities such as singers, actors etc. [38]. As an example, teenagers used to like dresses like Elvis Presley [39]. Phoebe Alexander [40] has reported how celebrities can influence the general public into wearing new styles of clothing. For example, Kanye West who is a world famous rapper, writer and producer has his own style of clothing that draws great attention from sections of the public. CuteCircuit is a fashion design company that is based in London. They produce interactive fashion garments and wearable electronics. Some examples of these garments are as shown in Figures 2.19 & 2.20 [41]. They use LED strips to produce illuminated garments. Over twenty thousand LEDs are used to produce a garment called a galaxy dress [42]. This company also produce other types of wearable electronics such as hug T-shirt that creates a sensation of touch. A person who is at a distance can send a signal from his/her mobile to another wearing a hug T-shirt to activate the hug effect [42]. In addition, M-dress enables answering of a mobile phone by lifting of the wrist without touching the phone [43].

Currently, CuteCircuit produce fashion garments using the latest technology, for example in their twitter Dress. Tweeted messages and animation are displayed in real time on the LED's in the garment. However, all these garments still remain part of the second generation of electronic textiles as they involve attachment of electronic components to the fabric surface. Therefore, the fabric's original performance has been compromised and it may not be possible to wear the garments for long periods comfortably.

FIGURE 2. 17: CUTECIUTE GALAXY DRESS [44]

FIGURE 2. 18: CUTECIUTE M-DRESS [43]

In 2013, two companies, Visijax and Eleksen, merged to strengthen their range of products. Visijax manufactured second generation Visijax highlight jackets [45] which could be used by cyclists who wanted to be visible for safety reason. High intensity LEDs were attached into this jacket's front and back (Figure 2.21).

FIGURE 2.19: VISIJAX HIGH VISIBILITY JACKETS [45]

2.3.4 Integration of Electrically Conducting Fibres

Engineered Fibre Structures Ltd. (EFS) reported the development of a control glove which could be used to control computers, games consoles, machines, electronic devices and equipment [46]. The EFS control glove consisted of electro-conducive areas (ECA) incorporated into the fingertips of a knitted glove (Figure 2.22). The wearer could activate certain functions by touching these ECAs together.

FIGURE 2.20: EFS CONTROL GLOVE [46]

Fibertronic Ltd. has commercialised wearable devices such as textile switches, flexible keypads, iPod & iPhone controllers, mobile phone interfaces, garment heating systems, fabric sensors and wearable lighting systems (Figure 2.23). The textile switch technology was originally developed by the New Zealand Company Canesis Ltd who trademarked it as 'Softswitch'. However, in all these products electronic components were attached to fabrics resulting in degradation of the textile characteristics [47].

FIGURE 2.21: EXAMPLES OF WEARABLE ELECTRONIC DEVICES FROM FIBROTRONICS [12].

A garment that was integrated sensors for knee joint monitoring has been developed by Gioberto in 2014 [48]. Three types of stitched stretch sensors were used in this garment such as a bottom thread cover stitched sensor, top thread cover stitched sensor and overlock stitched sensor. A textile based strain sensor, using elastic conductive webbing, was designed to monitor the flexion angle of elbow and knee movements. The webbing was produced by using conductive yarns and elastic yarns as shown in Figure 2.25. The strain sensor was placed on the arm and leg as shown in Figure 2.24 [48].

FIGURE 2.22: THE STRAIN SENSOR DEVICES FOR MONITORING THE FLEXION ANGLE DURING (A) ELBOW AND (B) KNEE MOVEMENTS [48]

FIGURE 2.23: THE ELASTIC CONDUCTIVE WEBBING WITH A PLAIN STRUCTURE [48]

2.3.5 Semi-Conductors Embedded Within Yarn.

In order to overcome the above disadvantages of first and second generation e-textiles, a novel concept for developing electronically active fibres and yarns was proposed by Dias in 2005 [10, 14, 15]. He suggested the development of a smart yarn by encasing semiconductor chips within the fibres of a yarn, which is a mixture of conventional textile fibres and conductive fibres as shown in Figure 2.26. The encasing of the chip has to be achieved in such a manner as to protect it from all forms of mechanical and thermal stresses. Such a smart yarn could then be used to manufacture electronically-active fabrics and garments. The concept will enable the creation of smart yarns containing different microchips and such smart yarns will be the building blocks of the next

generation of wearable electronics. Moreover, this will facilitate solutions to overcome current problems and difficulties which the manufacturers of wearable textiles are experiencing and open the doors for designers to develop the next generation of truly-wearable computers which are comfortable, flexible and washable [49, 50]. The technology to realise Dias' concept has been developed and is demonstrated within the programme of research that is documented in the following chapters of this thesis

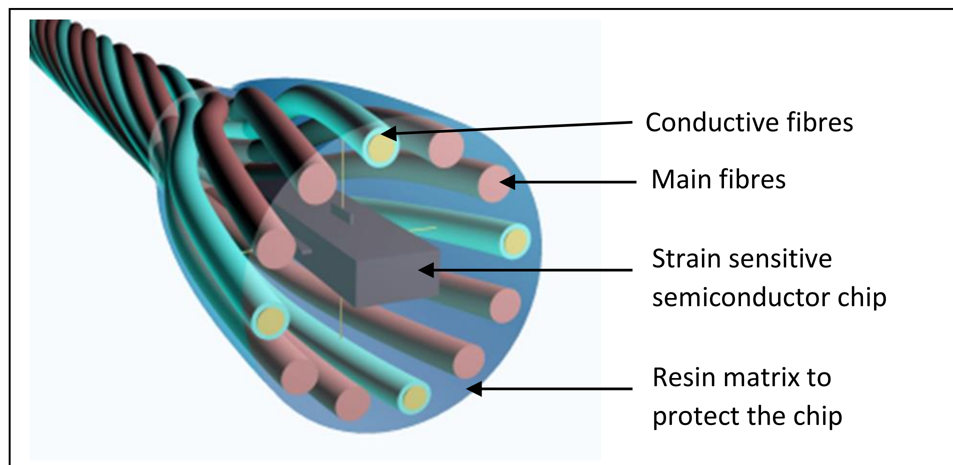

FIGURE 2.24: A SCHEMATIC ILLUSTRATING DIAS' CONCEPT OF AN ELECTRONICALLY-ACTIVE YARN [51]

In 2012 a French company Primo1D developed an electronic yarn called E-Thread in which RFID and LEDs chips were embedding into yarn [52]. However those electronics were visible on the outside because they were not integrated within the yarn structure [4]. Therefore, the interconnections and electronic components may not be strong enough to withstand mechanical stress which occur during the textile manufacturing process and end uses.

2.3.6 Highlighted Funded Projects on E-Textiles

There have been a number of projects on e-textiles, funded by the European Commission, and some of these projects are summarised below.

WEALTHY (Sept 2002 to Feb 2005): The focus of the project was to develop clothing for monitoring vital signs of patients. A Lycra-based knitted garment was developed with electrodes, which were knitted from a conductive yarn in order to determine ECG. The fabric of the garment was coated with carbon-black and silicone rubber to monitor the breathing patterns of the patient. The aim was to develop a garment to monitor a patient's health condition during rehabilitation without the need to remain in hospital unnecessarily [11, 53, 54, 55].

MY HEART (Dec 2003 to Oct 2007): This was a collaborative project with WEALTHY resulting in the development of a garment which made from woven fabric with insulated copper wire, a pressure sensing matrix and electrodes for recording of the heart rate was developed. The research consortium consisted of thirty partners from ten European countries. [11, 53, 54, 56].

BIOTEX (Oct 2005 to Feb 2008): The aim of this project was to develop a garment with biochemical-sensing techniques. The focus was on monitoring sweat and blood of the human body. A textile structure with sensing patches and textile sensors was developed for monitoring physiological measurements. Eight partners from four European countries were involved in the project [11, 53, 54, 57].

PROETEX (Feb 2006 to Jan 2010) was a project to develop a smart garment for first responders. The garment could monitor one's health, activity, position and the environmental conditions of the user (Figure 2.12) [11, 53, 54].

STELLA (Feb to Jan 2010) was a project aimed at developing stretchable electronics for large area applications. The main objective of the project was to develop new stretchable substrates with conductors to connect stretchable electronics such as energy supplies, sensors, actuators, display and switches. The target application areas were health care, wellness and functional clothes [11, 53, 54, 58].

OFSETH (Mar 2003 to Jan 2009): the aim of the project was to embed optical fibre sensors into textiles for healthcare applications. The project's focus was on use of silica and polymer optical fibres for monitoring vital signs of the human body, such as respiration, cardiac activities pulse oximetry and body temperature. Optical fibres with gratings and near infrared spectroscopy techniques were used [53, 54, 59, 60]

There have been a number of other EU founded projects such as CONTEXT (2006 to Jun 2008) that focused on the creation of smart textiles that have integrated contactless sensors for monitoring muscle activities and heart rate signals. The project MICROFLEX (May 2008 to May 2012) was co-ordinated by the University of Southampton with 13 partners. The project was focused on developing MEMS processing capability for the production of flexible smart fabrics using screen and inkjet printing and the development of new, functional inks to be compatible with fabrics [61, 62]. DEPHOTEX (Nov 2008 to Oct 2011) was a European collaborative research project focused on developing photovoltaic textiles based on novel fibres that can convert solar radiation to electric energy. The applications were textiles for sports, leisure, car interiors, solar tents, umbrellas, tennis rackets and everyday clothing [63, 64]. PLACE-it (Feb 2010 to Jun 2013) was called a 'platform for large area conformable electronics' by integration. This

project was led by Philips to develop electronic textiles by integrating foil-based electronics and LEDs into stretchable fabrics. As a result, Philips launched the product 'blue touch pain relief patch' in 2012 [65, 66].

Recently, a new research project commenced to develop manufacturing processes for integrating sensors, micro-controllers and other electronic components by embedding into textile yarn, which will be produced with printed electronic techniques. The project started in March 2015 with grant funding from the Engineering Physical Sciences Research Council in the UK. This is a collaborative research project between Southampton University and Nottingham Trent University with ten industrial partners. The project will enable the development of yarns with powerful electronic circuits [67, 68].

2.3.7 Current Situation of Global Wearable Electronics and Electronic Textiles

As mentioned in the beginning, electronic textiles are used, to produce smart textiles. There is another category called wearable computers or wearable electronics. Even though electronic components are used in e-textiles, all wearable electronics are not e-textiles. Therefore, wearable electronic products can be categorised as hand worn products (including smart watch, wrist wear and finger wear); head worn products (including smart glasses, head mounted display (HMD) and head up display (HUD); body worn products (including smart textiles, wearable patches, foot wear and arm wear) [69]. At the moment, according to Figure 2.27 and 2.28, the most popular wearable electronic products in 2013 and 2014 were hand-worn products (smart watches, for example): BBC News reported that Apple sold between 2.5 and 3 million smart watches in 2013 – 2014 [70]. However, 'Your Business Intelligence & Strategy Partner' (BIS) Research predicted that head-worn products would be more popular from 2016 (see Figure 2.27 and 2.28). Moreover, the total global wearable electronics market value is predicted to increase from USD 421.2 million to USD 17.47 billion by 2024 [71].

FIGURE 2.25: A SNAPSHOT OF THE GLOBAL WEARABLE ELECTRONICS COMPONENT MARKET VALUE [71]

FIGURE 2.26: A SNAPSHOT OF THE GLOBAL WEARABLE ELECTRONICS FORECAST [71]

IDtechEx (Identification Technology Exchange), has demonstrated that over 3 billion units of wearable sensors will be sold (worth USD 5.5 billion) by 2025 (Figure 2.29). Furthermore, IDtechEx explain that, even though the first wave of wearable sensors has come to market with other products such as mobile phones, and textile-based sensors will come to the market as a second wave [72] (Figure 2.30).

FIGURE 2.27: THE WEARABLE SENSORS MARKET FORECAST [72]

FIGURE 2.28: THE TRENDS OF SENSORS WHICH ARE IN WEARABLE ELECTRONICS [72]

All of smart textiles do not have an electronic functionality. The global smart textiles market was worth USD 289.5 million in 2012. Those smart textiles were used in medical applications; fashion and entertainment; protection and military; sports and fitness; transportation; architecture, and their market revenue share by application in 2012 is shown in Figure 2.31 [73]. The global smart textiles market is expected to grow to USD 2 billion by 2018 [74].

FIGURE 2.29: SMART TEXTILES MARKET REVENUE SHARE BY APPLICATION IN 2012 [73]

Currently, the highest demand for smart textiles is from Europe and North America, for a wide range of application such as transportation, military and healthcare. However, the fastest growth rate for smart textiles, rising at a compound annual growth rate (CAGR) of 20.2% from 2014 to 2020, was in Asia Pacific due to the fast growing industries in Asian countries such as China [73, 75]. At the moment, the major players in performance clothing are Adidas, Nike, and Reebok. Other high-end smart textiles manufactures are

Philips, Firetronic, Textronics, Peratech Ltd, Clothing+, ohmatex [73]. Other main E-textiles manufactures are Cute Circuit, Hovding, Moon Berlin, Myontex, No-Contact, Stealth Wear, Utope and Warmx [54].

According to IDTechEx there are active research programmes on electronic textiles in many universities worldwide; the universities involved in electronic textiles are listed in Appendix 1. [76, 77].

2.4 Conclusion

Today the demand for wearable devices is growing. To continue to meet this demand engineers, designers and commercial pioneers are conceptualising new applications. Textiles have a major role to play in this strategically-important area and offer many advantages over traditional materials such as support for technologically-advanced products, flexibility, softness, and high-strength-to-weight ratios. The highly developed mass production techniques that characterise the textile sector facilitate a path for the development of new products and their cost effective manufacture for many applications. These concepts are of particular benefit to certain groups who have specific requirements for wearable systems including the emergency services, military, elite athletes, patients and fashion innovators. Realising these concepts will expand an exciting new manufacturing sector, bringing together advanced textiles and electronics manufacturing. Most wearable technologies were developed in laboratories or as clothing that was specially made and bore little resemblance to garments that users would regard as normal. In the first generation of wearable technologies, electronic devices were simply attached to garments or included in pockets. In the second generation, electronic functionality was achieved by incorporating conducting yarns into the textile structure.

However, research has demonstrated their major drawbacks caused by inherent hysteresis of textile structures, which limits their application to relative measurements only [78, 79, 80]. Therefore, Dias has taken a major step forward by proposing the third generation of electronic textiles where integrated circuits are fully incorporated into yarns prior to fabric or garment production. The intensive literature survey, which was carried out by the author has confirmed the novelty of the concept as currently all activities in electronic textiles are limited to first and second generation products.

The aim of the research was to develop a new platform technology - ‘Fibre Electronics’ whereby semiconductor micro devices are directly embedded within the fibres of a yarn. Once produced, these electronically functional yarns will be incorporated into fabrics using conventional textile machinery or used as sewing thread in garment manufacture.

The resultant smart yarn technology will have a profound effect on the production and use of electronic textiles in wearable applications by providing robust functionality that is resistant to wear, washing and drying, and can be produced at lower costs than the electronic textiles available today where functionality is often added to the fabric and/or garment at the manufacturing stage.

CHAPTER THREE

3.0 Raw Materials Analysis

It was very important to understand the fundamental properties of selected raw materials before carrying out development tests for the creation of interconnects between micro-devices, in order to identify the compatibility of each materials and the performance of individual materials. Therefore, the physical, mechanical and electrical properties of the conductive filaments/threads/yarns and the solder pads of electronic semiconductor packaged dies were analysed. Tests included the determination of physical parameters (diameter, width, length, thickness, yarn count, tensile strength) and electrical properties. The results are included in this chapter.

3.1 Conductive Yarns/Threads/Strands

The interconnections of the micro devices were formed by using very fine conductive micro-strands (50 – 100 µm diameter) with very low electrical resistances. Ideally, the conductive strands should demonstrate good mechanical properties, excellent soldering ability and be covered by a thin non-conductive polymer film to prevent short-circuiting of the terminals of the microchips. Commercially available conductive threads can be classified as fine metal strands (single and multi-strands), synthetic polymer fibres with their surface covered with a micro millimetre thin conductive sheath of either silver, copper, nickel or gold, carbon fibres and silicone fibres impregnated with carbon nano particles [81]. Moreover, conductive polymers are also available such as Polypyrrole [82], which is a type of organic polymer produced by polymerisation of pyrrole [83]. However, most polymer-based conductive fibres are not suitable for creating interconnections due to their low melting points which would interfere with the soldering processes. The high melting point polymer based conductive fibres are very expensive. As such, it was decided to utilise fine metal strands to form interconnections between the terminals of the semiconductor micro devices. Silver is the most conductive metal by volume (Figure 3.1). However, it is only 5% more conductive by volume than copper and there are several benefits with copper compared to silver. For example, copper is cheaper, more malleable and more ductile. Consequently, copper is easier to form into different shapes and can be put under stress without damage. Moreover, it is possible to build up cracks when silver wire twists or kinks whist copper is less likely to build up cracks. Gold is also used as an electrical conductor as gold is corrosion resistant and reliable but it is very expensive [84, 85, 86]. Therefore, single and multi-strands copper wires were used in this research work.

FIGURE 3.1: ELECTRICAL CONDUCTIVITY OF MATERIALS [84]

Different configurations of Copper wires (Figure 3.2) from Luxion Technologies Incorporated Ltd in Wellingborough were examined for their suitability for the programme of research.

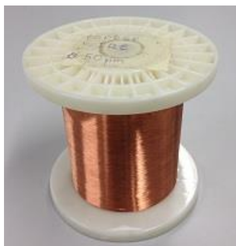

a. Single stand copper wire

b. Coated single strand copper wire A

c. Coated single strand copper wire B

d. Uncoated 4 strands copper wire

e. Uncoated 7 Strands copper wire

FIGURE 3.2: COPPER WIRES FROM LUXION INDUSTRIES INC. LTD.

3.1.1 Physical Properties Analysis of Copper Wires

3.1.1.1 Microscopic Analysis and Diameter Measuring Test

Microscopic analysis was carried out to determine the diameter of the copper wires. A digital microscope (Olympus model BX41) was utilised for these experiments. The diameters of the copper wires were measured in five different positions along the length of the copper wires within an image by using image-processing software (Cell^B). This test was repeated five times for each sample of copper wires. Examples of the images of the copper wires are shown in Figures 3.3 to 3.5. The results of the measurements of diameter are summarised in Table 3.1.

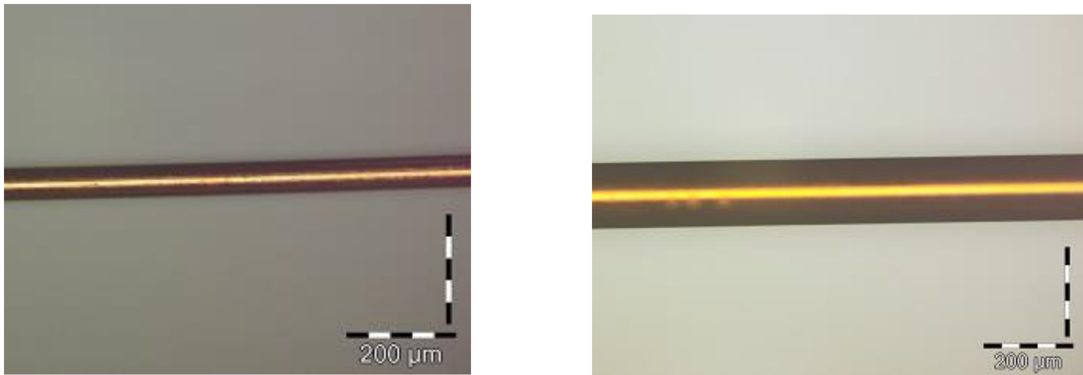

FIGURE 3. 3: SINGLE STRAND COPPER WIRE (LEFT: UNCOATED, RIGHT: COATED B)

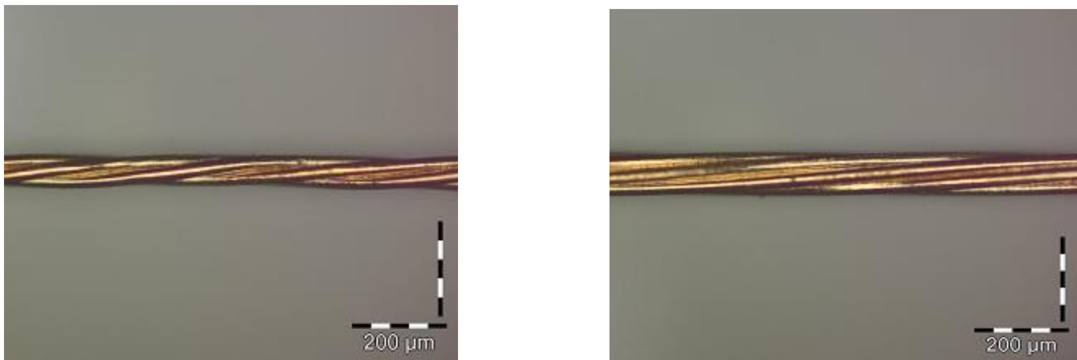

FIGURE 3. 4: UNCOATED 4 STRAND (LEFT), 7 STRAND (RIGHT) COPPER WIRES

FIGURE 3. 5: UNCOATED 8 STRANDS COPPER WIRE

Type of Copper Wires	Average Diameter (µm)	Standard Deviation (µm)
Single strand copper wire	55.20	4.87
Polymer coated strand copper wire A	76.60	1.36
Polymer coated single strand copper wire B	149.80	3.06
4 Strands twisted strand copper wire	65.80	1.72
7 Strands twisted strand copper wire	99.80	1.47
8 Strands twisted strand copper wire	127.80	1.72

TABLE 3. 1: THE RESULTS OF DIAMETERS OF THE COPPER WIRES

The diameters of polyester-coated single strand copper wire B and eight-strand copper wire were more than 100 µm. The diameters of the other copper wires were between 50 µm and 100 µm. The surfaces of copper wires were smooth without faults and the low standard deviations indicate that the diameters were uniform along the length. It was noticed that the twist of 4 strand copper wire was higher than that of 7 and 8 strands copper wires. Twist factor is a characteristic of a textile yarn that is expressed below, in formula 3.1 [87]. A higher twist factor leads to a smaller diameter of the yarn (either twisted spun yarn or filaments yarn) [88]. The breaking tensile force of a spun yarn is increased when the twist factor is increased up to certain point, but starts to decrease when the twist factor is increased further, as shown as in the Figure 3.6.

Twist Factor (kt) = Twist (turns per metre) x $\sqrt{\text{Tex}}$ ………………3.1

FIGURE 3. 6: RELATIONSHIP BETWEEN YARN BREAKING FORCE, BREAKING ELONGATION AND TWIST OF A SPUN YARN [88]

3.1.1.2 Measurement of Linear Density of Copper Wires

In textile science and technology, the term linear density is used to indicate the thickness of a yarn. This is also known as the 'yarn count'. This is determined by measuring the weight of a defined length of yarn. The most widely used yarn count system is the Tex System, where the linear density is defined by the weight of a 1000m length of yarn in grams. As the end product (electronic yarn) is a yarn, it was decided to measure the Tex count of copper wires used in the research. Due to the limited availability of copper wires, the weight of 1 m was measured by using a precision digital scale (model: PW214, Adam equipment) and the corresponding Tex counts were determined. In order to achieve a high degree of accuracy the length measurement of the copper wires was carried out with a crimp tester and 10 samples were used for each type of copper wire. The results are as summarised in Table 3.2:

Type of Copper wire	Average Count (Tex)	Standard Deviation (Tex)
Single strand copper wire A	25.1	0.34
Coated single strand copper wire	28.4	0.35
Coated single strand copper wire B	112.7	2.32
4 strand copper wire	26.8	1.02
7 strand copper wire	58.1	0.54
8 strand copper wire	70.5	0.08

TABLE 3. 2: THE LINEAR DENSITY OF COPPER WIRES

Table 3.1 shows that the single strand copper wire had the smallest yarn count, and polymer-coated single strand copper wire B had the highest yarn count.

3.1.2 Mechanical Properties of Copper Wires

The stress-strain behaviour of the copper wires was evaluated by using a Zwick-Roell, Z2.5 tensile testing machine according to the DIN EN ISO 2062:2009 standard. The tests were repeated 10 times for each sample and the results are given in Table 3.3. (Appendix 3 to 8).

L_v: Gage Length

F_H: Maximum Tensile Force

R_H: Fineness related breaking force

e_H: Elongation at maximum tensile force

Type of Copper Wires	L_v mm	Average F_H cN	Standard Deviation		Average e_H %	R_H cN/tex
			F_H (cN)	e_H (%)		
Single strand copper wire A	250	71	1.2	1.5	20	2.82
Coated single strand copper wire	250	86	3.2	2.8	19	3.04
Coated single strand copper wire B	250	272	27.0	12	19	2.42
4 Strand copper wire	250	116	12.6	3.6	23	4.32
7 Strand copper wire	250	300	11.9	1.2	16	5.15
8 Strand copper wire	250	357	8.0	1.8	17	5.06

TABLE 3. 3: TENSILE TEST RESULTS FOR COPPER WIRES

The results in Table 3.3 demonstrate that the multi-stand twisted copper wires performed better than single strand copper wires in term of R_H values. Overall, the seven-strand copper wire exhibited the best performance in terms of tensile strength per yarn count. The tensile and elongation behaviour of copper wires are shown in Figures 3.7 to 3.12.

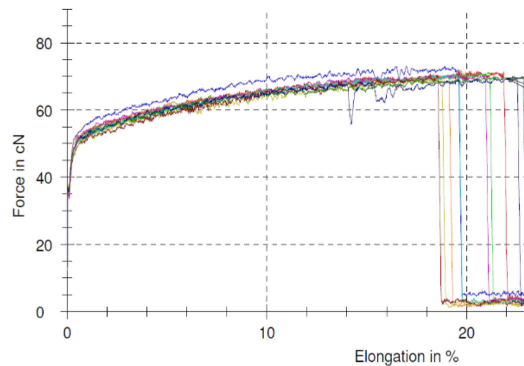

FIGURE 3. 8: GRAPH OF SINGLE STRAND WIRE

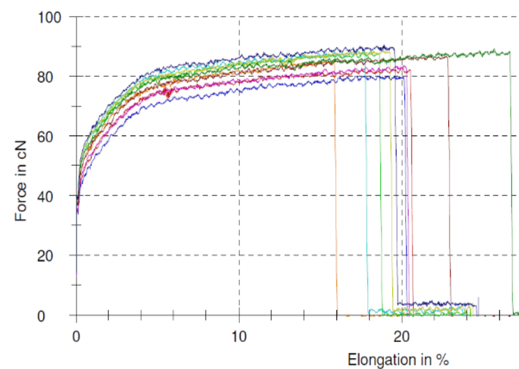

FIGURE 3. 7: GRAPH OF COATED SINGLE STRAND WIRE

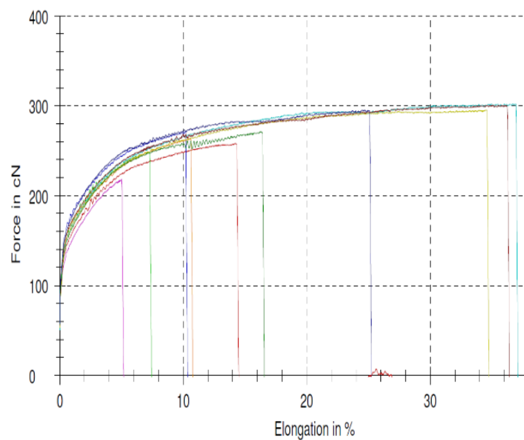

FIGURE 3. 9: GRAPH OF SINGLE STRAND WIRE B

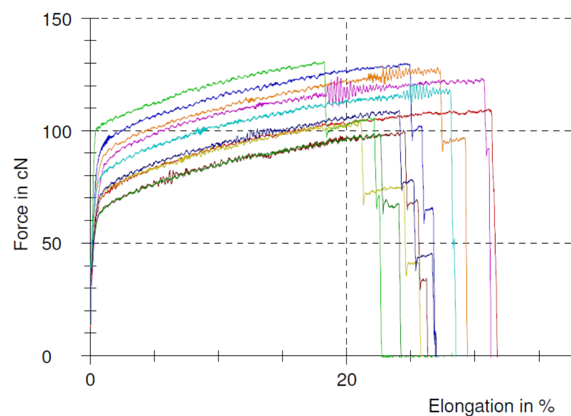

FIGURE 3. 10: GRAPH OF 4 STRAND WIRE

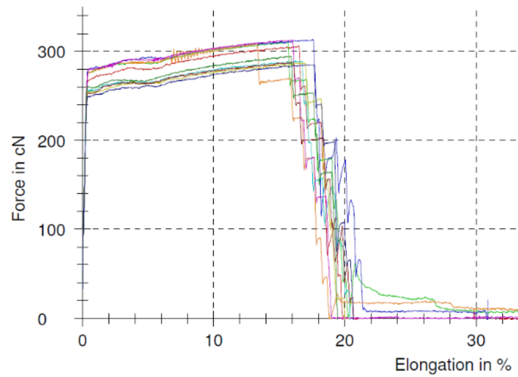

FIGURE 3. 12: GRAPH OF 7 STRAND WIRE

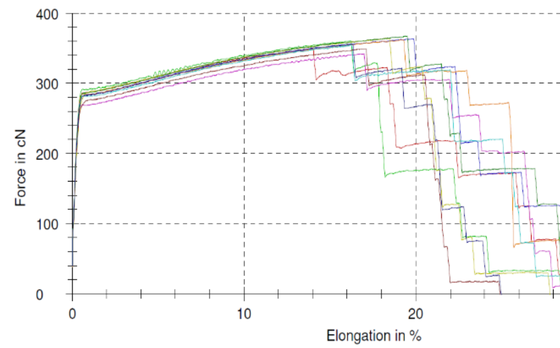

FIGURE 3. 11: GRAPH OF 8 STRAND WIRE

The observed elongation of the single wire copper B was highly variable (Figure 3.7), as confirmed from the high standard deviation for elongation of the single wire copper B shown in Table 3.3. The four-stand copper wires exhibited higher elongation as due to their higher twist level, as shown in Figure 3.6 [88].

3.1.3 Mechanical Properties of Polyester Yarn

During fabric manufacture textile yarns are subjected to high tensile stresses, and due to the low breaking strength of copper wires used in the research the interconnects and the semiconductor chips were strengthened with polyester yarn (150dTex/48 textured yarn). The polyester yarns were also tested and the results are given below. The yarns were tested using the procedures described in section 3.1.2 and results are given Table 3.4 (Appendix 9).

Polyester Yarn (150/48)	L_v mm	Average F_H cN	Standard Deviation		Average e_H %	R_H cN/tex
			F_H (cN)	e_H (%)		
Single yarn	250	674	33.5	2.3	21	4.5
Two polyester yarns	250	1352	50	1.7	21	4.5

TABLE 3. 4: TENSILE TEST RESULTS FOR POLYESTER YARN

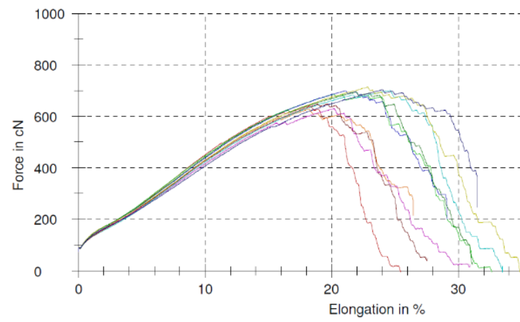

FIGURE 3. 13: GRAPH OF ONE POLYESTER YARN

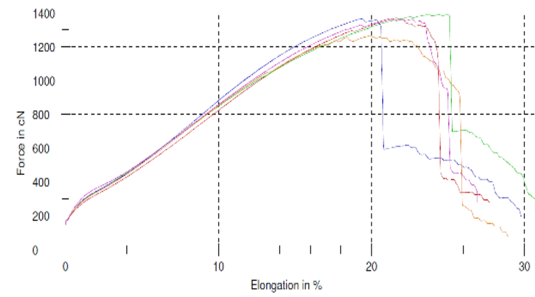

FIGURE 3. 14: GRAPH OF TWO POLYESTER YARN

3.1.4 Mechanical Properties of Polyester Yarn and Copper Wires Combination

As stated earlier, copper wires were not used on their own in the making of electronic functional yarn. They were integrated with polyester fibres to improve the strength, durability, flexibility, comfort and washability. As such it was necessary to analyse the physical properties when they were combined together. Therefore, further tensile tests were carried out with combinations of copper and polyester yarn (textured, 150/48) and the tensile test results are shown in Table 3.5 and Figure 3.15 to 3.18 (Appendix 10 to 13).

Combination of Copper wires and polyester yarns	L_v mm	Average F_H cN	Standard Deviation		Average e_H %	R_H cN/tex
			F_H (cN)	ε_H (%)		
A Polyester yarn & single copper wire	250	631	104	4	18	3.60
Two Polyester yarns & single copper wire	250	1392	45	2.1	20	4.28
A Polyester yarn & a 7 strand copper wire	250	734	35	1.2	15	3.53
2 Polyester yarns & a 7 strand copper wire	250	1370	118	2.1	17	3.84

TABLE 3. 5: TENSILE TEST RESULTS FOR COMBINATIONS OF POLYESTER YARN AND COPPER WIRE

The tensile breaking strength of the single strand copper wire was 71 cN, and seven-strand copper wires was 300 cN (Table 3.3). For example, at 10% elongation point, they both were not broken but the tensile force was very low at 10% elongation (Figure 3.7 & 3.11). However, when the copper wire was combined with polyester yarn, the tensile forces were higher at 10% elongation point (Figure 3.15 & 3.16). The single strand copper wires were not broken at 10% of elongation even though the forces are much higher than 71 cN (Figure 3.15). A similar result was noticed in seven strands copper wire too. Moreover, the breaking forces were similar for single strand copper wire and seven-strand copper wires when they combine with polyester yarn (table 3.5) whist single strand copper wire was very much weaker than seven strands copper wire without polyester yarn (table 3.3), as the polyester yarn was taking the tensile load when copper wire combine with polyester yarn. Therefore, the tensile tests result exhibited that it was important to use additional, strong textile yarns combined with copper wires to achieve the required strength.

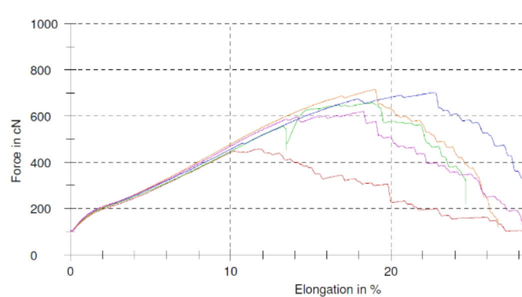

FIGURE 3. 16: GRAPH OF ONE POLYESTER YARN AND SINGLE STRAND COPPER WIRE

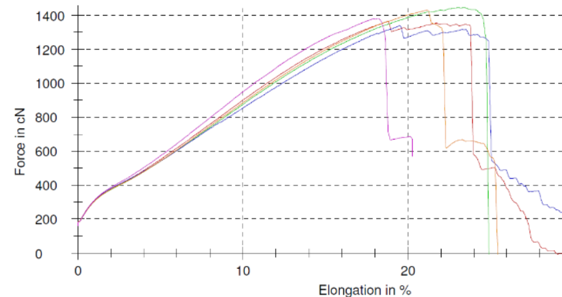

FIGURE 3. 15: GRAPH OF TWO POLYESTER YARNS AND SINGLE COPPER WIRE

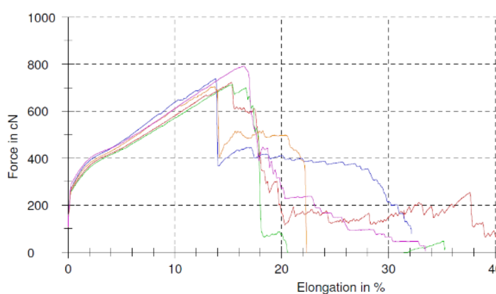

FIGURE 3. 18: GRAPH OF ONE POLYESTER YARNS AND 7 STRAND COPPER WIRE

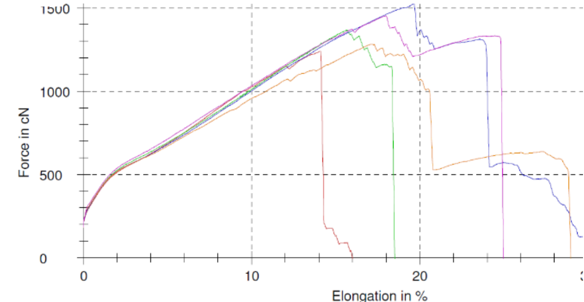

FIGURE 3. 17: GRAPH OF TWO POLYESTER YARNS AND 7 STRAND COPPER WIRE

3.1.5 Electrical Properties of Copper Wires

Batteries are often used for providing the required electrical power for circuits in electronic textiles, particularly in wearable devices. Batteries invariably add weight to the e-textiles. Therefore, it is important to reduce the required battery power of the system in order to avoid using higher-weight batteries. Because of that, the resistivity of conductive yarns is a very important factor. A digit multi-meter (Type Agilent 6 ½) was used to

measure the resistances of copper wires. The meter is shown in Figure 3.19. Resistances were measured per meter of copper wires for ten samples of each and every copper wire. The result is shown in Table 3.6.

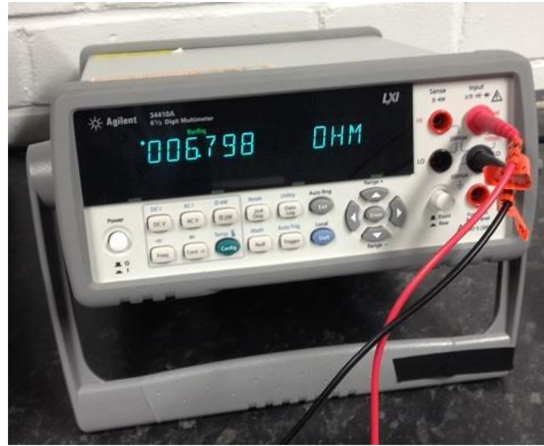

FIGURE 3. 19: AGILENT 6 ½ DIGIT MULTI-METER

Selected Copper Wires	Diameter of Copper Wires	Average of Resistance (Ω/m)	Standard Deviation of Resistance (Ω/m)
Single strand copper wire	55.20	6.81	0.12
Coated single strand copper wire A	76.60	6.29	0.24
4 Strand copper wire	65.80	56.16	0.72
7 Strand copper wire	99.80	17.78	0.29
8 Strand copper wire	127.80	14.32	0.26

TABLE 3. 6: THE RESISTANCE OF COPPER WIRES

3.2 Materials Used for Electrical Connection

Electrically-conductive materials are used by the electronics industry to create connections between electronic components such as semiconductor packaged dies, batteries, and input and output devices, via a printed circuit or wires. There is a number of materials commercially available for electrical connection including solder for hand soldering, solder paste conductive glue and conductive ink in the printed-electronics industry to create the required interconnects. Solder and a soldering iron from Xytronic (model: Auto-Temp 136 ESD) were used in the beginning of the research work reported here. During hand soldering, the soldering tip of the soldering iron has to be in contact

with the objects to be soldered. i.e. the solder pads of the semiconductor packaged dies and the copper wire used in the research. Micro-scale semiconductor packaged dies were used, therefore it was decided to use a non-contact soldering technique to prevent damaging semiconductor dies. Hence solder paste was used as it can be reflow the solder paste with non-contact technique. Moreover, solder paste can be dispensed precisely at a micro-gram scale using dispenser devices. Generally, a soldered bond is stronger than one formed with conductive adhesive. Solder paste forms a metallic bond whilst conductive adhesive forms a mechanical and chemical bond. Solder is more thermally-conductive than an adhesive (Solder: 60-65 W/mK, Adhesive: 3-25 W/mK). The resistivity of solder is lower than adhesive (Solder: 0.000015 Ω.cm and Adhesive: 0.0006 Ω.cm) [89]. The shearing force of an adhesive joint is less than soldered joint [90]. It was necessary to produce mechanically-strong, reliable conductive joints between semiconductors, packaged dies and copper wires in order to improve the robustness of electronic yarns. For these reasons, conductive adhesive was not used for these experiments.

3.2.1 Solder Paste

Solder paste consists metal powder (consist of millions of micro-metal balls dispersed) and flux, as shown in Figure 3.20. The formulation of Solder paste is at gel level, it is used in the electronics industry to create solder joints as it is efficient and accurate in use. Historically, solder paste contained lead but today most solders are lead free.

FIGURE 3. 20: A MICROSCOPE IMAGE OF SOLDER PASTE (91)

Solder paste dispenser systems are used to dispense solder paste precisely and efficiently. There are different types of solder paste classified according to the size of the metal balls contained within them. For an example, particle size of EFD type ii is 45 to 75 microns and EFD type vi is 5 to 15 microns (technical data sheet: Annex 8) [92]. Solder pastes are contained in slingers, there are different sizes and types of slinger tips use to dispense the solder paste. It is necessary to select a suitable slinger tip size according to the metal ball size. An example of a dispenser, slinger and slinger tips are shown in the Figure 3.21.

FIGURE 3. 21: SOLDER PASTE DISPENSER, SLINGER AND TIPS [93]

The use of lead in electrical products was banned due to health and safety reasons in 2006. The legislation was called Restriction of Hazardous substances (RoHS) and was set up by the European Union [94]. EFD Ltd market both lead and lead free version of solder paste. Both versions were tested, but the lead free version was used in this research work. The formulation, Sn96.5Ag3.0Cu0.5 type VI was used for soldering. It consists of Tin (96.5%), Silver (3%) and copper (0.5%). According to the technical data sheet (Annex 10), the alloy particle size is 5 to 15 microns in type VI. Microscopic analysis was undertaken as shown as Figure 3.22.

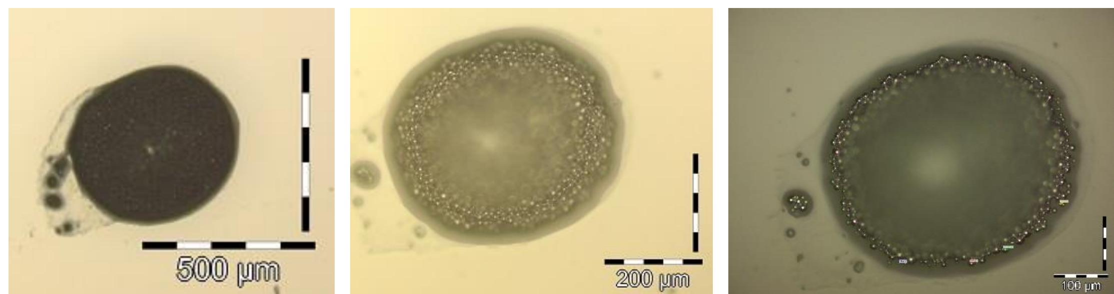

FIGURE 3. 22: MICROSCOPE IMAGES OF SN96.5AG3.0CU0.5 TYPE VI SOLDER PASTE

The middle of the solder paste drop could not be focused on due to the limited depth of field of the optical microscope. However, from microscope images of solder paste (Figure 3.20), small metal balls (diameters in between 5 and 15 micron) were observed.

3.3 SMD Type Electronics Packaged Dies

The packaging format used in surface mount devices (SMD) is the most suitable for creating electronic yarns (e-yarns) due to the absence of pins and leads. The miniature size of the SMDs will enable the creation of fine electronic yarns. Examples are SMD 0201 (600 x 300 x 230 µm) and SMD 0402 (1000 x 500 x 500 µm) shown in Figure 3.23, which were used in this project to produce e-yarns. A range of SMD-type packaged dies were used to create electronic yarns with specific functions. These included LEDs, resistors, thermistors and RFID (Radio Frequency Identification) packaged dies. Microscopic analysis was carried out for those packaged dies and the results are given bellow.

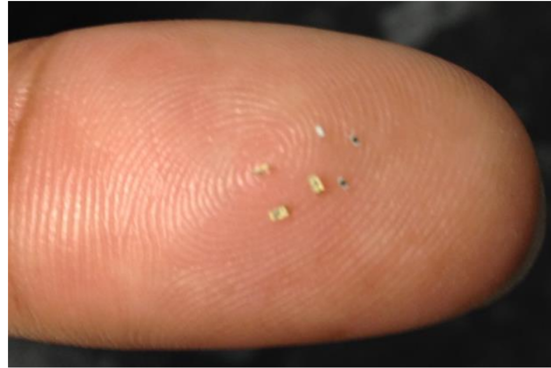

FIGURE 3. 23: EXAMPLE OF SMD 0402 LEDS (YELLOW) AND 0201 RESISTORS (BLACK)

3.3.1 Microscopic Analysis of Semiconductor Packaged dies

Microscopic analysis was carried out by using a digital microscope (Olympus model BX41) to identify the physical appearance of the semiconductor packaged dies, the dimensions (length, width and thickness) and the dimensions of the solder pads (length and width).

3.3.1.1 LED Silicon Wafer Bare Die

A few samples of LED Silicon bare dies were supplied by Plessey Semiconductors Ltd for tests. The standard SMD type LED packaged dies (package dies) are produced by using silicon wafer dies (bare dies). The LED bare dies supplied by Plessey, had gold wire interconnects, which are normally attached to the solder pads of packaged dies. Microscopic images of the silicon wafer are shown in Figure 3.24. It consists of silicon wafer bare die and two gold wires which were connected to the bare die.

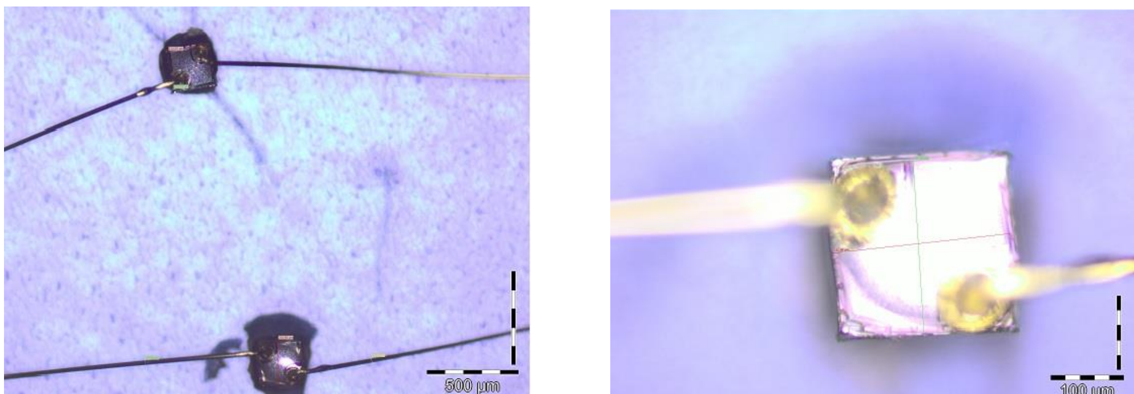

FIGURE 3. 24: MICROSCOPIC IMAGES OF LED SILICON WAFER BARE DIE (RIGHT: CLOSE IMAGE)

3.3.1.2 SMD Packaged Dies (0402 Type)

These are examples of package die that are made from a silicon wafer by adding a cover to protect the silicon wafer. Microscope images of the 0402 type LED packaged die (dimensions: 1.0 x 0.5 x 0.5 mm) and resistor are shown in Figures 3.25 and 3.26. These incorporate two solder pads (yellow-coloured anode and cathode) to facilitate electrical connections. A microscopic image of SMD resistor (0402 type) is also shown in Figure 3.26.

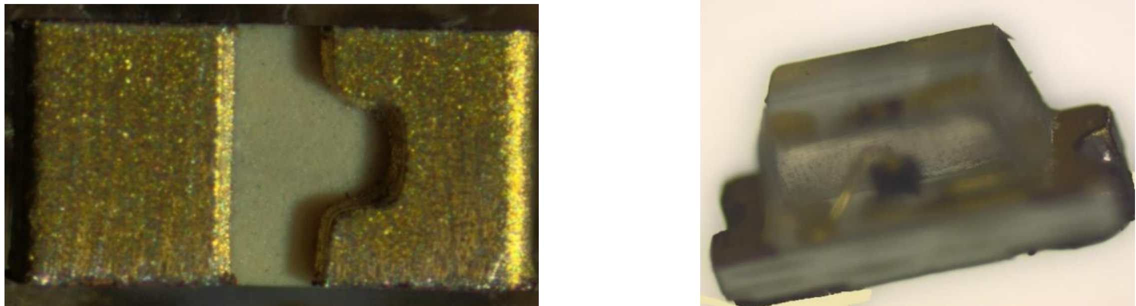

FIGURE 3. 25: MICROSCOPIC IMAGES OF 0402 TYPE LED PACKAGED DIE (LEFT: FRONT, RIGHT: BACK)

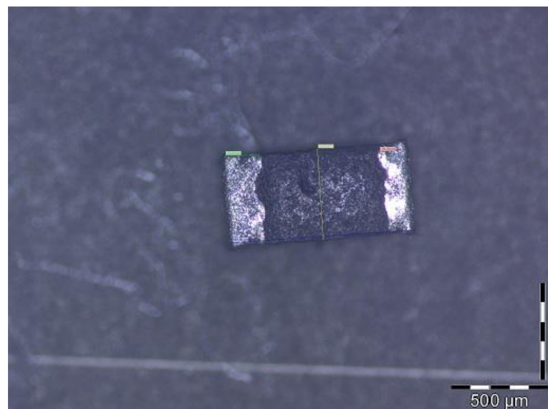

FIGURE 3. 26: MICROSCOPIC IMAGES OF RESISTOR PACKAGED DIE (0402 TYPE)

3.3.1.3 Radio Frequency Identification (RFID) Packaged Dies

Microscopic images of the RFID silicon wafer bare die and package die are shown in Figures 3.27, 3.28 and 3.29. Four solder pads in the wafer die and six solder pads in the package die were observed.

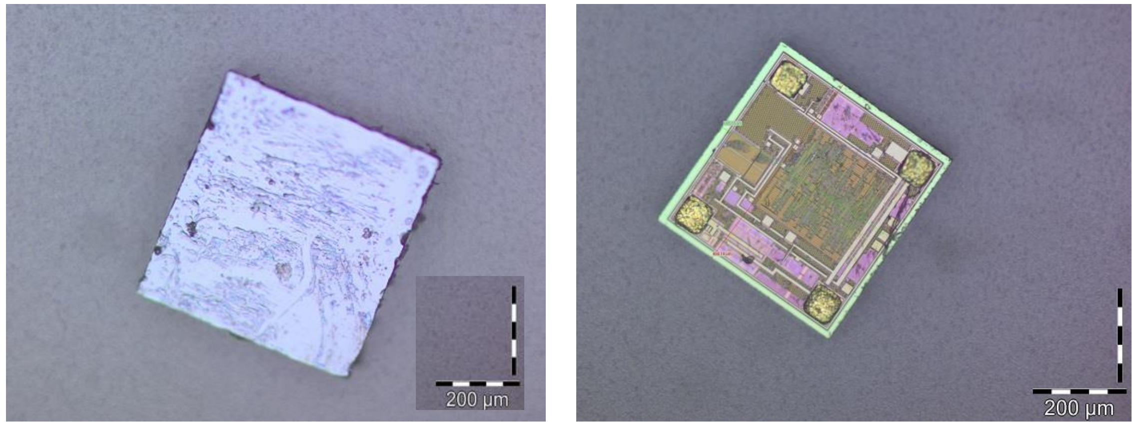

FIGURE 3. 27: MICROSCOPIC IMAGES OF RFID SILICON WAFER DIE (LEFT: BACK SIDE OF PACKAGED DIE, AND RIGHT: FRONT SIDE OF PACKAGED DIE)

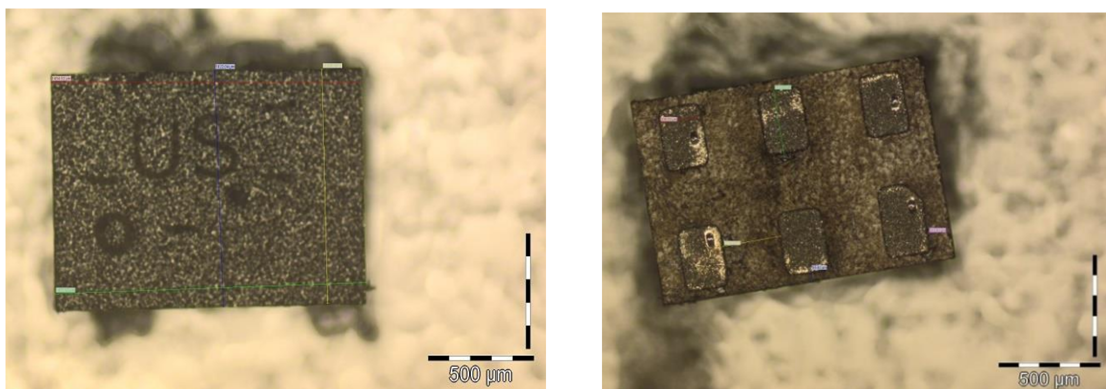

FIGURE 3. 28: MICROSCOPIC IMAGES OF RFID PACKAGE DIE (LEFT: BACK SIDE OF CHIP, AND RIGHT: FRONT SIDE OF CHIP)

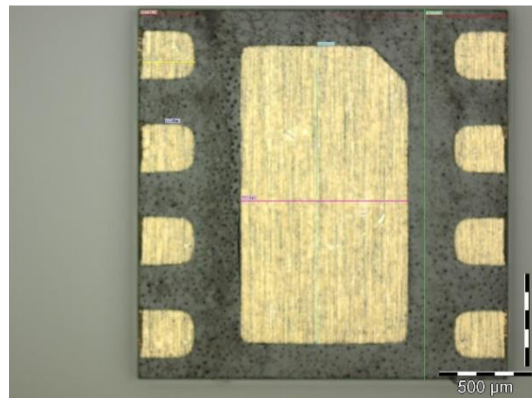

FIGURE 3. 29: MICROSCOPIC IMAGE OF 8-TERMINAL RFID PACKAGED DIE

3.3.2 Dimensions of Semiconductor Packaged Dies

All the dimensions of packaged dies were obtained using microscopic image analysis software (Cell^B). The results are shown in the Table 3.7.

Packaged die Type	Packaged die Dimensions (μm)	Solder pad Dimensions (μm)

	Length	Width	Thickness	Length	Width
LED Silicon wafer	230	220	100	N/A	N/A
LED 0402	1000	500	500	500	400
Resistor 0201	600	300	230	300	150
Resistor 0402	1000	480	350	480	180 & 130
RFID Silicon wafer	450	450	150	60	60
RFID 6 terminals packaged die	1450	1000	500	300	200
RFID 8 terminals packaged die	2000	2000	500	280	260

TABLE 3. 7: DIMENSIONS OF SEMICONDUCTOR PACKAGED DIES

3.4 Encapsulation Resin

Most electronics textiles available in the market today are not washable. For those that are washable, still it is necessary to remove the electronic components prior to washing. As a solution to address the washability, an encapsulation process was introduced, in order to develop washable electronic yarns. An encapsulating resin micro-pod protects the semiconductor packaged dies and solder joints. The encapsulation process is described in Chapter 5. There are many varieties of resin available in the market today, such as epoxy-based, silicone-based, polyurethane etc. and different curing techniques [95]. UV-curable resin was selected to use for encapsulation of E-yarns due to its many benefits such as the solvent-free liquid form, environmentally friendly due to low energy required for curing [96]. The UV, spot-curing technique is suitable for heat-sensitive electronics due to low heat generation and low curing times [97]. After an intensive market research, UV-curable Dymax 9001-E-V modified urethane conformable resins were used. This Dymax UV-curable resin is available in a number of different viscosity levels, such as 9001-E-V-3.1 (viscosity: 4500 cP), 9001-E-V-3.5 (viscosity: 17000 cP) and 9001-E-V-3.7 (viscosity: 45000 cP). It was necessary to do the initial curing tests for resins to determine curing time and the distance between UV source and resin which is to be cured, to optimise the efficiency of encapsulation process and performance. The tests were performed as shown below.

3.4.1 Testing for Distance between UV Light Source and Resin to be Cured

The aim of the investigation was to determine the optimum distance between the UV light guide tip and the two microscope slides that held the resin that was to be cured. The equipment was set up as shown in Figure 3.30. The equipment and raw materials used are

listed in Table 3.8. This test was recommended by the Dymax Company which provided the UV spot-curing system for the research; see Annex 14 for further details. The curing time of the Dymax blue wave 50 was set up for 5 seconds. Two microscope slides were placed on the work guide. Figure 3.31 shows a configuration with the ends of the microscope slides overlapping. A configuration with the two microscope slides placed end to end was found to be more practical and was used to produce the results shown in tables 3.9 to 3.10. The distance between UV light guide tip and microscope slide was set at 5 cm. Two milligrams of 9001-E-V 3.5 resin was deposited over the junction between the two microscope slides, as shown as Figure 3.32. UV light was applied for 5 seconds. The level of cure of the resin drop was tested by pulling the two microscope slides away from each other to find if the resin remained solid or if it was still liquid. The glass was then cleaned with anti-bacterial surface wipes before repeating the test. The distance between the UV light guide tip and the resin was varied to find the optimal distance. The results are shown in table 3.9. The results in table 3.9 show that a maximum distance of 1 cm between the light guide tip and the microscope slides was required in order to achieve full curing.

Equipment	Raw Materials
• A EFD dispenser unit	• A few pieces of glasses
• A compressor	• Dymax 9001-E-V 3.5
• Dymax blue wave 50 (UV source)	• Dymax 9001-E-V 3.7

TABLE 3. 8: THE EQUIPMENT AND RAW MATERIALS USED FOR THE CURING TEST

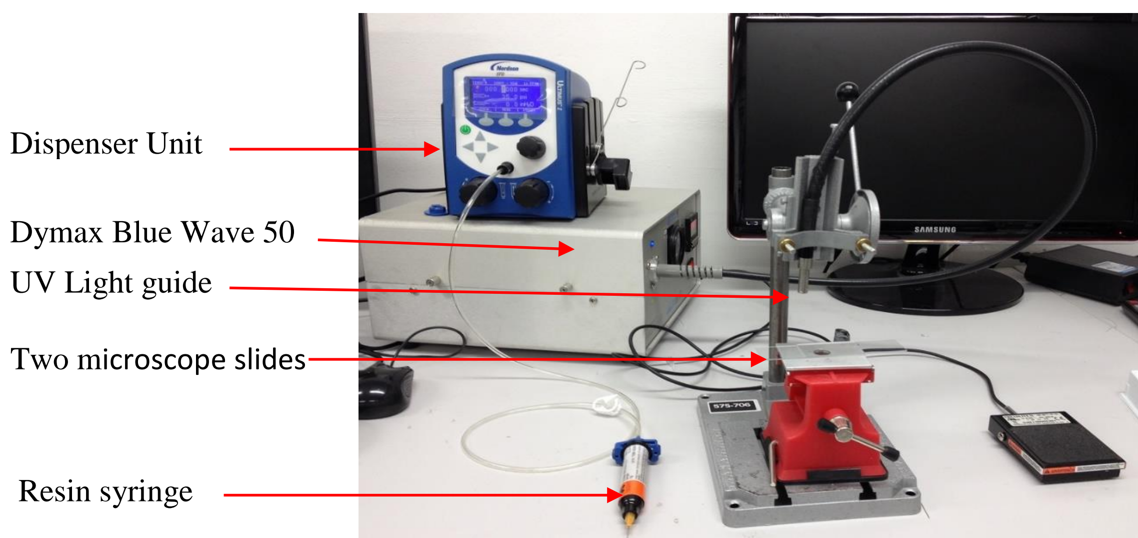

FIGURE 3. 30: EQUIPMENT SET UP FOR RESIN CURING TEST

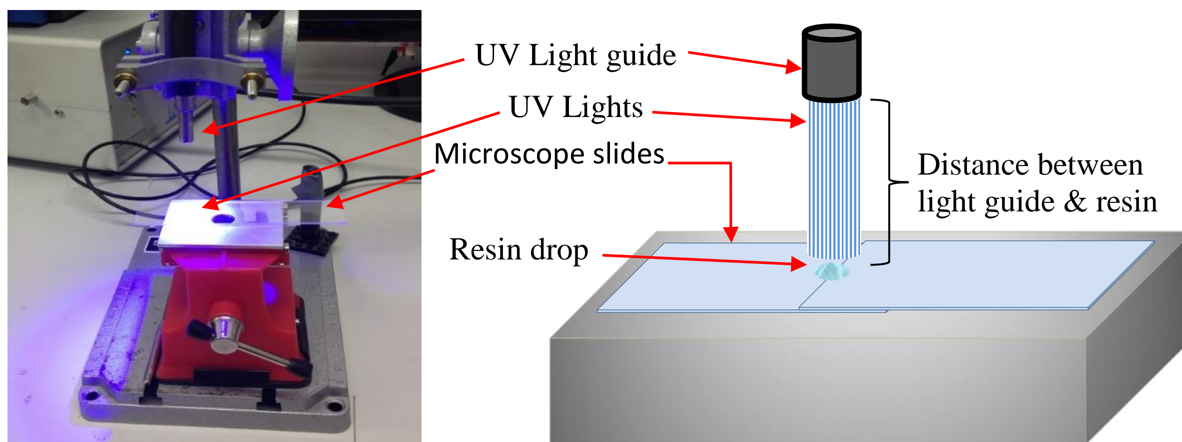

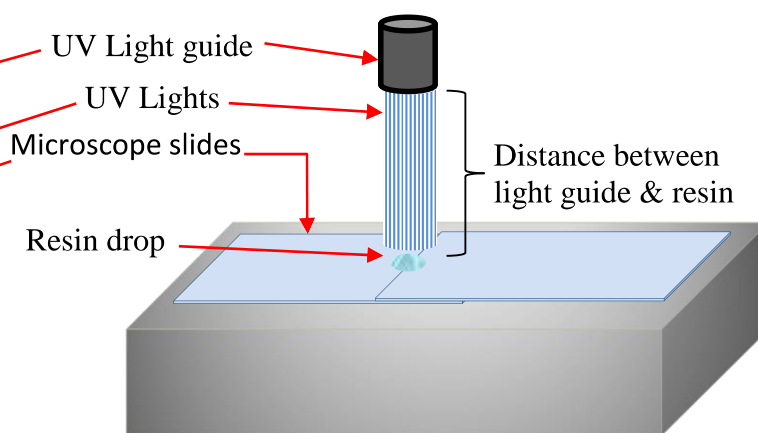

FIGURE 3. 31: EQUIPMENT SET UP FOR CURING

FIGURE 3. 32: : SCHEMATIC DIAGRAM OF EQUIPMENT SET UP

Distance between UV light guide tip & resin drop (cm)	Observation
7	Soft gel (not fully cured)
6	Soft gel (not fully cured)
5	Gel (not fully cured)
4	Hard gel (not fully cured)
3	Hard gel (not fully cured)
2	Appeared to be cured
1	Fully cured
0.5	Fully cured
0.3	Fully cured

TABLE 3.9: CURING TEST RESULT 9001-E-V 3.5 RESIN AT FIX UV EXPOSURE TIME (5 SECONDS)

3.4.2 Testing for Curing Time of UV Curable Resin

This aim of the experiment was to determine the optimum curing time of the UV-cure resins. The equipment was set up as shown in Figures 3.29 and 3.30. The distance between the UV light guide tip and the glass was set at 1 cm (as this had been found to be the optimal distance in the previous tests for which results are shown in table 3.8) and the test was repeated by altering the curing time of the 9001-E-V 3.5 and 9001-E-V 3.7 resins. The results are shown in tables 3.10 and 3.11.

Curing Time (seconds)	Observation
1	Soft gel (like liquid)
2	Gel (not fully cured)
3	Hard gel (not fully cured)
4	Appeared to be cured
5	Fully cured
10	Fully cured
20	Fully cured
30	Fully cured
40	Fully cured
50	Fully cured
90	Fully cured

TABLE 3.10: CURING TEST RESULT 9001-E-V 3.5 RESIN AT FIX DISTANCE OF 1 CM BETWEEN THE UV LIGHT GUIDE TIP AND THE GLASS

Curing Time (seconds)	Observation
1	Soft gel (like liquid)
2	Gel (not fully cured)
3	Hard gel (not fully cured)
4	Cured (but soft)
5	Fully cured
10	Fully cured
20	Fully cured
30	Fully cured
40	Fully cured
50	Fully cured
90	Fully cured

TABLE 3.11: CURING TEST RESULT 9001-E-V 3.7 RESIN AT FIX DISTANCE OF 1 CM BETWEEN THE UV LIGHT GUIDE TIP AND THE GLASS

Each test was done 5 times and the all of observations were as above tables (3.9, 3.10 and 3.11). The results shown in tables 3.8 to 3.10 show that the optimum curing time was 5 seconds and the optimum distance from UV light guide tip to resin was 1 cm for Dymax 9001-E-V 3.5 and 9001-E-V 3.7 resins. However, increasing the curing time is unlikely

to have any negative effect on the components, so a curing time of 10 seconds is recommended to ensure that the resin has been fully cured.

3.5 Conclusion

In this chapter, the physical, mechanical and electrical properties of copper wires and electronic packaged dies were analysed. In general, the conductivity of silver is 5% better (by volume) than copper but there are several benefits to copper compared to silver. Copper is more cost effective, more malleable and ductile than silver. Therefore, copper is easier to mould to different shapes and can be put under stress with less likelihood of damage.

The diameters of polyester-coated single strand copper wire (dark colour) and eight-strand copper wire were more than 100 µm, therefore these were too big for interconnection with semiconductor microchips. The diameters of the other copper wires were between 50 µm and 100 µm. Uncoated single strand copper wire had the lowest yarn count, whilst the highest yarn count was for polyester coated dark colour single strand copper wire, which was too big for this research work.

According to the tensile test results, seven-strand copper wire exhibited better performance, whilst single strand copper wire's tensile strength was lower. However, when copper wires were combined with polyester yarn, tensile strengths were similar for all of the copper wires, as polyester yarn had taken the tensile load. Therefore, it was important to use additional strong textile yarn to combine with copper wires to achieve the required strength.

Curing tests were carried for Dymax 9001-E-V 3.5 and 9001-E-V 3.7 resins to determine the optimum curing time and optimum distance between the UV light guide tip and the two microscope slides that held the resin that was to be cured. The results showed that the optimum curing time was 5 seconds and the optimum distance from UV light guide tip to resin was 1 cm.

CHAPTER FOUR

4.0 Creation of Interconnections of Micro-Devices

The creation of robust interconnects presented a number of challenges. Several techniques are demonstrated in this chapter (4.1). These are currently used in the electronics industry for creating interconnections between electronic devices. The most common technique is soldering which dates back 5000 years [98]. Generally, the electronics industry use soldering for electrical wiring and connecting electronic components on printed circuit boards (PCBs) [99]. Soldering techniques were selected to produce interconnections between copper wires and electronic components in this research work. Soldering micro scale semiconductor packaged dies (type SMD) to flexible fine wires (<100 micron) was a novel concept and was challenging when compared to soldering of package dies onto stiff surface of PCBs. And also electronic yarn (e-yarn) integrated with packaged dies and fine copper wires, should be able to flex and behave as a normal textile yarn, however, the solder joints should be mechanically strong. Hand soldering and reflow soldering techniques were studied in order to create good interconnections in terms of mechanical strength and electrical conductivity, and the findings including the optimisation of the process parameters are described in this chapter.

4.1 Available Techniques of Solder Bonding

Several metal bonding techniques for connecting copper conductors with the solder bonds of semi-conductor packaged dies (which will be referred to as chips in the following text) are commercially available, however, they all have their advantages and disadvantages. The most common heating sources used for reflow solder are described below briefly.

4.1.1 Hot Bar/Thermode Reflow Soldering

This involves contact heating to join parts together to create an electro-mechanical bond. The two parts which need to be bonded, have to be fluxed and coated with solder prior to applying heat by pressing a heated bar on to the top of the part and holding for a few seconds to reflow solder. This technique is suitable for joining together a few metal parts, which are away from semiconductor chips. Woznicki and others report that SMD-type chips would be damaged by the hot bar if this technique is used for soldering SMD-type chips [100, 101].

4.1.2 Hot plate

A hot plate is used for soldering in electronics industry. This is suitable for low-melting-point solder, which melts at 150 ^{0}C. Most lead free solders have melting points that are higher than 220 ^{0}C, so they are not suitable for use with the hot plate technique. Solder paste is deposited onto the soldering point (example: PCB), electronic components are then picked and placed onto the soldering point and the PCB is placed on a pre-heated hot plate (temperature around 160 ^{0}C). It will take approximately 30 seconds for the solder to reflow. Finally, the PCB is removed from the hot plate after 60 seconds [102]. This technique cannot be used due to the need to use lead-free solder in this research.

4.1.3 Resistance Soldering

This is a contact-soldering method in which the electrical current flowing through the contact surfaces of the parts to be soldered produces the heat required for the soldering process. This technique can generate high levels of heat rapidly and economically. As heat is generated only when necessary there is less risk of burning compared to techniques such as hand soldering where heat is generated continuously. It is suitable for soldering large items, and may not be suitable for soldering sensitive electronic devices such as microelectronic chips as they can be damaged due to the current flowing between the solder pads and interconnects during the heating process [103].

4.1.4 Flame Soldering

A flame is used as a heat source. Acetylene or propane gases can be used to burn with oxygen to create flame. Flame soldering can be used where higher degree of temperature required and not for semiconductor soldering in this project even though there is no physical contact with the parts [104].

4.1.5 Convection Oven

Convection ovens are used in industry to solder a number of items simultaneously. The heat is applied over a large area. This is a non-contact heating technique and uniform heat distribution across the area of application can easily be achieved [105]. However, this technique is not suitable for soldering interconnects to individual microelectronic chips, which was the focus of the research.

4.1.6 Focused Hot Air Soldering

In this technique, a stream of hot air is blown onto the soldering area. This is also a non-contact soldering technique. Heat is, generally, applied only to the soldering point. This is suitable for thermally-sensitive microelectronic components such as semiconductor chips, ceramic capacitors, glass diodes and SMD resistors [106].

4.1.7 Induction Soldering

An alternating electromagnetic field is generated by applying high-frequency current to an inductor (coil). If there is a metal surrounding the electromagnetic field, then it will be heated up due to the current induced in the metal. The inductor works like the primary winding and the work-piece functions like the secondary winding of a transformer. This technique is also not suitable for soldering small or sensitive electronic components [107].

4.1.8 Laser Soldering

In this technique a laser beam is used to transfer energy to solder alloy deposited between two parts. The solder alloy would absorb the energy and heat up to its melting point, thus forming an electro-mechanical joint between the two parts. This is a contactless technique and is suitable for soldering many varieties of electronic components using either solder paste or solder wire. There are mainly three types of lasers used today for soldering, such as carbon dioxide lasers (gas lasers), Nd YAG lasers (solid lasers) and diode lasers [108]. Due to health and safety considerations and the cost of equipment, this technique was not explored in this research.

4.1.9 Hand Soldering

The hand soldering techniques are used, to join two or more metals together by using flux and solder which has a lower melting point than the metals to be joined. It is believed that the technique was developed 5000 years ago and used for making jewelry, tools, stained glass and cooking items [109]. The electrical and mechanical properties of solder joints depend on the temperature of soldering iron, type of soldering tip, type of flux, amount of solder and the shape of the solder joint [110]. The flux is used to clean the surface of the metal from dirt, oil and oxides. There are three type of flux, namely water-soluble fluxes, no-clean fluxes and traditional rosin fluxes. Due to health and environmental issues, lead-free solders are promoted for use in Europe and Japan [111]. An example of hand soldering is shown in Figure 4.1.

FIGURE 4. 1: AN EXAMPLE OF HAND SOLDERING [112]

In hand soldering the heat necessary to melt the solder is provided with a pre-heated solder tip that has to be in contact with the two parts to be soldered. Proper selection and use of flux prevents oxidation during soldering, and the solder tip must be clean and pre-tinned with solder to ensure rapid heat transfer.

4.1.10 Infra-Red (IR) Reflow Soldering

It is necessary to transfer thermal energy from a heat source to the soldering point to melt and reflow solder between the terminals of the microchip and the conductive wire(s) in order to create good electro-mechanical bonds. There are four heat transferring mechanisms such as conduction, convection, radiation and phase changes [113]. The IR reflow soldering process provides a non-contact heat source for the soldering process, whilst in hand soldering technique described earlier the heat source (the soldering iron tip) is necessary to be physically in contact with the microelectronic chip and copper interconnects. IR reflow soldering is more efficient and leads to reducing the risk of damaging electronic components. There are different sizes of IR reflow soldering systems available in the market today. Small scale reflow soldering system are used in laboratories whist large scale systems are used in the industry. A small scale reflow soldering system from the company PDR Ltd was employed for this research work. That system is called 'PDR IR rework system' (Figure 4.2) (Annex 18)

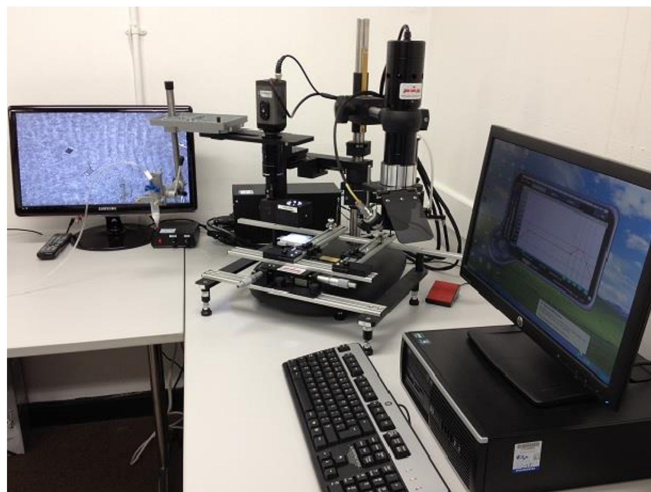

FIGURE 4. 2: AN EXAMPLE OF PDR IR REWORK SYSTEM USED IN THIS RESEARCH

The PDR IR rework system is controlled by a computer. The user-interface of the control software is shown in Figure 4.3. The software allows the operator to create or edit the heating profile required to create an efficient solder bond.

FIGURE 4. 3: THE USER INTERFACE OF THE CONTROL SOFTWARE OF THE PDR IR REWORK SYSTEM

Mainly, there are three steps in the reflow process. These are the deposition of solder paste accurately on the object; pick and place operation of the electrical components; and the application of heat to melt the solder. In the heating stage several steps are involved, to obtain a good solder bond. These are preheating, soaking (activation), reflow and cooling [113]. Each of these steps are important in optimising the electro-mechanical properties of solder joint. A typical reflow heating profile is shown in Figure 4.4.

Preheating: It is important to preheat the soldering area. This is important in PCB manufacture to avoid unnecessary thermal stress and spattering. In this stage, solvents and moisture are evaporated slowly and flux is transferred from the gel state to the fluid state.

Activation (Soaking): Flux reacts with the soldering surfaces and works as a cleaning agent by removing oil, oxides and other dirt. If the activation period is too long, it may affect the solder joints due to non-wetting or de-wetting of solder.

Reflow: In this phase the highest temperature of the heating profile is reached resulting in melting of the metal micro-spheres of the solder paste whilst flux helps to reduce surface tension and create a solder bond.

Cool Down: Finally, the soldering area (PCB) must be cooled down prior to safe handing. It is important, not to cool down rapidly to avoid thermal expansion or cracking the components [25].

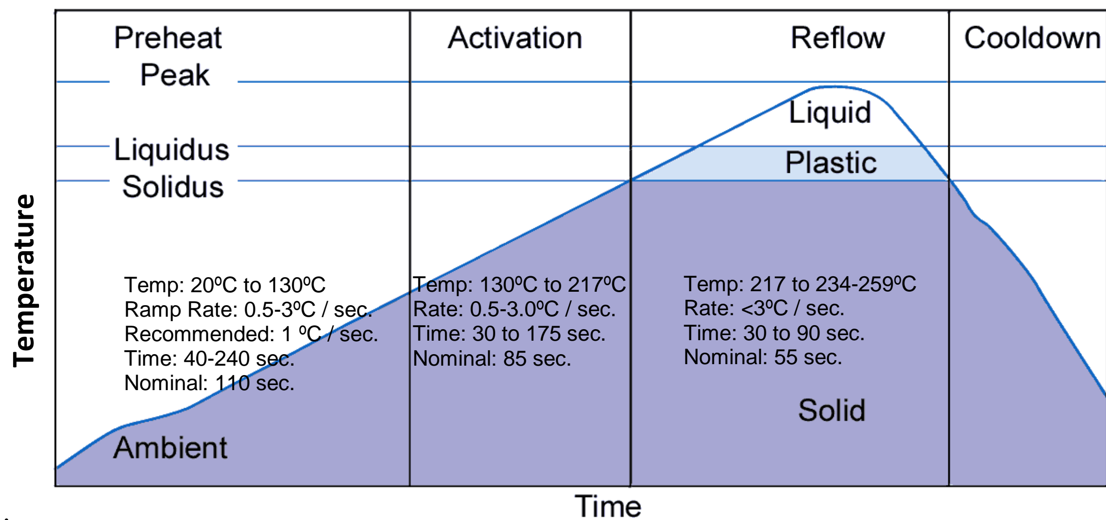

FIGURE 4. 4: A TYPICAL REFLOW HEATING PROFILE FROM EFD SOLDER PASTE SUPPLIER

4.2 Creation of Interconnections using Hand Soldering Technique

Preliminary laboratory work was carried out in order to identify the gaps in the current knowledge base for creating electronically-active fibres and yarns. The aim was to connect copper wires to the terminals of semiconductor devices (solder pads) prior to encapsulation with other fibres of the yarn. As this was one of the crucial steps, experiments were carried out to establish procedures that could be used to solder a single strand copper wire of 55 µm diameter to the anode and cathode of a 0402 SMD-type LED. The dimensions of the 0402 SMD type LED were length: 1000 µm, width: 500 µm and thickness: 500 µm. The dimensions of the solder pads were length: 500 µm and width: 400 µm. SMD type semiconductor packaged dies could be soldered onto PCBs using hand soldering [114, 115]. Soldering packaged dies onto the rigid surface of a PCB is not difficult, if one has a steady hand, good vision and a soldering iron with a small tip [116]. However, no literature, such as books, published papers and online resources, could be found on how to do hand soldering for such a micro-scale SMD-type electronic components onto flexible substrate such as textile yarn and fine copper wire. Firstly, it was very difficult to hold the chip whilst it was being soldered. After several failed attempts, it was decided to position the SMD 0402 type LED packaged die on double-sided tape prior to soldering as shown in Figure 4.5. A steel wire of diameter 150µm (manufacturer: SPRINT METAL) shown in Figure 4.1 was placed on the middle of the

chip to hold it down the chip. The wire also prevented molten solder from flowing between the two solder pads, which were 200µm apart, thus avoiding possible short-circuiting, which was an added advantage.

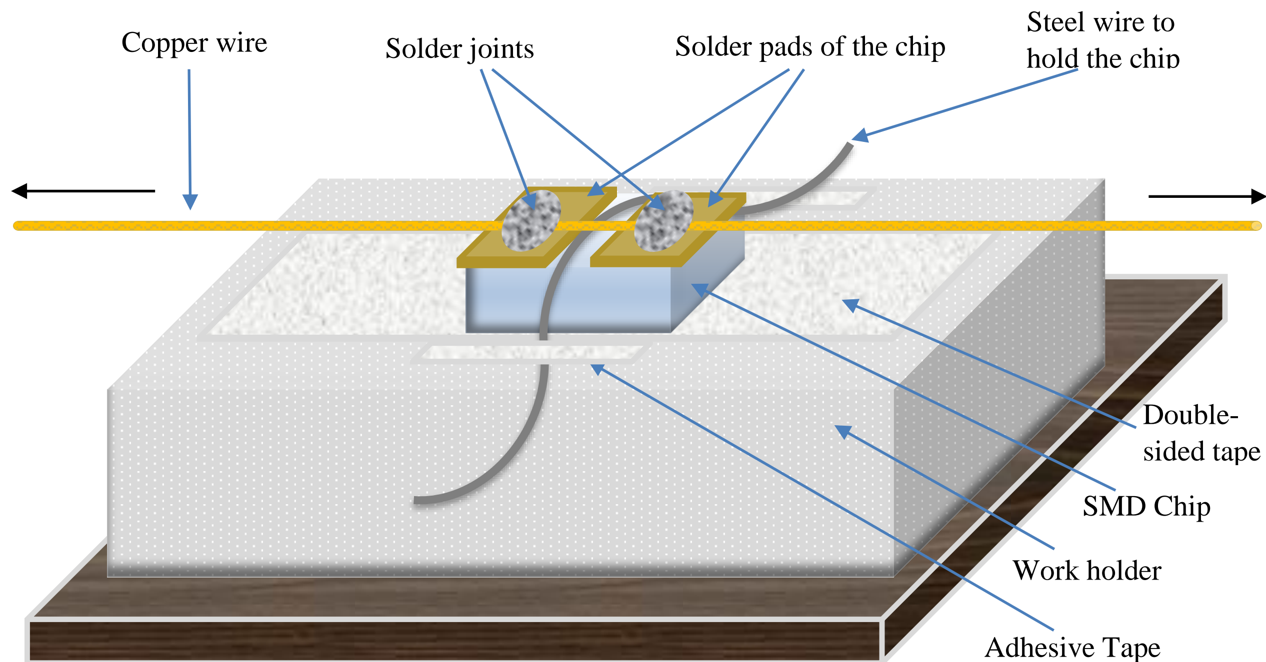

FIGURE 4. 5: SMD CHIP AND COPPER WIRE SET UP FOR HAND SOLDERING

After soldering both solder pads, it was necessary to cut the copper wire which was in between the solder pads; this was done by pulling away both ends of the steel wire together to break the copper wire between two solder pads.

An example of a hand soldered LED is shown in Figures 4.6 and 4.7. This activity was useful in identifying one of the key areas of the future research: the development of a technique for secure holding of the microchip and the creation of a secure solder bond between the solder pads and the copper wire.

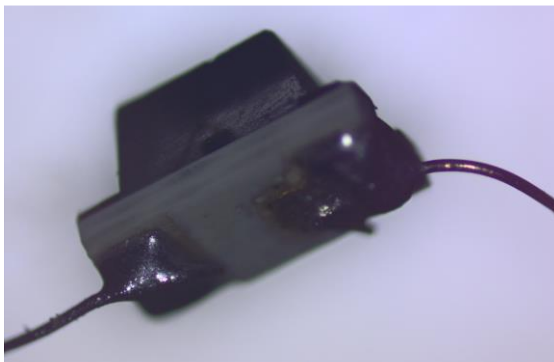

FIGURE 4. 7: MICROSCOPIC IMAGE OF SOLDERED MICRO LED CHIP (5 X MAGNIFICATION)

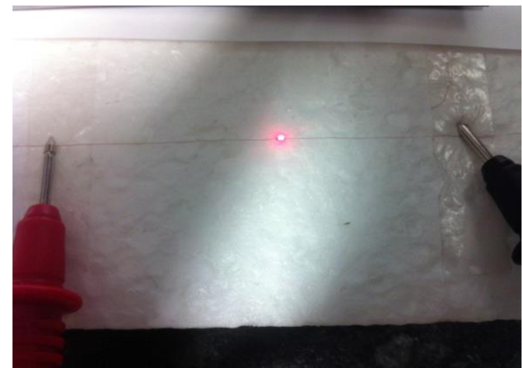

FIGURE 4. 6: A SOLDERED LED WHEN ENERGISED

The following areas of research were identified as important to progress the research from the preliminary experiments described above: Equipment was required that could form a strong and reliable solder joint between the terminals of microchips and conductive wires. This also included the identification of suitable conductive wires (fine single/multi-strand copper wires) and soldering materials (conductive solder pastes). This led to the use of a focused IR reflow soldering workstation, manufactured by PDR Ltd (referred to as the PDR IR Rework System in this thesis. (See Annex 18 for further details) and a precision dispenser system from EFD Ltd (EFD, model: Ultimus i). Many tests were carried out to analyse the strength and the reliability of the bonding between the solder pads and copper wires by using optical microscopy, tensile testing and washing trials. Moreover, the tests results were used to optimise the physical and electrical properties of the solder joints.

4.3 Creation of Interconnections using Reflow Soldering

The optimisation of reflow soldering techniques was a core part of this project. As explained earlier (section 4.1.10), the Rework System incorporates a radiation heat transfer mechanism, and employs IR electromagnetic rays to transfer focused heat energy required for the reflow soldering process. The PDR IR Rework System was a useful tool for creating good, soldered bonds between the solder pads of microchips and fine copper wires, without damaging the microchip circuitry, due to its contactless heat-transfer mechanism. As the PDR IR Rework System was developed for repairing PCBs, it was necessary to develop a new technique for soldering copper wires and packaged dies to create the necessary interconnects. A series of experiments was carried out to determine the efficient use of the PDR IR Rework System, as summarised below.

4.3.1: Determining the Solderability of Coated and Uncoated Copper Wires using the PDR IR Rework System

The aim of this experiment was to identify how to solder polyester coated copper wires to solder pads by using the reflow work station. The challenge was to remove the polyester coating prior to soldering. Uncoated copper wires were also soldered for comparison.

Equipment	Materials
• A PDR IR Reflow work system • A EFD dispenser (model: Ultimus i). • An air compressor • A multi-meter	• Lead-free solder paste (supplied by Koki Europe A/S, ref: 201265) Annex 10 • Uncoated, single-strand copper wire (supplied by Luxion, diameter 55µm) • Coated, single-strand copper wire (supplied by Luxion, diameter 70µm)

Procedure: A polyester-coated copper wire was laid on the work holder of the reflow work station, secured with adhesive tape and marked in ten places with one centimetre gaps between each point. The IR beam of the PDR IR Rework System was applied for sixty seconds at 300^0C for each marked place using a heating profile as shown in Figure 4.8. Pieces of uncoated copper wire were laid across each of the ten marked points and solder paste was applied to each. Heat was applied to produce solder joints between the coated copper wire and uncoated copper wires as shown in Figure 4.9 and 4.10. The test was then repeated using uncoated copper wire instead of coated wire. Finally, the electrical connectivity was checked for each soldered copper wire using a multi-meter.

FIGURE 4. 8: HEATING PROFILE

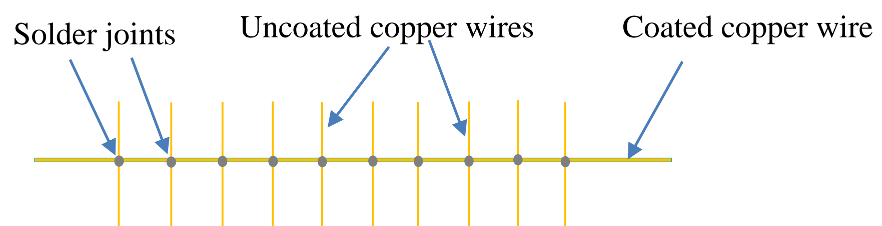

FIGURE 4. 9: SOLDERING ORIENTATION OF POLYESTER COATED COPPER

WIRE

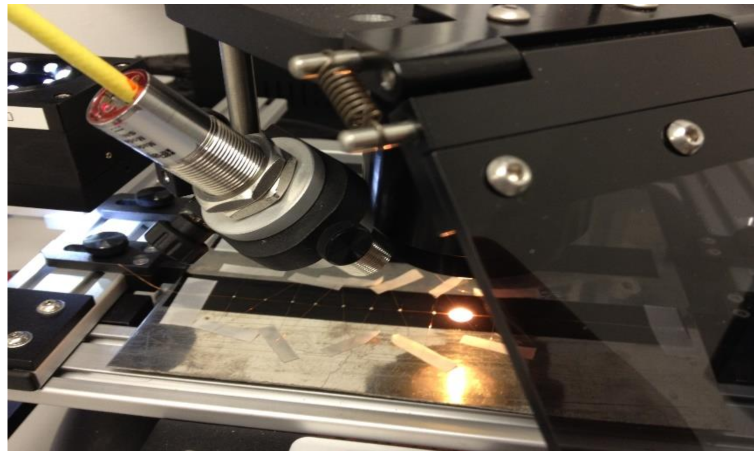

FIGURE 4. 10: THE SOLDERING PROCESS

Results and Discussion: All the solder joints of the uncoated copper wires were electrically connected, therefore it was shown that there were no issues with the solder paste and soldering process. However, none of solder joints of the coated copper wires were electrically connected as the polyester coating had not been removed successfully even though the temperature of 300 ^{0}C was higher than the melting point of polyester. The possible reason could have been that a fraction of the IR beam of the rework station has been reflected away by the copper wire without being absorbed by the coating layer. Therefore, it was determined that the polyester coating needed to be removed prior to soldering.

4.3.2: Polyester-Coated Copper Wire Soldering after Removal of the Coating

The polyester coatings of the copper wire were removed with a soldering iron and the procedure described in section 4.3.1 was repeated. A multi-meter was used to confirm the electrically connectivity of the wires.

Results and Discussion: The diameter of the polyester-coated, copper wires is 77 μm. Therefore, it was possible to damage the wires easily. It was noted that a few copper wires were damaged during removal of the coating by the hot soldering iron. It was still possible to remove coating in 10 places on a wire and to carry out the soldering process. It was observed that all ten joints were connected electrically (Figure 4.11).

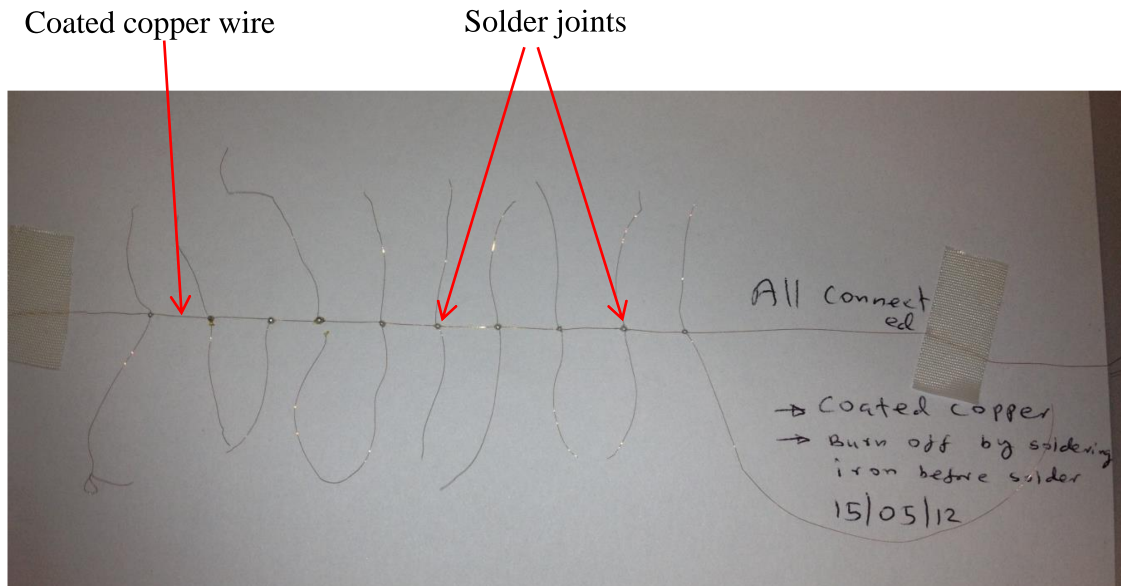

FIGURE 4. 11: THE COATED COPPER WIRE WHICH WAS SOLDERED SUCCESSFULLY

4.3.3: Method for Burning-off the Polyester Coating of the Copper Wire using Flux (Contactless Method)

The previous test proved that polyester coating could be removed from copper wires with a hot soldering iron. However, damage to the coated copper wire was observed. Therefore, a new experiment was carried out with the aim of determining whether the polyester coating of a copper wire could be removed by applying flux under the infrared beam of the PDR IR rework system.

Equipment	Materials
• A PDR IR Reflow system • A Multi-meter	• Coated, single-strand copper wire (supplied by Luxion, diameter 70 µm) • Flux (supplied by RS components • Adhesive glass tape (width: 25 mm and thickness: 0.15 mm) • Adhesive foil tape (width: 20 mm and thickness: 0.12 mm)

Procedure: Two layers of glass tape were adhered onto the aluminium plate (width: 1cm, length: 20 cm and thickness: 0.5 cm). The glass tapes are capable of withstanding heat and provide a gap between the aluminium plate and foil to create a micro-mould. A foil tape was then adhered onto the glass tape to create five micro-moulds (1.0 x 1.0 x 0.5 mm) by pressing a square piece of metal (cross section: 1.0 mm x 1.0 mm) onto the surface of foil tape. The micro-moulds were filled with flux, and a polyester-coated

copper wire was laid over the moulds as shown in Figure 4.12. The IR beam of the PDR IR Rework System was applied at each point for 40 seconds at 300^0C. (The heating profile was as shown in Figure 4.8.) The electrical connectivity was checked using a multi-meter at each place on the copper wire to determine whether the polyester coating had been removed.

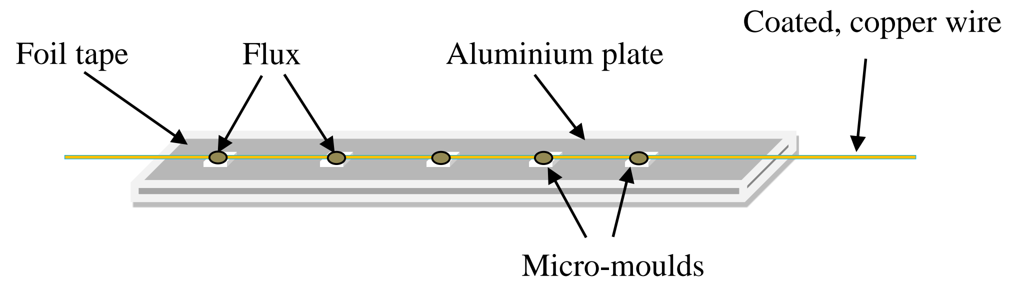

FIGURE 4. 12: THE ARRANGEMENT OF COATED, COPPER WIRE ON THE MICRO-MOULD ARRAY

Results and Discussion: Generally, flux is used for cleaning impurities of metal surfaces such as oil, dirt and oxide-films prior to soldering. Flux contains chemicals such as acids and chlorides and it is used to create a good solder bond during soldering of electronic components. Several methods exist to remove polyester coatings from wires, such as scraping using knives or blades, sanding using abrasive papers, melting using soldering irons or flames. However, fine wire may get damaged by these physical contact methods [117]. Therefore, novel techniques were found for removal of polyester coating without physical contact. It was observed that the polyester coating was successfully burned-off at all the required points on the copper wire, and no damage to the copper wire was detected. The chemicals in the flux may have contributed to the removal of the polyester layer of the copper wire. In addition, the flux provided a dark environment for the copper wire which was in the micro-mould, thus preventing any reflection of the IR beam by the surface of copper wire, resulting in the total energy of the IR beam being absorbed by the flux and copper wire.

4.3.4: Analysis of the Heating Profile Recommended by the Solder Paste Manufacturer for use with the PDR IR Rework System

The aim of this investigation was to study the suitability of the heating profile recommended by the solder-paste supplier.

Equipment	Materials
• PDR IR Rework System • EFD precision dispenser system (model: Ultimus i) • A Compressor	• Uncoated, 7-strand twisted copper wire (diameter: 100µm) • Solder paste (Ref: S62D500A6Z0, Lead version, Type VI, supplier: EFD) • Red LED, 0402 (ref: 4663633, supplier: RS) • Precision Tip: 25GA GP 0.01x0.5 Red (supplier: EFD)

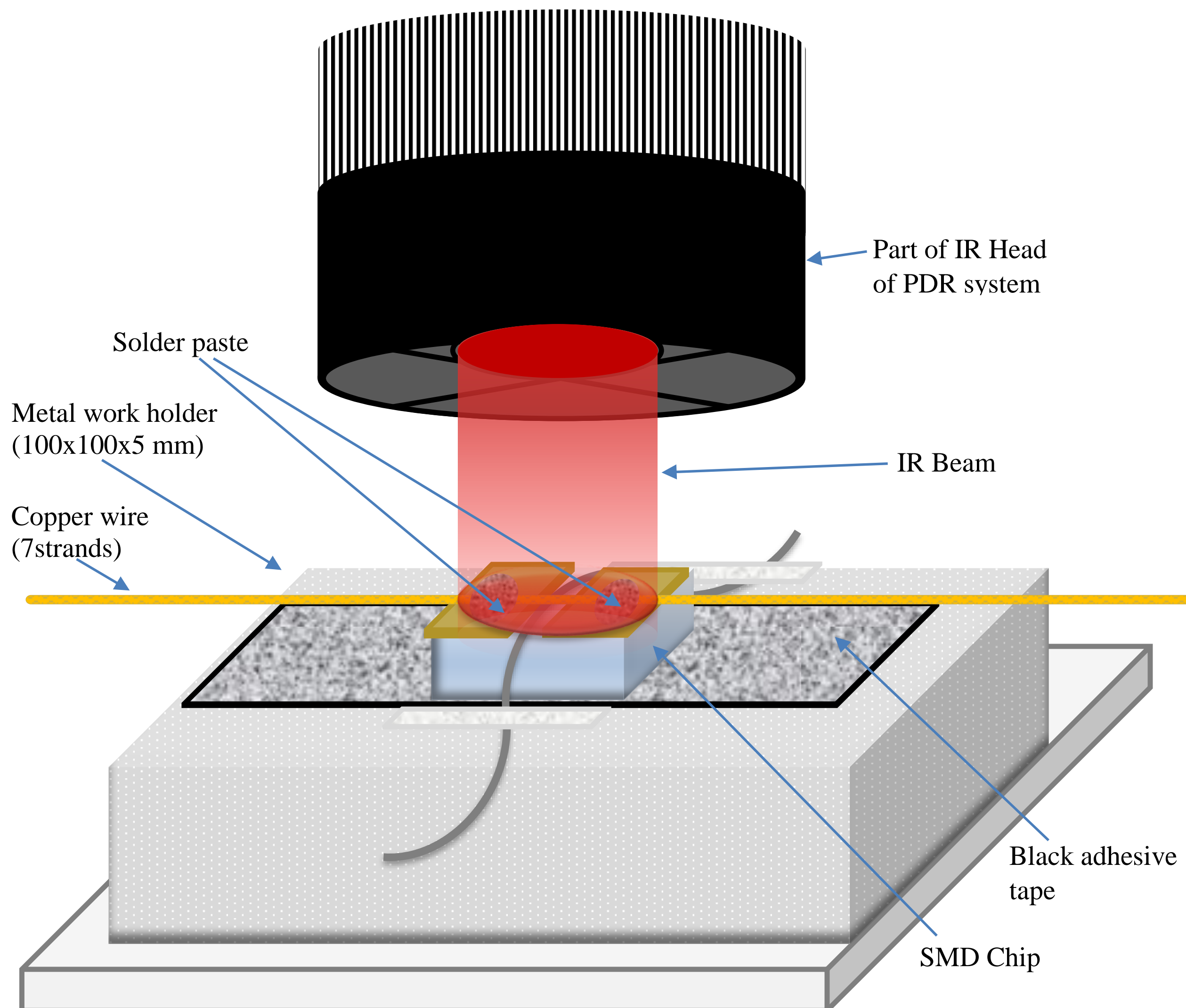

FIGURE 4. 13: SMD CHIP AND COPPER WIRE SET UP FOR REFLOW SOLDERING (NOT ACCORDING TO DIMENSIONS)

Procedure: Black adhesive tape of 2cm width was adhered to the metal work-holder plate using double sided tape (Note: According to the PDR IR rework system manufacturer's

instructions, the surface has to be black in order to obtain maximum energy absorption from the IR beam). A SMD 0402 type red LED (1.0x0.5x0.5mm) was then picked and placed onto the black tape. The LED was then secured with a steel wire of diameter 150µm. A seven-strand twisted copper wire was laid on the LED chip. Solder paste was deposited onto both solder pads of the LED chip using the EFD dispenser at a pressure of 228 kPa for 0.05 seconds. This resulted in 90 micrograms of solder paste being delivered by the dispenser system. The lead version was used in the beginning and changed to lead free version. The heating profile shown in Figure 4.14, which was recommended by solder paste manufacturer, was applied using the PDR IR rework system (with IR-spot diameter 5mm). The set-up of the test procedure is shown in Figure 4.13.

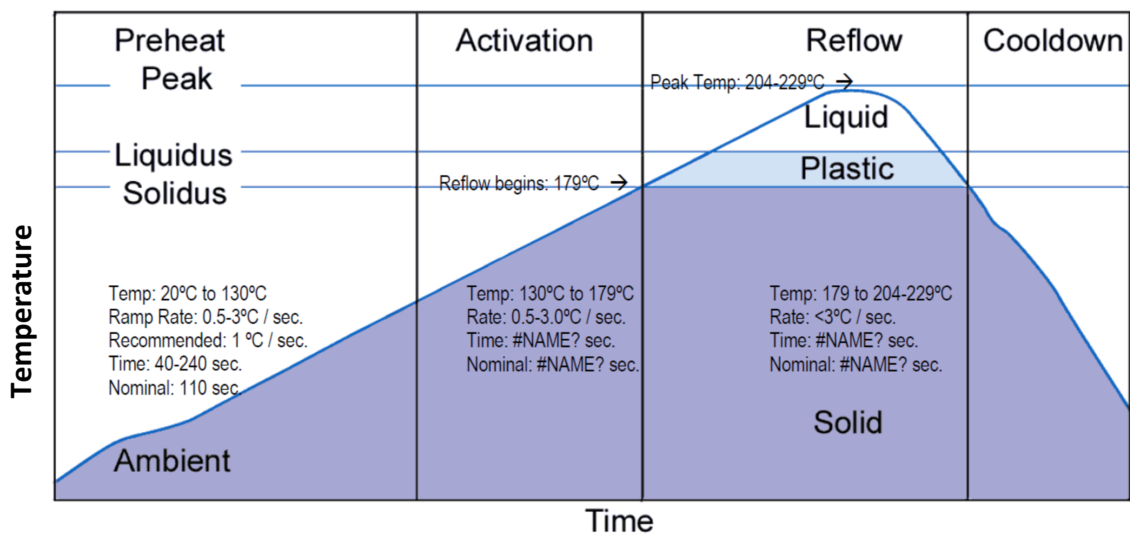

FIGURE 4. 14: THE PDR IR REWORK SYSTEM HEATING PROFILE AS RECOMMENDED IN THE TECHNICAL DATA SHEETS OF THE SOLDER PASTE MANUFACTURER

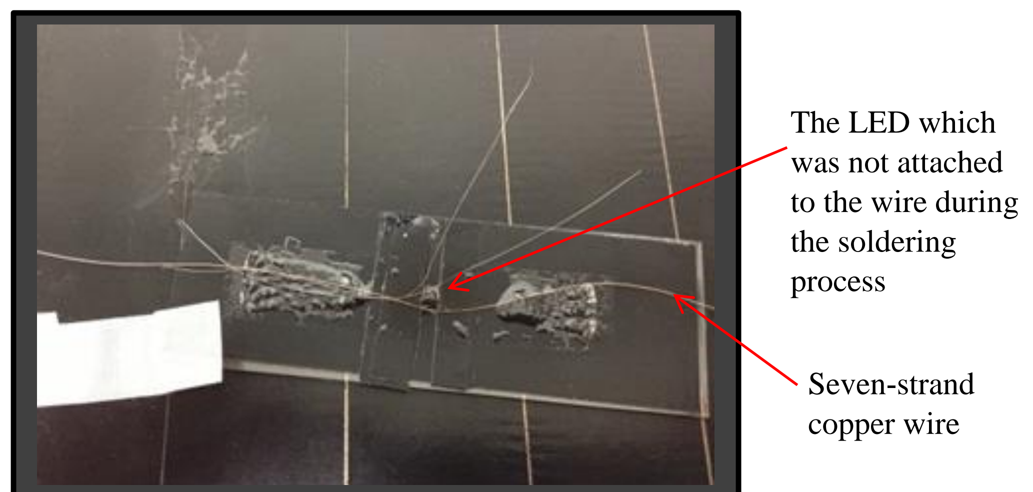

FIGURE 4. 15: LED CHIP AND COPPER WIRE AFTER APPLYING HEAT

Results and Discussion: The copper wire and LED chip were not joined together, as shown as Figure 4.15. The heating profile did not seem to be suitable for soldering SMD chips to copper wire. Ten tests were carried out by changing the above heating profile but none of them was successful.

4.3.5: Analysis of the Heating Profile Recommended by LED Manufacturer with PDR IR Rework System

The aim of this investigation was to identify whether the heating profile, which was recommended by the LED Company, was suitable for this project.

Equipment	Materials
• PDR IR rework system • EFD Dispenser system, (model: Ultimus i) • A Compressor	• Uncoated 7-strand, twisted copper wire (diameter: 100µm) • Solder paste (Ref: S62D500A6Z0, Lead version, Type VI, supplier: EFD) • Red LED, 0402 (ref: 4663633, supplier: RS) • Precision Tip: 25GA GP 0.01x0.5 Red (supplier: EFD)

Procedure: The same work holder plate as described above was used, and an SMD 0402 type red LED was placed onto the black tape. The LED was secured with the steel wire. A seven-strand, twisted copper wire wad laid on the LED chip. The same amount of solder paste 90 µg was deposited onto both solder pads of the LED chip and copper wire using the EFD dispenser. The heating profile, recommended by the manufacturer of the LED, was applied as shown in Figure 4.16. Finally, the portion of the copper wire that was between the two solder pads of the LED chip, was removed by using a sharp knife.

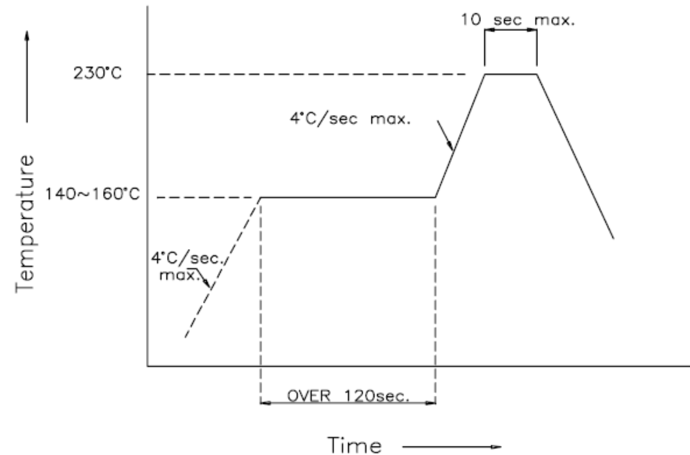

FIGURE 4. 16: PDR IR REWORK SYSTEM HEATING PROFILE WHICH IS RECOMMENDED IN THE MANUFACTURER 'S TECHNICAL DATA SHEET FOR THE 0402 SMD LED CHIP

Results and Discussion: The colour of the LED chip changed from clear to dark. The author believes this was due to overheating of the LED during soldering. Therefore, this temperature profile did not seem to be suitable for soldering LEDs to fine copper wires, even though the LED did light up when connected to a power supply. This heating profile was recommended for soldering SMD's onto printed circuit boards (PCB), which is the normal practice in the manufacture of electronic devices. In PCB manufacture the semiconductor chips are placed on top of conductive tracks on a board with the solder pads of the chip touching the conductive tracks (interconnects). Solder pads are not directly exposed to IR radiation in PCB manufacture, where the heat applied to the solder pads is provided through copper tracks and by preheating the PCB's.

4.3.6: Optimisation of the Heating Profile for Soldering Multi-Strand Copper Wires to Solder Pads

The experiments described in the above sections 4.3.4 and 4.3.5, demonstrated that the heating profiles recommended by the solder-paste and semiconductor chip manufacturer are not suitable for soldering copper wires to the solder pads of semiconductor packaged dies, because they had been recommended for soldering electronic components onto printed circuit boards (PCBs). It was observed that the heating times of those profiles were not suitable for soldering copper wires. Therefore, a detailed study was carried out to formulate a heating profile for creating the interconnections of micro devices for electronic yarn.

Equipment	Materials
• PDR IR rework system • EFD Dispenser system, (model: Ultimus i) • A Compressor • A laboratory power supply, TTi EX354T	• Uncoated 7-strand, twisted copper wire (diameter: 100µm) • Solder paste (Ref: S62D500A6Z0, Lead version, Type VI, supplier: EFD) • Red LED, 0402 (ref: 4663633, supplier: RS) • Precision Tip: 25GA GP 0.01x0.5 Red (supplier: EFD)

Procedure: Experiments were carried out in the same manner as outlined in sections 4.3.4 and 4.3.5, but using different heating profiles. The heating profiles are shown in Figure 4.17a to 4.17f. Finally, a 1.8 V voltage was applied using a laboratory power supply to check whether the LED's and copper wire had been soldered together.

FIGURE 4.17 A: HEATING PROFILE

FIGURE 4.17 B: HEATING PROFILE

FIGURE 4.17 C: HEATING PROFILE

FIGURE 4.17 D: HEATING PROFILE

FIGURE 4.17 E: HEATING PROFILE

FIGURE 4.17 F: HEATING PROFILE

FIGURE 4. 17: HEATING PROFILES WHICH WERE USED IN THIS EXPERIMENT

Results and Discussion: The heating profiles shown 4.17a to 4.17f were used. The rapid heating method was the most suitable (as shown Figure 4.17f). The system was setup to reach the optimum temperature in 10 seconds. The copper wire and LED solder pads were joined together successfully, as demonstrated by the LED functionality (Figure 4.18). The physical appearance of the LED chips was clear after soldering, and the solder joints were better than those created using the previous methods. The investigations of the electro-mechanical properties of the solder joints is reported in Chapter 6.

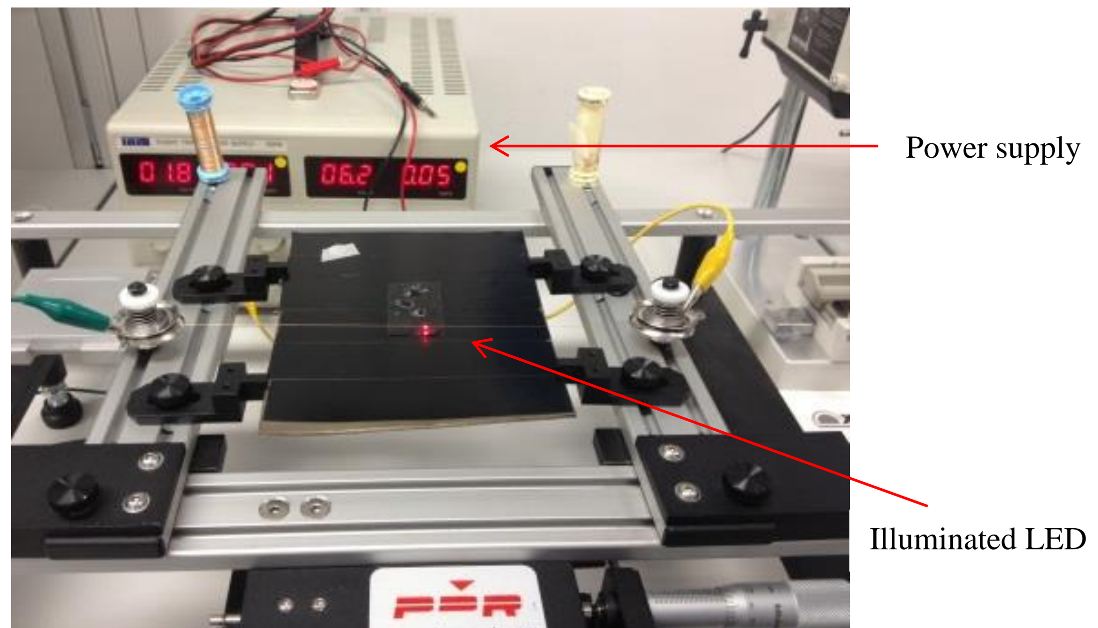

FIGURE 4. 18: AN EXAMPLE OF AN ILLUMINATED LED JUST AFTER SOLDERING

4.3.7: Development of Soldering Techniques for the 0201 Type Chips with Seven-Strand Copper

The aim of this experiment was to identify soldering parameters for SMD 0201 chips (600 x 300 x 230 µm). All experiments reported in the previous sections were carried out with SMD 0402 type chips (1000 x 500 x 500 µm). In this experiment, the parameters described in section 4.3.6 (pages 88 to 89) and the rapid heating profile were used.

Equipment	Materials
• A PDR IR rework system • A EFD Dispenser (Ultimus i) • A Compressor	• Uncoated 7-strand, twisted copper yarn (Diameter: 100µm) • Solder paste (ref: S62D500A6Z0, Lead version, Type VI and, supplier: EFD) • Resistor (0201, ref: 7550167 width: 300µm) • Precision Tip: 25GA GP 0.01x0.5 Red (supplier: EFD)

Procedure: This experiment was also carried out as in section 4.3.6, using the rapid heating profile. The amount of solder paste used was 70 µg.

Results and Discussion: It was necessary to cut and remove the 7-stands, twisted copper wire which remained between the two terminals of the resistor after soldering, to avoid sort circuiting. When this copper wire was cut, the solder joint was damaged due to weak solder joints (Figure 4.19). Ten experiments were repeated by using 7-strand, twisted copper wire, however none of them were successful. The area of the solder pad was 100 x 230 µm. The diameter of the 7-strand copper wire was 100 µm, and the surface area of the solder pads of the 0201 resistor chip was not enough to create a strong solder bond with the 7-strand copper wire.

FIGURE 4. 19: SOLDER JOINT FAILURE AFTER SOLDERING OF 0201 RESISTOR WITH 7 STRAND COPPER WIRE

4.3.8: Development of Soldering Techniques for the 0201 Type Chips with Single-Strand Copper Wire

As a good solder joint could not be created with the seven-strand, copper wire, as demonstrated in the previous section (4.3.7), the same experimental procedure was repeated with a single-strand copper wire of 55 µm diameter. The soldering joints were connected properly. Therefore, the results indicated that the finer copper wire (diameter: 55µm) was suitable for 0201 type SMD chips.

In view of the above success the experimental procedure was carried out with four-strand, copper wire (total diameter: 66 µm).

Results and Discussion: Ten resistor chips were soldered. Three solder joints were successfully created with good solder bonds whilst seven were created with very weak solder joints and they were broken when the copper wire was cut out from the gap in between the solder pads. The analysis showed that the diameter of the copper wire had to be selected according to the dimensions of the solder pads of the chip.

4.3.9: Development of Soldering Techniques for 0402 type Resistor Chips with Seven-Strand Copper

This experiment was carried out to identify whether 7-strand copper wire (Diameter: 100 µm) was suitable for soldering to SMD 0402 resistor chips. The experimental procedure described in section 4.3.8 was used.

Equipment	Materials
• A PDR IR rework system • A EFD Dispenser (Ultimus i) • A Compressor • A digital microscope (Olympus model BX41)	• Uncoated, 7-strand copper wire (Diameter: 100µm) • Solder paste (ref: S965D500A6Z0, Lead Free version, Type VI, supplier: EFD) • Resistor, 0402 (ref: 6678814, supplier: RS) • Precision Tip: 27GA TT 0.008” NAT

Results and Discussion: Ten trials were carried out with 7-strand copper wire, but all of them failed. The dimensions of the solder pads of the chips were examined using a microscope. As shown in Figure 4.20, one side of the solder pad is smaller than the other side. The dimension of the solder pad of the 0402 resistor in the technical data sheet (TDS) was 0.5 +/- 0.05 X 0.25 +/- 0.1 mm. However, the actual dimension of the smaller side

of the solder pad was 0.471 X 0.114 mm. The dimension of the other side of the pad was in accordance with the TDS. As one of the solder pads was smaller it was difficult to solder with 7-strand copper wire.

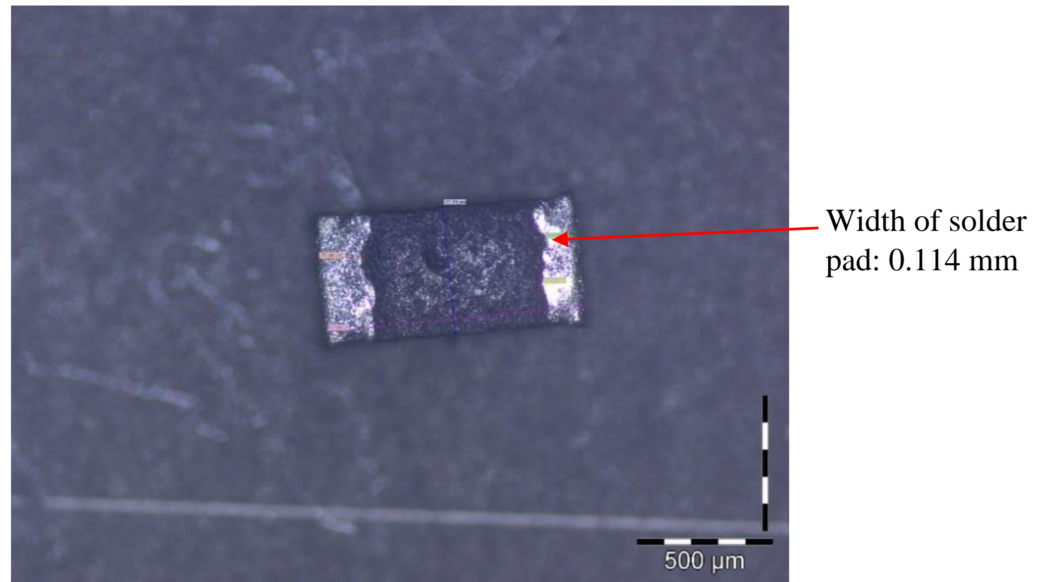

FIGURE 4. 20: A MICROSCOPIC IMAGE OF THE SOLDER PADS OF A 0402 RESISTOR CHIP

4.4 Analysis of Electrical Properties of Solder Joints

The electro-mechanical performance of solder joints is a very important factor in the electronics industry as it influences the performance and the reliability of the final product. This aim of the research was to develop the core technology to integrate microelectronics into yarns to produce electronic textiles. Textiles have to be flexible, washable, reliable, durable and able to withstand mechanical stress. Therefore, the electrical properties of solder joints are a crucial factor.

4.4.1 Development of a Method to Analyse the Electrical Properties of Solder Joints

The electrical resistance of the solder joint influences the performance of semiconductor devices. Therefore, a method to evaluate the electrical performance of the solder joints based on DC resistance was developed, which is described below.

There are few parts that contribute to the total resistance of final e-yarn such as interconnects (copper strands, solder joints and semiconductor chips (such as resistors and thermistors). For an example, the resistance at different points of the resistor with the interconnects can be divided into different name as shown in Figure 4.21.

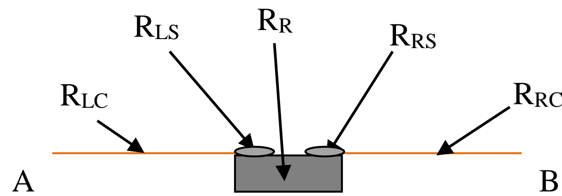

FIGURE 4. 21: SCHEMATIC OF RESISTANCES MEASURED IN SMD RESISTOR CHIP AND SOLDERED INTERCONNECTS

The resistance between A and B is;

$R_{AB} = R_{LC} + R_{LS} + R_R + R_{RS} + R_{RC}$ ……………………..7.1

Where;

Resistance of left copper wire: R_{LC}

Resistance of left solder joint: R_{LS}

Resistance of resistor chip: R_R

Resistance of right solder joint: R_{RS}

Resistance of right copper wire: R_{RC}

It is difficult to determine the resistances of solder joints, R_{LS} and R_{RS} individually. Because of this, the total resistance of the solder joints can be calculated as below formula 7.1a. This formula was used for experiments in section 4.4.2 and 4.4.3.

Total resistance of the solder joints (RLS + RRS) = RAB – RLC – RRC – RR……7.1a

4.4.2. Analysis of Solder Joints Created by Hand Soldering

A single strand of copper wire of length 100 cm was soldered onto the solder pads of SMD resistor chips type 0201 and the resistances of the different sections of the electrical circuit were measured with an Agilent 6 ½ Digit Multi-meter (model: 34410A) as described in previous section. The resistances of each resistor chip R_R were measured prior to soldering. The procedure used for soldering is given below.

Test Procedure:

- The resistance of 0201 type SMD resistor (ref number: 7550167) was measured by using Agilent multi-meter before soldering the resistor
- Double-sided tape was adhered to the work holder
- The resistor was laid on the adhesive tape

- A single copper wire (Diameter: 55μm) was placed in the middle of the resistor so that it was touching both terminals (solder pads) of the resistor chip
- Some flux and heat were applied to clean the solder pads of the resistors
- The soldering-iron tip was cleaned and tinned with solder
- The soldering iron was touched onto the two solder pads of the chip
- The solder joints were checked to see whether the soldering had been effective.
- The copper wire which remained, in between the 2 soldered joints, was removed to avoid creation of a short-circuit.
- The total resistance of resistors A to B, R_{LC}, R_{LS}, R_R, R_{RS}, R_{RC} (as described in section 4.4.1) were measured using the Agilent multi-meter
- The test was repeated for 10 resistors.

Results

The results are shown in Table 4.1. The results demonstrated that the total resistance of the two solder joints varied between 0.44 and 9.08 Ohms, and that there was a large standard deviation of 2.88.

No	Total R (A to B) Ω	R_R Ω	R_{LC} Ω	R_{RC} Ω	Resistances of solder joints (R_{LS} + R_{RS}) Ω
1	111.12	104.28	2.82	2.75	1.27
2	111.90	104.58	3.06	3.76	0.50
3	114.80	105.10	2.88	3.15	3.67
4	118.80	104.78	2.44	2.50	9.08
5	111.56	104.31	2.93	3.01	1.31
6	113.54	104.89	2.82	3.25	2.58
7	117.62	105.24	3.12	2.96	6.30
8	111.23	104.12	3.52	3.15	0.44
9	112.65	104.52	2.96	3.85	1.32
10	111.85	104.87	3.24	3.11	0.63
Avg	113.51	104.67	2.98	3.15	0.63
St Dev	2.74	0.37	0.29	0.41	2.88

TABLE 4.1: DC RESISTANCES OF HAND SOLDERED SOLDER JOINTS

4.4.3 Analysis of the Electrical Properties of Solder Joints Formed with the PDR IR Rework System

A single-strand copper wires were soldered onto the solder pads of SMD resistor chips using the PDR IR Rework System. The heating profile shown in section 4.3.6 (pages 88 to 89) was used with solder paste (ref: S965D500A6Z0, Lead Free version, Type VI, supplier: EFD) for the soldering process. Ten samples were made for evaluation. The results of the resistance measurements are given in Table 4.2 below.

Results

According to results shown table 4.2, the standard deviation was 0.62 which is lower than the results in table 4.1. It is evident from the results that better solder joints with less variability in resistance can be formed with a PDR IR rework system compared to those produced by hand soldering. The PDR IR rework system was therefore used to solder copper wires onto the solder pads of SMD microchips.

No	Total R (A to B) Ω	R_R Ω	R_{LC} Ω	R_{RC} Ω	Resistances of solder joints ($R_{LS} + R_{RS}$) Ω
1	112.55	105.14	3.0	3.73	0.68
2	111.83	104.68	2.75	3.30	1.10
3	113.10	104.69	2.94	2.86	2.61
4	111.50	104.80	3.30	2.94	0.46
5	111.46	105.08	2.85	3.01	0.52
6	110.90	104.58	2.96	2.78	0.58
7	112.29	104.63	3.15	3.65	0.86
8	112.21	104.95	2.83	3.28	1.15
9	110.91	104.15	2.91	2.97	0.88
10	111.99	105.32	2.78	2.87	1.02
Avg	111.87	104.80	2.95	3.14	0.99
Stdev	0.70	0.34	0.17	0.34	0.62

TABLE 4.2: THE RESULTS OF RESISTANCE MEASUREMENTS OF SOLDER JOINTS MADE WITH THE PDR IR REWORK SYSTEM

4.5 Analysis of Mechanical Performance of Solder Joints

Electronic yarn should be able to withstand mechanical stresses during the manufacturing processes and afterwards, during day to day use. The reliability of electronic textiles will depend largely on the mechanical strength of the solder joints. Therefore, it was necessary to analyse and improve the mechanical strength of the solder joints of the electronic yarn. Tensile tests were carried out on soldered, semiconductor chips, encapsulated chips (carrier yarns), and on the final, assembled electronic yarns encased within circular, warp-knitted sleeves.

4.5.1 Tensile Testing of Soldered 0201 Resistors with 4 Strands Copper Wires

In order to determine the strength of the solder joints, four strand-copper wires were soldered onto five SMD resistor chips type 0201 and tested for breaking strength. The solder joints were formed with the PDR IR rework system using the heating profile described in section 4.3.8 and EFD solder paste (ref: S965D500A6Z0, Lead Free version, Type VI, supplier: EFD). The tensile tests were carried out using a Zwick / Roell Z 2.5 (ref no: A707329). Tensile Testing Machine (Figure 4.22). An Agilent 6 ½ Digit Multi-meter (model: 34410A) was used to measure the resistance during the tensile tests.

Tensile Test Parameters:

- Tensile test standard: DIN EN ISO 2062:1995
- Pre-load: 0.5 cN/tex
- Test speed: 250 mm/min
- Grip to grip separation at the start position: 250 mm
- The Agilent multi meter was connected to both ends of the copper wire
- Resistance variation was monitored and recorded

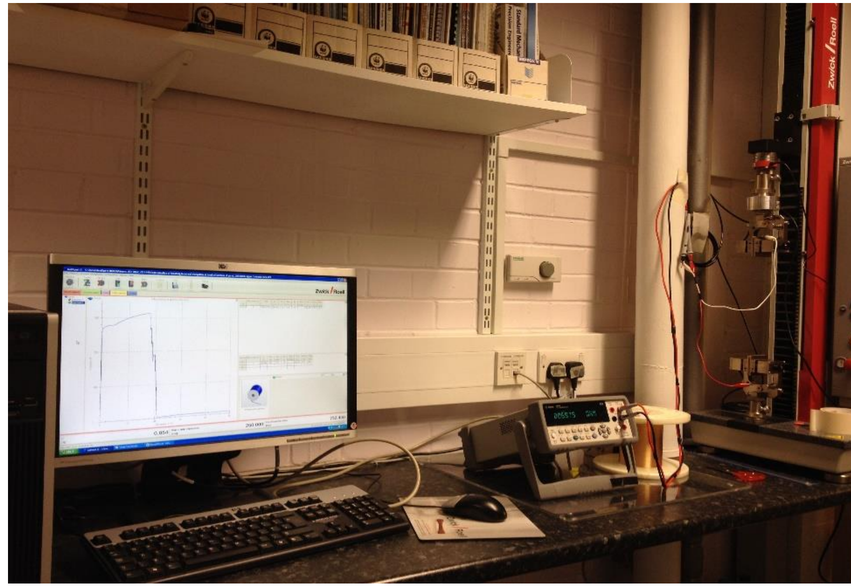

FIGURE 4. 22: TENSILE TEST AND RESISTANCE MEASUREMENT EQUIPMENT

Results and Discussion

An example of tensile test result is shown in Figure 4.23. It was observed that the solder joints were strong and had not been broken at solder joints. However, when the solder joints were examined under a digital optical microscope, Olympus (model: BX41), it was observed that the solder pads were detached from the chips as shown in Figure 4.24. This was observed for all five samples tested. The resistance measurements of the copper wire with solder-resistant chips demonstrated, as shown in Figure 4.23, that the resistance increased during the stretching of the test samples in the tensile tester. An infinite resistance was recorded by the multi-meter at the end of the tensile tests, due to the detachment of the solder pad from the chip. According to table 3.3 of chapter 3 (page 55), the average tensile breaking strength of the four-strand copper wire was 116 cN with a standard deviation of 12.6. However, in the results given in table 4.3, the average breaking strength of the four-strand copper wire with resister chip occurred at 98 cN due to the solder pads being detached from the packaged die. One could conclude that solder joints with good mechanical strength were formed with PDR IR rework system using the optimised heating profile and EFD solder paste. On the other hand, one cannot improve the bonding strength of the solder pads to the packaged die for off-the-shelf devices. Therefore, a study was undertaken to understand how one could improve the overall strength of the copper wire soldered to the chips. This is described in the following sections.

Specimen	L_v	F_H	R_H	Yarn Count
No.	mm	cN	cN/tex	Tex
1	250	99.5	3.71	26.8
2	250	98.0	3.66	26.8
3	250	101.1	3.78	26.8
4	250	95.5	3.57	26.8
5	250	96.5	3.60	26.8
Avg	250	98.12	3.66	26.8
Stdev	0	2.25	0.08	0

TABLE 4.3: RESULTS OF THE TENSILE TESTS OF FOUR-STRAND COPPER WIRES SOLDERED TO SMD RESISTOR CHIPS

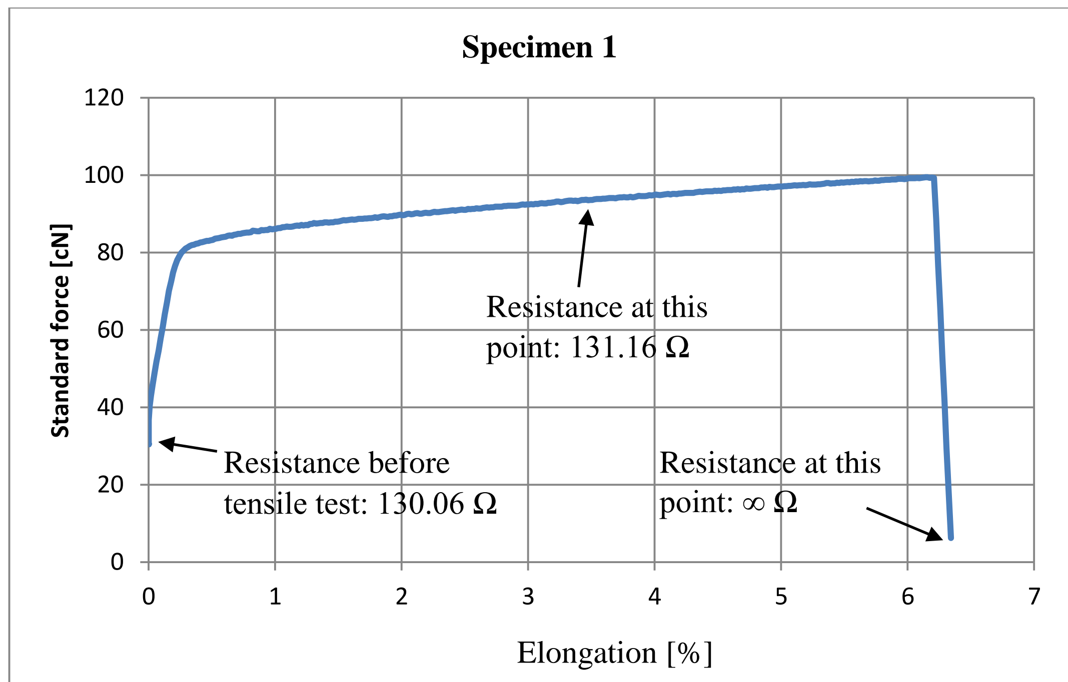

FIGURE 4. 23: THE LOAD – ELONGATION CURVE OF FOUR-STRAND COPPER WIRE SOLDERED TO AN SMD RESISTOR CHIP (SPECIMEN 1)

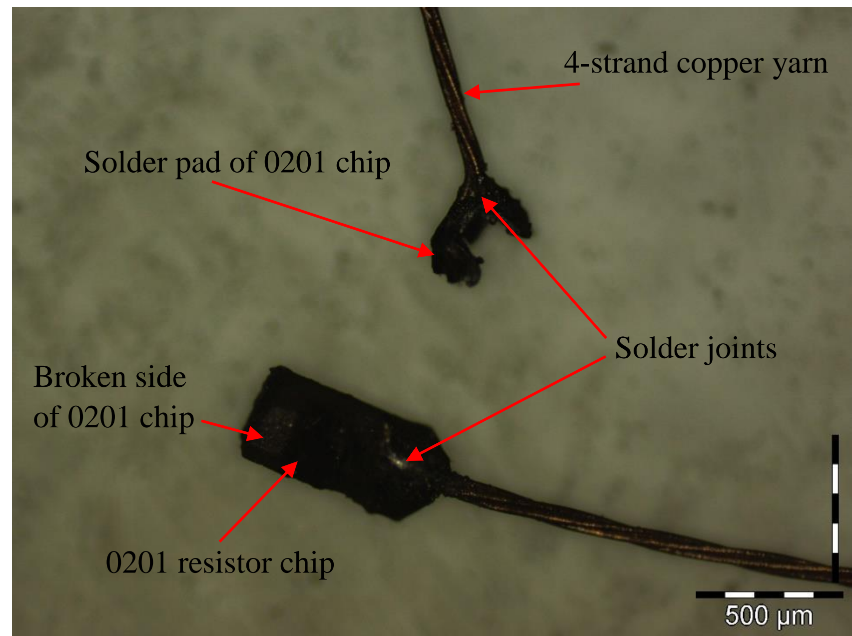

FIGURE 4. 24: MICROSCOPIC PICTURE OF SOLDERED 0201 CHIP AFTER TENSILE TEST

4.5.2 Tensile Testing of Copper Wire Soldered with LEDs

Two different types of SMD semiconductor chips were used in the research and, therefore it was necessary to evaluate the mechanical strength of seven-strand copper wires soldered to SMD chips type 0402. In the previous section, the mechanical strength of four-strand copper wire soldered to SMD resistor chips of type 0201 was analysed. Due to the dimensions of the solder pads only four-strand copper wire could be used in the analysis, and it was important to evaluate the mechanical strength of the solder joints when these were formed with copper wire with a higher number of strands. Therefore, the test procedure described in the previous section was repeated with seven-strand copper wire soldered to SMD blue and red LEDs type 0402. An example of seven-strand copper wire soldered with a blue LED is shown in Figure 4.25.

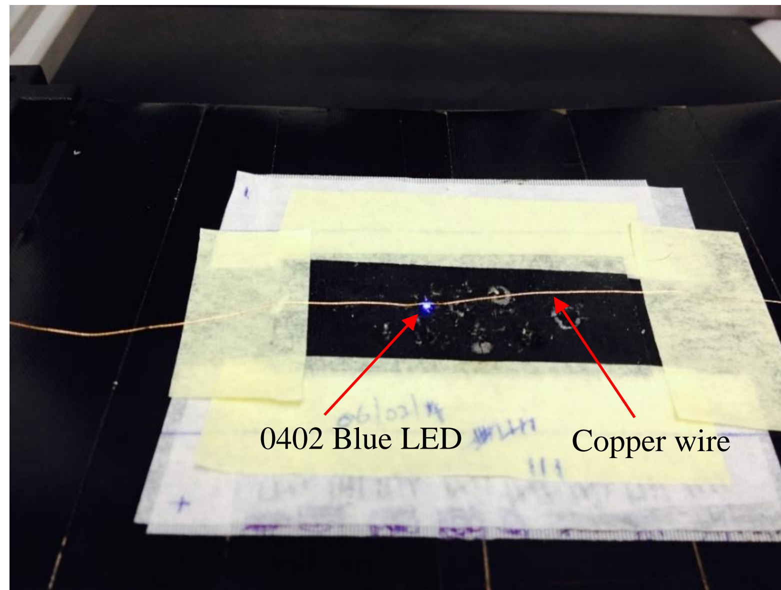

FIGURE 4. 25: AN EXAMPLE OF ILLUMINATED BLUE 0402 LED JUST AFTER SOLDERED

A copper wire with an LED was clamped between the jaws of the tensile tester, which were electrically insulated, and the LED was powered from a laboratory power supply (model: TTi EX354T) in order to determine when the solder joint had been broken during testing (see Figure 4.26). The results are shown in table 4.4 (Appendix 14), Figure 4.27 and Figure 4.28.

Tensile Test Parameters:

- Tensile test standard: DIN EN ISO 2062:1995
- Pre-load: 0.5 cN/tex
- Test speed: 250 mm/min
- Grip to grip separation at the start position: 250 mm
- TTi EX354T Triple Power Supply was connected to both ends of copper wire
- Five specimens were tested
- While tensile test was taking place, the illumination of LED was monitored

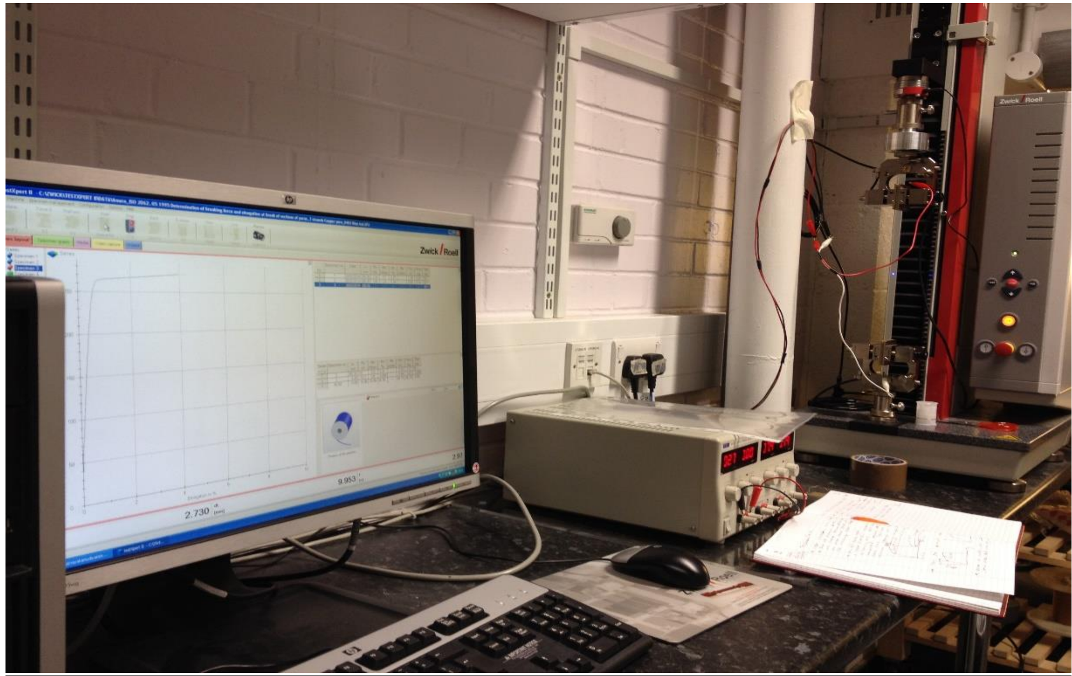

FIGURE 4. 26: TENSILE TEST AND POWER SUPPLY ARRANGEMENT

Results and Discussion

Observations undertaken with a microscope showed that the solder pads of the 0402 chips became detached from the 7-strand copper wire at the tensile breaking point (Figure 4.27). The copper yarn of the last specimen was broken without damaging soldered area. The strength of the attachment between the solder pads and the package die is a function of the die manufacturing process. However, one copper wire broke while the solder pads remained in place. It can be concluded that the solder joints between copper strands and solder pads of dies were strong.

Specimen	L_v	F_H	R_H	Yarn count	Which part was broken
No.	mm	cN	cN/tex	Tex	at the breaking point
1	250	213.99	3.68	58.1	Solder pad
2	250	168.39	2.89	58.1	Solder pad
3	250	277.98	4.78	58.1	Solder pad
4	250	250.05	4.30	58.1	Solder pad
5	250	246.80	4.25	58.1	Copper wire
Avg	250	231.44	3.98	58.1	
StDev	0	41.92	0.72	0	

TABLE 4.4: TENSILE TEST RESULTS FOR SOLDERED BLUE LEDS WITH 7-STRAND COPPER WIRE

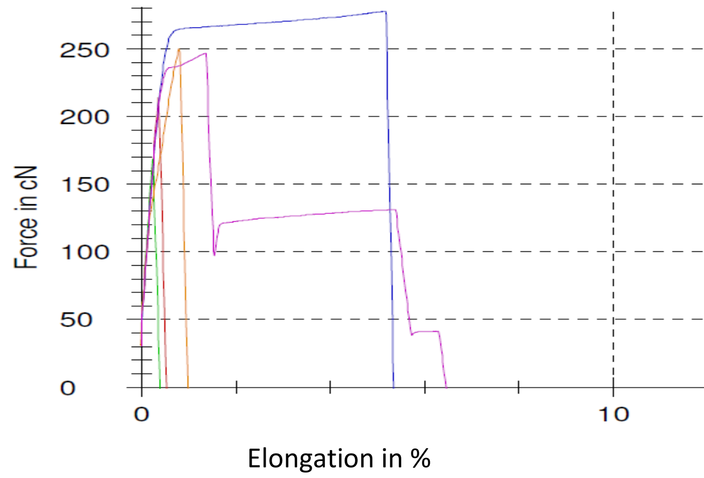

FIGURE 4. 27: GRAPH OF TENSILE TEST OF TABLE 4.4

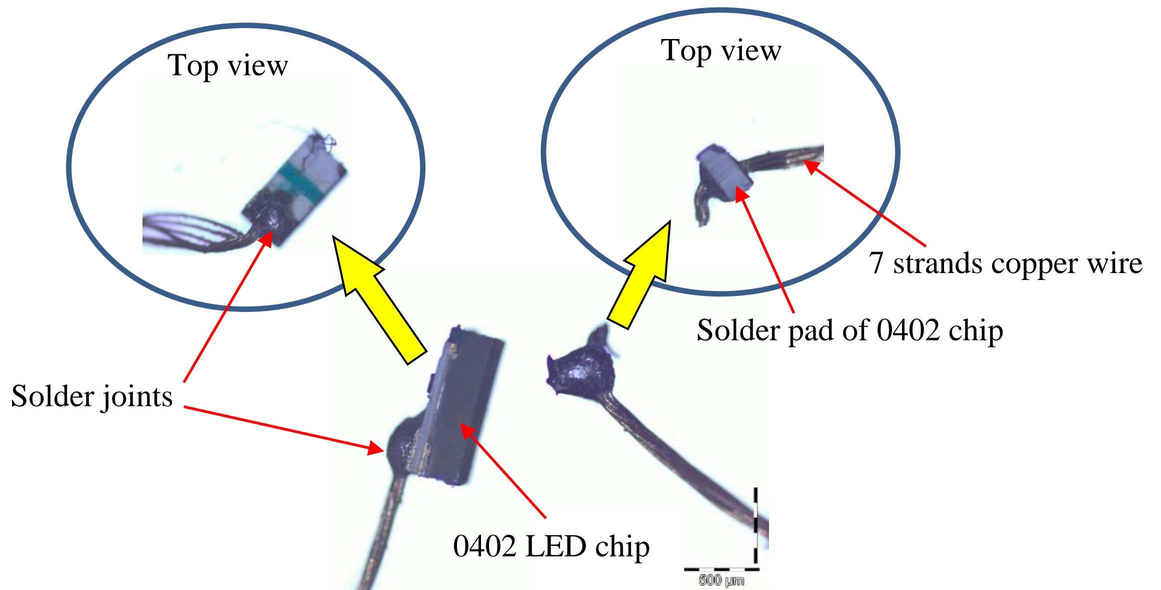

FIGURE 4. 28: MICROSCOPIC PICTURES OF SOLDERED 0402 CHIP AFTER TENSILE TEST

4.5.3 Tensile Test for Soldered 0402 Red LEDs with 7 Strands Copper Wires

The aim of this experiment was to analyse the strength of solder joints between 0402-type, red SMD LEDs and 7-strand copper wires. The test described in section 4.5.2 was repeated using red LED's instead of blue LED's.

Results and Discussion

The results show that in four of the samples tested the seven-strand copper wire broke, and in only one sample, one of the solder pads was detached from the chip. In all the four samples (i.e. 1 to 4 in table 4.5 (Appendix 15)) the corresponding LEDs did light up when the unbroken copper wires were connected to the power supply as shown in Figure 30, The results demonstrated that strong solder bonds were formed with the PDR IR rework system using the heating profile described in section 4.3.8 and EFD solder paste (ref: S965D500A6Z0, Lead Free version, Type VI).

Specimen No.	L_v mm	F_H cN	R_H cN/tex	Yarn count Tex	Which part was broken at the breaking point
1	250	308	5.29	58.1	Copper wire
2	250	197	3.39	58.1	Copper wire
3	250	307	5.27	58.1	Copper wire
4	250	305	5.24	58.1	Copper wire
5	250	246	4.23	58.1	Solder pad
Avg	250	272.60	4.68	58.1	
Stdev	0	49.77	0.85	0	

TABLE 4.5: TENSILE TEST RESULTS FOR SOLDERED RED LEDS WITH 7-STRAND COPPER WIRES

Series graph:

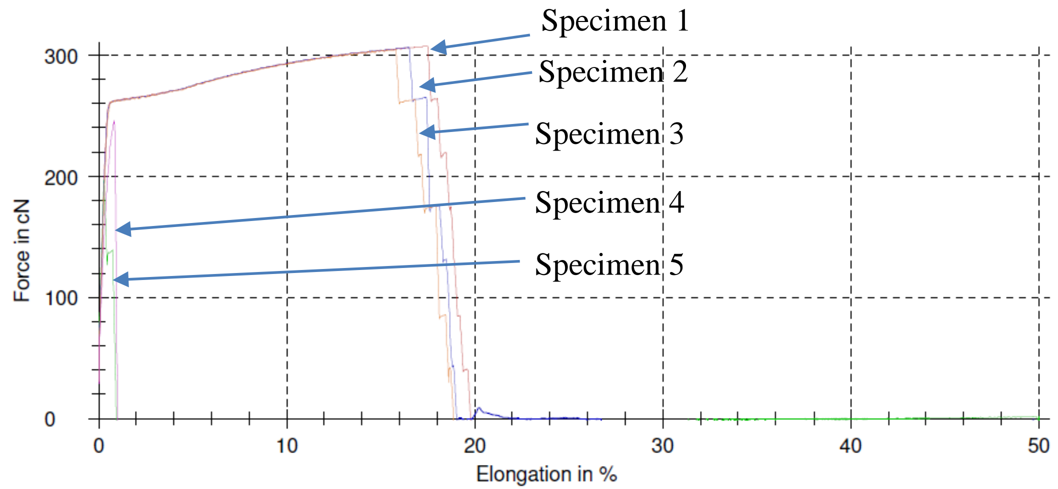

FIGURE 4. 29: LOAD – ELONGATION CURVES OF SEVEN-STRAND COPPER WIRE SOLDERED TO RED LED'S TYPE 0402

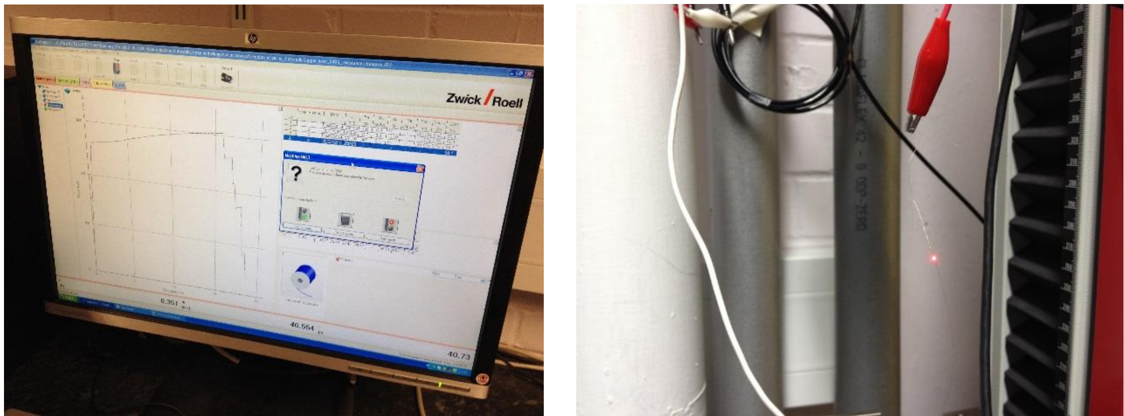

FIGURE 4. 30: AN LED THAT WAS STILL FUNCTIONAL AFTER BREAKING OF THE ATTACHED COPPER WIRE DURING TENSILE TESTING

4.4 Analysis of the IR Beam of PDR IR Rework System

It was necessary to understand the functionally of the IR beam, in order to utilize the PDR IR Rework system to obtain optimum usage of IR beam energy. The PDR IR Rework System was developed for PCB manufacture and the IR heating unit consists of an aperture to adjust the beam size and a lens system to project infra-red radiation onto the work piece (Figures 4.31 and 4.32) [118]. The IR beam size can be changed by rotating the aperture according to the soldering component size, without damaging other components of the PCB.

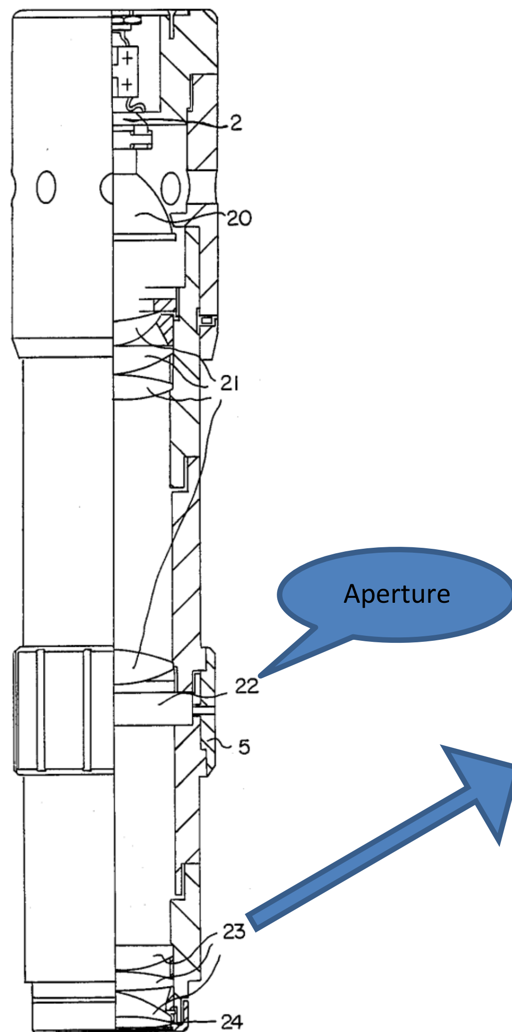

FIGURE 4. 31: A CROSS-SECTION OF LAMP AND IR REWORK LENS HOUSING OF THE PDR IR REWORK

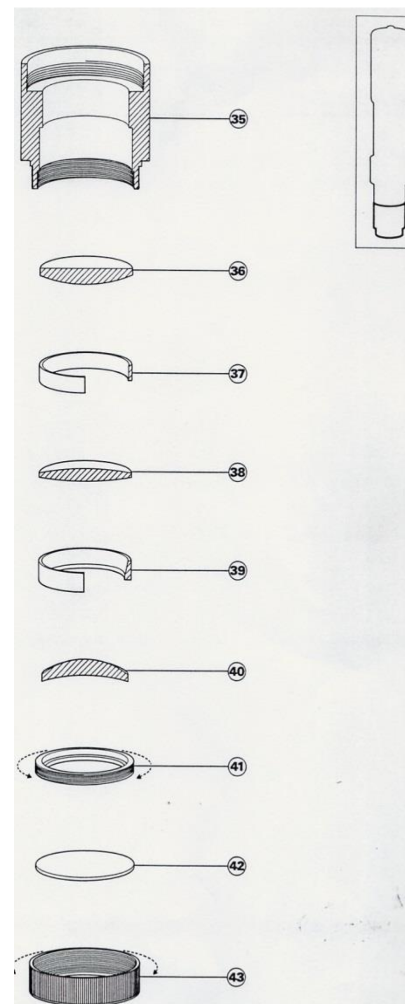

FIGURE 4. 32: LENSES OF PDR SYSTEM [21]

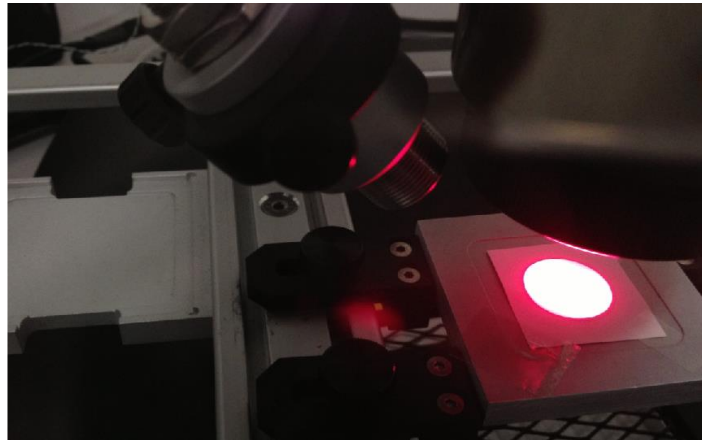

FIGURE 4. 33: THE MAXIMUM SIZE OF THE IR BEAM OF THE PRD SYSTEM

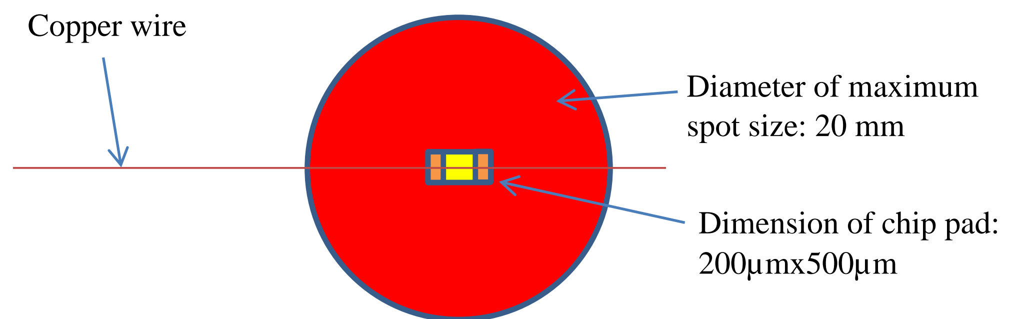

FIGURE 4. 34: COMPARATIVE DIMENSIONS OF THE IR SPOT AND THE 0402 LED CHIP, WHEN THE APERTURE IS FULLY OPEN

Calculation:

Area of Spot = $A = \pi r^2$

= 3.142 x 10^2 mm^2

= 314.2 mm^2

Area of chip pads = 2 x 0.2 x 0.5 mm^2

= 0.2 mm^2

The ratio of areas (chip pads: spot) = 0.2: 314.2

= 1: 1571 or chip pads area 0.06% of spot area

Discussion of the Results

The chip pad area is negligible compared with the IR spot area when the aperture is fully opened (at maximum spot size). The output of infra-red energy does not vary with spot size as an aperture is used to change the spot size. However, when one uses the highest

spot size, this will help to warm up quickly the supporting plate which use to hold the electronic components, and as a result, it will reach the heating temperature profile quickly. Otherwise the actual timing to achieve the heating profile would be longer than the profile setting timings. The PDR IR Rework System consists of another heating unit in the base which is called the back-heat unit. This is used for pre-heating and obtaining the maximum heating profile (i.e. 250 ^{0}C). The spot size has to be adjusted if there are other components around the work piece and if there is a risk of damaging those components from heating.

4.5 Conclusion

In the beginning of the project, hand soldering tests were undertaken to understand how to handle the electronic chips and copper wires using suitable raw materials and equipment. The heating profiles of a PDR IR Rework System which was recommended by the raw material suppliers, were not suitable for soldering micro-devices and copper wires. After several trials, a rapid heating profile was developed to optimise the mechanical and electrical properties of the soldered joints. A novel concept of contactless technique was developed to remove the polyester coating of the copper wire through use of flux combined with the IR beam of the PDR IR rework system.

Seven-strand copper wire (diameter: 100µm) was found to be the most suitable for soldering 0402 type chips as it exhibited good mechanical and electrical properties. However, seven-strand copper wire was too big to solder to 0201-type chips. Single-strand copper wire (diameter: 55µm) was suitable for 0201 type chips.

CHAPTER FIVE

5.0 Encapsulation

5.1 Introduction

The washability of electronic textiles is one of main challenging areas in the E-textiles industry [119]. Most E-textiles in the market today are not washable like normal garments as the electronic components of E-textiles are not fully protected and can be easily damaged. Some of those E-textiles can be washed but the electronic devices have to be removed prior to washing to protect them from water. Therefore, such E-textiles in the market today may not be user friendly. The current trend is to wear easy-care and more user-friendly garments, and washability is a basic requirement. Therefore, the encapsulation of the chip and solder joints to create the polymer micro-pod is very important. The micro-pod will also protect the electronic components and solder joints from tensile, bending and torsional stresses that the electronically-functional yarns will be subjected to during fabric manufacture and dyeing and finishing processes, while retaining basic textiles characteristics in the rest of the yarn. Moreover, the encapsulated resin micro-pod protects and improves the durability of the electronic components.

Different types of resins are used in industry for encapsulating printed circuit boards (PCBs). Popular resins are epoxy, hot melt, unsaturated polyester, urethane and silicones [120]. The selection of the type of resin to create the micro-pod will depend on the end user application, for example, a clear resin should be used for embedding LED’s in yarns; and thermally-conductive resin should be used for designing temperature-sensing yarn by encapsulating thermistors in yarns. A number of techniques can be used to cure resins. A traditional encapsulation method is to mix two components together [121]. Those two components consist of two different chemical groups which react when they are mixed together; When the two components are mixed polymerisation takes place [122], resulting in generation of heat which could be harmful to semiconductor devices Therefore, ultraviolet (UV) curing techniques are used in the electronics industry due to their ability to cure certain resins without generating heat. In addition, no mixing is required, shrinkage is low and a smooth, non-tacky surface is created. Moreover, the two-component method has disadvantages as it may be messy when mixing, will waste unused mixed resin, may exhibit a slow curing process, may require oven heating and have a limited shelf life [121]. The micro-scale semiconductor packaged dies used in this project are sensitive to heat. Therefore, it was decided to use the UV-curing technique for the research work. The UV-curing theory and experiments are described in this chapter.

5.1.1 Ultraviolet (UV) Radiation

Ultraviolet (UV) radiation is an electromagnetic wave with wavelengths between 100 to 380nm. The wavelengths of UV radiation are between those of X-rays and visible light (Figure 5.1) [123]. Depending on the wavelength, UV radiation is classified into three groups such as UV-A (315-400nm), UV-B (280-315nm) and UV-C (100-280nm) [123].

FIGURE 5. 1: UV SPECTRUM [123]

The relationship between UV exposure and irradiation intensity is described below. When UV-curing techniques are used for curing resin, the required irradiation time can be calculated using Equation 5.1.

$$E = (I) \times (T) \quad \text{…………………… 5.1}$$

Where

E: UV exposure (mJ/cm^2);
I: Intensity (mW/cm^2);
T: Irradiation time (s).

5.1.2 UV Curing Technique

The UV-curing technique is a method for converting a liquid resin into a hard polymer by using ultraviolet energy. A UV-curable resin consists of monomers, oligomers, photoinitiators and other components such as fillers, pigments etc. The polymerisation process is initiated by photoinitiators of the UV-curable resin absorbing UV light energy and becoming excited. These excited photoinitiators instigate bonding of monomers and oligomer molecules, resulting in a three-dimensional polymerisation. Generally, within a few seconds, the liquid resin becomes a solid material. While in conventional curing techniques, heat is applied to evaporate solvents to cure the resin, UV-curing techniques do not involve solvents and the polymerisation takes only a few seconds. The UV-curing polymerisation process of a chip encapsulated with a UV-curable resin is illustrated in Figures 5.2 to 5.4 [124].

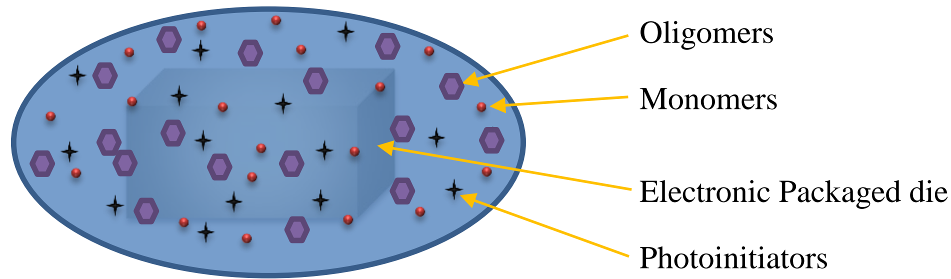

FIGURE 5. 2: THE SCHEMATIC OF AN SMD CHIP ENCAPSULATED WITH UV-CURABLE RESIN BEFORE APPLICATION OF UV ENERGY [124]

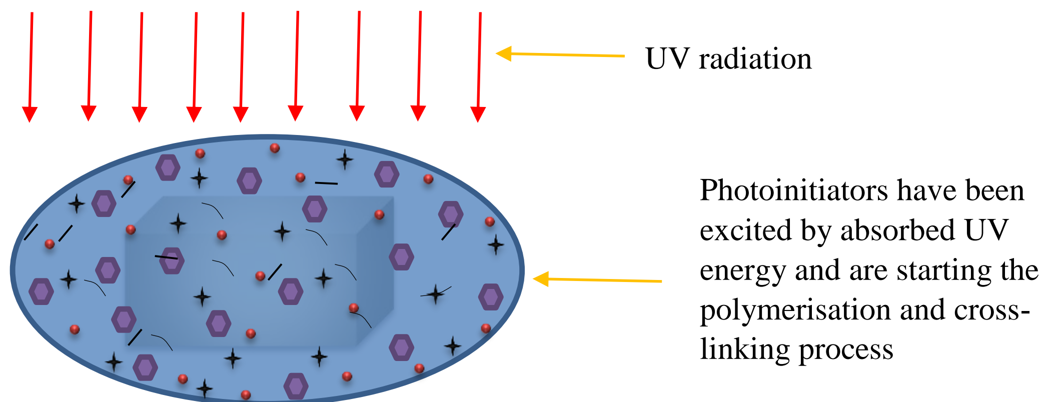

FIGURE 5. 3: THE SCHEMATIC OF AN SMD CHIP ENCAPSULATED WITH UV-CURABLE RESIN DURING APPLICATION OF UV ENERGY [124]

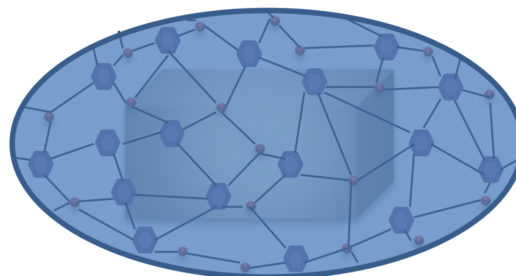

FIGURE 5. 4: THE SCHEMATIC OF AN SMD CHIP ENCAPSULATED WITH UV-CURABLE RESIN AFTER CROSS-LINKING AND BECOMING A SOLID POLYMER MICRO-POD [124]

5.2 Preliminary Encapsulation Test

A simple, experimental rig was constructed (Figure 5.5) and initial tests were carried out to understand the encapsulation of individual SMD packaged dice with the fibres of yarns. The experimental rig consisted of a rotatable yarn-holding unit for yarn packages, a metal plate on the top to hold the copper wire soldered with semiconductor packaged dies, guide rollers, a UV light source (Dymax Blue Wave 50) and a yarn-winding unit. Each yarn

was fed through a tensioning device. The copper wire was twisted with a polyester yarn prior to creating the polymer micro-pod as shown in Figure 5.6.

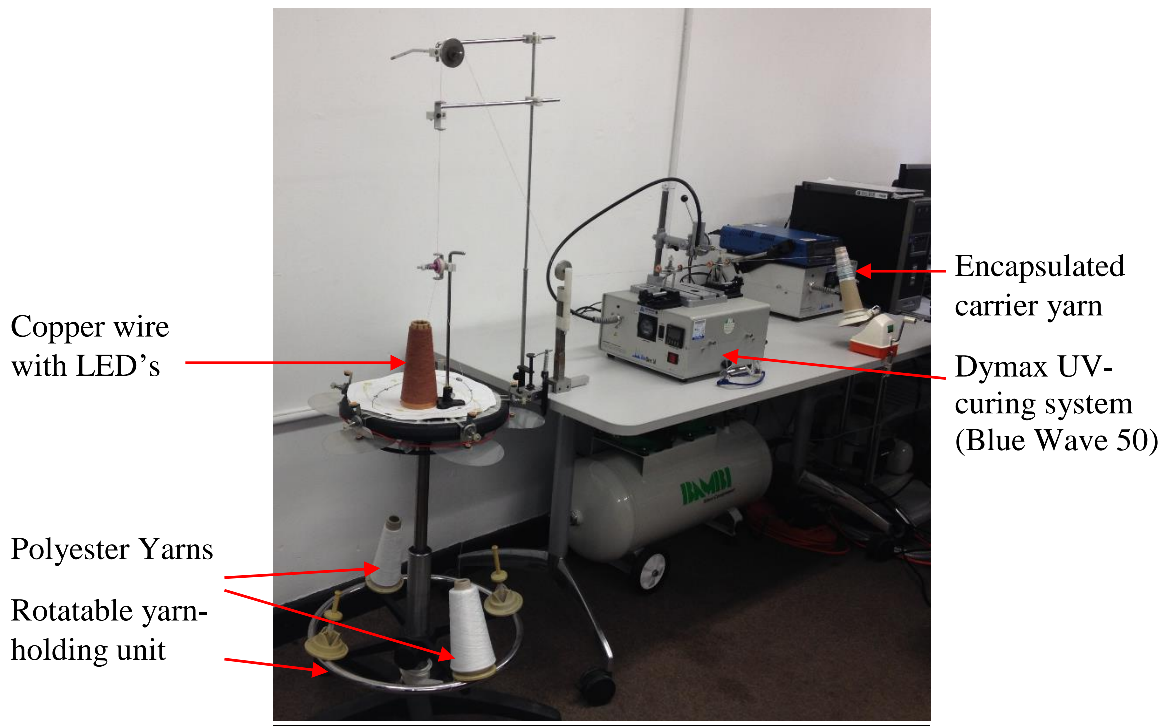

FIGURE 5. 5: THE EXPERIMENTAL RIG BUILT TO ENCAPSULATE SMD CHIPS

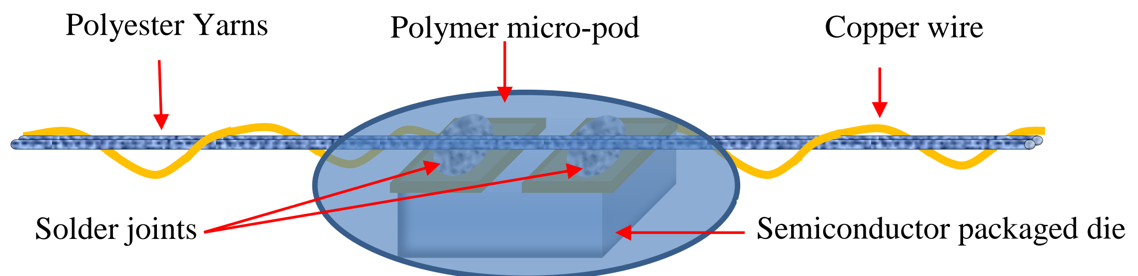

FIGURE 5. 6: SCHEMATIC OF AN ENCAPSULATED, PACKAGED DIE

Procedure: The, yarns and equipment were set up as shown in Figures 5.5 above. UV-curable resin, Dymax 9001-E-V-3.5, was applied around the soldered semiconductor packaged die using a small brush, and a UV light spot was used for 10 seconds exposure as shown in Figure 5.7. The test was repeated with ten, soldered SMD-type LED packaged dies.

Equipment	Raw Materials
• Dymax blue wave 50 (UV source) • A small brush	• Dymax 9001-E-V 3.5 • Polyester yarn (Textured, 150/48) • Soldered 0402 LEDs with 7 strands copper wire

TABLE 5.1: THE EQUIPMENT AND RAW MATERIALS FOR THE ENCAPSULATION PROCESS

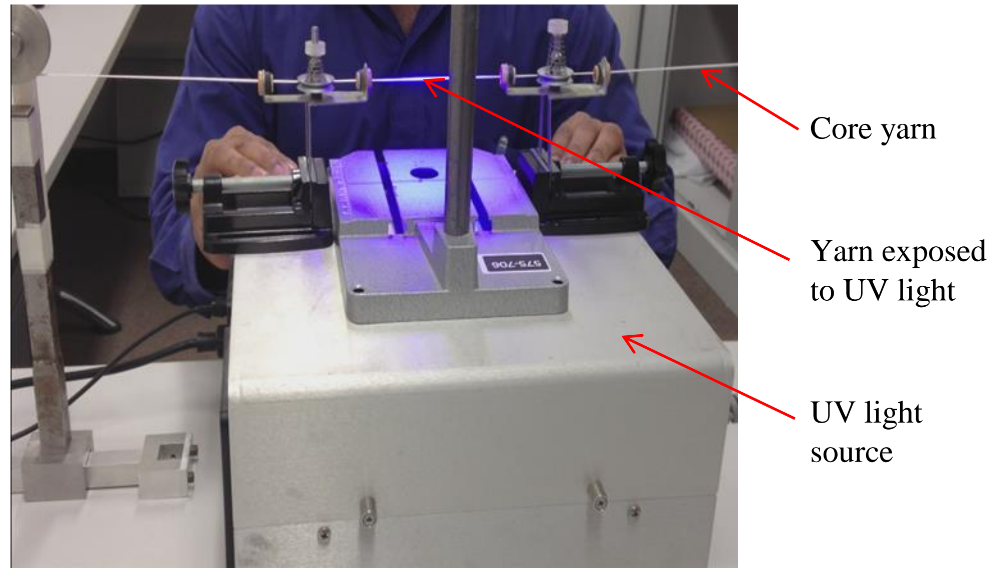

FIGURE 5. 7: A CLOSE-UP PICTURE OF THE ENCAPSULATION PROCESS.

Observation: One could form a polymer micro-pod to protect the solder joints and semiconductor devices by using this method. However, it was not possible to control the amount of resin applied during the encapsulation. Therefore, the amount of resin and size of micro-pod varied considerably.

5.3 Encapsulation Process Using EFD Dispenser Unit

The aim of this investigation was to apply resin precisely using an EFD unit which was capable of dispensing resin precisely at micro-litre scales.

Equipment	Raw Materials
• A EFD dispenser unit • A compressor • Dymax blue wave 50 (UV source)	• Dymax 9001-E-V 3.5 • Polyester yarn (Textured, 150/48) • Soldered 0402 LEDs with 7 strands copper wire

TABLE 5.2: THE EQUIPMENT AND RAW MATERIALS FOR THE ENCAPSULATION PROCESS

Procedure: The copper wire which was soldered with electronic packaged dies was twisted around two 150dTex/48 filaments polyester yarns. As shown in the Figure 5.8, 0.3 µl of UV curable Dymax 9001-E-V 3.5 resin was dispensed to cover the whole packaged die. The resin was then exposed to UV light for 10 seconds to cure the resin. Finally, the yarn, which is called the core yarn in this thesis, was wound onto a yarn package. This process was repeated for 10 encapsulation specimens.

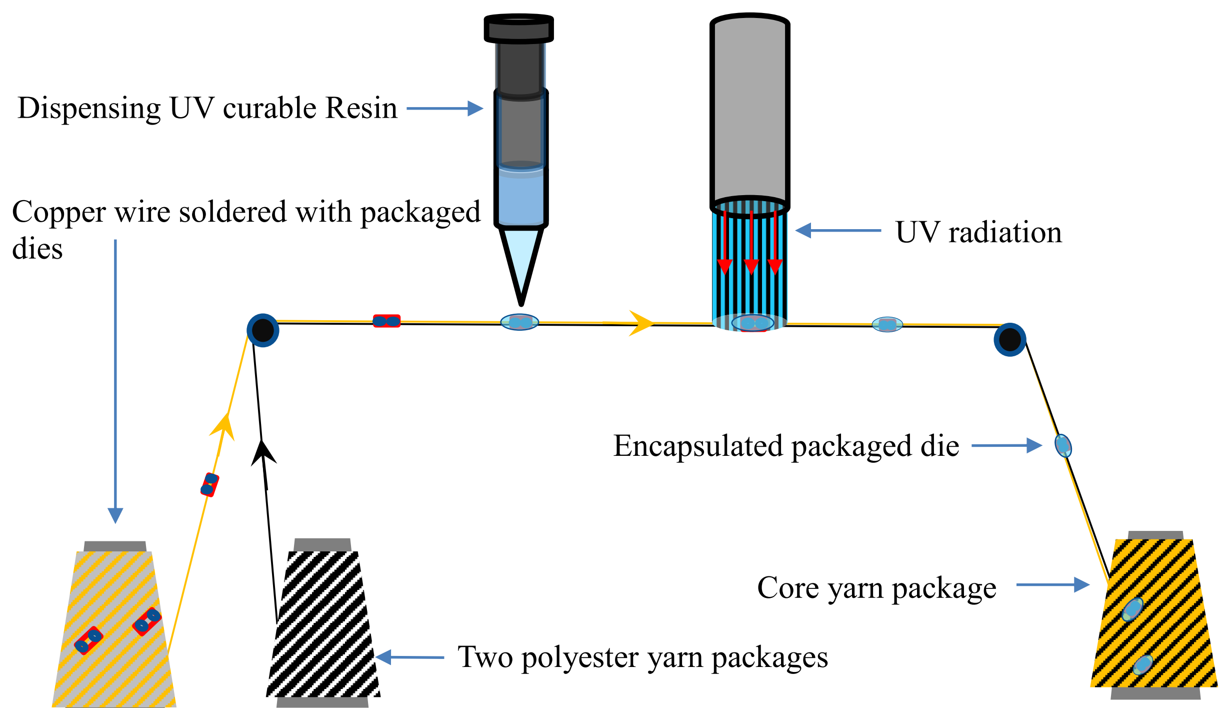

FIGURE 5. 8: SCHEMATIC OF THE ENCAPSULATION PROCESS

Results and Discussion

Using this method, it was possible to control the amount of resin (0.3µl) to ensure that this was same for 10 LED chips. However, the geometrical shape of the encapsulated packaged die was not the same even for the same type of SMD packaged die. Therefore, it was decided to use a mould for the resin curing process.

5.4 Encapsulation Process Using EFD Dispenser Unit and Teflon Tube Mould

It was necessary to select a material with a very low coefficient of friction to use as a mould for creating the encapsulated polymer micro-pod. Polytetrafluoroethene (PTFE) which is commonly known as Teflon is a thermoplastic polymer with a very low coefficient of friction (0.05 to 0.10) [125]. Therefore, PTFE can be used for non-stick surfaces as it has non-adhesiveness properties [126]. A short Teflon tube (inner diameter: 0.8 mm, outer diameter: 1.6 mm and length: 2.5 cm) was used for these experiments as it was easy to remove the micro-pods from the Teflon tube after curing. A seven-strand copper wire and a soldered packaged die with a copper wire were pulled through the Teflon tube with two 167dTex/47 polyester yarns. The packaged die was positioned in the middle of the Teflon tube as shown in Figure 5.9 and 5.10. The yarns were kept under tension (Figures 5.9 and 5.10). Dymax 9001-E 3.5 resin (0.4 µl) was dispensed from the EFD dispenser with a long needle into each open end of the Teflon tube UV light was then applied for 10 seconds to cure the resin. Then, the core yarn was pulled out to remove the polymer micro-pod from the Teflon tube. The test was repeated for 10 soldered packaged dies.

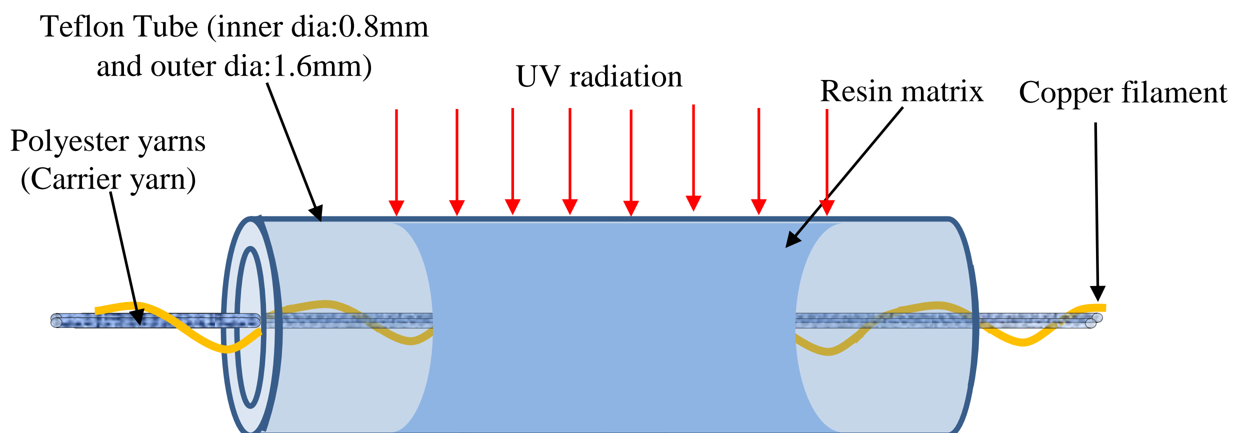

FIGURE 5. 9: SCHEMATIC DIAGRAM OF THE ENCAPSULATION PROCESS USING TEFLON TUBE

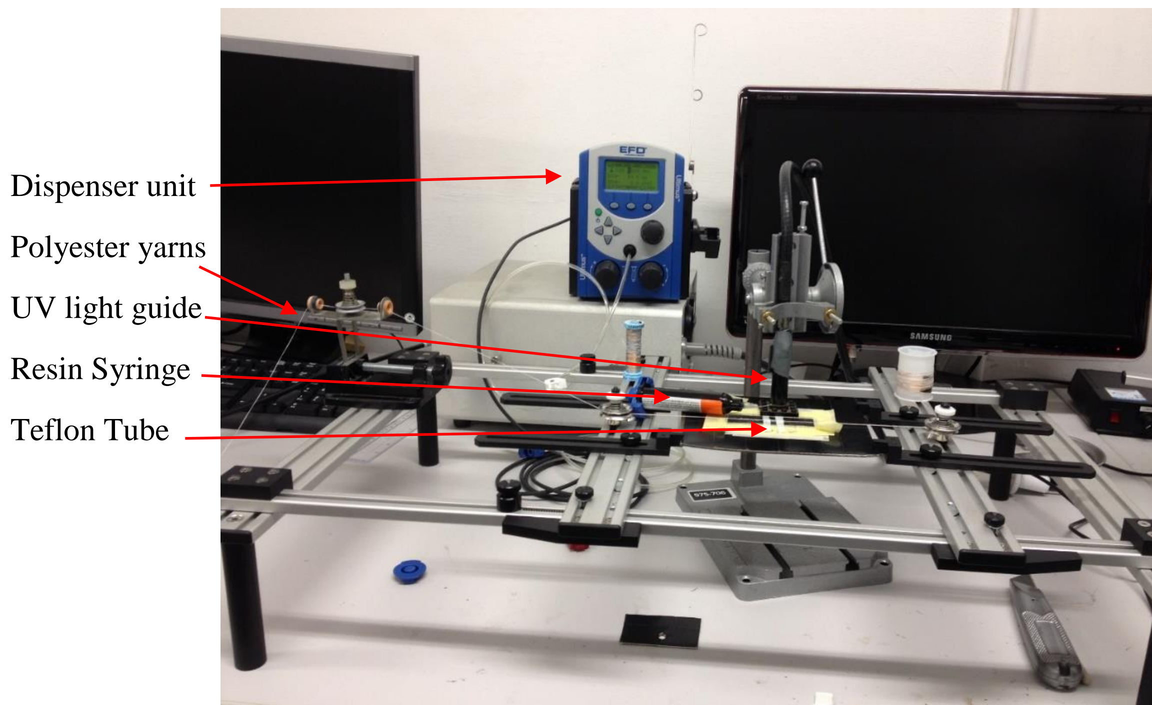

FIGURE 5. 10: THE EXPERIMENTAL RIG BUILT TO ENCAPSULATE CHIP AND SOLDER JOINTS

Results and Discussion

As expected the geometrical shape of all the micro-pod (encapsulated packaged die) was the same. Two example images are shown in Figure 5.11. The micro-pods formed are of tubular shape which is comparable to the shape of fibres. The cross-sectional dimensions of the micro-pod can be controlled by the selection of Teflon tubes of different diameters.

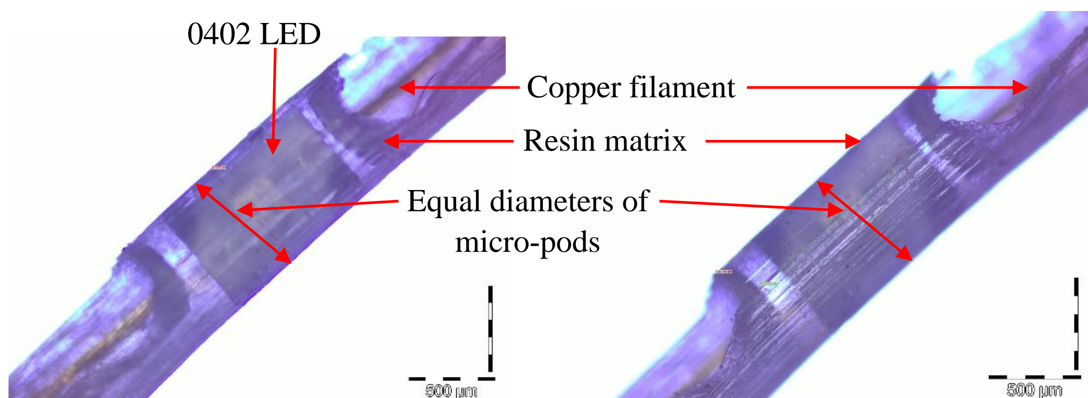

FIGURE 5. 11: MICROSCOPIC IMAGES OF ENCAPSULATED 0402 TYPE LEDS USING TEFLON TUBE

5.5 Tensile Test of Soldered and Encapsulated 0402 Blue LEDs with 7-Strand Copper Filaments

The focus of this investigation was to analyse whether the strength of solder joints was improved after they had been soldered with 7-strand copper filaments and encapsulated with resin in comparison with non-encapsulated solder joints. The test procedure described in section 4.3.6 of Chapter 4 (pages 88 to 89) was used to solder the 5 samples and the test procedure described in section 5.3 of Chapter 5 (page 113) was used to encapsulate the solder joints. The test procedure described in section 4.5.2 of Chapter 4 (page 99) was used to carry out the tensile test for these samples. Pictures taken during the tests are shown in Figure 5.12.

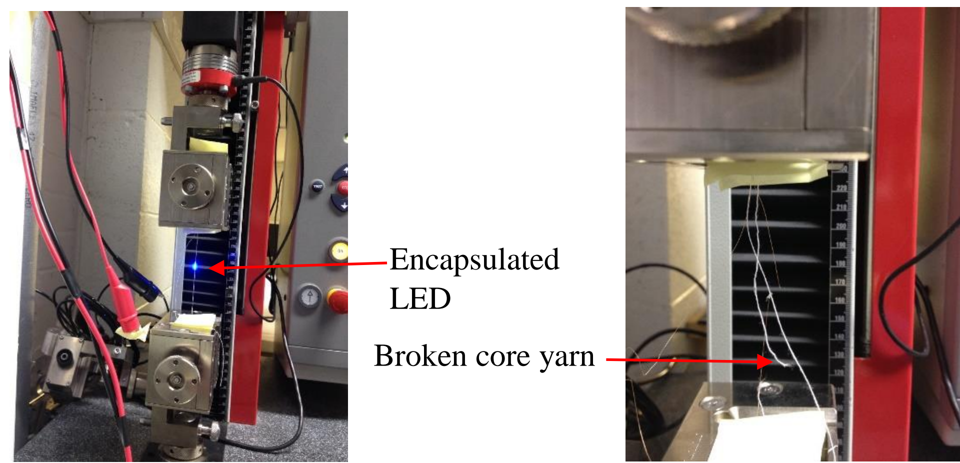

FIGURE 5. 12: BEFORE (LEFT) AND AFTER (RIGHT) TENSILE TEST

Results and Discussion

During tensile testing, the solder joints of four core yarns were broken. In second sample (see table 5.3, Appendix 16), the seven-strand copper wire was broken at away from the solder joint. As explained earlier in section 5.3. the seven-strand copper wire with LED's attached by soldering was twisted around two 167dTex/47filaments polyester yarns and, therefore, the tensile strength of the core yarn was increased (see table 5.3). However, the solder joint was still the weakest point. Therefore, further improvements made are discussed in chapter 6.

Specimen no.	L_v	F_H	R_H	ε_H	Yarn count	Location of Breaking Point
	mm	cN	cN/Tex	%	Tex	
1	250	1060	2.7	18	92	Solder joint
2	250	1160	2.9	17	92	Copper wire
3	250	943	2.4	16	92	Solder joint
4	250	974	2.5	16	92	Solder joint
5	250	973	2.5	17	92	Solder joint

TABLE 5.3: TENSILE TEST RESULTS FOR SOLDERED & ENCAPSULATED BLUE LED'S WITH 7-STRAND COPPER FILAMENTS

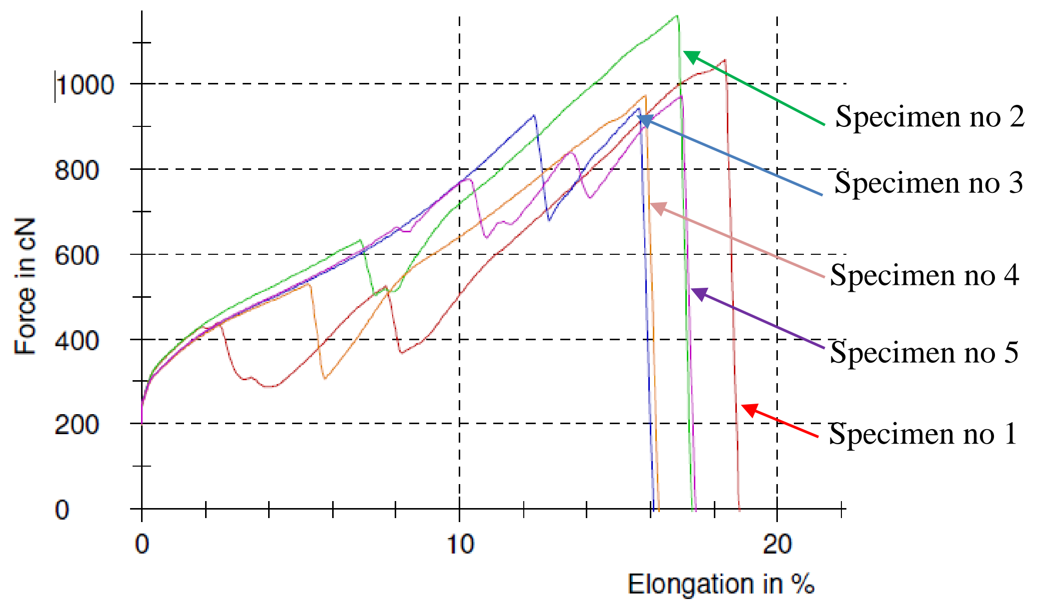

FIGURE 5. 13: GRAPH OF TENSILE TEST OF CORE YARN SAMPLES IN TABLE 5.1

5.5 Conclusion

Encapsulation of the electronic components is essential for ensuring the washability and durability of electronic yarn. Moreover, it provides robustness to the yarn prior to feeding through a conventional mini circular warp knitting machine in order to produce the final, electronic yarn. A traditional encapsulation method is to use two-component resin. However, UV curing is the method employed in the electronics industry and has more benefits than use of two-component resins, therefore, a UV curing technique was used with UV-curable resin to create micro-pods around the semiconductor package die. Three methods were used to apply resin to the electronic packaged dies which had been soldered

onto seven-strand copper wires. In first method, it was not possible to control the amount of resin applied to each packaged die, as resin was applied with a paint brush. Therefore, the size of micro-pods and geometrical shapes of the encapsulated packaged dies varied. In the second method, resin was applied using a syringe with a long needle. The volume of resin could be controlled but the geometry of the micro-pods varied. In the third method, the packaged die was located within a Teflon tube and resin was then applied and cured. This encapsulation method was more successful than the others as it was able to create geometrically-uniform micro-pods for each electronic packaged die.

CHAPTER SIX

6.0 Electronic Yarn Formation

Integrating micro-scale semiconductor, packaged dies within the fibres of yarn is a novel concept. However, it was a challenging task to develop robust interconnections with the electronic devices to withstand mechanical stresses and chemical processes which usually take place during textile manufacturing and later during textile use. The encapsulation process was explained in the chapter 5. The core yarn with micro-pod that was developed, had insufficient mechanical strength. Mechanical strength and the basic textile characteristics of e-yarns are defined by the properties of the final yarn, such as fibre and yarn type, and yarn formation method. Therefore, this chapter focuses on textile qualities of the e-yarn. The yarn formation techniques for manufacture of e-yarns such as twisting, braiding and covering and optimisation of yarn quality are explained in this chapter.

6.1 Electronic Yarn (e-Yarn)

Normal spun yarns are produced from short or long staple fibres twisted together. For example, cotton yarn is a spun yarn which is made by twisting cotton fibres. It is a long process and involves a number of steps [127]. Therefore, it would be very complicated if semiconductor packaged dies integrated yarns (e-yarns) were to be produced using the normal route for cotton yarn manufacture. Therefore, it was necessary to select a technique suitable for producing the final e-yarns by using conventional textile yarns (either staple spun or multi-filament yarns from synthetic or natural fibres). The final e-yarn is a hybrid yarn, assembled together with fine standard yarns, fine copper interconnects, semiconductor packaged dies, resin micro-pods and carrier yarn. Conventional hybrid yarns are formed by different techniques such as twisting, covering and braiding. The twisting technique and issues with this are discussed in 6.2. The circular warp knitting technique was used to produce e-yarns, as it has distinctive properties which are described in 6.3. Optimisation of the properties of the e-yarn is also discussed in 6.3. Tensile tests were carried out for final e-yarns as discussed in section 6.4.

6.2 Study of Twisting Technique for e-Yarn Formation

This investigation was undertaken to identify the suitability of twisting the core yarn with conventional textile fibres to produce e-yarns. A simple experimental rig was developed to produce e-yarns by twisting the core yarn, which consists of carrier yarns, seven-strand copper wire populated with soldered SMD chips and micro pods, and conventional textile fibres (see Figures 6.1 and 6.2). The yarn-package holding unit could be manually rotated.

The tensioning devices were fixed for each and every yarn to provide tension. This rig was also used for encapsulation processes to produce core yarns by using two main yarns (carrier yarns) and copper wire which had electronic chips soldered onto it as described in chapter 5.2 (page 111).

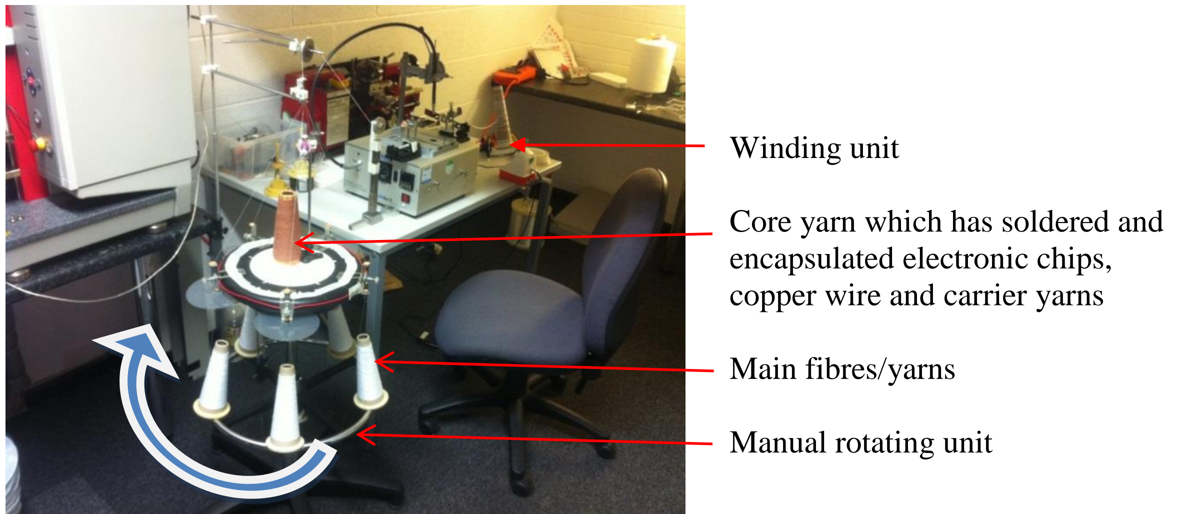

FIGURE 6. 1: THE EXPERIMENTAL RIG WHICH WAS BUILT TO TWIST CORE YARN WITH TEXTILE YARNS TO PRODUCE E-YARNS

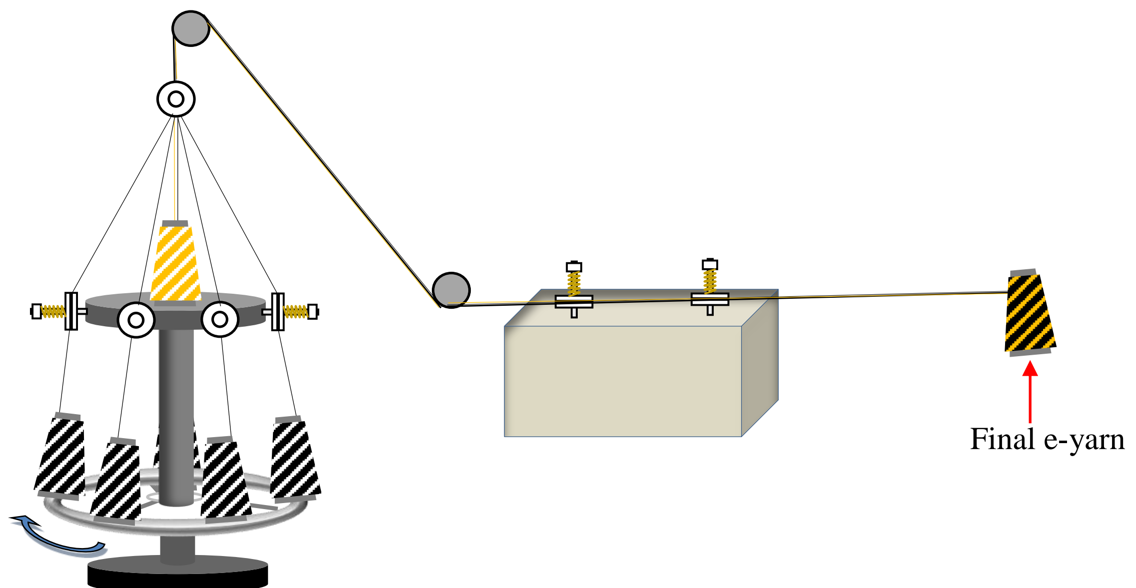

FIGURE 6. 2: A SCHEMATIC DIAGRAM OF THE EXPERIMENTAL RIG WHICH WAS BUILT TO TWIST CORE YARN WITH TEXTILE YARNS TO PRODUCE E-YARNS

6.2.1 The Issues of the Twisting Technique

As shown Figure 6.3 and 6.4, when several yarns are twisted together, due to fibre migration, it is not possible to prevent one particular yarn from appearing on the outer surface of the final yarn, even when it is twisted with double or multiple yarns. The

motivation for twisting the core yarn with a number of conventional textile yarns was to form an e-yarn with the core yarn being held in its centre, in order to protect the interconnects (fine copper wires) from unwarranted mechanical stresses such as rubbing during use. According to Table 3.3 and Table 3.4 of chapter three (pages 55 and 57), the fine copper wires used are weaker than conventional textile yarns such as polyester. However, it was necessary to use fine copper wires to form the interconnects to the SMD chips utilised to produce e-yarns, and this required protection. Therefore, the twisting method is not suitable for production of e-yarns as copper interconnects can be damaged easily.

FIGURE 6. 3: A SCHEMATIC DIAGRAM SHOWING TWISTED YARNS [128]

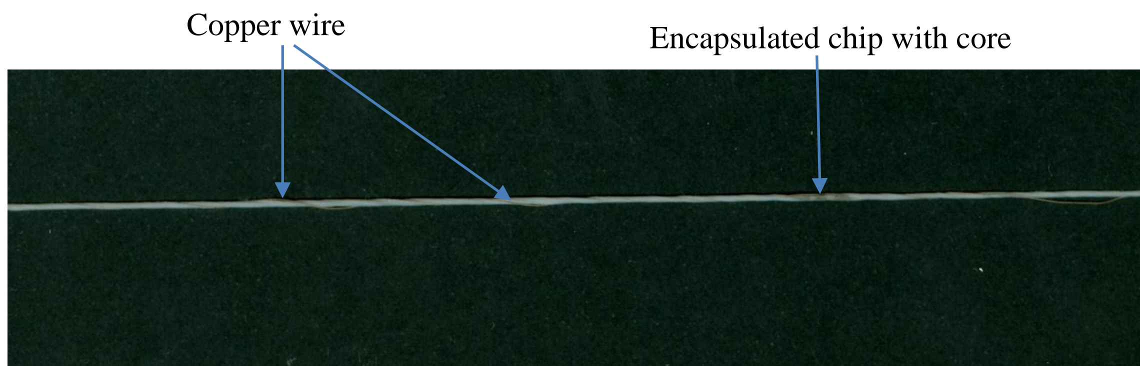

FIGURE 6. 4: AN EXAMPLE OF THE FINAL, TWISTED E-YARN

6.3 Mini Circular Warp Knitting Technique for e-Yarn Formation

In order to protect the micro-electronic devices, one could surround the core yarn with a fibre sheath, which could be in the form of an interlaced or interlooped structure. Braiding is a well-known technique which can be used to produce tubular structures which are formed by interlacing of at least three yarns diagonally to the axis of the braid. Industrial braiding machines consist of carriers of yarn driven by horn gears, and the length of the braid that can be produced is determined by the length of yarn wound onto the carriers. On the other hand, one could use a small-diameter warp knitting machine to produce a continuous fibre sheath by interloping 4 to 16 yarns. Therefore, it was decided to investigate the possibility of using a small-diameter Raschel warp knitting machine from RIUS, Model MC. The warp knitted structure is more suitable for manufacturing e-yarns

due to its properties, and as four yarns can be supplied directly from yarn packages to the latch needles on the machine the process is efficient and economical.

6.3.1 Preliminary Testing

In order to produce finer e-yarns a RIUS MC with a needle cylinder with an internal bore size of 1.5mm diameter was utilised. The needle cylinder was equipped with four latch needles (gauge 18). The aim of preliminary testing was to identify the suitability of the RIUS machine to craft the e-yarn and practical issues of e-yarn formation. The latch needles were threaded with multi-filament texturized polyester yarns (150dTex/48) to form the tubular warp knitted structure (knitted sleeve). A schematic of the concept of forming e-yarn is shown in Figure 6.5, and the arrangement of the four PE yarns and the core yarn is illustrated in Figure 6.6. The machine speed was set to 50 rpm and the machine was adjusted to produce a tubular warp knitted sleeve with ten courses per inch. The core yarn was delivered to the centre of the needle cylinder as shown in Figure 6.7. The SMD 0402 type semiconductor chip (length: 1.0 mm, width: 0.5 mm and thickness 0.5 mm) was used.

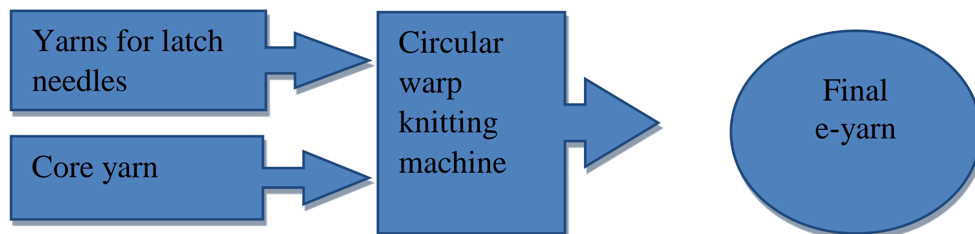

FIGURE 6. 5: SCHEMATIC OF THE FORMATION OF THE FINAL E-YARN.

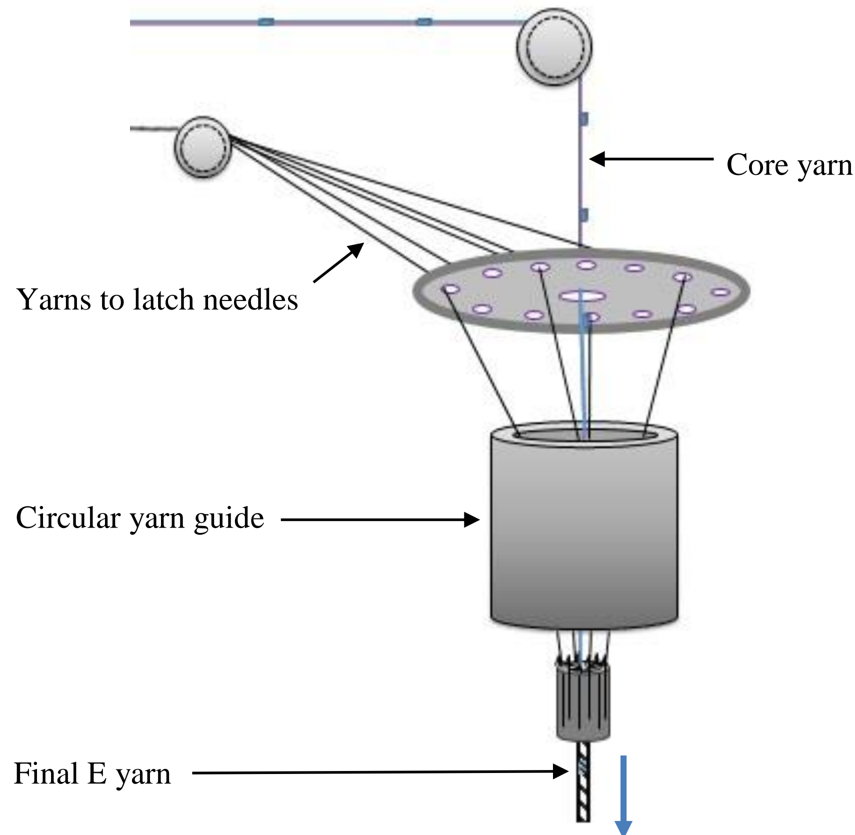

FIGURE 6. 6: A SCHEMATIC OF THE ARRANGEMENT OF YARN IN THE CIRCULAR WARP KNITTING MACHINE

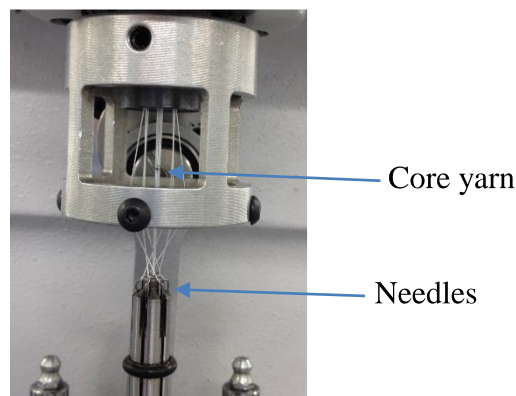

FIGURE 6. 7: THE NEEDLE CYLINDER OF THE WARP KNITTING MACHINE AND YARN ARRANGEMENT

Results and Discussion

E-yarns were successfully produced using the small-diameter warp knitting machine from RIUS without encountering problems with the machine. However, the evenness of the warp knitted e-yarn was compromised by micro pods on the core yarn as shown schematically in Figure 6.8 and 6.9. The diameter of the e-yarn in the semiconductor packaged die embedded area was larger than in other areas. The e-yarns should be able to undergo further

manufacturing processes such as weaving, knitting, sewing and embroidering without snagging. Therefore, it was necessary to improve the evenness of the e-yarn.

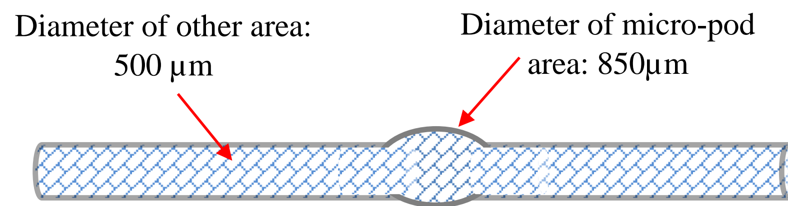

FIGURE 6. 8: A SCHEMATIC DIAGRAM OF THE FINAL E-YARN

FIGURE 6. 9: AN EXAMPLE OF FINAL E-YARN

6.3.2 Optimisation of the Uniformity of E-yarn

The aim of this investigation was to improve the evenness of the e-yarn by introducing extra filler yarns in parallel with the carrier yarn. Therefore, four extra 150/48 textured polyester yarns were delivered to the warp knitting zone with carrier yarn. The important components of the RIUS small-diameter circular warp knitting machine are shown in Figure 6.10.

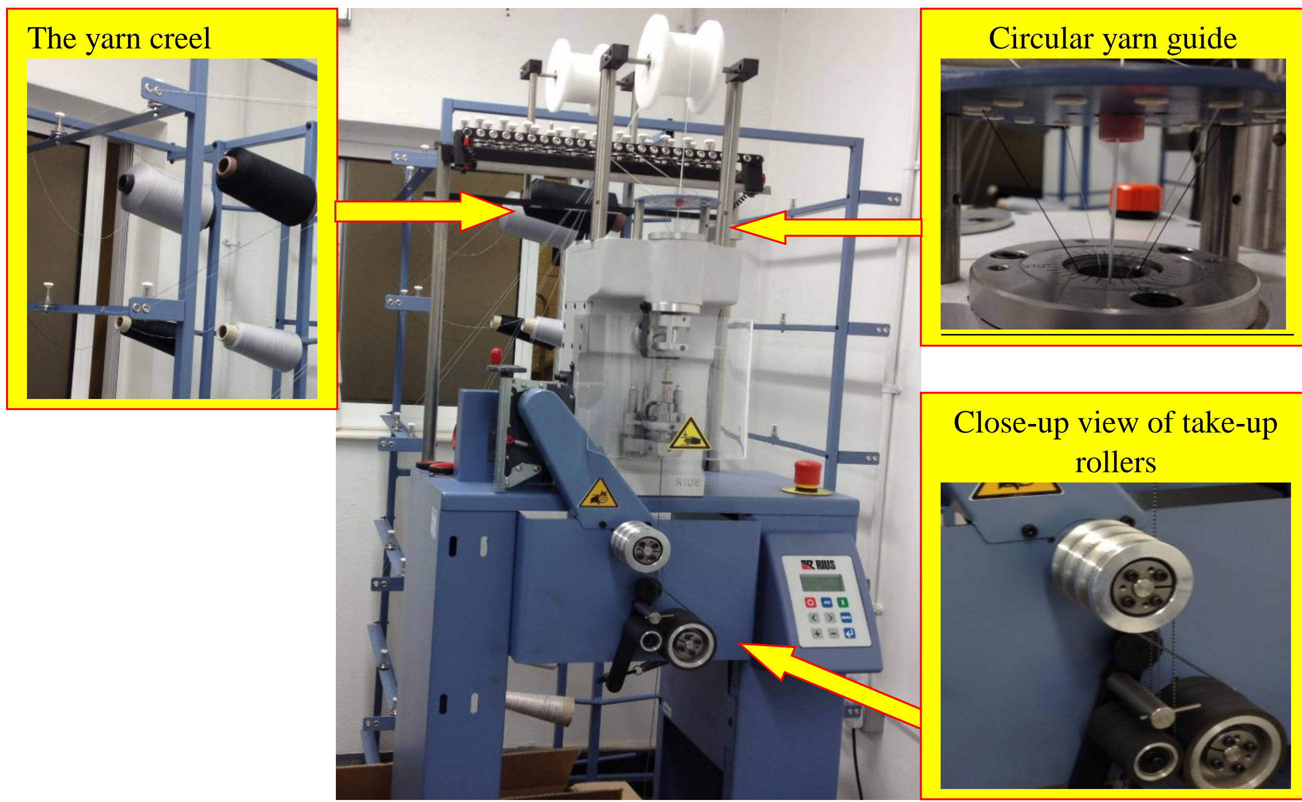

FIGURE 6. 10: SMALL-DIAMETER CIRCULAR WARP KNITTING MACHINE RIUS MC WITH YARN CREEL

Results and Discussion

The extra filler yarns were well accommodated inside the e-yarn. As shown below in Figure 6.11, these yarns maintained a uniform yarn diameter, which was larger along the length of the e-yarn. However, it was observed that the filler yarns were squeezed at the micro pod area. Therefore, although the evenness of the yarn was improved, part of the micro pod did emerge onto the surface of the e yarn sometimes as illustrated in Figure 6.12 and shown in Figure 6.13.

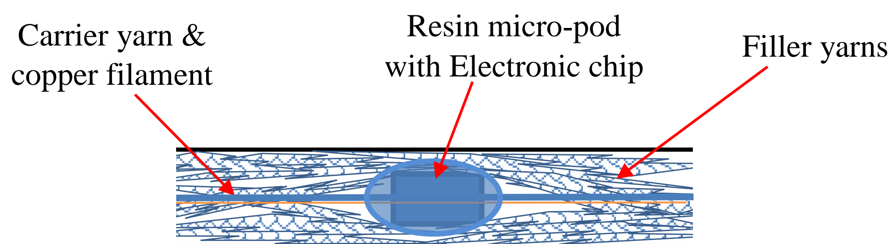

FIGURE 6. 11: SCHEMATIC TO ILLUSTRATE THE PREFERRED POSITION OF MICRO POD WITHIN E-YARN.

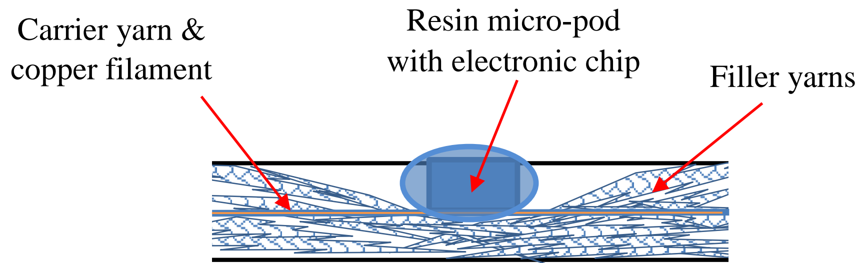

FIGURE 6. 12: SCHEMATIC TO ILLUSTRATE THE MICRO POD BEING SQUEEZED UP TO THE E-YARN SURFACE BY FILLER YARNS

FIGURE 6. 13: A PICTURE OF E-YARN WITH MICRO POD BEING PUSHED UP TO THE YARN SURFACE

Two possible reasons were postulated for the shifting of the micro pod to the surface of the e yarn. One reason was that filler yarns were not guided properly into the circular yarn guide of the machine. All filler yarns stuck together at the circular yarn guide causing the micro pod of the core yarn to be pushed aside. Therefore, a newly-designed circular disc was introduced to separate the packing yarn evenly around the inside of the circular guide. The other reason was that the core yarn and the seven-strand copper wire were not placed symmetrically in the micro pod, i.e. they were both positioned on one side of the packaged die as shown in Figures 6.14 and 6.15. The solution was to introduce two PE yarns on either side of the packaged die during the encapsulation process, as shown in Figure 6.16, thus the carrier yarn consisted of two PE yarns, seven strand copper wire and micro pods.

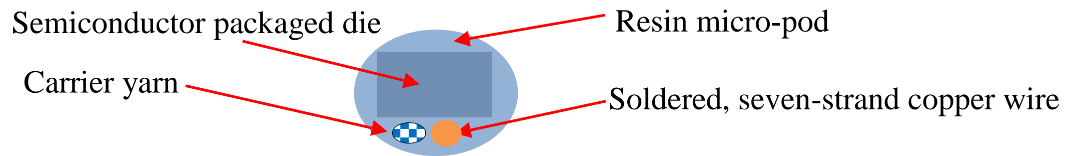

FIGURE 6. 14: SCHEMATIC ILLUSTRATING THE CROSS SECTION OF THE MICRO POD WITH CORE YARN AND SEVEN-STRAND COPPER WIRE ON THE SAME SIDE OF THE PACKAGED DIE

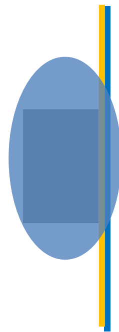

FIGURE 6. 165: SCHEMATIC OF THE SIDE VIEW OF THE MICRO POD WHEN CARRIER YARNS ARE TOGETHER

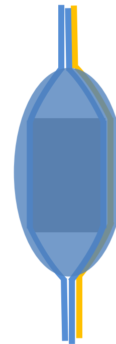

FIGURE 6. 156: SCHEMATIC OF THE SIDE VIEW OF THE MICRO POD WHEN THE CARRIER YARNS ARE EITHER SIDE

As explained in the previous section, a new yarn guide disc was fabricated. This was made from acrylic plate which was cut to the desired shape precisely with a laser cutting system. A needle cylinder with a central bore size of 2.0 mm was used when investigating the new concept. The new needle cylinder was equipped with six latch needles, and the arrangement of the yarns is as shown in Figures 6.17 and 6.18.

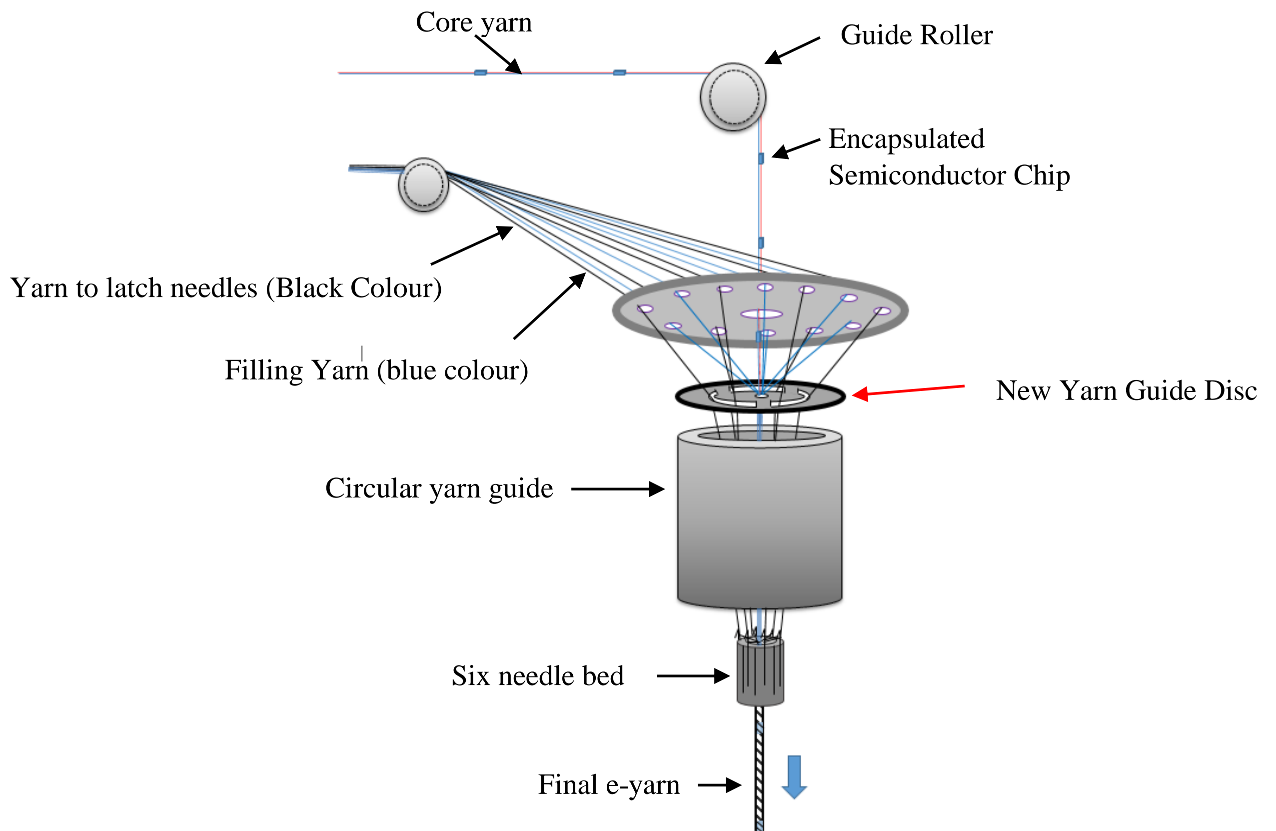

FIGURE 6. 17: SCHEMATIC OF YARN ARRANGEMENT ON RIUS KNITTING MACHINE WITH THE NEW FILLER-YARN GUIDE DISC

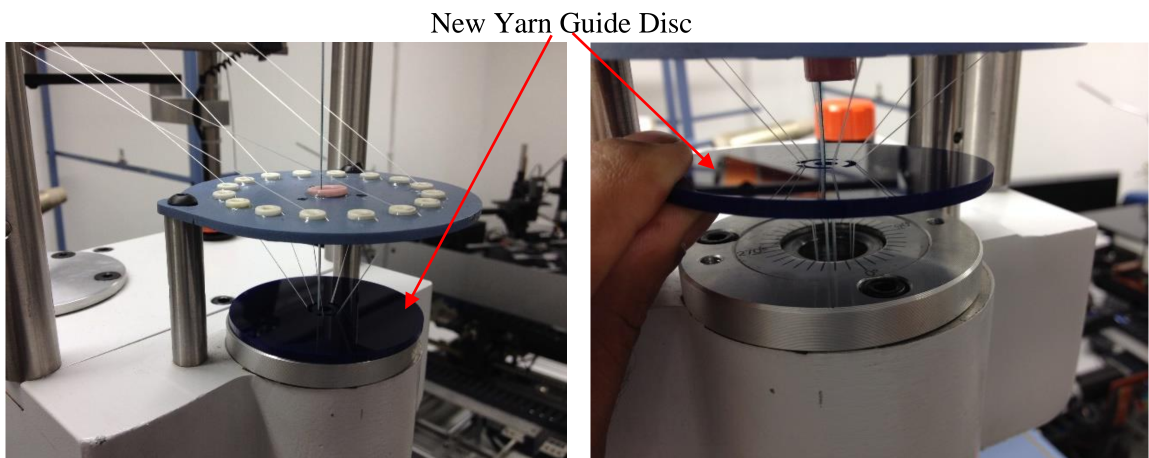

FIGURE 6. 18: PICTURES OF THE FILLER YARN GUIDE DISC

Results and Discussion

The extra filler yarns were well arranged around the carrier yarn as shown in Figures 6.19 and 6.20, therefore the evenness of the yarn was improved as shown Figure 6.21.

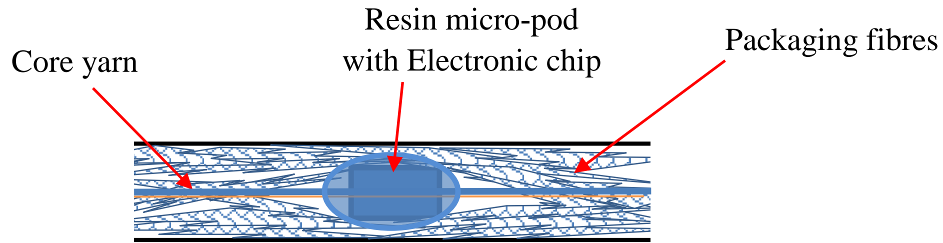

FIGURE 6. 19: A SCHEMATIC DIAGRAM OF FIBRE-ORIENTATION IN THE FINAL E-YARN

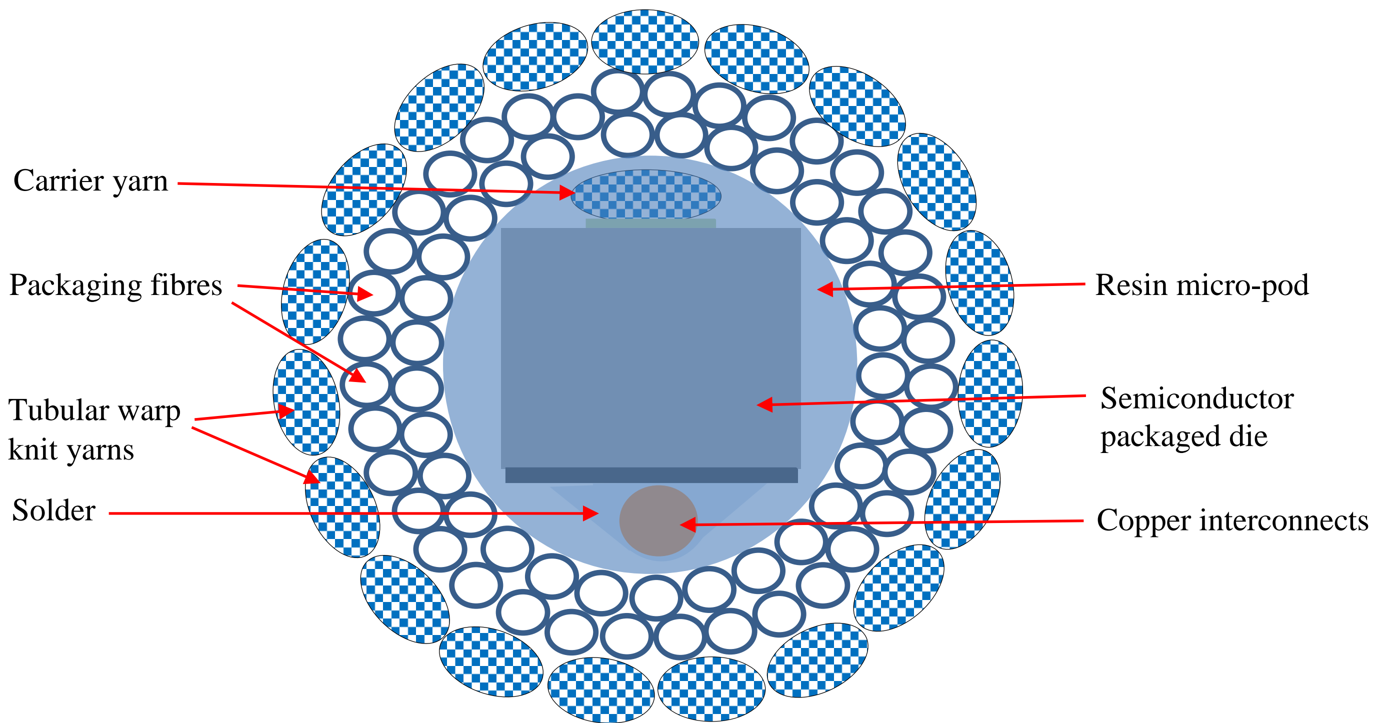

FIGURE 6. 20: A SCHEMATIC DIAGRAM OF SHOWING A CROSS-SECTIONAL VIEW OF THE FINAL E-YARN

FIGURE 6. 21: AN EXAMPLE OF THE FINAL E-YARN

6.4 Tensile Test e-Yarns

6.4.1 Tensile Testing of Warp-Knitted Sleeves (Without Electronics)

The aim of this evaluation was to analyse the tensile strength of the warp knitted sleeves, designed to surround the core yarn of the e-yarn. The procedure described in 6.3.2 (page 124) was used to form the knitted sleeve using a 4-needle braiding machine. The test method described in section 4.5.1 (page 95) was used to evaluate the tensile properties of the warp-knitted sleeve samples.

Results and discussion

The results of the tensile tests (Tables 6.1, Appendix 17 and Figure 6.22) showed that the minimum breaking tensile strength of the warp-knitted sleeve samples was 6660 cN (6.6 Kg). The tensile strength can be increased further by using stronger yarns as carrier yarns or as knitting yarns or by changing the needle bed with higher numbers of latch needles. For example, if Zylon yarn is used as a carrier yarn instead of polyester yarn, the resultant yarn will be stronger (tensile strength of Zylon yarn: 37 cN/dTex and polyester: 8 cN/dTex (129)).

L_v: Gage Length

F_H: Maximum Tensile Force

R_H: Fineness related breaking force

Specimen no.	L_v	F_H	R_H	Yarn Count
	Mm	cN	cN/tex	Tex
1	250	7540	19.0	397
2	250	6660	16.8	397
3	250	8960	22.6	397
4	250	8330	21.0	397
5	250	8030	20.2	397

TABLE 6.1: TENSILE TEST RESULTS FOR WARP KNITTED SLEEVES PRODUCED WITH SIX NEEDLES

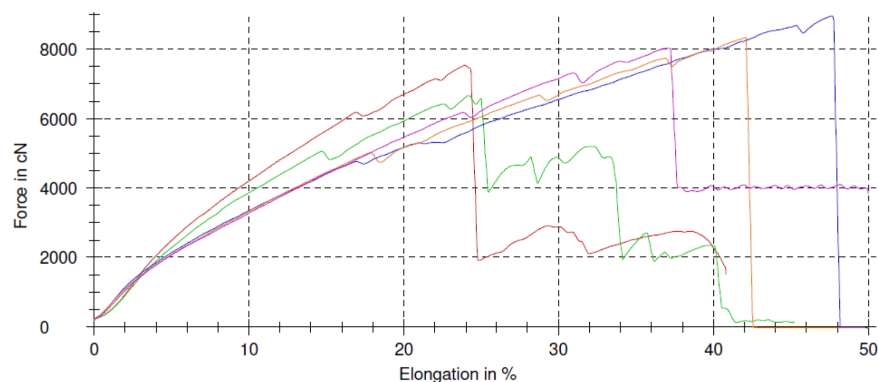

FIGURE 6. 22: GRAPH SHOWING TENSILE TEST RESULTS FOR THE SAMPLES LISTED IN TABLE 6.1

6.4.2 Tensile Testing of E yarn with Blue LEDs

The aim of this investigation was to analyse the tensile strength of the e-yarns that consisted of 0402 Blue LEDs and interconnects, at 10% elongation. The method described in section 4.3.6 (pages 88 to 89) was used to solder packaged dies to seven-strand copper wire to create the interconnects, and the method described in section 5.4 (pages 114 to 115) was used to encapsulate the packaged dies and solder joints. Finally, the method described in section 6.3.3 of this Chapter was used to craft the final e-yarn. The test method described in section 4.5.1 (page 95) was used to carry out the tensile testing of the samples. An example of an e-yarn under test is shown in Figure 6.23.

FIGURE 6. 23: BEFORE (LEFT) AND AFTER (RIGHT) TENSILE TEST

Results and Discussion

According Tables 6.2 (Appendix 18) and Figures 6.24, none of yarns was broken at 10% elongation. E-yarn with polyester warp-knitted sheaths were able to withstand more than 4 kg load. However, the breaking strength of E-yarn could vary according to type of yarn used as core yarn and the type used to form the warp-knitted fibre sheath.

Specimen no.	L_v	F_H	R_H	Yarn count	Which part was broken
	mm	cN	cN/tex	tex	at Breaking Point
1	250	4050	10.1	400	None
2	250	4420	11.0	400	None
3	250	4250	10.6	400	None
4	250	4410	11.0	400	None
5	250	4570	11.4	400	None

TABLE 6.2: TENSILE TEST RESULTS FOR SOLDERED WITH BLUE LED'S AND 7-STRAND COPPER WIRE, ENCAPSULATED AND BRAIDED

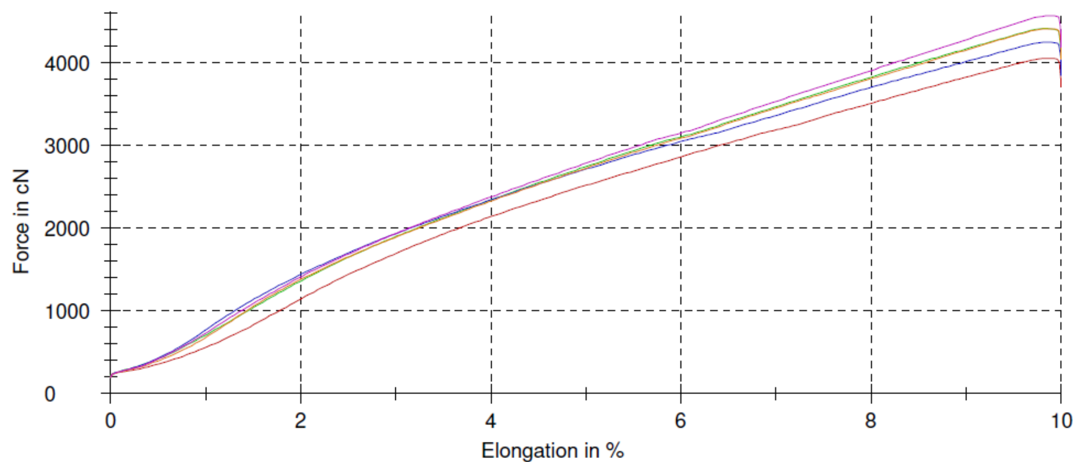

FIGURE 6. 24: GRAPH OF TENSILE TEST OF TABLE 6.2

Note: The covering techniques could also be recommended for future production of e-yarns, but it was not feasible to carry this out during in this research due to lack of availability of equipment.

6.5 Conclusion

The staple spun yarn manufacturing process is a long and complex process. It would be almost impossible to manufacture e-yarns by using that process. Therefore, it was necessary to investigate alternative yarn manufacturing techniques.

If yarns are twisted together, all the yarns including conductive wires used to create the interconnects to the packaged dies would appear on the outer surface of the final yarn. Therefore, the copper wires could get damaged when they come into contact with other objects. Therefore, it was concluded that twisting of yarns to produce e-yarn was not a suitable option.

The inner part of a braided yarn is covered completely with the outer, braided yarn. Therefore, the braiding technique was suitable for manufacturing e-yarns. Carriers populated with yarn are used in normal braiding machines, and this lead to production of braided yarn with limited lengths. This is labour intensive because of the winding, loading and unloading of carriers from a braiding machine. However, there are no such issues with small-diameter circular warp knitting machines. Moreover, the rate of production of such machines is much greater than that of normal braiding machines, and the structure of tubular-warp knitted structures are more suitable for e-yarns due to the tight, secure structure of the central filler yarns. Therefore, a carrier yarn with semiconductor packaged dies could be held securely in place in the middle of the e-yarn.

Uneven e-yarns could be caused due to two main reasons. One reason was that filler yarns were not guided before reaching the circular knitting barrel of the knit braider. To improve this, filler yarns were guided around the carrier yarn by introducing a new guide plate. The other reason was that the carrier yarn and copper filament were not at the central axis of the encapsulated, packaged die. This issue was solved by introducing two carrier yarns to the other side of the packaged die during the encapsulation process.

CHAPTER SEVEN

7.0 Development of Prototype Demonstrators with e-Yarn

7.1 Introduction

E-yarn is a novel concept, so its potential can be established only by creating textile fabrics. Novel concepts are quite difficult to establish without developing prototype demonstrators. Prototype demonstrators generate the opportunity for learning the functionality of the products and highlight practical issues, manufacturing limitations and quality control issues. Also one can gain valuable experience by creating prototype demonstrators. They could enhance one's creative thinking and provide a platform for the development of new skills. Prototype demonstrators also help to draw attention and interest to the technology.

Therefore, several prototype demonstrators were developed within the framework of this program of research, and this chapter is devoted to reporting these developments. Different SMD packaged dice were used to produce e-yarns with distinctive, unique electronic functionality, and then these were incorporated into textile fabrics using weaving and knitting techniques. LED's were used to produce light-emitting yarns; thermistors were utilised to craft temperature sensor yarns; vibration sensors were embedded to produce vibration sensing yarns; micro magnets were applied to create magnetic yarns; and RFID chips were exploited to develop yarns with unique electronic signatures. Different prototype demonstrators were fashioned with these e-yarns. Some demonstrators were used to undertake laboratory tests such as tensile and wash testing.

7.2 Illuminated Yarns

7.2.1 Producing Single-Colour LED Yarns

A number of single-colour LED yarns were produced to identify the following:

- The feasibility of manufacturing E-yarns;
- The identification of practical issues;
- To demonstrate the technology for potential partners.

Procedure: The procedure which was explained in Chapter 4 in Section 4.3.6 (pages 88 to 89), was used for soldering copper interconnects to LED chips, and their encapsulation was undertaken according to the procedure described in Chapter 5.4 (pages 114 to 115). The final yarn formation was undertaken according to the method explained in Chapter 6.

E-Yarns Containing Blue Colour LED's: Five SMD 0402 type blue colour LED's (part number: 860-9018 from RS components, Annex 2) were soldered to 7-strand of copper

wires, two 150dTex/48 texturized polyester yarns were encapsulated to produce the core yarn. The final e-yarn was produced on a RIUS small-diameter, circular warp knitting machine using four cotton yarns to create the outer tubular warp-knitted casing. Each e-yarn contained one blue LED with a working voltage of three volts. The LED's were connected in a parallel circuit and powered with a coin-cell battery as shown in Figures 7.1 and Figure 7.2.

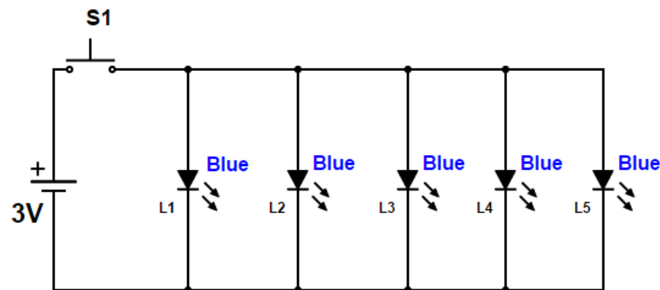

FIGURE 7. 1: CIRCUIT DIAGRAM OF YARNS CONTAINING BLUE LED'S

FIGURE 7. 2: E-YARNS CONTAINING BLUE LED'S BEFORE AND AFTER ACTIVATION

E-yarns Containing Yellow Colour LED's: Twenty SMD 0402 type yellow LED's (part number: 4663649 from RS components Annex 6) were used to produce five e-yarns. The core yarn of each e-yarn consisted of five LED's soldered in series to seven-strand copper wire, two 150dTex/48 texturized polyester yarns and five micro pods which is cured resin around those LED's. The e-yarn was produced with a tubular, warp-knitted casing made from four, textured, polyester yarns (150dTex/48). The five LED's in each e-yarn were positioned at 10 mm intervals. These yarns were connected in a parallel circuit as shown in Figure 7.3 and connected to a 10V power supply, and a photo of the e-yarns, when activated, is shown in Figure 7.4.

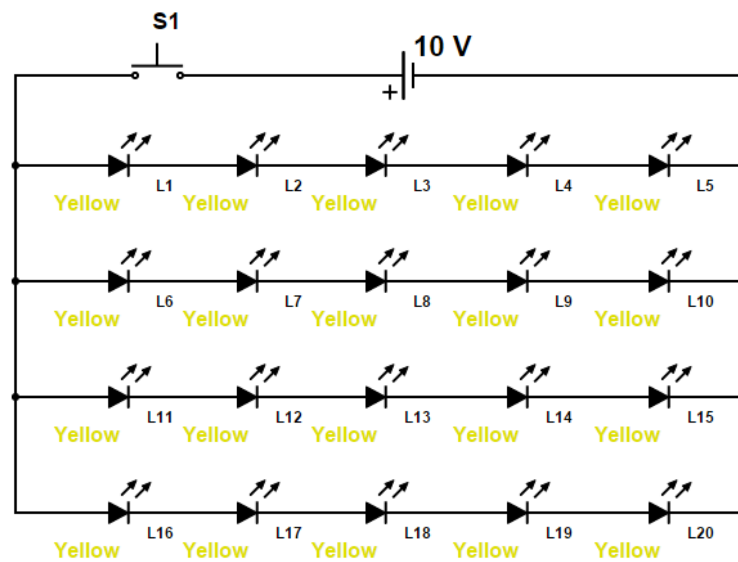

FIGURE 7. 3: CIRCUIT DIAGRAM OF E-YARNS CONTAINING YELLOW LED'S

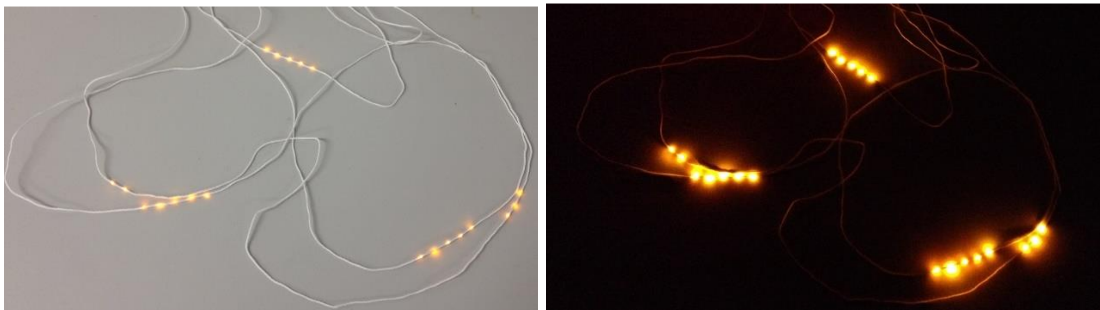

FIGURE 7. 4: ILLUMINATED E-YARNS CONTAINING YELLOW LED'S

E-Yarns Containing White LED's: Eight e-yarns were made up with twenty-four SMD 0402 type white LED's (part number: 6973840 from RS components Specs: Annex 4). The core yarn of each e-yarn consisted of three LED's soldered in series to seven-strand copper wire, two 167/47dTex texturized polyester yarns and three micro pods (which is cured resin around those LED's). The e-yarn was produced with a tubular, warp-knitting machine using four, textured polyester yarns (167dTex/47). The four LED's in each e-yarn were positioned at 50 mm intervals. These e-yarns were connected in a parallel circuit as shown in Figure 7.5 and connected to a nine Volt battery. The e-yarns are shown in Figure 7.6.

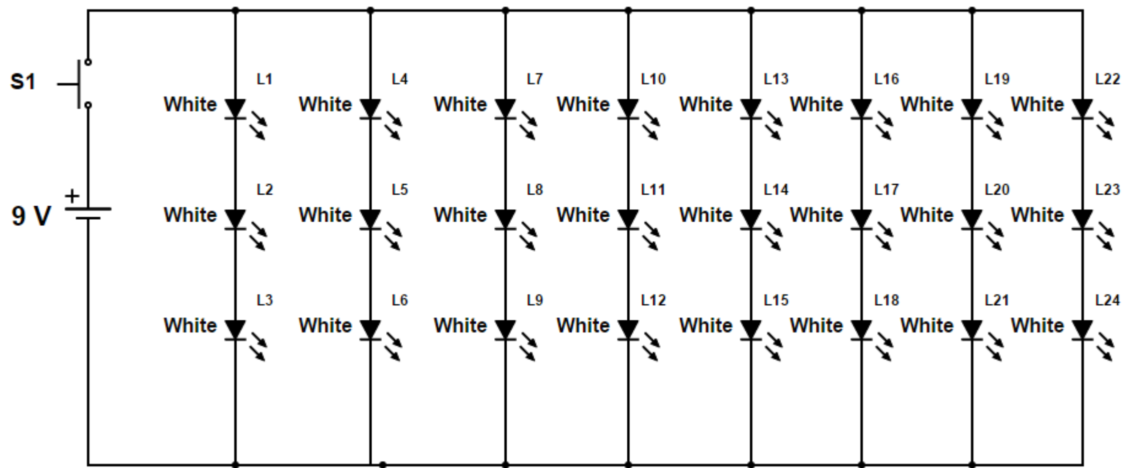

FIGURE 7. 5: CIRCUIT DIAGRAM OF WHITE YARNS

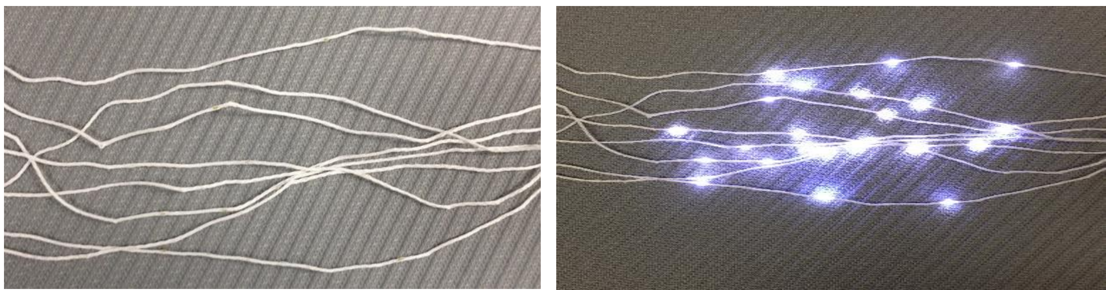

FIGURE 7. 6: E-YARNS WITH WHITE LED'S BEFORE AND DURING ACTIVATION

7.2.2 Production of Multi-Colour LED Yarns

In some electronic textiles it may be necessary to create e-yarns with multiple interconnects. In such situations one has to use multi-strand copper wires coated with a thin layer of PE for insulation to solder the interconnects. The aim of this experiment was to study removal of the polyester coating of the copper wire and creation of multiple connections within a yarn without causing short circuits.

Procedure: The method described in 4.3.3 (page 81) was used to remove the polyester coating from a single strand of copper wire at five different places. The coating was removed from 1.0 mm of the copper wire, at intervals of 10 mm. Five, red LED's (part number: 4663633 from RS Components, spec: Annex 3) were picked and placed onto a 25 mm wide black adhesive tape on the work-holder plate, ensuring that there was a 10 mm gap between each chip. The single-strand copper wire was laid on the LED's by aligning the areas in which the coating had been removed from the copper wire with the tops of the solder pads of the LED chips. Finally, the copper wire was soldered onto the solder pads using the procedure described in 4.3.6 (pages 88 to 89). The above procedure was repeated with yellow and green LED's, to produce three, different polyester-coated, single-strand,

copper wires, each soldered with five LED's of three different colours (red, yellow and green), and these were then combined to form the core yarn. The core yarn was then processed further on the small-diameter, circular, warp-knitting machine to craft an e-yarn containing LED's in three different colours (Figure 7.9). Each different coloured LED had to be supplied with a different voltage, which was achieved by connecting three load resistors in series with PE-coated copper wires as shown in Figure 7.7. The calculation of the load resistors is given in Appendix 2.

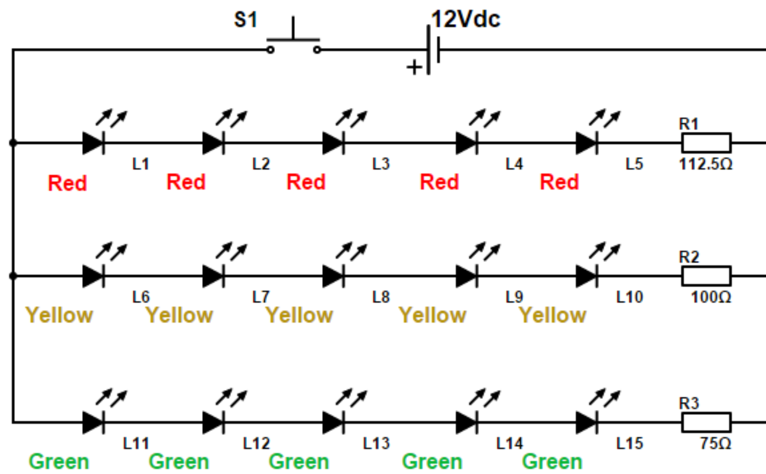

Figure 7. 7: The circuit used to power e-yarn with three colour LED's

Results and Discussion: All the LED's were soldered successfully, as shown as Figure 7.8. This experiment was undertaken to prove that the polyester coating can be removed only at the soldering area, thus preventing any short circuits. The final yarn containing three-colour LED's is shown in Figure 7.9.

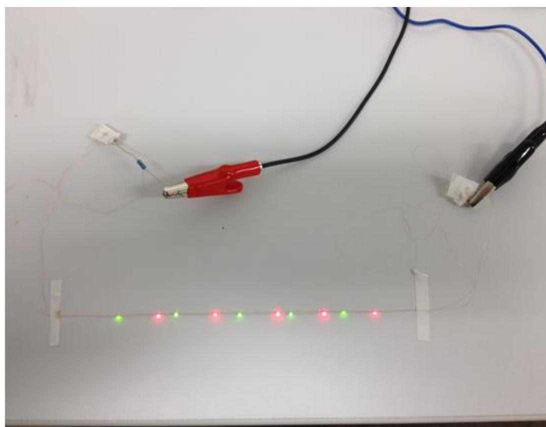

Figure 7. 8: After soldering 2 colours of LED

Figure 7. 9: Three- colour illuminated yarn

7.3 Development of Illuminated Car Seat Cover

E-yarn containing LED's (LEDY) will have multiple applications, especially in the cockpits of vehicles, e.g. door panels, headliners, dashboards, car seats, safety belts and carpets. Therefore, a prototype demonstrator of a car-seat cover was designed and produced and exhibited at the Automotive Engineering Show 2013 in Birmingham. The prototype demonstrator is shown in Figure 7.10, and its development is described in the following sections.

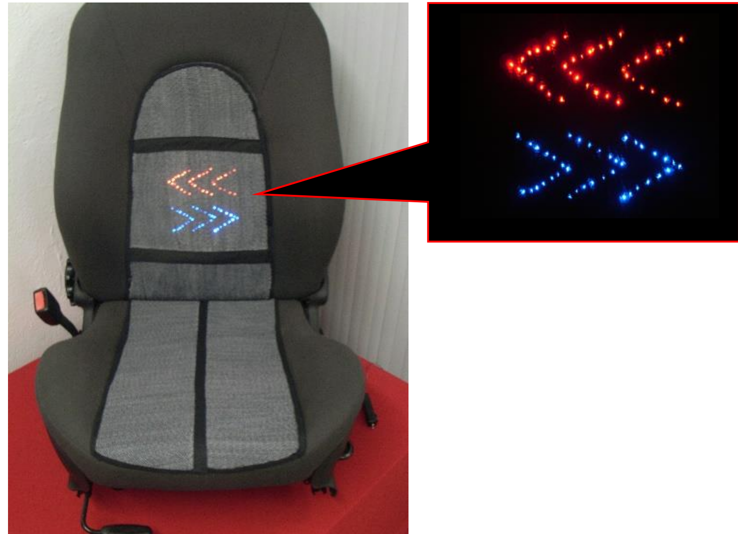

FIGURE 7. 10: THE PROTOTYPE DEMONSTRATOR OF AN ILLUMINATED CAR-SEAT COVER

7.3.1 Design of the Positions of LED's in the Fabric

A number of motifs were designed by the postgraduate research student (Dilusha Rajapaksha) at NTU. The two-colour arrow-shaped motif was selected as it was suitable for the automobile industry (Figure 7.11).

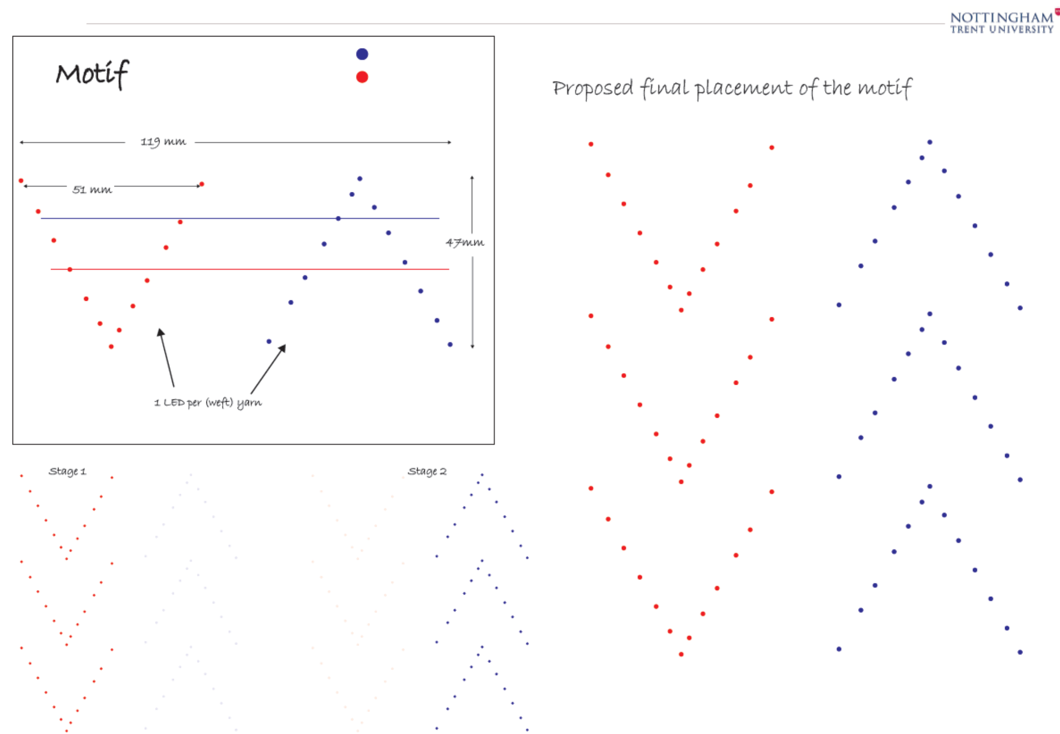

FIGURE 7. 11. POSITIONS OF RED AND BLUE LED'S IN THE CAR-SEAT COVER

7.3.2 Formation of LED Yarns for Car Seat Cover

Test 4.3.6 of Chapter 4 (pages 88 to 89) was used to solder LED's using a rapid heating profile. Thirty-nine red LED's (0402 type, RS components part number: 4663633, Spec: Annex 3), thirty-nine blue LED's (0402 type, RS components part number: 8609018 Spec: Annex 2), seven-strand copper wire, solder paste (lead free version, type VI from EFD ltd) were used. All the LED's (78 LED's) were soldered without issues. The method described in section 5.3 was used to encapsulate each LED using Dymax 9001-3.5 UV-curable resin (Spec: Annex 12). LED's soldered to copper wire were twisted onto the two 176 dTex/45 textured polyester yarns prior to encapsulation. The UV spot light was applied for 10 seconds to cure the resin. The core yarns were then processed further on the small-diameter circular warp knitting machine to craft e-yarns. Two, black-coloured 176 dTex/45 textured polyester yarn and two grey coloured 167 dTex/47 textured polyester yarns were used for knitting. The encapsulated core yarn and four white coloured 176 dTex/45 textured polyester yarn were used as packing fibres.

7.3.3 Production of Car Seat Fabrics

The car seat fabric was woven by Vajira Peiris (130), lecture of NTU. Details of the weaving specifications are shown in Figure 7.12.

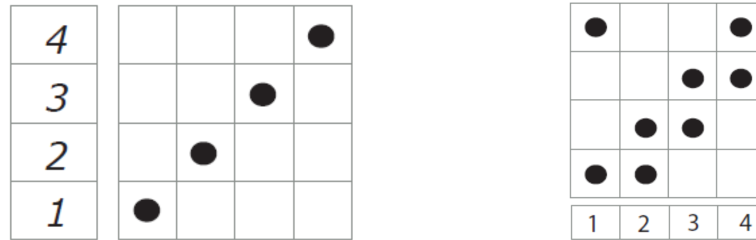

FIGURE 7. 12: WARP PLAN (LEFT) AND LIFTING PLAN (RIGHT)

7.3.3.1 Technical Specifications of Weaving the Car Seat Fabric.

The width of the warp before weaving was 30 cm. The width of warp after weaving was 26.5 cm. Two, different types of yarns were used for the weft: e-yarns with one LED and filling yarn which was produced on the RIUS with identical packing yarn and tubular warp knitted covering, however, without the core yarn which contain LED's. This enabled a uniform fabric to be woven. During weft insertion, the LED's were placed according the arrow shape motif diagram. The ends per inch of woven fabric was 8. The total length was 1.52 m.

7.3.4 Electronic-Circuit Design

According to the motif design, there were 13 LED's in total for each arrow (6 LED's on the left hand side of an arrow and 7 on the right-hand side of each arrow). As shown in Figure 7.10, there were three arrows in red and three arrows in blue. The LED's were connected as shown in Figure 7.13. As the number of LED's on the two sides of an arrow was not equal, different voltages were required to power all 13 LED's of an arrow. An Arduino pro mini board [131], which had a programmable micro controller, was used control the LED's to create blinking effects. However, the Arduino board was not capable of driving 13 LED's, so a power circuit was designed to drive the LED's with the Arduino pro-mini board. The electronic circuit and power circuit are shown in Figures 7.13 & 7.14. Even though two power circuits were designed and produced, only one circuit which was designed for use with the red LED's was used as it sufficient for all the connections. According to Figures 7.13 and 7.14, there were two groups of LED's containing 6 and 7 LED's each. However, the 6 and 7 LED's were connected together to make one group of 13. Then 12 groups of blue and red LED's were connected to make 6, larger groups.

Therefore, 6 connections from the Arduino circuit were required, instead of 12 which was original idea.

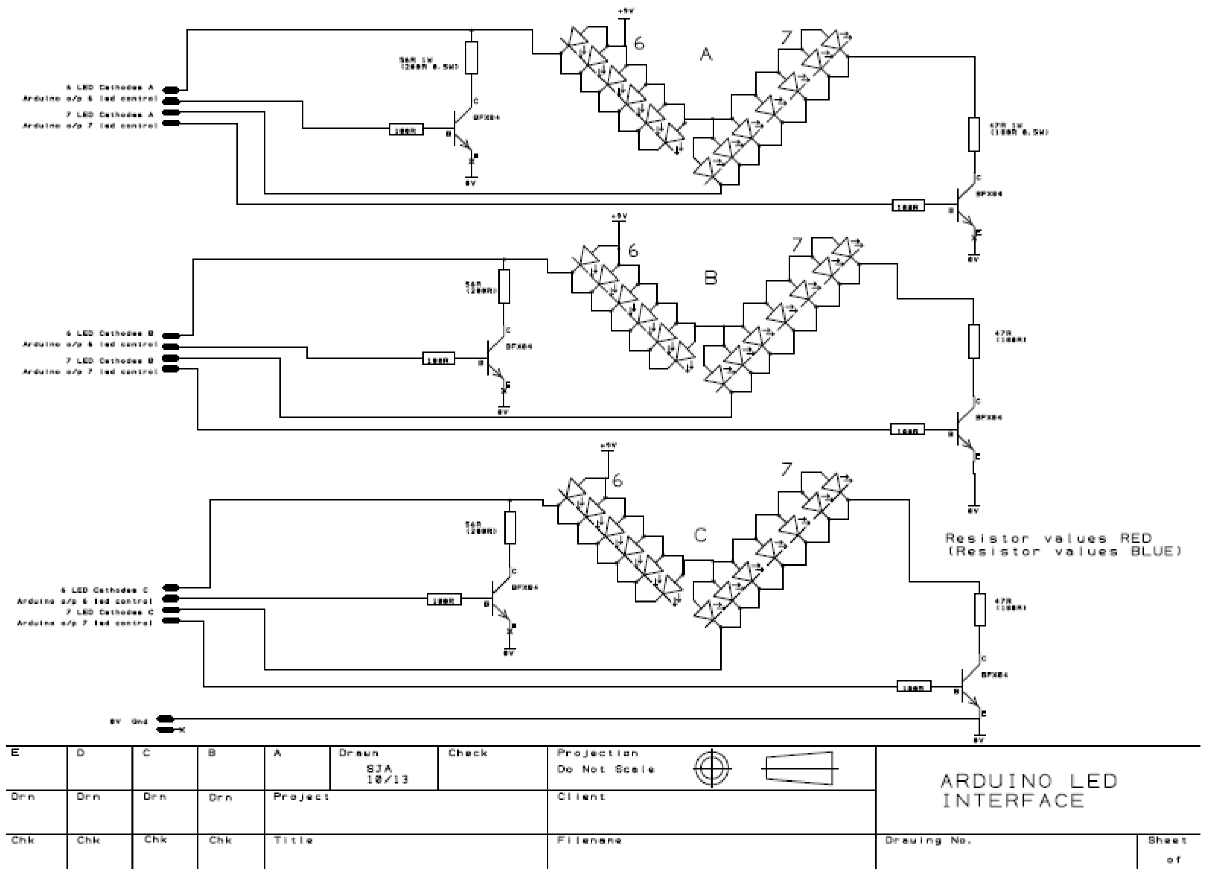

FIGURE 7. 13: ARDUINO-LED INTERFACE – SCHEMATIC

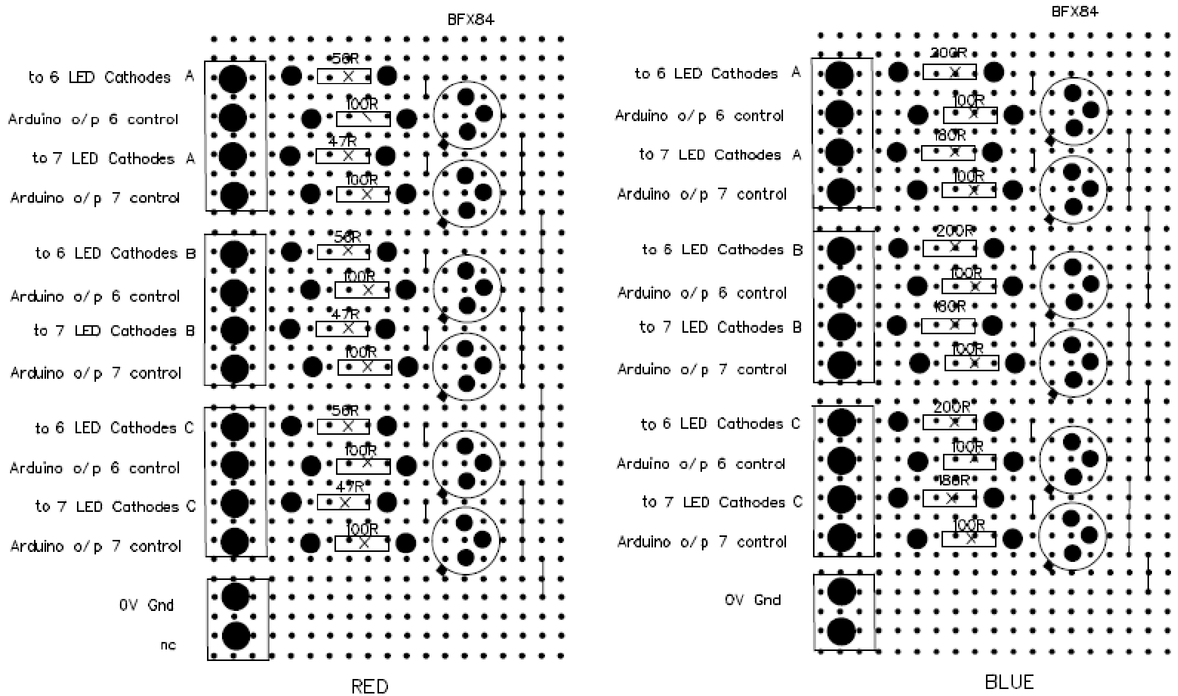

FIGURE 7. 14: SCHEMATIC DIAGRAM OF POWER CIRCUIT BOARDS

7.3.5 Circuit Programming

Two blinking functions were designed: a blinking effect and a sequence effect for the red and blue LED's. The Arduino programmes were as demonstrated below.

7.3.5.1 Arduino Programming for the Blinking Effect

```
// The Lilypad 328 has PWM on pins 5,6,9,10,11
/* Pin Definitions */
// LED's: white LED's are connected to 5, 6, A2, A3, A4
int ledPins[] = {1, 2, 3};
void setup()
{
  for(int i=0; i<8; i++)  //Set all LED pins to outputs
  {
    pinMode(ledPins[i], OUTPUT);  //Set pin as output
    if(i>4)
    {
      digitalWrite(ledPins[i], HIGH);  //If RGB LED then make pin high to turn OFF
    }
  }
}
 void loop()
{
   // Blink LED's for 60 seconds
  for(int j=1; j<30; j++)  // LED's ON for 1 second, OFF for 1 second * 30 for minute
  {
    for(int i=0; i<8; i++)
    {
     if(i>4)
      {
       digitalWrite(ledPins[i], LOW);  // If RGB LED pin then set pin low to light
      }
      else
      {
       digitalWrite(ledPins[i], HIGH);  // High for normal LED
      }
    }
    delay(50);  // Wait for 1 second
    for(int i=0; i<8; i++)
    {
     if(i>4)
      {
       digitalWrite(ledPins[i], HIGH);  // If RGB LED pin then set pin high for off
      }
      else
      {
       digitalWrite(ledPins[i], LOW);  // Low for normal LED
      }
    }
    delay(50);  // Wait for 1 second
```

```
  }
}
```

7.3.5.2. Arduino Programming for the Sequence Effect

```
// The Lilypad 328 has PWM on pins 5,6,9,10,11
/* Pin Definitions */
// LED’s: white LED’s are connected to 5, 6, A2, A3, A4
int ledPins[] = {5, 6, 7, 8, 9, 10};
int delTime = 300;
void setup()
{
  for(int i=0; i<6; i++)  //Set all LED pins to outputs
  {
    pinMode(ledPins[i], OUTPUT);  //Set pin as output
    if(i>4)
    {
      digitalWrite(ledPins[i], HIGH);  //If RGB LED then make pin high to turn OFF
    }
  }
}
 void loop()
{
// Sequence all LED’s
  for(int i=0; i<6; i++)  // This for loop will run 5 times
  {  // blink the white LED’s (first 5 LED’s in ledPins array)
    pinMode(ledPins[i], OUTPUT);  // set pin as output
    digitalWrite(ledPins[i], HIGH);  // turn LED on
    delay(delTime);  // wait for a quarter second
    digitalWrite(ledPins[i], LOW); // turn LED off
    //delay(500);
  }
  }
```

7.3.6 Pilot Run with standard LED’s

A pilot run was undertaken using an Arduino main board Uno [132] (open source interface, available in the market) and standard LED’s. The main advantage of an Arduino main board is that it can be connected using wires without soldering. The initial objective was to check the power circuit board and Arduino programme. The LED’s and connections from the power board and Arduino main board were placed on a breadboard. The Arduino main board was connected to a computer using a mini USB cable (Figure 7.15). The Arduino programme was uploaded to the Arduino main board and checked. The programme was changed, uploaded and checked until a satisfactory of blinking effect was obtained. This procedure was repeated for the second programme.

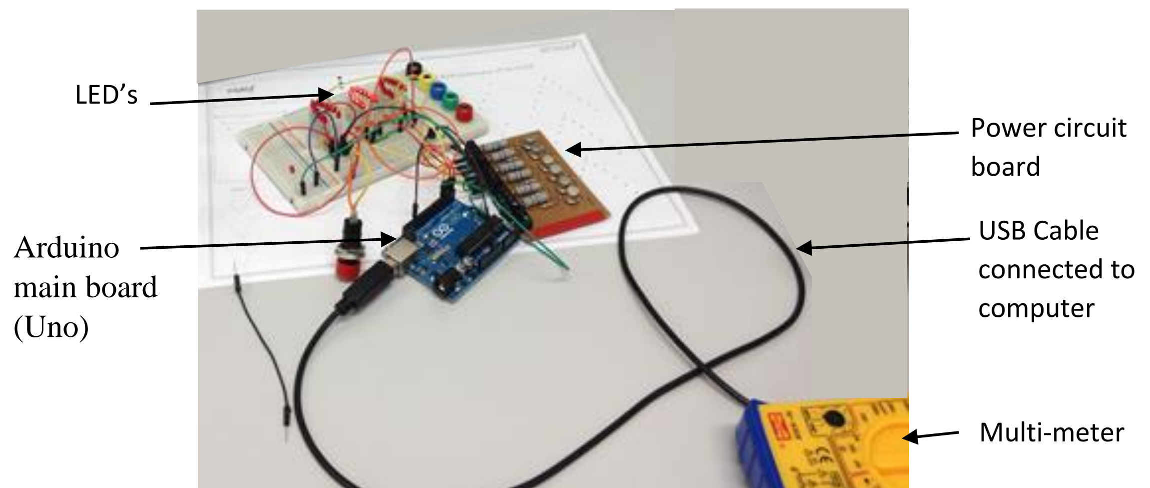

FIGURE 7. 15: A PICTURE OF PILOT RUN ON BREADBOARD

7.3.7 Pilot Run with Illuminated Fabric Piece

The above circuit was connected to the illuminated fabric for testing (Figure 7.16).

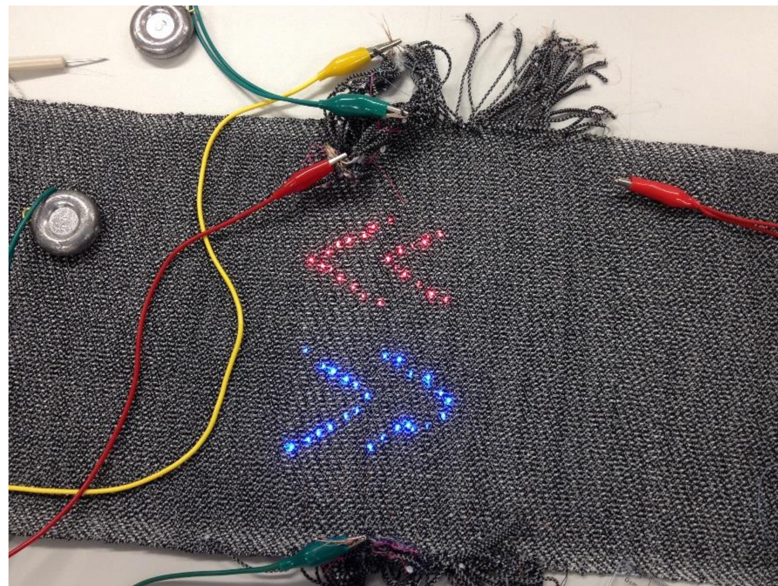

FIGURE 7. 16: A PICTURE OF PILOT RUN ON ILLUMINATED FABRIC

7.3.8 Finishing the Car Seat Edge

It was necessary to remove excess polyester yarns whilst copper wires of e-yarns were remaining for interconnection. Thirteen copper wires connected to one arrow were twisted together and soldered individually to a tubular, warp-knitted yarn which contained six, coated-copper wires inside. Both edges of the fabric were finished by hand sewing (Figure 7.17). Then this piece of fabric was sewn to two pieces of fabric and finished the edges as shown Figure 7.18.

FIGURE 7. 17: THE ILLUMINATED FABRIC WHILST FINISHING THE EDGES

7.3.9 Pilot Run with Illuminated Car Seat and Packing the Circuit Boards

The final pilot run was carried out with the illuminated fabric using the Arduino main board (Figure 7.21). After that, all the wires were disconnected from the breadboard and Arduino main board. The connections were soldered to Arduino pro mini boards which were equal to the main board but much smaller. Finally, the circuit boards were inserted into a box and attached to a switch and to the circuit board.

FIGURE 7. 18: THE FINAL PILOT RUN WITH ILLUMINATED CAR SEAT COVER

The illuminated car seat was exhibited (Figure 7.19) at the Advanced Engineering Exhibition, Birmingham between the 12 and 13 November 2013 [133]. The Advanced Engineering UK 2013 group of events was comprised in Aero Engineering Show 2013, Composites Engineering Show 2013, Automotive Engineering Show 2013, Auto Electronics 2013 & Printable Electronics for Industry. It was 2-day attendance of 12,000, representing some 5000+ companies, 600+ exhibiting supply chain companies and 200+ Presentations

FIGURE 7. 19. THE AUTHOR AT THE AUTOMOTIVE ENGINEERING SHOW IN BIRMINGHAM

7.4 Illuminated Garment

"The high performance area of textiles contributes £1.2 billion to the UK's economy each year and employs more than 20,000 people. Future Textiles looked at how this industry is supported: by inspiring young people at school; by university courses that focus students on the latest technologies" [135]. An exhibition called 'Future Textiles Exhibition at the Palace of Westminster (UK Parliament) on 10th to Friday 14th December 2012 [134, 135]. There were eight exhibitors and Advanced Textiles Research Group of Nottingham Trent University was one of them. A prototype demonstrator garment was designed and produced to show case the e-yarn technology to stake holders, and the manufacturing process is described in this section.

FIGURE 7. 20: THE ILLUMINATED GARMENT

7.4.1 Design of LED's Position in the Fabric

It was decided to integrate fifty LED's into the garment, and the LED positions are shown in Figure 7.21 which was designed by a MA Student (Anna Piper) of the School of Art and Design at Nottingham Trent University. There were ten LED's in each row and the design consisted altogether of five rows.

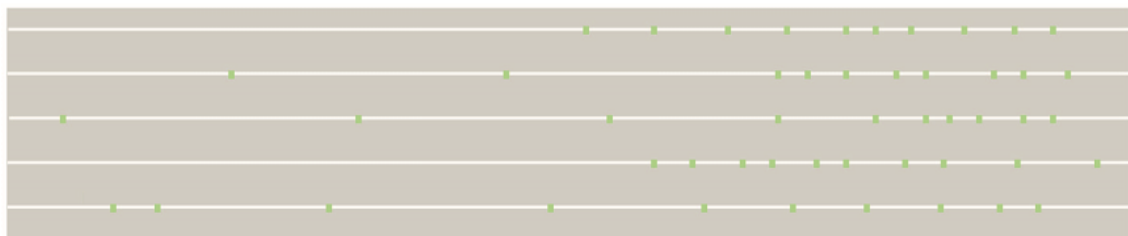

FIGURE 7. 21. LED'S POSITIONS IN THE ILLUMINATED GARMENT FABRIC

7.4.2 Fabrication of E-Yarn with LED's

According to the design illustrated in Figure 7.21, five e-yarns with ten green LED's (0402 type, RS components part number: 4663611, Annex: 5) were produced. Ten LED's were soldered on to seven-strand copper wire using solder paste (lead free version, type VI from EFD Ltd). Five, different core yarn of LED's was formed, i.e. a total of 50 LED's were soldered without any issues. The LED's in the core yarns were soldered according to the design in Figure 7.21, in which the LED's were placed at uneven distances apart in order to break the even nature of illumination across the design. The design was printed onto an A4 sheet and the distances between each LED were directly copied to the core yarn during soldering of the LED's, rather than measuring each and every distances between LED's.

As the next step, micro pods were created to protect the LED's using Dymax 9001-3.5 UV curable resin. However, prior to encapsulation of the LED's the interconnects (multi strand copper wire) were twisted on to two 176dTex/45 white, textured polyester yarns. The above procedure, which was explained in 5.4 (pages 114 to 115) was adopted to build the core yarn. This was then covered with the tubular, warp-knitted structure using the RIUS MC machine to form the e-yarns as explained in section 7.3.2 and the yarns were labelled according to the design.

The e-yarns with LED's were checked before being woven into the fabric. Figure 7.22 shows the five e-yarns when activated.

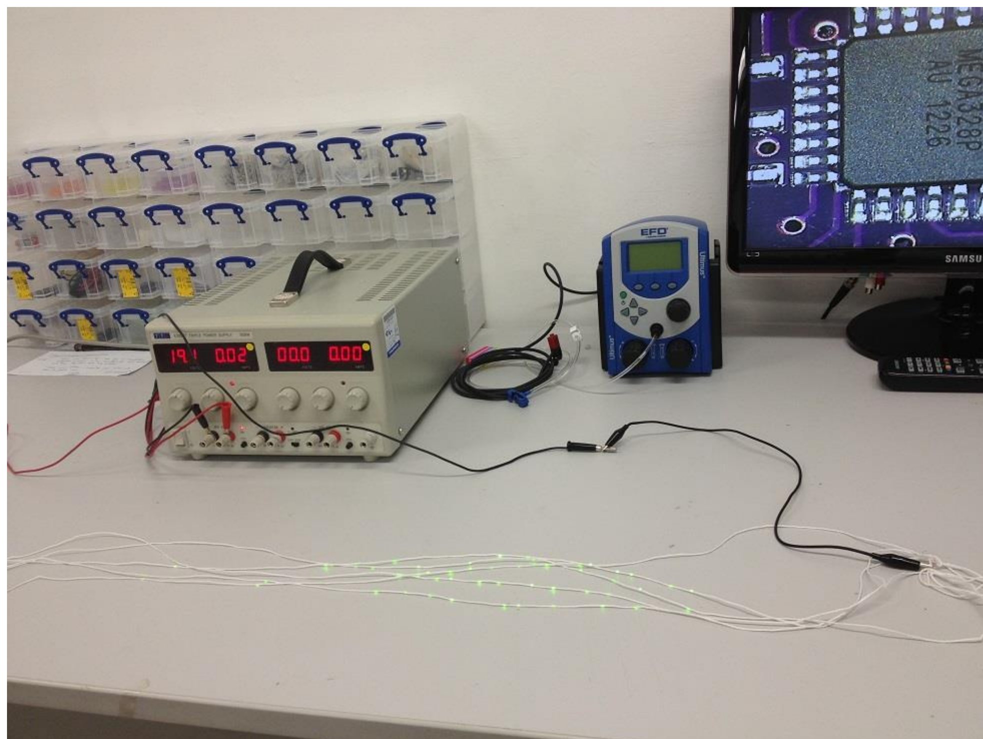

FIGURE 7. 22 : ILLUMINATED E – YARNS

7.4.3 Weaving the Illuminated Garment

The illuminated garment was woven on a handloom as a seamless tube construction [136]. During the weaving process the e-yarns were introduced as the weft at positions defined by the design.

FIGURE 7. 24: THE WEAVING OF THE GARMENT BY ANNA PIPER

FIGURE 7. 23: THE GARMENT JUST AFTER REMOVAL FROM WEAVING LOOM

7.4.4 Electronics and Power Circuit Board and Design

On each e–yarn there were ten LED’s connected in series. According to the technical data sheet for the green LED’s [Annex 5], a DC voltage of between 2.1 and 2.5 Volts has to be supplied to activate one LED, so 21 – 25V was required to activate all the LED’s in one e-yarn. In order to create a visually attractive lighting pattern the individual electronic yarns were controlled from a LilyPad Arduino microcontroller (Figure 7.25). According to the technical specification, a LilyPad micro controller can provide an output between 2.7 to 5.5 V [Annex 19]. However, as at least 21V is required to power the LED’s. Additional hardware was developed to boost the 5.5V output of the LilyPad circuit (Figure 7.26).

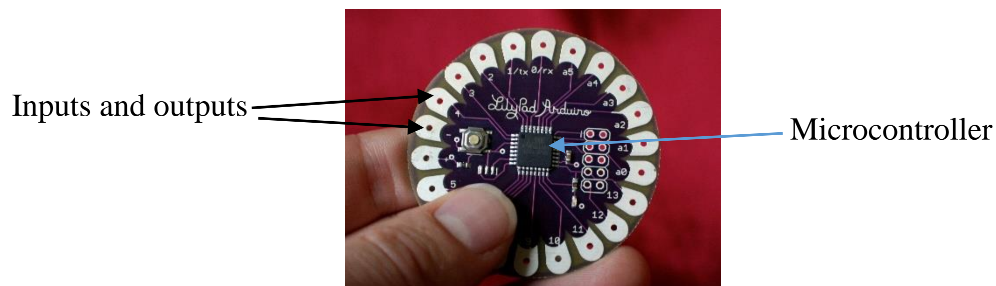

FIGURE 7. 25: IMAGE OF LILYPAD ARDUINO MICROCONTROLLER

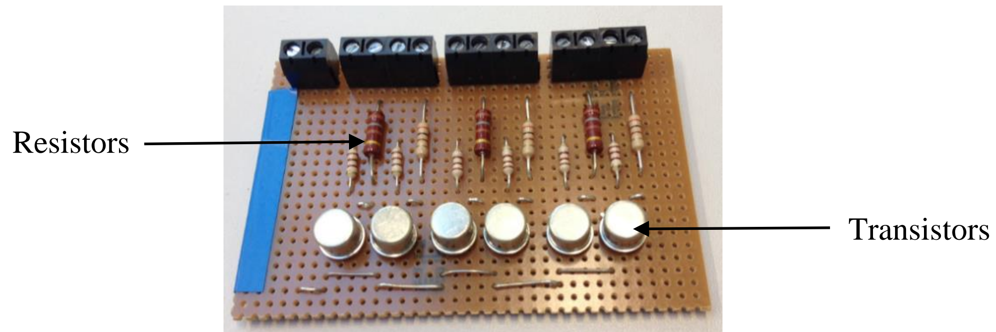

FIGURE 7. 26: ELECTRIC POWER MANAGEMENT CIRCUIT BOARD

7.4.5 Arduino Software Programming

A software programme was developed with three blinking patterns: a sequence pattern (each LED row switching on and off from bottom to top) repeated three times; a blink pattern (all the LED's switching on and off) lasting60 seconds; and a fade pattern (starting from zero, up to the maximum intensity of the LED's) lasting for 60 seconds. These three patterns were continuously repeated. The software programme as developed is given below.

```
// The Lilypad 328 has PWM on pins 5,6,9,10,11
/* Pin Definitions */
// LED's: white LED's are connected to 5, 6, A2, A3, A4
int ledPins[] = {5, 6, A2, A4, A3, 9, 10, 11};
void setup()
{
   for(int i=0; i<12; i++)  //Set all LED pins to outputs
  {
   pinMode(ledPins[i], OUTPUT);  //Set pin as output
   if(i>4)
   {
     digitalWrite(ledPins[i], HIGH);  //If RGB LED then make pin high to turn OFF
   }
  }
  }
 void loop()
{
 int q=1;
 while(q<2){

// Sequence all LED's
   for(int i=0; i<8; i++)  // This for loop will run 5 times
  {  // blink the white LED's (first 5 LED's in ledPins array)
   pinMode(ledPins[i], OUTPUT);  // set pin as output
   digitalWrite(ledPins[i], HIGH);  // turn LED on
   delay(250);  // wait for a quarter second
```

```
    digitalWrite(ledPins[i], LOW); // turn LED off
   }
   for(int i=0;i<8;i++)  // This for loop will run 3 times
   {   // blink the RGB LED's (last 3 LED's in ledPins array)
    pinMode(ledPins[i], OUTPUT);   // set the pin as an output
    digitalWrite(ledPins[i], LOW);  // turn RGB LED on
    delay(250);  // wait a quarter second
    digitalWrite(ledPins[i], HIGH);  // turn the RGB LED off
    // Note that a HIGH turns the RGB LED off, LOW is on
    // that's backwards from the white LED's
   }
 // Blink LED's for 60 seconds
   for(int j=0; j<30; j++)  // LED's ON for 1 second, OFF for 1 second * 30 for minute
   {
    for(int i=0; i<8; i++)
    {
     if(i>4)
      {
       digitalWrite(ledPins[i], LOW);  // If RGB LED pin then set pin low to light
      }
      else
      {
       digitalWrite(ledPins[i], HIGH);  // High for normal LED
      }
    }
    delay(100);  // Wait for 1 second
    for(int i=0; i<8; i++)
    {
     if(i>4)
      {
       digitalWrite(ledPins[i], HIGH);  // If RGB LED pin then set pin high for off
      }
      else
      {
       digitalWrite(ledPins[i], LOW);  // Low for normal LED
      }
    }
    delay(100);  // Wait for 1 second
   }
 // Fade LED's for 60 seconds
   for(int j=0; j<2; j++)
   {
    for(int i=0; i<251; i++)  // i = LED brightness
    {
      analogWrite(5, i);
      analogWrite(6, i);
      analogWrite(9, i);
      analogWrite(10, i);
      analogWrite(11, i);
      delay(10);  // Delay for 1mS
    }
      for(int i=250; i=0; i--)  // i = LED brightness
```

```
    {
     analogWrite(5, i);
     analogWrite(6, i);
     analogWrite(9, i);
     analogWrite(10, i);
     analogWrite(11, i);
     delay(10);  // Delay for 1mS
    }
   }
  q=1;
   }
 }
```

7.4.6 Pilot Run with LilyPad Development Board and Illuminated Garment

A LilyPad development board [137] (Figure 7.27) which has a built in LiyPad controller and LED's was used to develop and test the software programme. It was easy to upload the Arduino programme from a personal computer (PC) and software was written to create blinking patterns with LED's. Once the new software had been tested and optimised, it was tested with the illuminated garment (Figure 7.28) before finishing off the connections to the e-yarns at the edges of the garment.

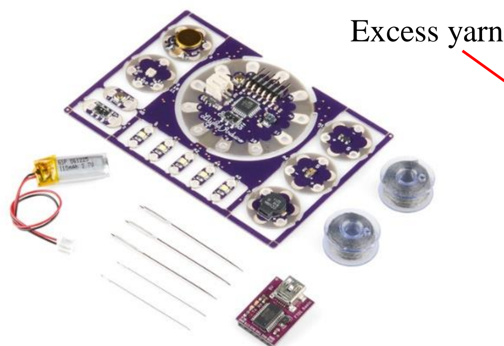

FIGURE 7. 27: LILYPAD DEVELOPMEN BOARD

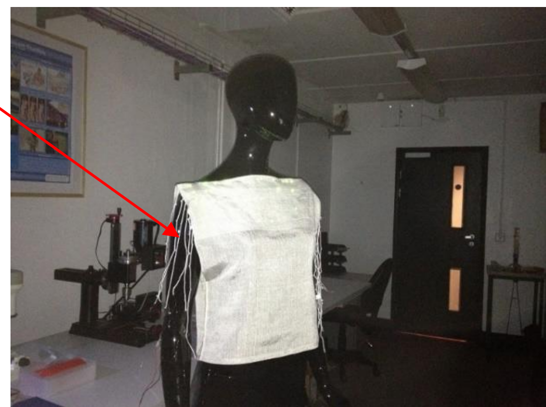

FIGURE 7. 28: A PICTURE TAKEN DURING THE PILOT RUN ON THE ILLUMINATED GARMENT

7..4.7 Finishing of the Illuminated Garment and Connectivity of e-Yarns.

All the excess yarns were removed. The ends of the multi-strand copper wires in the e-yarns were soldered and connected to metal press-studs (female). The fabric edges at the arm holes were folded and hand stitched to give a neat finish. The LilyPad circuit board and the power board (which contained hardware designed to boost the output voltage of the LilyPad controller) were connected together and inserted into a box. The output

connections from the power board were connected to metal press-studs (male) on a rectangular woven fabric piece of 15x10 cm, which was then folded to form a fabric connector as shown in Figure 7.29. In order to demonstrate the illuminated garment for longer periods, especially at exhibitions the hardware was designed to be powered from a twenty-four Volt power pack.

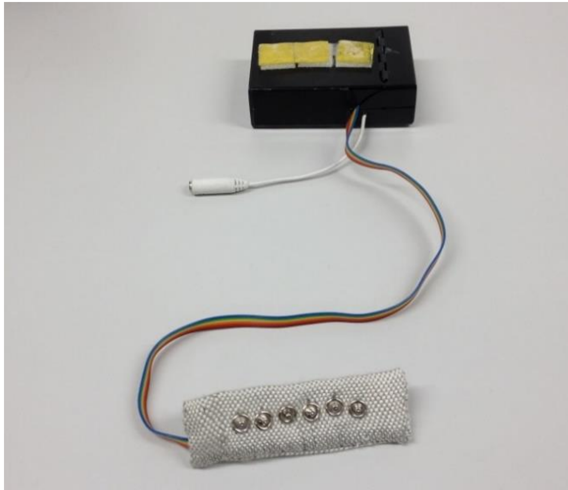

FIGURE 7. 29: THE FABRIC CONNECTOR, WHICH WAS DEVELOPED TO CONNECT CONTROL HARDWARE TO THE GARMENT

FIGURE 7. 30: THE FINISHED, ILLUMINATED GARMENT

7.5 Development of Temperature-Sensor Yarns and Fabrics

7.5.1 E-Yarns for Temperature Sensing

The aim of this development was produce a temperature-sensing e-yarn by using thermistors. A thermistor is a temperature-sensitive resistor. There are two type of thermistors. Negative temperature coefficient (NTC) thermistors decrease in resistance when the temperature increases. In contrast, positive temperature coefficient (PTC) thermistors increase in resistance when the temperature increases [138]. A SMD type thermistor from Murata Corporation (10kΩ 100mW 0402 NTC Thermistor 1.0 x 0.5 x 0.5mm) was used [139] in this development; the technical data is given in Annex 7. According to the manufacturer's data, at 25^{0}C the thermistor had a resistance of 10kΩ. The manufacturing process of e-yarn with thermistors (Soldering, encapsulation and braiding) was undertaken using the method reported in Section 7.4. Both ends of the multi-strand copper wire of the thermistor e-yarn were connected to a multi-meter (Figure 7.31) in order to demonstrate the change in resistance at different temperatures. For example, on touching the e-yarn where the thermistor is located, the resistance reading changed immediately.

FIGURE 7. 31: A PROTOTYPE THERMISTOR E - YARN

7.5.2 Development of a Fabric to Measure Temperature

Several thermistor e-yarns were integrated into a knitted fabric to develop a prototype demonstrator for sensing temperature. Five thermistor e-yarns were produced following the procedure explained in the previous section (7.5.1). A rib-knitted fabric of 25x20 cm was produced from 167dTex/47 PE yarn. The fabric was knitted with 2 mm wide channels so that thermistor e-yarns could be inserted into them. The knitted fabric containing thermistor e-yarn is shown in Figure 7.32. Red colour threads were tagged on to the fabric surface in order to indicate the thermistor locations in the temperature-sensor fabric.

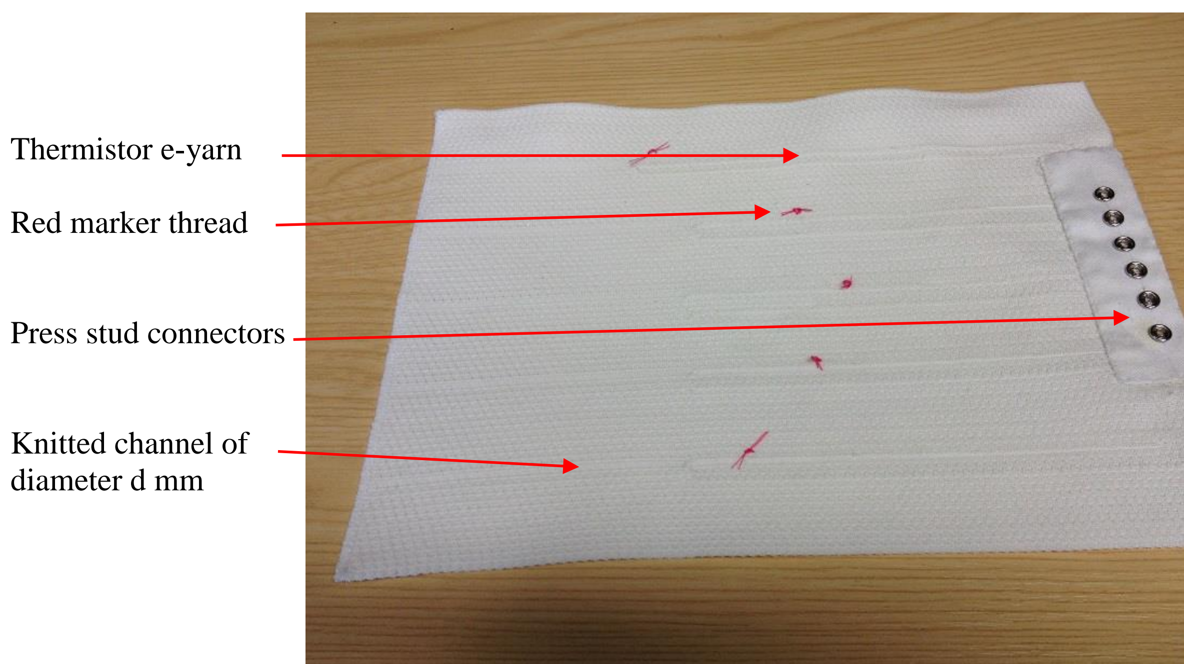

FIGURE 7. 32: PICTURE OF THE TEMPERATURE-SENSOR FABRIC MAT

7.5.2.1 Hardware Development

One end of each thermistor e-yarn was connected together and soldered to a metal, female press-stud and the other 5 ends were soldered to 5 metal female press studs. Six male metal press studs were mounted on to a woven fabric of 15x10 cm, and these were soldered to the relevant terminals of the circuit shown in Figure 7.33. A potential-divider circuit was used to determine the resistance of the thermistors, and the relevant voltages were measured with an Ardiuno pro mini micro controller unit [Annex: 20]. The fabric edges were folded and covered with Silicone rubber (Figure 7.35)

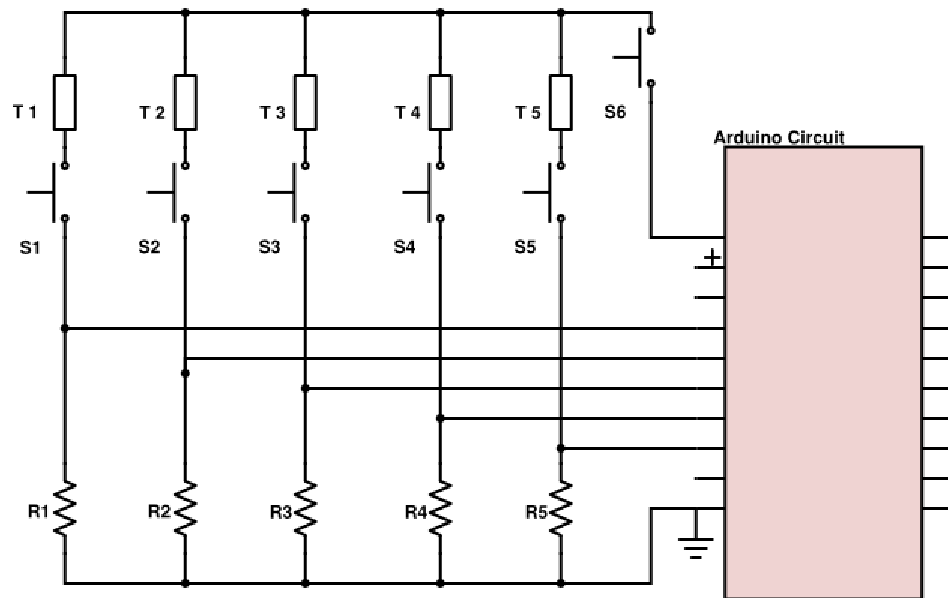

FIGURE 7. 33: ELECTRONIC CIRCUIT DIAGRAM (SCHEMATIC)

Thermistors: T1, T2, T3, T4, T5

10KΩ Resistors: R1, R2, R3, R4, R5

Metal press studs: S1, S2, S3, S4, S5

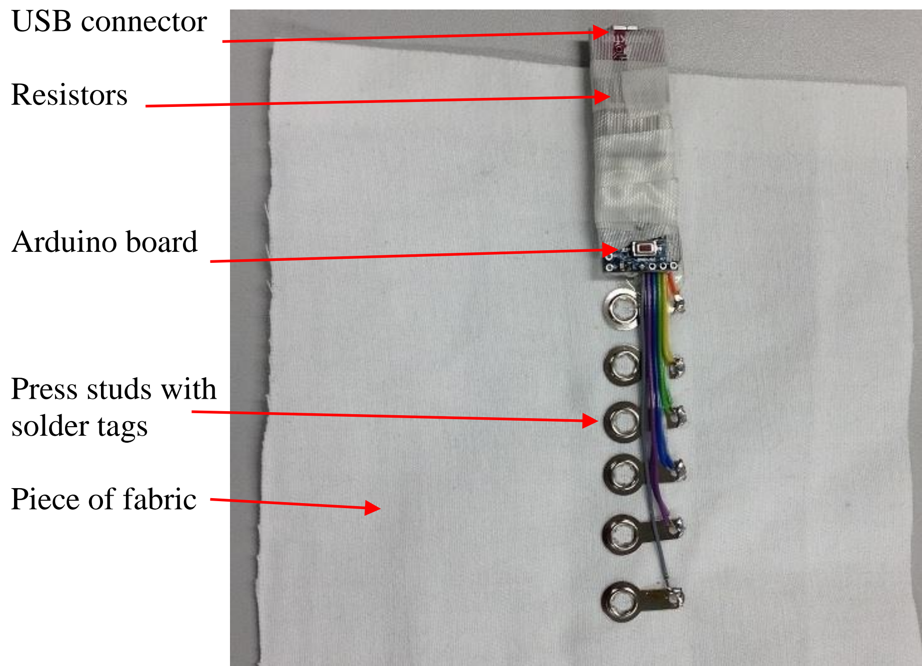

FIGURE 7. 34: PICTURE OF THE ELECTRONIC CIRCUIT BOARD

FIGURE 7. 35: PICTURE OF THE CIRCUIT BOARD WHICH IS COVERED WITH SILICONE RUBBER

7.5.2.2 Development of hardware to measure temperature with temperature sensor fabric

LabVIEW software was developed to demonstrate the temperature sensing fabric mat. This is shown below in Figure 7.36 and 7.37.

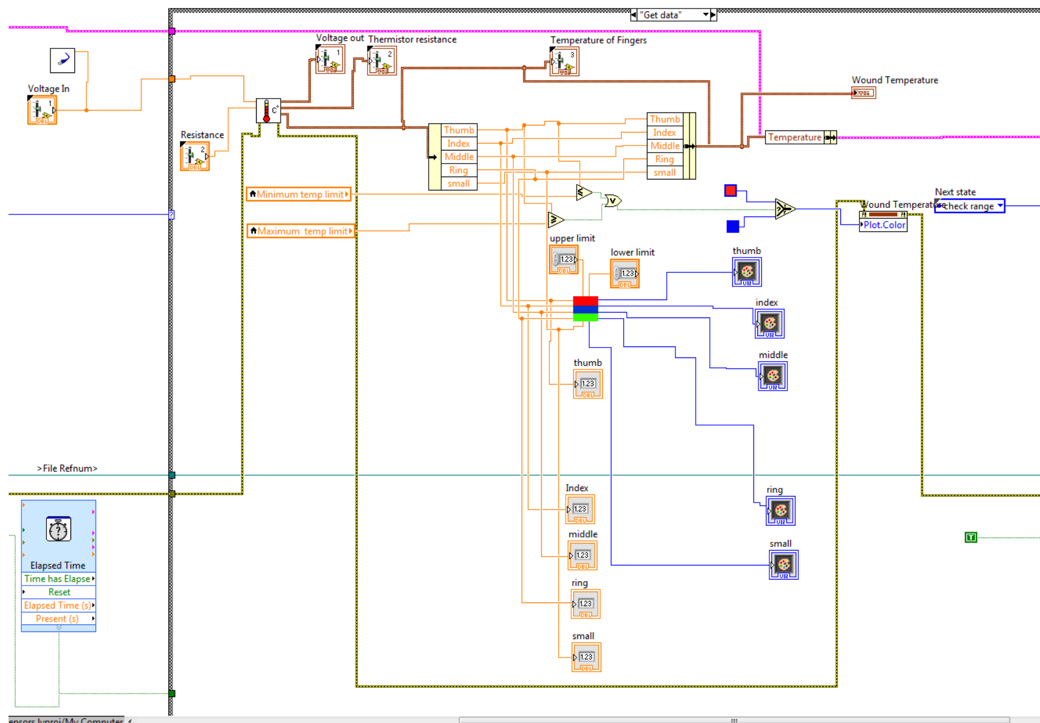

FIGURE 7. 36: LABVIEW BLOCK DIAGRAM

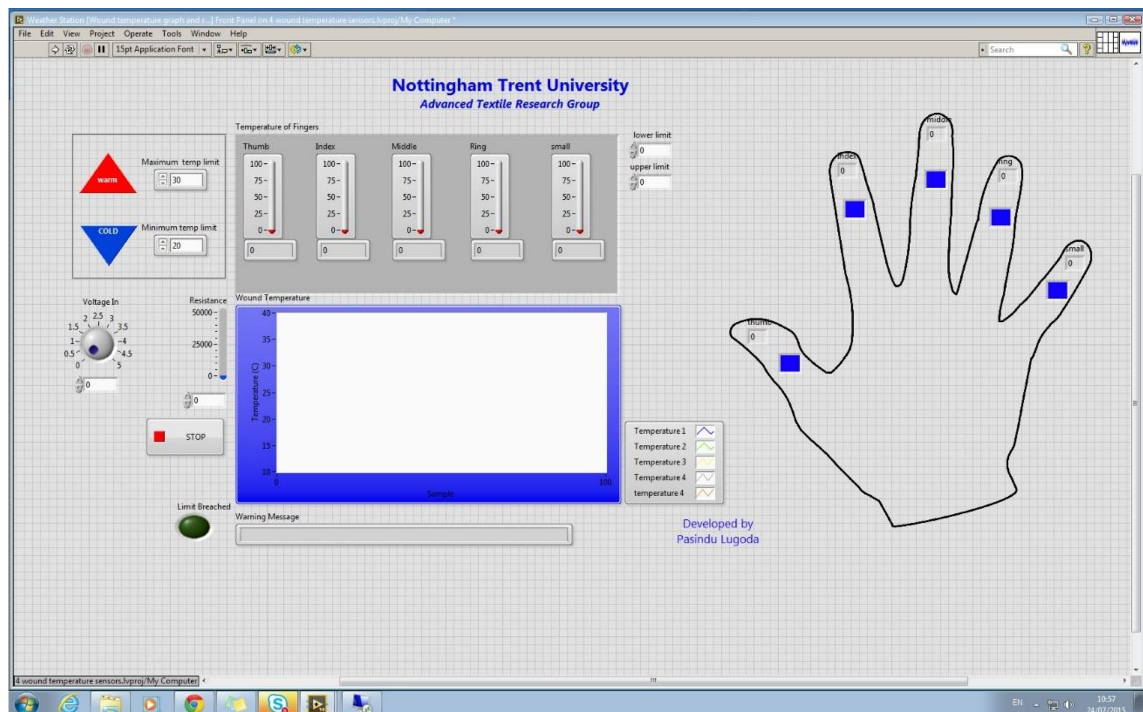

FIGURE 7. 37: LABVIEW GRAPHICAL USER INTERFACE DEVELOPED TO SHOW THE MEASURED TEMPERATURES

7.5.2.3 A Pilot Run

The connector with the electronic circuit was connected to the temperature sensing mat, and was also connected to the computer using an USB cable. The LabVIEW interface was set-up in run mode. A hand was placed on the mat and the temperature readings were noted. The colour image of the hand on the hand screen changed from blue to red when the temperature exceeded 30 ^{0}C. In Figure 7.38 the spot on the little finger in the image is a blue colour, as the little finger of the hand was not touching the thermistor e-yarn of the temperature sensing mat. When all the fingers were touching the thermistor e-yarns of the temperature sensor fabric mat, all fingers in the image on the computer screen changed to a red colour as shown as Figure 7.39.

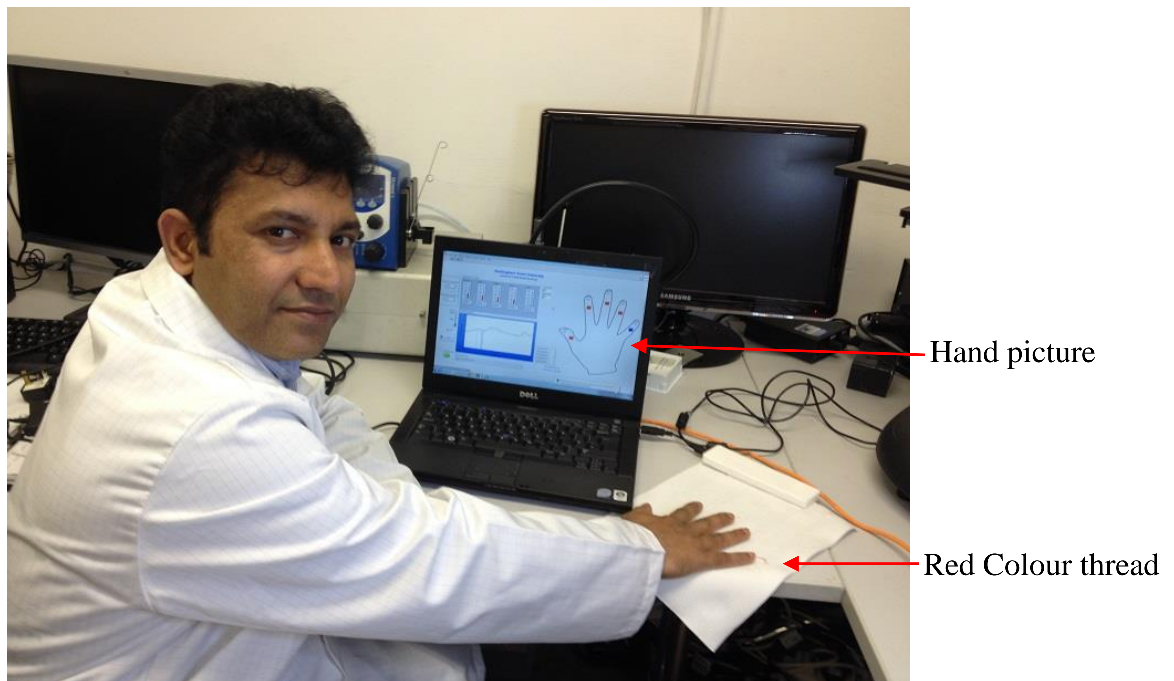

FIGURE 7. 38: DEMONSTRATION OF THE RESPONSE OF TEMPERATURE WHEN FOUR FINGERS OF THE AUTHOR'S HAND ARE IN CONTACT WITH THE TEMPERATURE-SENSOR FABRIC MAT

FIGURE 7. 39: DEMONSTRATION OF THE RESPONSE WHEN ALL FIVE FINGERS OF THE AUTHOR'S HAND ARE IN CONTACT WITH THE TEMPERATURE-SENSOR FABRIC MAT

7.5.3 Development of Temperature Sensor Socks

As shown in Figure 7.40, a pair of thermistor socks were developed to measure foot temperature for the management of non-freezing cold injury and diabetic foot ulcers. The ultimate aim of the medical community is to identify the symptoms and manage feet damage.

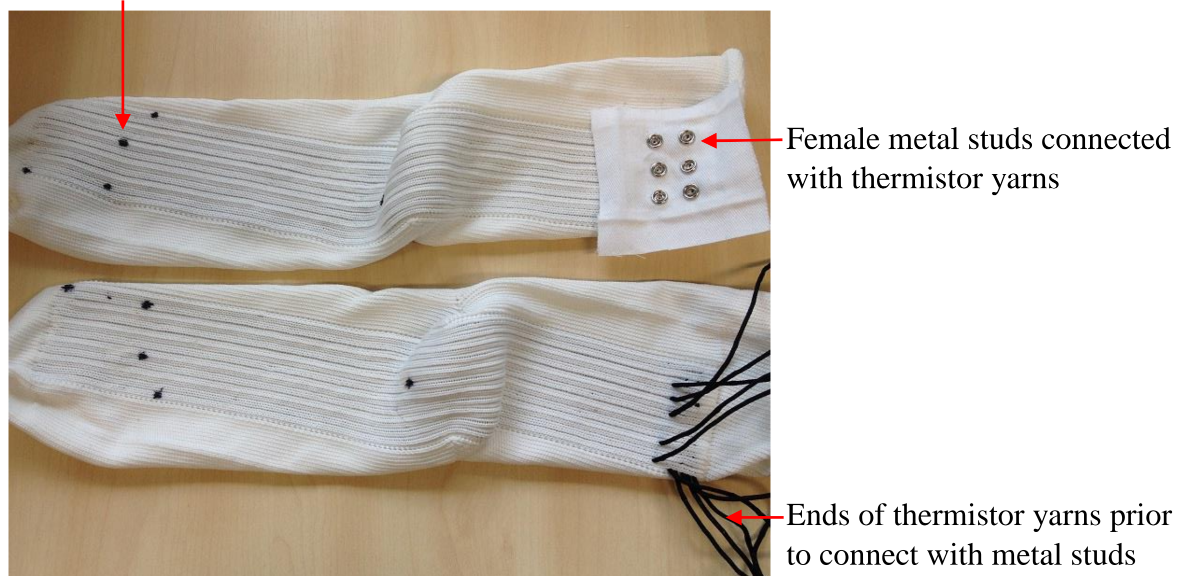

FIGURE 7. 40: A PAIR OF THERMISTOR SOCKS

Ten thermistor yarns were produced following procedure as described in the section 7.5.2. The seamless garment socks were knitted on Shima Seiki flate bed knitting machine (model: SWG, needle Gauge: 15, needle hook gauge: 15). Seven ends of texturized polyester 167dTex/48 yarns (white colour) a Lycra yarn were used for knitting the pair of sock. The sole part of the socks was knitted with five channels (2mm wide tube) of 2 needles and six channels (3mm wide tube) of three needles, so that thermistor e-yarns could be inserted into them. Knitting technical specs are shown in Figures 7.41 and 7.42. Five thermistor yarns were serted into sole part of each sock. The thermistor yarns were conneted to metal studs as explained as section 7.5.2.1. A detail analysis of improvement, washing trials and clinical trials could not be carried out within the framework of this PhD research programme.

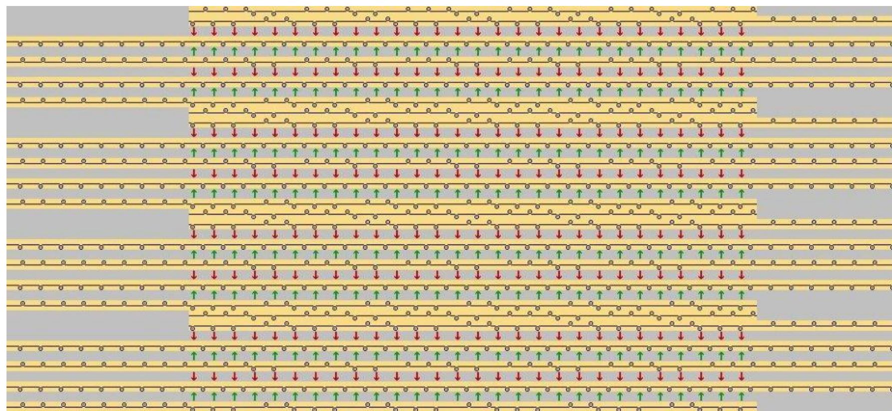

FIGURE 7. 41: TECHNICAL SPEC OF KNITTING MACHINE

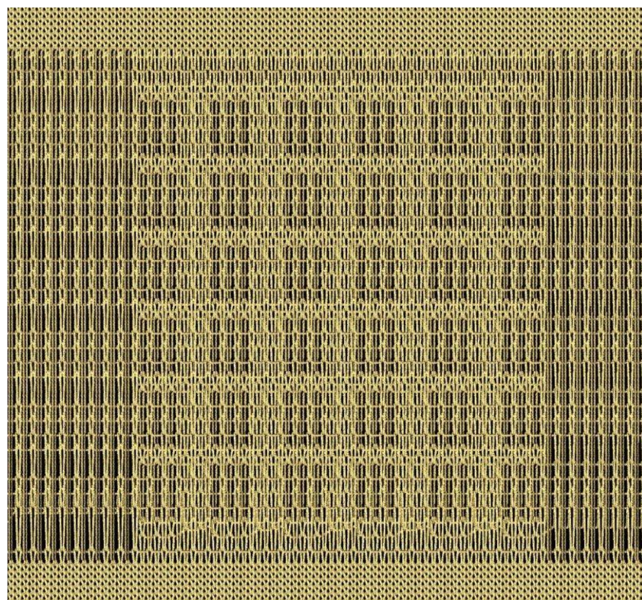

FIGURE 7. 42: SIMULARSION OF KNITTED FABRIC STRUCTURE OF SOCK

7.6 Development of e-Yarns with Electronic Signatures

Radio frequency identification (RFID) is a technology which uses microwaves or ultra-high frequency (UHF) electromagnetic signals within the radio spectrum to identify and track objects wirelessly [140]. Even though RFID technology is 50 years old, recently it has moved from obscurity into common use to handle or monitoring of manufacturing processes through to the end use of products and materials efficiently. RFID technology is able to identify objects at a distance for large numbers of products within a few seconds. In the case of bar codes, which are a widely-used and established technology for identifying products and objects today, it is necessary to position a bar code scanner in a line of sight at close distance [141]. Examples of a barcode and an RFID tag are shown in Figures 7.43 and 7.44.

FIGURE 7. 44: AN EXAMPLE OF A BAR CODE [142]

FIGURE 7. 43: AN EXAMPLE OF AN RFID TAG [141]

7.6.1 RFID Technology

An RFID tag contains a semiconductor chip to store memory and an antenna to receive and transmit radio waves (Figure 7.44). The current RFIDs can be categorised into three groups, as active, passive and semi-passive. Batteries are used to power the chip in order to transmit signals to the reader in active RFID tags, whilst passive tags do not use a battery. The antenna of passive tags receive the electromagnetic waves sent out by a reader and energise the chip, so that a predetermined interference pattern is created by the chip depending on the information stored in its memory. This interference pattern is received by the reader to identify the chip. The battery power and wave sent out by the reader are both used in semi-passive tags to transmit data to the reader. Active and semi-passive tags are comparatively expensive and are used in high-value goods, and can be read from longer distances than passive RFID tags [143].

FIGURE 7. 45: SCHEMATIC DEMONSTRATING RFID TECHNOLOGY (144)

7.6.2 Creation of antenna for the RFID device

Commercial RFID tags are made by printing an antenna onto a substrate, which could either be thin paper or plastic films, mounting the semiconductor chip onto the substrate and then connecting the antenna to the chip. An example is given in Figure 7.46.

However, such a design cannot be used to create e-yarn. In order to create e-yarn, seven-strand copper wire (total diameter: 100µm) was soldered to the solder pads of an SMD type RFID chip SL3S1013FTB0 from NXP. The RFID chip was a six-terminal package die (1x1.45x0.5 mm), and by using the soldering technique which was described section 4.3.6 (pages 88 to 89) the seven-strand copper wire was soldered onto the solder pads to create the antenna as shown in Figure 7.46. A microscopic image of the soldered chip is shown Figure 7.47. In the final e-yarn the soldered copper wire would rest inside the yarn and perform as a dipole antenna.

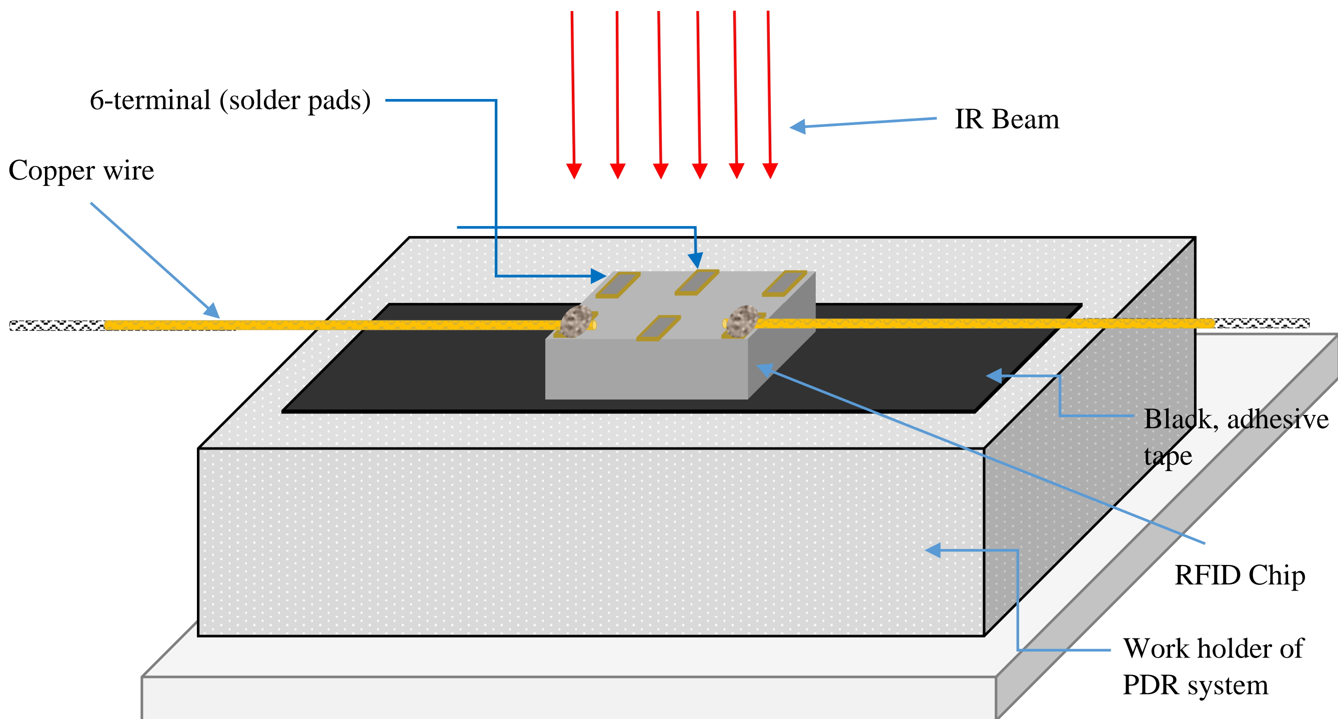

FIGURE 7. 46: SMD CHIP AND COPPER WIRE SET UP FOR REFLOW SOLDERING

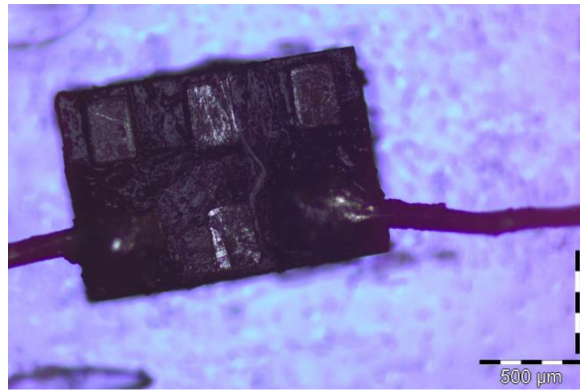

FIGURE 7. 47: A MICROSCOPIC IMAGE OF AN RFID CHIP WITH SOLDERED, SEVEN-STRAND COPPER WIRES

The packaged die was encapsulated using the method described in section 5.4 of this thesis (pages 114 to 115) to create the core yarn for forming the final RFID e-yarn, shown in Figure 7.48.

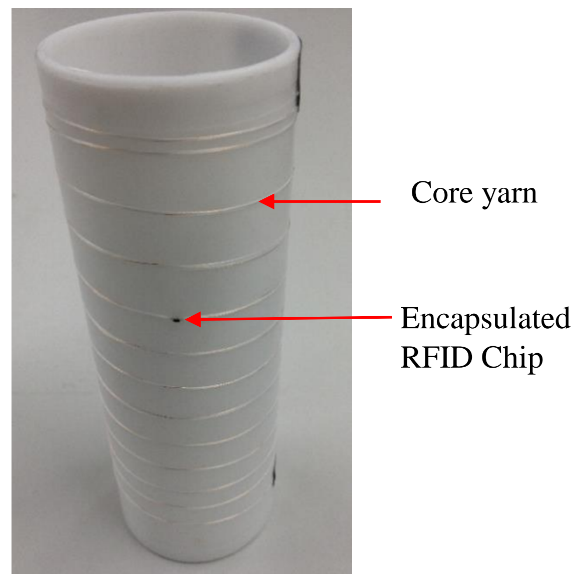

FIGURE 7. 48: THE CORE YARN CONTAINING RFID PACKAGED DIE, SOLDERED SEVEN-STRAND COPPER WIRE, TWO 167DTEX/47 PE YARNS AND MICRO PODS.

The core yarn was then processed further in the RIUS small-diameter warp knitting machine using six needles to create the RFID e-yarns. The formation of the warp-knitted sleeve using six 167dTex/47 PE yarns was as explained in section 5.4 of the thesis (pages 114 to 115). The performance of the RFID e-yarn was tested using an RFID reader from Technology solutions UK Ltd, an 1128-UHF_bluetooth_reader and the iPhone app provided by the manufacturer, as shown in Figure 7.49.

FIGURE 7. 49: TESTING OF RFID E-YARN USING AN RFID READER AND IPHONE APP

7.6.3 Optimisation of Read Distance

It was necessary to tune the length of the dipole antenna of the RFID e-yarns to the communication frequency of the RFID chip and the reader to achieve the maximum read distance. One metre of seven-strand copper wire was soldered to the RFP and RFN solder pads of the RFID chip and the reading distance was measured. The test was continued by cutting the dipole length (copper length) and again measuring reading distance. The results are shown in Table 7.1. The optimum shorted length of antenna was 10cm.

No	Antenna Length on each side of RFID chip (cm)	Reading Distance (Reader to RFID Tag) (cm)
1	100	160
2	75	160
3	50	130
4	25	400
5	15	100
6	10	400
7	5	100

TABLE 7. 1: EFFECT OF DIPOLE LENGTH ON READ LENGTH

7.6.4 Integration of RFID e-Yarn with Garments

Four RIFD e- yarns with 10cm-long dipole antennae were integrated into the seams of a shirt, two T-shirts and one army uniform (Figure 7.50) and the read distance was

measured: in each case the read length was 4 meters. As the RFID e-yarns were very small and flexible, it was very easy to insert these into the seams of the garments.

FIGURE 7. 50: RFID E-YARN AND RFID E-YARN-INTEGRATED GARMENTS

7.6.5 Washing of RFID e-Yarn Integrated Garment

A T-shirt was washed on a domestic washing machine (Bosch, Logixx 8), at 30^{0}C, spin speed 800 rpm and washing cycle duration 47 minutes (machine original settings for sport wear). The read distance was determined before washing and after washing (Figure 7.51). The T-shirt was subjected to nine wash cycles and the results are shown in Table 7.2.

FIGURE 7. 51: TEST PROCEDURE FOR MEASURING READ DISTANCE

Number of wash and drying cycles	Reading Distance (m)
0	4.00
1	4.50
2	4.55
3	4.55
4	4.55
5	4.55
6	4.55
7	4.55
8	4.55
9	4.55

TABLE 7.2: TEST RESULTS OF READ DISTANCE AFTER WASHING AND TUMBLE DRYING

7.6.6 Results Discussion

The total length of the RFID e-yarn was 20 cm. It was the finest, smallest flexible RFID tag according to a literature survey and feedback from experts [145, 146, 147, 148, 149]. The RFID e-yarn could easily be integrated into three different types of garments and it was almost impossible to detect. Performance was retained after washing and tumble drying, in fact the read length increased by 55 cm after the first wash. This may be due to the washing away of lubricants and chemicals that are used in textile and garment manufacturing processes. A detailed analysis of this behaviour (improvement) of read length could not be carried out within the framework of this PhD research programme. Recently one of the T-Shirts integrated with an RFID yarn was tested for its performance by a company which is one of the leading RFID-tag manufacturers, RFID e-yarn performed to the company's satisfaction. Due to confidentiality agreements between the company and the University, the details of their investigation cannot be included in this thesis.

7.7 Other Prototype Demonstrators with e-Textiles

Additional prototype demonstrators which were produced using electronic yarns are as shown in Figures 7.52 to 7.53.

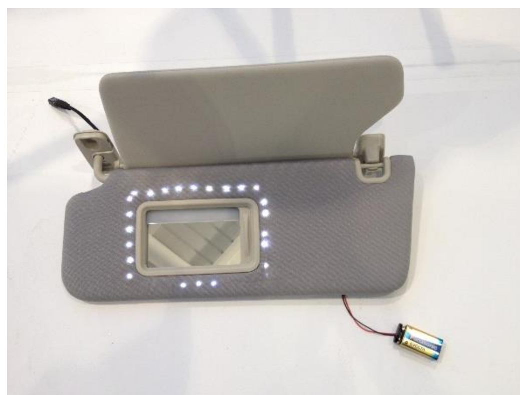

FIGURE 7. 52: A PROTOTYPE ILLUMINATED SUN VISOR FOR FUTURE CARS

FIGURE 7. 53: PROFESSOR TILAK DIAS HOLDING MAGNETIC YARN

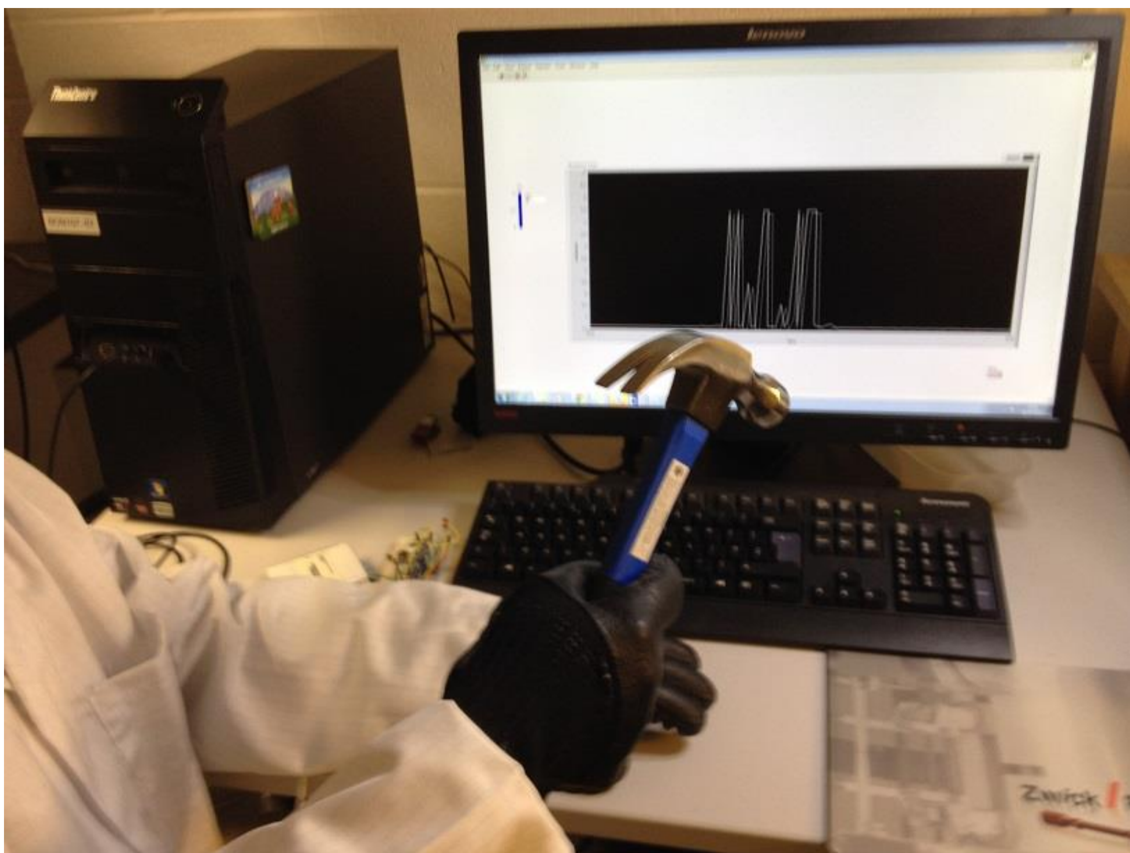

FIGURE 7. 54: A PICTURE OF A VIBRATION-SENSING GLOVE

FIGURE 7. 55: AN ILLUMINATED YARN-INTEGRATED BLANKET

FIGURE 7. 56: ILLUMINATED YARN INTEGRATED INTO A COMPOSITE LAMINATE

7.8 Conclusion

Integrating micro-scale semiconductor chips into yarn is a new concept which has been pioneered at Nottingham Trent University [67, 68]. However, without prototype demonstrators with e-yarns, it is difficult to demonstrate the impact that this technology could make on society. The research reported in this thesis has provided a platform in order to receive funding from the British Government and Industry to advance the technology to a higher Technology Readiness Level (TRL 6).

CHAPTER EIGHT

8.0 Conclusion and Future Work

8.1 Thesis Summary

The research work described in this thesis started with a literature survey that proved that micro-scale semiconductor chips have not been integrated into yarns. Therefore, it was necessary to start this work from scratch. The first task was to choose suitable materials: SMD type semiconductor chips were selected as there are no pins or legs that could interfere with the final appearance and dimensions of e-yarn; multi-strand copper wires were selected as conductive yarns as these are solderable and have other benefits compared to other metal wires: copper is cheaper, more malleable and more ductile than silver and gold. Therefore, copper is easier to mould into different shapes and can be put under stress without damage. However, the resistance of copper could change due to oxidisation. Therefore, it is necessary to use enamel-coated copper wire. Lead-free solder paste was selected as it can be applied precisely at micro-litre scales. On the other hand, due to European legislation, it is a legal requirement to use lead-free versions of solder paste. UV-curable resin was selected for encapsulation of solder joints and semiconductor chips. The results showed that the optimum spot curing time was 5 seconds and the optimum distance from the UV light to the resin was 1 cm.

It was a challenging task to find a suitable method for creating interconnections. A hand soldering technique was used, to identify the best method of handling the microelectronic components and fine copper wires using suitable raw materials and equipment. Then later, a PDR rework system was employed as it had significant benefits compared with manual soldering. After several experiments (which are described in chapter 4), a rapid heating profile was developed to optimise the mechanical and electrical properties of the soldered joints. A novel concept of a contactless technique was developed to remove the polyester coating of copper wire by using flux combined with the IR beam of the PDR reflow workstation.

A UV-curing technique was used in this research work. A number of methods were tested for application of resin to the electronic packaged dies which had been soldered with multi-strand copper wires. In the first method, a paint brush was used to apply resin, however it was not possible to control the amount of resin applied to each packaged die. In the second method, resin was applied using a syringe with a long needle. The volume of resin could be controlled but the geometry of the resulting micro-pods varied. In the third method, the packaged die was located within a Teflon tube and resin was then

applied and cured. This encapsulation method was more successful than the others as it created geometrically-uniform micro-pods for each electronic, packaged die.

A small diameter circular warp knitting technique was used to produce the final e-yarn. It was shown that the technique was suitable for manufacturing e-yarns. After several experiments (which are described in chapter 6), an e-yarn with an even appearance was produced. E-yarns integrating prototypes of e-textiles (an illuminated garment, an illuminated car seat, RFID garments, a temperature sensor fabric mat and socks) were produced as part of this PhD research and exhibited at various events as demonstrated in the other academic activities (page xix) and chapter 7.

8.2 Conclusion

General textiles have a history covering thousands of years. However, the electronic textiles (e-textiles) industry is still at a young stage. The first generation of e-textiles was developed by adding electronic devices such as mobile phones and MP3 players into pockets (For example the ICD+ jacket in 2000). There were many practical issues with these garments which were heavy and bulky, not washable, and inflexible. Second generation e-textiles incorporated conductive threads into the fabric or were made by attaching PCB's to fabrics or garments. There were still similar issues as in the first generation. Therefore, integrating functionality into flexible fibre form is thus the next logical evolution in wearable electronics which has been developed in this research work. Such electronically functional yarns (e-yarns) will be the building blocks of the next generation of wearable electronics. Moreover, this will facilitate solutions to overcome current problems and difficulties which the manufacturers of wearable textiles are experiencing and open the doors for designers to develop the next generation of truly-wearable computers which are comfortable, flexible and washable. The e-yarns could be used in medical applications such as monitoring of ECG, respiratory patterns, blood pressure and skin temperature, in industries such as automotive, retail, manufacturing, military, the internet of soft things, consumer products, sports, fashion and entertainment.

Researchers from universities and companies all over the world have been working on e-textiles during the last decade and the field of e-textiles has a rapid growth rate. This research has developed a new generation e-textiles as is described in this thesis. The main objective of the research was to develop the platform technology to integrate semiconductor packaged dice within the fibres of yarns, in order to craft novel electronically active yarn (EAY). The core technology was developed and a patent was

filed (Patent no: PCT/GB2015/052553). Moreover, the work drew significant attention and great interest from government bodies, industries, Universities and research centres as a result of exhibiting e-textiles at various events. Subsequent, successful development of the technology led to receipt of EPSRC funds (2.8 million pounds) for further development of e-yarns by creation of multi-functional, complex connections, and scaling-up of manufacturing processes of e-yarn through development of fully-automated systems [150].

8.3 Contribution to Knowledge

- Critical analysis of literature review on wearable technologies.
- Selection of suitable raw materials to create robust e-yarns by conducting physical and chemical scientific tests.
- Generation of a technique for creation of interconnections between semiconductors and copper filaments.
- Creation of a suitable encapsulation method for e-yarns.
- Introduction of braiding techniques for e-yarn formation in order to produce e-yarn that is even and strong.
- Production of prototypes of e-yarns using LEDs, Thermistors, RFIDs and vibration sensors.
- Production of prototype e-textiles; illuminated garment, illuminated car seat cover, temperature monitoring mat, RFID integrated garments, temperature monitoring socks.

8.4 Future Work

The manufacturing processes of electronic yarns were demonstrated in chapters 3 to 6. These process were carried out manually. Therefore, it was a very time-consuming process. As this was a novel platform technology, no machinery to carry out the processes is available commercially. Therefore, it is necessary to develop fully automated e-yarn production systems to produce e-yarns on small to medium quantities as the first stage to commercialising the technology. A fully-automated pick and place machine (SMTmax, model: QM-1100) was employed after carrying out market research. These machineries were designed for interconnection of PCBs in the electronics industry. Therefore, further work is necessary to modify the machine. The author proposes the modification illustrated in Figure 8.1.

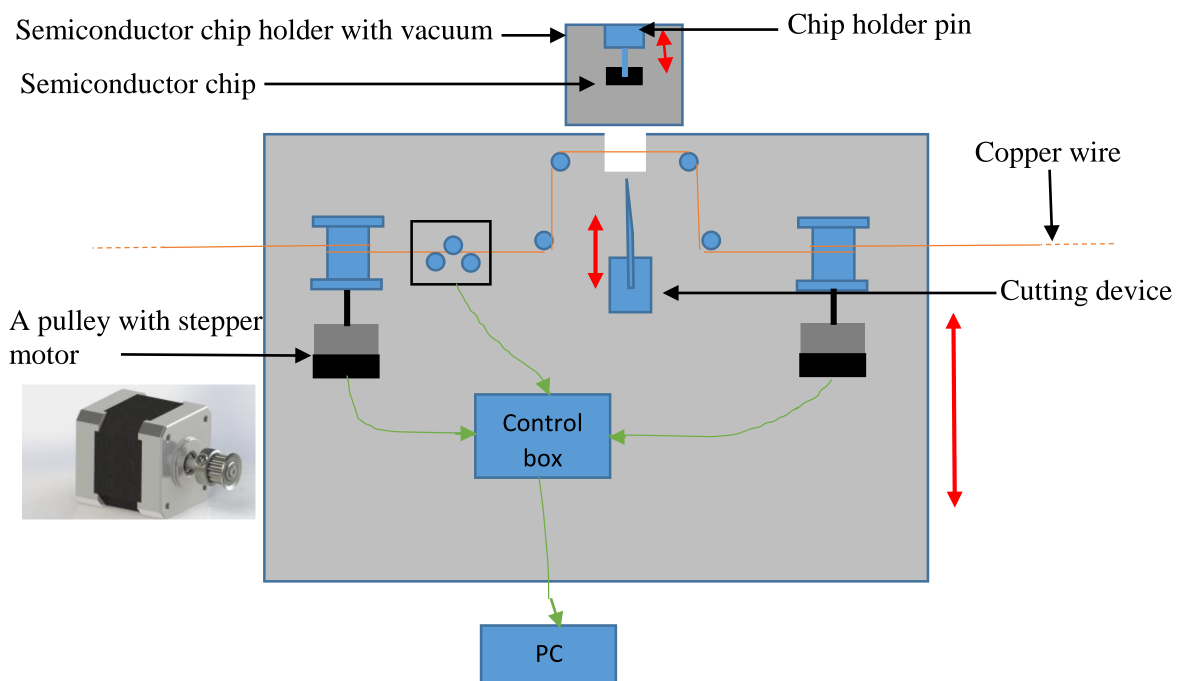

FIGURE 8. 1: SCHEMATIC OF PICK AND PLACE MACHINE MODIFICATION

Almost every electronic device requires electrical power to operate its electronic and mechanical functions. Devices such as laptops, smart phones and wearable electronics use batteries. The battery life will depend on the battery capacity in milliamperes per hour (mAh) and device consumption in milliamperes (mA) [178]. Batteries generate extra weight to products and limit their practicability. Therefore, it is necessary to carry out detailed studies of the limitations imposed by battery life in various applications in future research work.

During the PhD research, a few prototypes to demonstrate different applications of e-yarns were produced, as explained in chapter seven. However, it is necessary to carry out research for each and every application, requiring individual projects to investigate the reliability of e-yarns, further improvements in current practical issues and further improvements in performance, for example, clinical trials on medical e-textiles such as temperature sensor gloves, socks, moisture sensors and pressure sensor-integrated textiles, and further washing trials on e-textiles.

Many SMD packaged dice consist of multiple terminals (solder pads). In this project, the focus was limited to only two-terminal interconnections. However, in future developments it is necessary to create multi-terminal connections using multi-terminal semiconductor devices with electronically-insulated copper filaments as shown in Figure 8.2. This research work has also been started as an EPSRC-funded project (2015 to 2019).

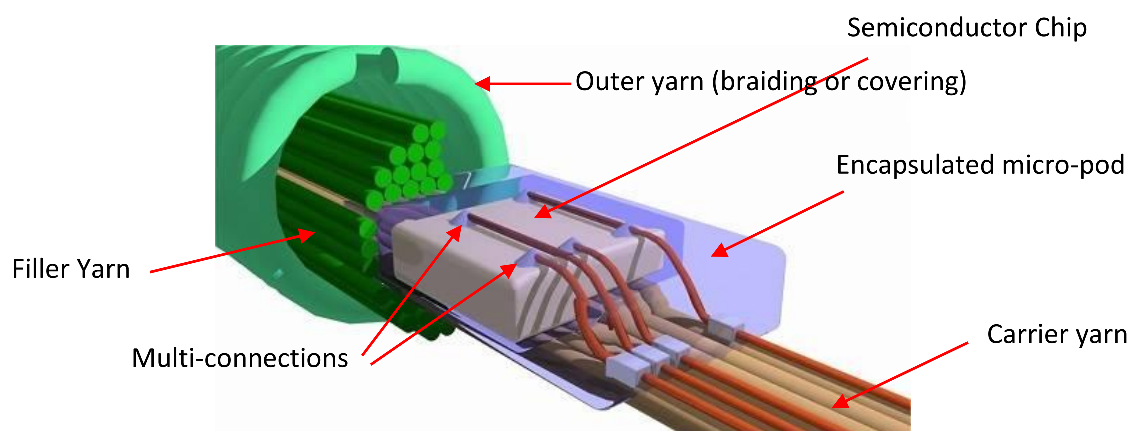

FIGURE 8. 2: A SCHEMATIC IMAGE OF MULTI-TERMINAL CONNECTIONS OF FUTURE E-YARN [151]

As e-yarn is a novel product, there are no test standards for testing e-yarns as for other textiles. Therefore, it necessary to develop testing equipment, testing procedures and standard for e-yarns.

It has been noticed that circular yarn guide of the small diameter circular warp knitting machine used to produce the final e-yarn is oscillated when the machine is running. Therefore, the warp yarns could be damaged or become entangled together. Therefore, further study needs to be carried out to optimise the textile characteristics of the e-yarns and the limitation of mass production. The author suggested to introduce new guides as shown Figure 8.3.

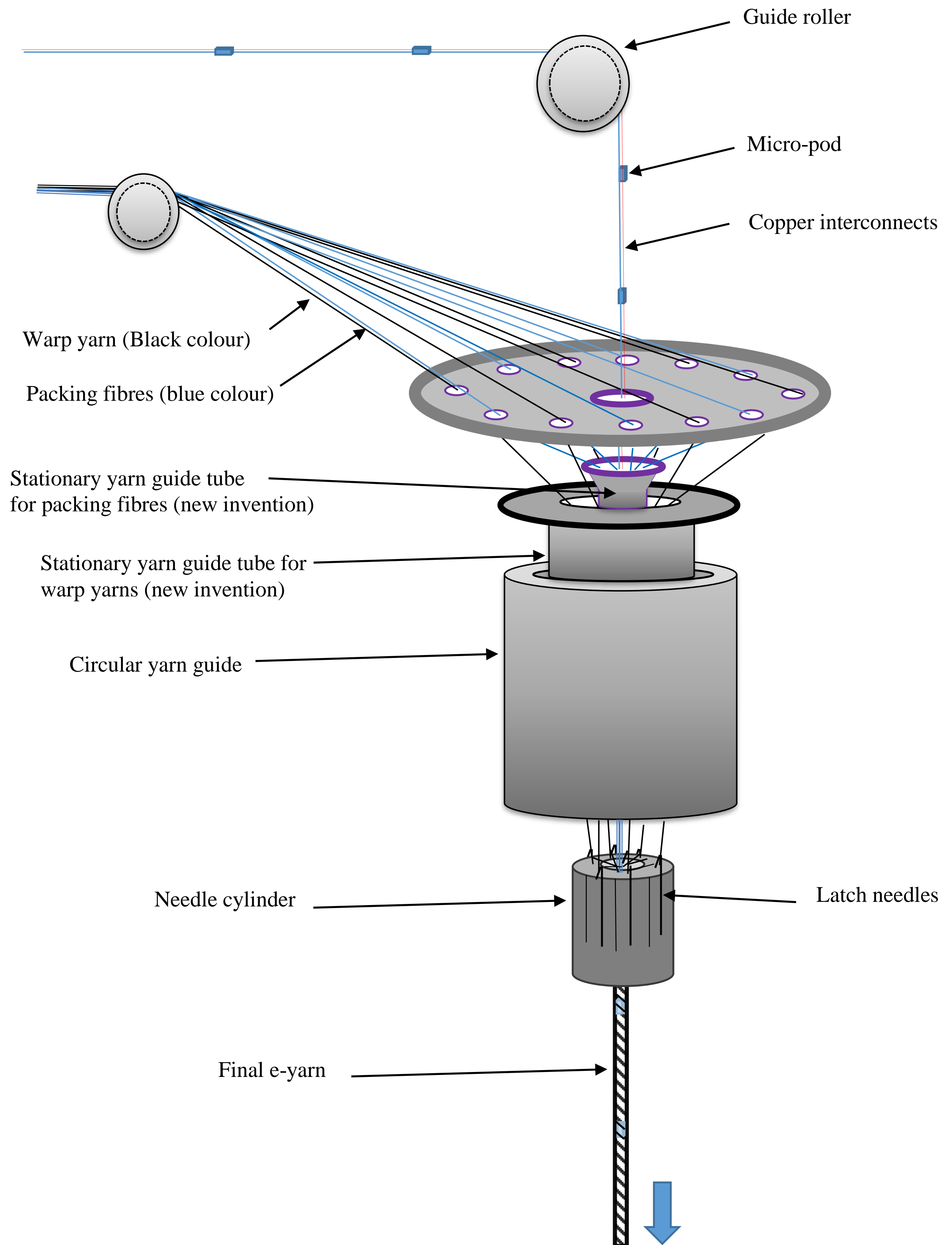

FIGURE 8. 3: SCHEMATIC OF YARN ARRANGEMENT RIUS KNITTING MACHINE WITH NEW GUIDES

REFERANCES

1. Wearable Electronics and Technology Market by Applications (Consumer, Healthcare, Enterprise), Products (Eyewear, Wristwear, Footwear), Form Factors and Geography - Analysis & Forecast to 2014 - 2020. *MarketsandMarkets.com.* [Online] September 2014. http://www.marketsandmarkets.com/Market-Reports/wearable-electronics-market-983.html?gclid=Cj0KEQjwwIKxBRDKhOz7ytT30vkBEiQAT1NaPb_qJJd_K6EbKZG-CXqROh2leGk_3rnY8rpJEHm6q60aAg_h8P8HAQ. Report Code: SE 2763.
2. Global smart, intelligent, digital & interactive fabrics/textile market revenue from 2012 to 2018 (in billion U.S. dollars)*. [Online] statista.com. http://www.statista.com/statistics/302526/smart-fabrics-market-revenue-worldwide/.
3. Harrop, P., and Raghu,. *E-Textiles: Electronic Textiles 2014-2024, Wearable Technology Report.* s.l. : IDTechEx, 2014.
4. Dias, T., and Rathnayake, A.,. Intergration of micro-electronics with yarns for smart textiles (chapter 5). [book auth.] T. Dias. *Electronic Textiles Smart Fabrics and Wearable Technology.* Nottingham : Woodhead, 2015.
5. Rathnayake, A.,. *A Module of MSc Research, Integrated Learning Package of Fibre/Textile Fundamentals. University of Bolton.* s.l. : Not been published, 2007.
6. Wijendra, H.,. Textile Spinning Process of Cotton Yarn. *Classification of Yarn.* [Online] Sri Lanka Institute of Textile & Apparel Technology (SLITA). http://textilelearner.blogspot.co.uk/2013/12/textile-spinning-process-of-cotton-yarn.html.
7. Domskiene, J., and Strazdiene, E.,. *Investigation of Fabric Shear Behaviour.* s.l. : Fibres & Textiles in Eastern Europe, 2005. Vol. 13 (2).
8. Akhilvijayakumar. *Basic Classification of Electronic Components* . [Online] 16 July 2013. [Cited: 03 May 2015.] https://simplectronics.wordpress.com/2013/07/16/basic-classification-of-electronic-components/.
9. Smith, H. T. P.,. *Introduction to Microelectronics.* 1998.
10. Semiconductor. [Online] [Cited: 02 April 2015.] http://en.wikipedia.org/wiki/Semiconductor.
11. Matteo, S., and Alessandro, C.,. *Wearable Electronics and Smart Textiles: A Critical Review.* s.l. : Sensors, 2014. pp. 11957-11992. Vol. 14.
12. *Fibretronic Ltd.* [Online] [Cited: 10 March 2014.] www.fibretronic.com.
13. Vivonoetics Ltd. [Online] [Cited: 10 March 2014.] http://vivonoetics.com/.

14. Hunter, B.,. [Online] Control Glove, 2010. [Cited: 27 March 2013.] http://www.fibrestructures.com/innovations.php.
15. Textronics Inc. [Online] [Cited: 27 March 2013.] http://www.textronicsinc.com.
16. Van, L. L.,. *Smart textiles for medicine and healthcare: materials, systems and applications.* s.l. : Elsevier., 2007.
17. Carron, A.,. *Electric-heated glove. US1011574* 1911. US Petent.
18. Grisley, F.,. *Improvements in blankets, pads, quilts, clothing, fabric, or the like, embodying electrical conductors. GB445195 (A)* 1936.
19. Summers, A. V.,. *Improvements relating to Electrical Heated Clothing, Flying Equipments and the like. GB571985A* 1945.
20. Lee, G.,. *PhD Thesis: An Investigation into the Feasibility of the Integration of Microwave Circuitry Into a Woven Textile.* s.l. : Loughborough University, 2012.
21. Diaries, F.,. [Online] November 2013. http://femmediaries4.blogspot.co.uk/2013_11_01_archive.html.
22. Mattila, H.,. *Chapter 15 – Yarn to Fabric: Intelligent Textiles, Textiles and Fashion.* s.l. : Woodhead, 2015. Vols. Pages 355–376.
23. Curone, D., Secco, E.L., Tognetti, A., Loriga, G., Dudnik, G., Risatti, M., Whyte, R., Bonfiglio, A., and Magenes, G.,. *Smart garments for emergency operators: the ProeTEX project. Information Technology in Biomedicine.* s.l. : IEEE Transactions, 2010.
24. Bluetooth-enabled Zegna Sports Icon Jacket with joystick controls. [Online] [Cited: 4th April 2015.] http://www.damngeeky.com/2013/10/09/14496/bluetooth-enabled-zegna-sports-icon-jacket-joystick-controls.html.
25. QTC Material . [Online] Peratech Ltd. [Cited: 07 April 2015.] http://www.peratech.com/qtc-material.html.
26. Leitch, P., Tassinari, T., Winterhalter, C., Fairneny, J., Herbert, J., Lee, C., and Hoyt, R.,. *Interactive Textiles Front End Analysis.* 1998. pp. Natick/TR-99/004. Vol. Phase 1.
27. Hardy, G. V.,. *Design and construction of smart structures for technical textiles.* University of Leeds : PhD thesis, May 2008.
28. Dadi, H. H.,. *Literature Over View of Smart Textiles.* s.l. : Swedish school of Textiles, June 2010.
29. Martin, S.,. Smart Clothing. [Online] [Cited: 15 March 2015.] http://ldt.stanford.edu/~jeepark/jeepark+portfolio/cs147hw8jeepark.html.

30. Sungmee, P.,. Georgia Institute of Technology. [Online] [Cited: 15 March 2015.] http://www.gtwm.gatech.edu/team/sungmee/sungmee.html.
31. Tech, The University of Southern California and Virginia. Battle hardened e-textiles set for trials. [Online] 2nd October 2002. [Cited: 29 March 2015.] http://www.theengineer.co.uk/news/battle-hardened-e-textiles-set-for-trials/279914.article .
32. Advanced Textiles Source. E-Textiles for Military Markets. [Online] 11th Jan 2014. [Cited: 29 March 2015.] http://advancedtextilessource.com/2014/01/e-textiles-for-military-markets/.
33. Hopkins, J.,. Intelligent Textiles Limited. [Online] October 2012. [Cited: 30th March 2015.] http://www.plustex.eu/wp-content/uploads/2012/12/SOUTHAMPTON-GP_-Intelligent-Textiles-Limited.pdf.
34. Coosemans, J., Hermans, B., and Puers, R.,. *Integrating wireless ECG monitoring in textiles. Sensors and actuators.* s.l. : A, Physical, 2006. pp. 48-53. Vol. 130.
35. Linz1, T., Vieroth1, R., Dils1, C., Koch1, M., Braun1, T., Becker1, K., Kallmayer1, C. *Embroidered Interconnections and Encapsulation for Electronics in Textiles for Wearable Electronics Applications Institute for Reliability and Microintegration IZM.* s.l. : Germany Advances in Science and Technology, 2008. pp. 85-94. Vol. 60.
36. Numetrex. *The heart rate monitor sports bra.* [Online] [Cited: 10 December 2014.] http://www.numetrex.com/.
37. Fashion. [Online] [Cited: 06 April 2015.] http://en.wikipedia.org/wiki/Fashion .
38. Influence in Fashion . [Online] [Cited: 06 April 2015.] http://moreintelligentlife.co.uk/content/lifestyle/rebecca-willis/influence-fashion.
39. Cynthia Durcanin, What is Fashion. [Online] 12th Oct 1999. [Cited: 06 April 2015.] http://www.pbs.org/newshour/extra/1999/10/what-is-fashion/ .
40. Alexander, h.,. Why Do Celebrities Influence Fashion Trends? *Style Flair Fashion.* [Online] 07 May 2014. http://www.styleflair.com/why-do-celebrities-influence-fashion-trends/.
41. CuteCircuit Ltd. [Online] [Cited: 2nd April 2015.] http://cutecircuit.com.
42. CuteCuircuit. [Online] [Cited: 2nd April 2015.] http://en.wikipedia.org/wiki/CuteCircuit .
43. Fashion of the Future: Is That Your Dress Ringing. *abc News.* [Online] 23rd Aug 2010. [Cited: 2nd April 2015.] http://abcnews.go.com/Technology/fashion-future-dress-ringing/story?id=11448779.

44. Yuka, Y.,. LED Galaxy Dress by CuteCircuit is World's Largest Wearable Display. *http://www.ecouterre.com/.* [Online] 11th Nov 2009. [Cited: 2nd April 2015.] http://www.ecouterre.com/bewitching-led-galaxy-dress-by-cute-circuit-is-worlds-largest-wearable-display/.
45. Visijax. Innovative Wearable Electronic Products. [Online] [Cited: 26 March 2015.] http://www.visijax.com/ .
46. Fibrestructures. [Online] [Cited: 06th Feb 2012.] http://www.fibrestructures.com/innovations.php.
47. Peratech. *SOFTswitch.* [Online] July 2006. [Cited: 28 March 2015.] http://www.peratech.com/softswitch.html.
48. Gioberto, G.,. *Garment-integrated wearable sensing for knee joint monitoring.* Seattle : Adjunct Program, ACM, 2014.
49. Dias, T.,. *Electronically Active Smart Textiles.* Manchester Conference Centre, Days Hotel : BCS Health Northern Specialist Group, 16th Mar 2011. http://www.bcs.org/content/conEvent/5915.
50. Adding Value to Sri Lankan Textiles The Electronic Textiles. [Online] Technology, Business, Lifestyle, Nov 2009.
51. PhD Studentship in Development of Smart Yarn capable of measuring its stress-strain behaviour. [Online] Innovation in Textiles, Mar 2011. http://www.innovationintextiles.com/phd-studentship-in-development-of-smart-yarn-capable-of-measuring-its-stress-strain-behaviour/.
52. Primo1D. Electronics in a yarn : E-Thread® integration. [Online] 2015. http://primo1d.com/technology/.
53. Related projects. *Wealthy.* [Online] ProeTEX. http://www.proetex.org/related_projects.htm.
54. Berglin, L.,. Smart Textiles and Wearable Technology - A study of smart textiles in fashion and. *clothing. A report within the Baltic Fashion Project.* [Online] the Swedish School of Textiles, University of Borås., 2013. http://www.hb.se/Global/THS/BalticFashion_rapport_Smarttextiles.pdf.
55. Sorensen, D.,. What is a wearable health system? [Online] Wearable health, 14 May 2015. http://www.wealthy-ist.com/2015/05/14/what-is-a-wearable-health-system/.
56. Habetha, J.,. MyHeart – Fighting Cardiovascular Diseases by Prevention and Early Diagnosis. [Online] Philips. http://csnej106.csem.ch/sfit/pdf/concertation_lucerne_myheart.pdf.

57. Luprano, J.,. Biotex, Bio-sensing textile for health management. *1st Concertation meeting on smart fabrics & wearable flexible systems & applications.* [Online] 01 Feb 2006. http://csnej106.csem.ch/sfit/pdf/concertation_lucerne_biotex.pdf.
58. Klatt, C.,. Stella Newsletter 1. *Stretchable electronics for large area applications.* [Online] 28 Nov 2006. http://csnej106.csem.ch/sfit/pdf/stella_newsletter_1.pdf.
59. Régis, L.,. *D1.1 – Report on the requirements of the application.* s.l. : OFSETH, 2006. http://www.ofseth.org/IMG/pdf/OFSETH_ITM_D1.1_PU_a.pdf.
60. Ofseth. Project Description: OFSETH in short. [Online] 2007. http://www.ofseth.org/.
61. Beeby, S., Torah, R., Yang, K., Wei, U., and Tudor, T.,. *Microflex Project - Microtechnology in Smart Fabrics.* 4th International Conference "Smart Materials, Structures and Systems" (CIMTEC) - June 2012 - Italy : University of Southampton.
62. Beeby, S., Torah, R., Yang, K., Wei, Y., and Tudor, J.,. Microflex. *Microflex Project Summary.* [Online] http://microflex.ecs.soton.ac.uk/dissemination.html.
63. Project Overview. *Dephotex.* [Online] http://www.dephotex.com/?q=node/2.
64. Editor, N.,. Power suits: wearable fabric that can generate electricity from the sun. *The EU Framework Programme for Research and Innovation.* [Online] 04 Feb 2015. http://ec.europa.eu/programmes/horizon2020/en/news/power-suits-wearable-fabric-can-generate-electricity-sun.
65. Introduction to PLACE-it (IST-0248048). *Summary.* [Online] http://www.place-it-project.eu/Introduction/tabid/36/Default.aspx.
66. Sterrett, C. D., and Rachael,. *White paper on smart textile garments and devices:a market overview of smart textile wearable technologies.* Denmak : Ohmatex smart textile technology, 2014.
67. Southampton to share in ?20 million to advance UK's manufacturing capability . [Online] University of Southampton, Dec 2014. http://www.southampton.ac.uk/news/2014/12/19-advance-uk-manufacturing-capability.page.
68. Nottingham Trent University shares in £20 million to manufacture fibre of the future . [Online] Nottingham Trent University, Jan 2015. http://www.ntu.ac.uk/apps/news/168226-15/Nottingham_Trent_University_shares_in_%C2%A320_million_to_manufacture_fibre_of_t.aspx.
69. Rupal, S.,. Wearable electronics product market analysis 2014 2024 - a global perspective-sample. [Online] June 2014.

http://www.slideshare.net/RupalSSharma/wearable-electronics-product-market-analysis-2014-2024-a-global-perspectivesample-35830655.

70. Dave, L.,. Apple Watch: How many have been sold? [Online] North America technology reporter, BBC News, 21 July 2015. http://www.bbc.co.uk/news/technology-33618485.
71. Wearable Electronics/ Technology Compnents (Memory, Battery, Display, Connectivity, Sensors & Others) Market Study A Global Analysis, Forecast & Insights 2014-2024. *Report description.* [Online] http://bisresearch.com/wearable-electronics-technology-components-memory-battery-display-connectivity-sensors-others-market-study-a-global-analysis-forecast-insights-2014-2028.html.
72. *Opportunities in Wearable Sensors: an overview of the market and technologies.* Presentation, Webinar. s.l. : IDTechEx, 2015.07.23.
73. Smart Textiles Market Analysis And Segment Forecasts To 2020. *Grand View Research, Marcket research and consulting* . [Online] Jan 2014. http://www.grandviewresearch.com/industry-analysis/smart-textiles-industry. ISBN Code: 978-1-68038-061-3.
74. Statista. Global smart, intelligent, digital & interactive fabrics/textile market revenue from 2012 to 2018 (in billion U.S. dollars). *Global smart textile/fabrics market revenue 2012-2018.* [Online] 2015. http://www.statista.com/statistics/302526/smart-fabrics-market-revenue-worldwide/.
75. Smart and Interactive Textiles Market for Industrial, Military and Defense, Medical and Healthcare, Retail and Consumer, Transportation and Other Applications - Global Industry Analysis, Size, Share, Growth, Trends and Forecast, 2014 - 2020. *Free Market Analysis.* [Online] July 2014.
76. Indvik, L.,. Google Levi's Partner to Develop "Smart Fabric". [Online] 29 May 2015. http://fashionista.com/2015/05/google-levis-jacquard.
77. Project Jacquard. *Introducing Project Jacquard.* [Online] https://www.google.com/atap/project-jacquard/.
78. *Automatic identification of gait events using an instrumented sock.* Dias, T., Preece, S., Kenney, L., Major, J., Lay, E. and Fernandes, B.,. s.l. : Journal of NeuroEngineering and Rehabilitation , 2011, Vols. vol. 8, pp. 1-10. http://www.jneuroengrehab.com/content/.
79. *Knitted strain gauges* . Dias, T., Wijesiriwardana, R. and Mukhopadhyay, S.,. s.l. : “SPIE’s International Symposium on Microtechnologies for the New Millennium 2003, 2003.

80. *Resistive Fibre-Mesh Transducers.* Dias, T., Wijesiriwardana, R. and Mukhopadhyay, S.,. October 2003 : "7th IEEE Conference of wearable computers".
81. *Electrical Conductivity Meassurement of Fibers and Yarn* . GRÉGR, Veronika ŠAFÁŘOVÁ and Jan. Liberec, Czech Republic : 7th International Conference - TEXSCI 2010, 2010.
82. Cork, C.R. Conductive fibres for electronic textiles: an overview. [book auth.] Tilak Dias. *Electronic Textiles* . Nottingham Trent University : The Textiles Institute , 2015.
83. Polypyrrole. *Wikipedia.* [Online] https://en.wikipedia.org/wiki/Polypyrrole.
84. Blue Sea System. *Electrical Conductivity of Materials.* [Online] October 2011. https://www.bluesea.com/resources/108/Electrical_Conductivity_of_Materials.
85. Copper. *Edison Tech Center.* [Online] October 2011. http://www.edisontechcenter.org/wires.html.
86. Wires. *Edison Tech Center.* [Online] October 2011. http://www.edisontechcenter.org/wires.html.
87. Mandal, Md. Jasimuddin. Yarn Twist, Relationship Between Yarn Count and Twist, Principles of Twist Measuring Methods. [Online] http://textilelearner.blogspot.co.uk/2013/03/yarn-twist-relationship-between-yarn.html.
88. Meier, R. Further and S. *Uster Zweigle Twist Tester 5.* s.l. : Uster Zweigle Ltd, 2009.
89. BIOCCA, DARRYL J. SMALL AND PETER. Lead-free solders vs. conductive adhesives. [Online] http://electroiq.com/blog/2000/10/lead-free-solders-vs-conductive-adhesives/.
90. Petra Gratz, Sven Rzepka, Gerhard Schubert and Ekkehard Meusel. Solder Joints VS Conductive Adhesive Bonds: A direct comparison for SMT packaging technology . *University of Technology, Dresden, Germany.*
91. luigi. A really close look at solder paste from Evil Mad Scientist. *The tinkering studio.* [Online] Jun 2013.
92. Solder Formulations. [Online] Nordson EFD. [Cited: 20 May 2014.] http://www.nordson.com/en-us/divisions/efd/products/solder-paste/Pages/solder-formulations.aspx .
93. EFD Nordson. [Online] [Cited: 10 12 2011.] http://www.nordson.com/.
94. Directive 2002/95/EC of the European Parliament and of the Council of 27 January 2003 on the restriction of the use of certain hazardous substances in electrical and

electronic equipment . *Directive 2002/95/EC of the European Parliament and of the Council of 27 January 2003 on the restriction of the use of certain hazardous substances in electrical and electronic equipment.* [Online] [Cited: 24 June 2012.] http://eur-lex.europa.eu/legal-content/EN/TXT/?uri=CELEX:32002L0095.

95. Encapsulation Resin. [Online] Electrolube Ltd. [Cited: 10 Nov 2011.] http://www.electrolube.com/pdf/encapsulation-resins-brochure-electrolube.pdf.
96. UV Coatings. [Online] BASF Group. http://www.intermediates.basf.com/chemicals/coatings/uv-coatings.
97. UV CURING Technology. [Online] [Cited: 05 June 2015.] http://www.senlights.com/gijyuu/uvcure/UVcuring.html.
98. Brady, George et al. *Materials Handbook.* s.l. : McGraw Hill pp. 768–70, 1996. ISBN 0-07-007084-9..
99. Soldering. [Online] Wikipedia. [Cited: 06 Feb 2012.] https://en.wikipedia.org/wiki/Soldering.
100. Woznicki, Tom. Hot-Bar Soldering. [Online] Flex Circuit News, November 2000. [Cited: 10 March 2012.] http://www.flexdude.com/Back%20Issues/FCN11-00A.PDF.
101. HOT BAR REFLOW. [Online] Amada Miyachi Europe, 2013. [Cited: 08 May 2015.] http://www.amadamiyachieurope.com/cmdata/documents/Hot-Bar-Reflow-Soldering-Technology-10-2014.pdf.
102. Gladwin, Dave. Hot plate reflow soldering using low temperature solder. [Online] Cit Technology. [Cited: 08 May 2015.] http://cittechnology.com/articles/hotplate-soldering-low-temperature-solder.html.
103. Resistance Soldering. [Online] Brunel Hobbies. [Cited: 08 May 2015.] http://www.brunelhobbies.com.au/soldering/instruct/rsinstruct.htm.
104. KELSEY, JOHN. How to Use Torches, Heat Guns, and Soldering Irons-and When. [Online] [Cited: 08 May 2015.] http://www.thisoldhouse.com/toh/article/0,,449698,00.html.
105. Vivari, M.J. and M.A. Kasman,. *Laser Solder Reflow: A Process Solution Part I.* 2007.
106. SMD HOT AIR PENCIL. [Online] [Cited: 08 May 2015.] http://www.zeph.com/pencil.html.
107. Induction-Soldering. [Online] Wolf Produktions Systeme. http://www.orion-industry.com/robot_laser/Ind_loet_engl.pdf.

108. Ogochukwu, Ezeonu Stella. Laser Soldering, Chapter 15. [Online] [Cited: 09 May 2015.] http://cdn.intechopen.com/pdfs-wm/38865.pdf.

109. Soldering . [Online] [Cited: 15 May 2014.] http://en.wikipedia.org/wiki/Soldering .

110. Metcal Hand Soldering Basics . [Online] [Cited: 10 March 2014.] http://ecee.colorado.edu/~mcclurel/Metcal_Hand_Soldering_Basics.pdf .

111. Bradley, E. *Lead-free Solder Assembly: Impact and Opportunity in Electronic Components and Technology Conferance.* s.l. : IEEE, 2003.

112. Introduction to Soldering SMDs. *Electronics Yorkshire Training Centre.* [Online] [Cited: 18 May 2014.] http://www.eytraining.org.uk/t/Services/Skills-in-Electronics/Introduction-to-soldering-SMDs.aspx.

113. Reflow soldering. [Online] [Cited: 13 June 2014.] http://www.radio-electronics.com/info/manufacture/soldering/reflow_soldering/infrared_reflow_soldering.php.

114. SMD Soldering Information & Instructions. [Online] SparkFun Electronics, Inc. [Cited: 12 Nov 2011.] https://www.sparkfun.com/marcomm/SFE03-0010-KitCard-SolderingSMD-ReaderSpreads.pdf.

115. *Hints and Tips for using Surface Mount Technology (SMT).* Enriquez, Luke. Australia : http://www.wdv.com/Electronics/Fab/SMT-GuideV1-3.PDF, 2001.

116. Surface Mount Soldering Procedure. [Online] [Cited: 05 Dec 2011.] http://www.fpga4fun.com/external/SMD/SMDProc.pdf.

117. Ghosh, Anindo. How to remove enamel from wire? [Online] 05 Jan 2013. [Cited: 25 June 2015.] http://electronics.stackexchange.com/questions/53028/how-to-remove-enamel-from-wire.

118. al, Gibbs et. Infra-red rework station. *Patent Number 4843216* . [Online] 1989. [Cited: 13 03 2013.] http://www.freepatentsonline.com/4843216.pdf. .

119. Paula, G.,. *Textiles gain intelligence.* s.l. : Materials Today, ScienceDirect, 2003. Vol. 6. Page 38 - 43.

120. Stockhausen, J., and McClenachan, C.,. Selecting the Right Potting Compound for Your Application. [Online] E LANTAS PDG, Inc. [Cited: 04 July 2015.]

121. Solving Ultraviolet Curable Potting & Encapsulating Problems With. [Online] April 2012.
http://www.epoxies.com/_resources/common/userfiles/file/Solving%20Ultraviolet%20Curable%20Problems%20-%20LH.pdf.

122. Paints. [Online] Essential Chemical Industry, 18 March 2013. [Cited: 16 June 2014.] http://www.essentialchemicalindustry.org/materials-and-applications/paints.html.

123. Disinfection by Ultraviolet Light. [Online] [Cited: 15 April 2015.] http://www.lenntech.com/library/uv/will1.htm#effect.

124. A Primer on UV-Curable Inkjet Inks. [Online] [Cited: 02 May 2014.] http://www.signindustry.com/flatbed_UV/articles/2008-11-17-SGIA_Primer_on_UV-Curable_Inkjet_Inks.php3.

125. Teflon. [Online] World of Molecules. [Cited: 10 June 2015.] http://www.worldofmolecules.com/materials/teflon.htm.

126. Teflon PTFE fluoropolymer resin. *Properties Handbook.* [Online] Dupont . [Cited: 12 July 2015.] http://www.rjchase.com/ptfe_handbook.pdf.

127. How Cotton cloth was made at the Yard Works in Preston. *Activities Follow the Yarn.* [Online] [Cited: 14 July 2015.] http://www.cleo.net.uk/followtheyarn/activities/cprocess2.html#top.

128. Process: Twisting. [Online] Verdol. http://www.verdol.eu/twisting,135.html.

129. Eyerer, Peter, ed. Polymers-opportunities and risks I, general and environmental aspects. . *Vol. 11. p 155.* Springer, 2010.

130. Vajira Peiris. [Online] Advanced Textiles Research Group NTU, 10 June 2014. https://ntuadvancedtextiles.wordpress.com/2014/06/10/vajira-peiris/.

131. Arduino Pro Mini. [Online] https://www.arduino.cc/en/Main/ArduinoBoardProMini.

132. Arduino / Genuino UNO. [Online] https://www.arduino.cc/en/Main/ArduinoBoardUno.

133. 2013 Review. *2013 post-show official press release (dated Nov 19, 2013).* [Online] Nov 2013. http://www.advancedengineeringuk.com/2014-review/.

134. Future Textiles Exhibition. *Sponsored by Simon Danczuk MP, and endorsed by Secretary of State for Business.* [Online] organised by Policy Connect and All-Party Parliamentary manufacturing Group, 10 to 14 December 2012. UK Parliament's Upper Waiting Hall showcased an area. http://www.policyconnect.org.uk/apmg/sites/site_apmg/files/exhibition_summary.pdf.

135. Cork, Colin. Future Textiles Exhibition. [Online] Advanced Textiles Research Group, Nottingham Trent University, 14 Dec 2012. https://ntuadvancedtextiles.wordpress.com/2012/12/14/future-textiles-exhibition/.

136. Piper, Anna. Future Textiles Collaboration Project:. [Online] Advanced Textiles Research Group, NTU, 19 Nov 2012. https://ntuadvancedtextiles.wordpress.com/2012/11/19/future-textiles-collaboration-project-post-by-anna-piper/.
137. PROTOSNAP - LILYPAD DEVELOPMENT BOARD(NEW). [Online] PROTO-PIC. http://proto-pic.co.uk/protosnap-lilypad-development-board-new/?gclid=CNLV_t_69cYCFeXLtAodUTgA2A.
138. WHAT IS A THERMISTOR? [Online] U.S. Sensor Corp Innovative Temperature Sensing Solutions. http://www.ussensor.com/technical-info/what-is-a-thermistor.
139. Murata 10kΩ 100mW 0402 NTC Thermistor, 1 x 0.5 x 0.5mm. *RS Components Ltd.* [Online] Murata. http://uk.rs-online.com/web/p/thermistors/7259041/.
140. RFID. [Online] [Cited: 10 04 2015.] http://endtimestruth.com/mark-of-the-beast/rfid/.
141. Want, Roy. An Introduction to RFID Technology. [Online] Intel Research, 28 11 2005. [Cited: 25 04 2015.] https://www.cs.cmu.edu/~15-821/CDROM/PAPERS/want2006.pdf.
142. sellis. You Might Need a Barcode. [Online] Entrepreneur Launch Pad, 08 08 2013. [Cited: 25 04 2015.] http://www.elpnow.org/2013/08/08/you-might-need-a-barcode/.
143. [Online] [Cited: 20 05 2015.] http://www.tandfonline.com/doi/pdf/10.1201/1078/44912.22.1.20051201/85739.7.
144. About RFID Technology. [Online] Infinium Solutionz. [Cited: 15 05 2015.] http://122.182.4.125/infiniumwebsite/Tech_RFID.aspx.
145. Birkle, Chris. Garments with 'invisible' chips to revolutionise clothing industry. [Online] Nottingham Trent University, 01 07 2015. [Cited: 15 10 2015.] http://www.ntu.ac.uk/apps/news/174980-22/Garments_with_invisible_chips_to_revolutionise_clothing_industry.aspx.
146. Radio Frequency Identification (RFID) Tags. *Tilak Dias.* [Online] Advanced Textiles Research Group , 02 03 2015. [Cited: 20 10 2015.] https://ntuadvancedtextiles.wordpress.com/2015/03/02/radio-frequency-identification-rfid-tags/.
147. Cork, Colin. Fully embedded RFID devices in textile yarns. [Online] Advanced Textiles Research Group, NTU, 08 04 2015. [Cited: 20 10 2015.] https://ntuadvancedtextiles.wordpress.com/2015/04/08/fully-embedded-rfid-devices-in-textile-yarns/.

148. Admin, nfc Tagify. Researchers unveil breakthrough in weaving NFC chips into clothes. [Online] nfc TAGIFY.com, 03 07 2015. [Cited: 20 10 2015.] https://nfctagify.com/researchers-unveil-breakthrough-in-weaving-nfc-chips-into-clothes/.

149. Boden, Rian. Researchers unveil breakthrough in weaving NFC chips into clothes. *NFC World.* [Online] 03 07 2015. [Cited: 20 10 2015.] http://www.nfcworld.com/2015/07/03/336391/researchers-unveil-breakthrough-in-weaving-nfc-chips-into-clothes/.

150. Nottingham Trent University shares in £20 million to manufacture fibre of the future. [Online] 7 January 2015. [Cited: 10 September 2015.] http://www.ntu.ac.uk/apps/news/168226-15/Nottingham_Trent_University_shares_in_%C2%A320_million_to_manufacture_fibre_of_t.aspx.

151. Dias, Tilak. ntuadvancedtextiles.wordpress.com. [Online] https://ntuadvancedtextiles.wordpress.com/2015/04/13/research-fellow-in-the-manufacture-of-functional-electronic-textiles/.

152. Harrop, P.,. Why the interest in e-textiles? [Online] May 2014. http://www.printedelectronicsworld.com/articles/6531/why-the-interest-in-e-textiles.

153. TE Connectivity CRG Series Thick Film Surface Mount Fixed Resistor 0201 Case 105Ω ±1% ±200ppm/°C. [Online] RS components. [Cited: 15 10 2015.] http://uk.rs-online.com/web/p/surface-mount-fixed-resistors/7550167/?searchTerm=7550167&relevancy-data=636F3D3126696E3D4931384E525353746F636B4E756D6265724D504E266C753D656E266D6D3D6D61746368616C6C26706D3D5E5C647B367D247C5E5C647B377D247C5E5C647B31307D242670.

154. Kingbright KPHHS-1005QBC-D-V Blue LED, 465 nm, 1005 (0402) SMD Package. [Online] RS Components. [Cited: 15 10 2015.] http://uk.rs-online.com/web/p/visible-leds/8609018/?searchTerm=860-9018&relevancy-data=636F3D3126696E3D4931384E525353746F636B4E756D6265724D504E266C753D656E266D6D3D6D61746368616C6C26706D3D5E5C647B337D5B5C732D2F255C2E2C5D5C647B332C347D2426706F3D313426736E3D.

155. Bradley, E.,. *Lead-free Solder Assembly: Impact and Opportunity in Electronic Components and Technology Conferance.* s.l. : IEEE, 2003.

156. Semiconductor. [Online] [Cited: 10 June 2014.] www.medlibrary.org.

157. Conductive Fibre and Fabric. [Online] [Cited: 05 April 2014.] www.conductivefibreandfabric.co.uk.

158. Research at ITA. *Smart Textiles.* [Online] [Cited: 10 May 2014.] http://www.ita.rwth-aachen.de/andere_sprachen/englisch/3-05-smarttextiles.html.

159. Industrial Hand Spldering. [Online] [Cited: 19 March 2014.] http://www.eevblog.com/forum/reviews/what-metcal/60/.

160. Gladwin, D.,. Hot plate reflow soldering using low temperature solder. [Online] Cit Technology. [Cited: 08 May 2015.] http://cittechnology.com/articles/hotplate-soldering-low-temperature-solder.html.

161. Woznicki, T.,. Hot-Bar Soldering. [Online] Flex Circuit News, November 2000. [Cited: 10 March 2012.] http://www.flexdude.com/Back%20Issues/FCN11-00A.PDF.

162. Vivari, M.J., and Kasman, M.A.,. *Laser Solder Reflow: A Process Solution Part I.* 2007.

163. Ogochukwu, E. S.,. Laser Soldering, Chapter 15. [Online] [Cited: 09 May 2015.] http://cdn.intechopen.com/pdfs-wm/38865.pdf.

164. Hot Bar Reflow . [Online] Amada Miyachi Europe, 2013. [Cited: 08 May 2015.] http://www.amadamiyachieurope.com/cmdata/documents/Hot-Bar-Reflow-Soldering-Technology-10-2014.pdf.

165. SMD Hot Air Pencil . [Online] [Cited: 08 May 2015.] http://www.zeph.com/pencil.html.

166. Kelsey, J.,. How to Use Torches, Heat Guns, and Soldering Irons-and When. [Online] [Cited: 08 May 2015.] http://www.thisoldhouse.com/toh/article/0,,449698,00.html.

167. luigi. A really close look at solder paste from Evil Mad Scientist. *The tinkering studio.* [Online] Jun 2013. http://tinkering.exploratorium.edu/tinkering/2013/06/14/a-really-close-look-at-solder-paste-from-evil-mad-scientist.

168. Dias, T., Rathnayake, A.,. *Electronic Textiles Smart Fabrics and Wearable Technology.* [ed.] T. Dias. Advanced Textiles Research Group, Nottingham Trent University : Woodhead, The Textile Institute, 2015. pp. 109-116.

169. Cork, C., Dias, T., Rathnayake, A., Acti, T., Mbise, E., Anastasopoulos, I., and Piper, A.,. *The next generation of electronics textiles, Advanced Textiles Research Group, Nottingham Trent University.* Manchester : 1st International Conferance on Digitl Technologies for the Textiles Industies, 2013.

170. MC. [Online] RIUS-Comatex. http://www.rius-comatex.com/eng/maquinaria/cuerdas_cordones/mc.php.

171. Constructed Textiles . *Braided structures.* [Online] 23 10 2010. [Cited: 20 05 2015.] http://constructedtextiles.blogspot.co.uk/.

172. Dias, D., and Rathnayake, A.,. *Electronic Textiles Smart Fabrics and Wearable Technology.* [ed.] T. Dias. Advanced Textiles Research Group, Nottingham Trent University : Woodhead, The Textile Institute, 2015. pp. 109-116.

173. Harrop, P., and Raghu, D.,. *E-Textiles: Electronic Textiles 2014-2024, Wearable Technology Report.* s.l. : IDTechEx, 2014.

174. Zeidman, M. I., Sawhney, P. S., and Herrington, P. D.,. *Fiber migration theory of ring-spun yarns.* s.l. : Indian Journal of Fibre & Textile Research, 2003. Vols. 28. pp. 123-133.

175. Wijendra, H.,. Textile Spinning Process of Cotton Yarn. *Classification of Yarn.* [Online] Sri Lanka Institute of Textile & Apparel Technology (SLITA). http://textilelearner.blogspot.co.uk/2013/12/textile-spinning-process-of-cotton-yarn.html.

176. Smith, Ross Travers. Workshop: An Introduction to prototyping with the Arduino for the Software Engineer. [Online] PERVASIVe/ISWC 2012 page 55, 18-22 June 2012. http://www.iswc.net/iswc12/iswc-program.pdf.

177. LilyPad Arduino. [Online] https://www.arduino.cc/en/Main/arduinoBoardLilyPad.

178. Battery Life Calculator [online] [cited] 14 06 2016 http://www.digikey.co.uk/en/resources/conversion-calculators/conversion-calculator-battery-life